IDENTIFICATION OF ENDOGENOUS MECHANISMS THAT AFFECT
KLEBSIELLA PNEUMONIAE GROWTH IN THE MURINE HOST

by

Helen Yuen-Fun Lau

A dissertation submitted in partial fulfillment
of the requirements for the degree of
Doctor of Philosophy
(Microbiology and Immunology)
in the University of Michigan
2007

Doctoral Committee:

        Assistant Professor Thomas A. Moore, Co-Chair
        Professor Gary B. Huffnagle, Co-Chair
        Professor Victor J DiRita
        Professor Harry LT Mobley
        Professor Gabriel Nunez

Because she has to be everywhere.

To Kathryn who is forever too sweet and innocent to remain here.

And to those who have ever wanted something so badly,

went against numerous obstacles

and obtained it.

Acknowledgements

First and foremost, I must thank all the scientific people in the Pulmonary Division and the Department of Microbiology and Immunology, both current and past members, who have either taught me specific techniques or have given me valuable input and suggestions about my research.

I must also thank the members of the Huffnagle Lab: Toby, John ED, Nicole, Rod, Andy, Tiffany, Katie, Daniel, Gwo-Hsiao, and Michal. You guys are a talented, intelligent and friendly group of people. I am forever grateful for your suggestions, technical help and supply sharing. And thanks for "adopting" me into your lab meetings as well.

To my dissertation committee, Tom Moore, Gary Huffnagle, Vic DiRita, Gabriel Nunez and Harry Mobley, thank you all for your comments, suggestions and ideas about my thesis. Thanks Tom for taking me into your lab, letting me go about things on my own, and creating a comfortable lab environment in which to conduct research. You never looked over my shoulders and always had faith in me.

And thank you Gary so VERY much. I don't think my thesis would be what it is today without you. Actually, I KNOW it would not be what it is today without your help and guidance. Your leadership abilities, scientific knowledge, enthusiasm, positive attitude and warmth amazes me still. I have nothing but the deepest respect for you. Thanks again for being there for me when I needed help the most.

To all my friends that have encouraged me, believed in me and kicked me back onto this path when I dared to veer, thank you all; especially to Jenn and Yen for being in my life since the 7th grade, my little sister Nancy, and my college buddies, Michelle and Jim.

And thanks to Bender, Fry and Leela for being cute and furry and for bringing a smile to my face **EVERYDAY**.

Table of Contents

List of Figures

Figure

List of Tables

Abstract

     Klebsiella pneumoniae is an opportunistic pathogen and a normal component of the host flora. The aim of this project was to investigate mechanisms that determine mucosal tissue colonization and infection by *K. pneumoniae*. In this study, a clinical respiratory isolate of *Klebsiella pneumoniae*, strain IA565, was found to be both non-pathogenic in a murine model of bacterial pneumonia and unable to colonize the lungs even during extreme immunosuppressive conditions. Strain IA565 was inoculated intranasally and intragastrically into immunocompetent and immunocompromised mice, germ-free mice, and mice with intestinal inflammation. When strain IA565 was both intranasally instilled and orally gavaged into wild type mice, this strain stably colonizes and persists in the nares and GI tract. Interestingly, intranasal inoculation of wild type (WT), germfree (GF), and severely immunocompromised mice with strain IA565 displayed similar CFU levels in the nasal cavity. Conversely, strain IA565 gastrointestinal (GI) tract CFU levels in GF mice are significantly higher than in WT mice suggesting that, in the presence of the normal gut microbiota, IA565 growth is controlled and maintained at low levels. In addition, mice with *Citrobacter rodentium*-induced gut inflammation displayed no change in IA565 GI colonization, compared to WT mice, and no change in the disease outcome. However, DSS-treated mice displayed significantly higher levels of IA565 gut CFU compared to WT levels demonstrating that host mediated inflammation can alter microbial colonization. Collectively, these data

indicate that strain IA565 nasal cavity colonization can be achieved in immunocompetent, immunocompromised, and GF mice. Thus, nasal cavity colonization is independent of host factors and the indigenous microbiota. This is in contrast to IA565 GI colonization where host factors mediating certain types of inflammation can alter CFU levels and absence of the gut microbiota leads to increased IA565 growth. This study is the first to identify and describe mechanisms influencing the growth and behavior of a murine commensal organism.

Chapter I

An Introduction to *Klebsiella pneumoniae*

Clinical Significance

Klebsiella pneumoniae is part of the family *Enterobacteriaceae* and is named

after the 19th century German microbiologist, Edwin Klebs to honor his work in

identifying the etiological cause of diptheria. *K. pneumoniae* is a rod-shaped, gram-

negative bacterium most commonly encountered by physicians worldwide as a

community-acquired and a hospital-acquired pathogen. Unique biochemical

characteristics that enable identification of this bacterium in clinical and environmental

samples are production of urease and citrate, lack of ornithine decarboxylase and

motility, inability to produce indole, and ability to ferment glucose and lactose.

Community-acquired *Klebsiella* pneumonia is also called Friedländer's

pneumonia named after Carl Friedländer who identified *K. pneumoniae* as the cause of

fatal cases of pneumonia in 1882. Although *K. pneumoniae* is historically known as an

important cause of community-acquired pneumonia, the incidence of these cases has

significantly declined in the United States [1]. However, nosocomial *K. pneumoniae*

pneumonia is still problematic with substantial morbidity and mortality.

In the United States, urinary tract infections (UTIs) comprise about 30% of

nosocomial infections, followed by pneumonia at 27%, and bloodstream infections at

19%. *K. pneumoniae* is responsible for about 4-8% of these cases continually ranking in

the top 5 causative agents for each type of infection [2]. For nosocomial pneumonia, patients who are in the neonatal intensive care units, 65 years of age or older, and have severe underlying disease, immunosuppression, and/or cardiopulmonary disease are mostly at risk for *K. pneumoniae* infections [3, 4].

Pulmonary *K. pneumoniae* disease is often complicated by multilobular involvement, formation of lung abscesses, and dissemination of bacteria from within the pulmonary airspace into the bloodstream [5, 6]; all of which are accompanied by the characteristic rapidly progressive clinical course. The lungs of these patients display high levels of necrosis, inflammation, and hemorrhage with the production of thick, bloody, mucoid sputum described as currant jelly sputum. Factors associated with pulmonary colonization and establishment of pneumonia are depicted in Figure I.1. These include mechanically assisted intubation, oral, tracheal and gastric colonization, and antibiotic therapy all leading to the development of respiratory disease.

K. pneumoniae respiratory infections have been complicated by the extensive use of broad-spectrum antibiotics in hospitals selecting for drug resistant strains that produce extended-spectrum β-lactamase (ESBL). Thus, the emergence of ESBL producing *K. pneumoniae* strains limits therapeutic options contributing to the overall high mortality rates in these patients [6-9].
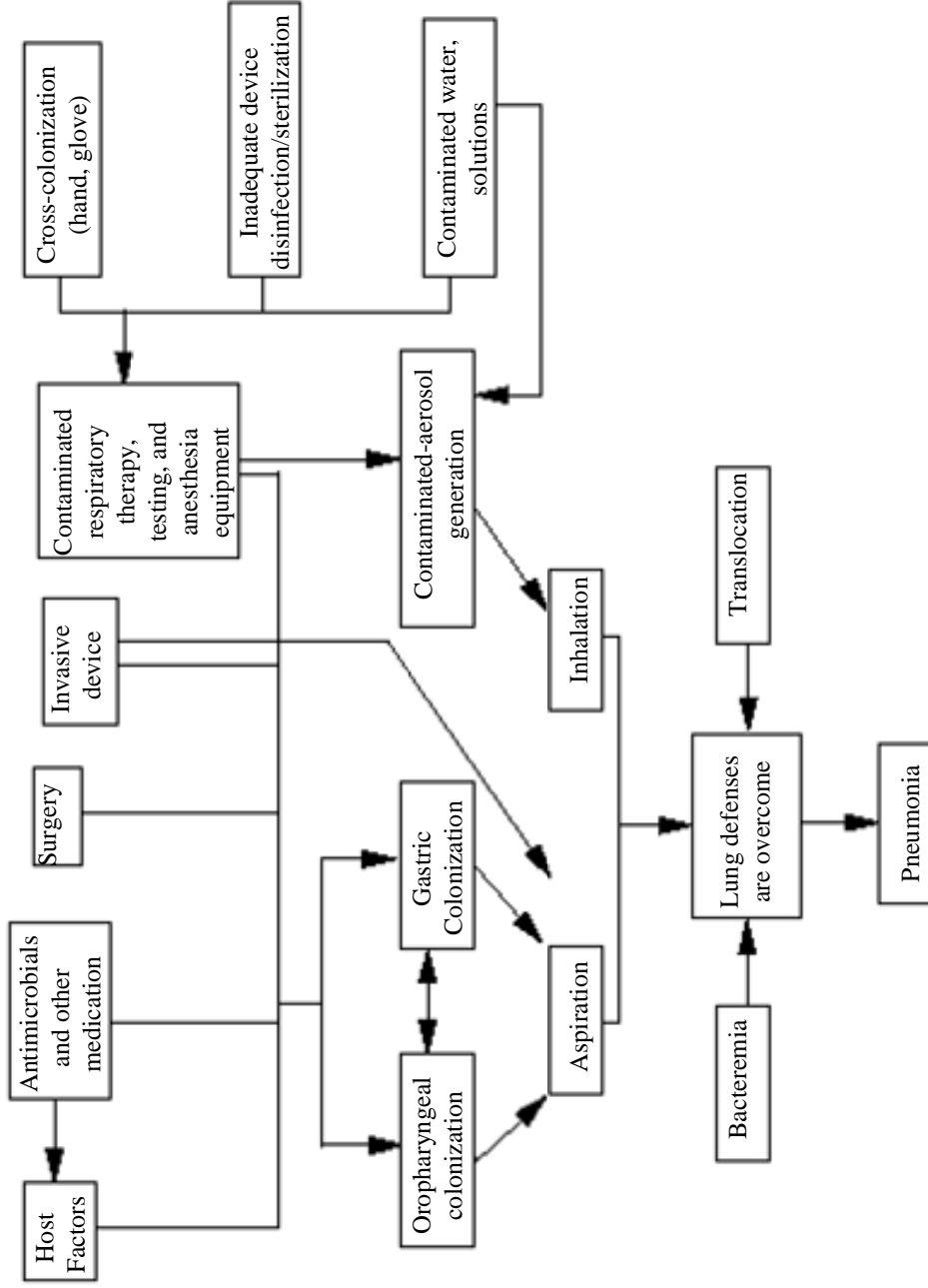
Figure I.1 Factors Associated with Nosocomial Bacterial Pneumonia
(Adapted from the Center for Disease Control, Guidelines for prevention of Nosocomial Pneumonia.)

Host Responses during *Klebsiella pneumoniae* Respiratory Infection

The respiratory tract serves as one of the three interfaces between the host and the environment. Therefore, the lung is equipped with complex and effective defense mechanisms for the rapid clearance of microbes from the respiratory tract. The surface of the lung is protected by non-specific factors such as the barrier of the airway epithelium, the cough reflex, ciliary beat and mucus clearance. In addition to these mechanical factors, highly complex cellular and non-cellular components of pulmonary innate immunity play a role in microbial clearance as well.

Toll-like receptors (TLRs)

Toll-like receptors (TLRs), collectins (surfactant A and D and mannose-binding lectin), defensins, and complement are part of the non-cellular portion of the innate immune system. TLRs are pattern-recognition receptors that are highly specific for conserved sequences on microbes known as pathogen-associated molecular patterns. TLRs are responsible for the initiation of host responses via the recognition of invading microbes. Signaling through TLRs results in immune activation via the release of cytokines, chemokines and antimicrobial substances such as collectins and defensins [10].

TLR4 is responsible for recognizing lipopolysaccharide (LPS) and initiating early innate immune responses to this bacterial antigen. Schurr et al. found that as early as 4 hours post *K. pneumoniae* pulmonary challenge, mice increased lung expression of TLR4-dependent genes such as cytokines required for neutrophil activation and recruitment, the TLR adaptor protein, MyD88, growth factor receptors, and adhesion

molecules [11]. Their data suggested that rapidly induced expression of TLR4-related genes in response to bacterial challenge is important for clearance and host survival.

Collectins

Collectins, members of the C-type lectin superfamily, are collagen-binding lectins responsible for recognizing and binding to sugar moieties on microbial surfaces to increase adhesion and phagocytosis by alveolar macrophages [12]. Surfactant protein A (SP-A) and D (SP-D) and mannose-binding receptors (MR) are collectins found in the respiratory tract and are believed to contribute to pulmonary innate immunity to *K. pneumoniae* [13].

SP-A and MR have been shown to recognize *K. pneumoniae* capsular polysaccharide [14]. In addition, SP-A increases phagocytosis of *K. pneumoniae* during respiratory infection by serving as a opsonin and by activating macrophages and thus increasing the activity of MR [15]. Similarly, SP-D, which is responsible for recognizing *K. pneumoniae* LPS [16], also promotes opsonization and phagocytosis of this organism during pulmonary infection [17, 18]. Thus clearance of this organism from the lung is dependent upon these collectins.

Alveolar Macrophages, Neutrophils and Lymphocytes

Animal models have proven useful in identifying the specific host: pathogen interactions and crucial elements of lung innate defense during *K. pneumoniae* pulmonary infection. Utilizing a murine model of *K. pneumoniae* pneumonia, many different cell types and cytokines have been shown to play an important role in mediating lung

antibacterial host responses during *K. pneumoniae* infection. Increased lung bacterial clearance and improved survival have all been attributed to the influx of polymorphonuclear cells (PMNs) into the lungs as well as to the action of resident alveolar macrophages during *K. pneumoniae* infection.

Resident alveolar macrophages (AMϕs) are capable of eradicating invading organisms during low levels of microbial challenge. When AMϕ depleted mice are given sublethal doses of *K. pneumoniae*, 100% mortality is observed as well as increased bacterial burden in the lungs [19]. In addition, macrophage inflammatory protein-1 alpha (MIP-1α) is important for AMϕ activation since MIP-1α deficient AMϕs had a lower phagocytic index for *K. pneumoniae* compared to wild-type AMϕs [20]. However when AMϕs are overwhelmed, such as during high microbial challenge or during exposure to a virulent organism, various cytokines and chemokines are produced to recruit and activate circulating neutrophils and monocytes to aid in microbial clearance.

Through studies done with the chemotactic cytokines, macrophage inflammatory protein-2 (MIP-2) and keratinocyte chemoattractant (KC), PMNs have been shown to be indispensable during *K. pneumoniae* pulmonary infection [21, 22]. Transgenic expression of KC decreases mortality and bacterial burden while increasing lung neutrophilic influx. *In vivo* depletion of MIP-2 results in a significant decrease in neutrophil numbers and bacterial clearance. Furthermore, $\gamma\delta$-T cells contribute to the survival of *K. pneumoniae* infected mice as well as the control of bacterial dissemination from the lung into the blood [23].

Cytokines

In addition to the cytokines mentioned above, absence of interferon gamma (IFNγ), tumor necrosis factor alpha (TNFα), interferon-inducible protein 10 (IP-10), and interleukin(IL) -17, during pulmonary *K. pneumoniae* infection results in increased mortality and bacterial burden in the lungs [24-27]. This illustrates the important role proinflammatory cytokines play in mediating lung antibacterial host responses during *K. pneumoniae* infection. *In vivo* neutralization of TNFα also reduced levels of lung PMNs suggesting a role for TNFα in neutrophil recruitment [24]. IL-10 is known to suppress the production of proinflammatory cytokines and inhibit microbicidal activities of macrophages and neutrophils. Neutralizing IL-10 in *K. pneumoniae* infected mice deceased mortality and lung bacterial burden aiding the host in pulmonary clearance and long term survival suggesting the dampening effects of IL-10 had on innate immunity [28]. TNFα, MIP-2 and MIP-1α levels in the lungs of IL-10 depleted mice were above wild-type levels confirming the beneficial effects these cytokines elicit during *K. pneumoniae* infection. However, no increase in neutrophil recruitment was observed in those mice [28]. Interestingly, IFNγ KO infected mice displayed higher amounts of lung IL-10 further suggesting that IL-10 downregulates the immune response exacerbating the disease in these mice [25].

Thus cytokines are not only important for amplifying the host defense against invading microbes, a balance of type 1 and type 2 cytokines have been shown to modulate the intensity of innate immunity and to polarize and transition from innate immunity to adaptive immunity [29].

Virulence Factors

K. pneumoniae contains several well studied virulence factors that include capsular polysaccharide, lipopolysaccharide, type 1 and type 3 fimbriae, and siderophores depicted in Figure I.2 (adapted from [30]).
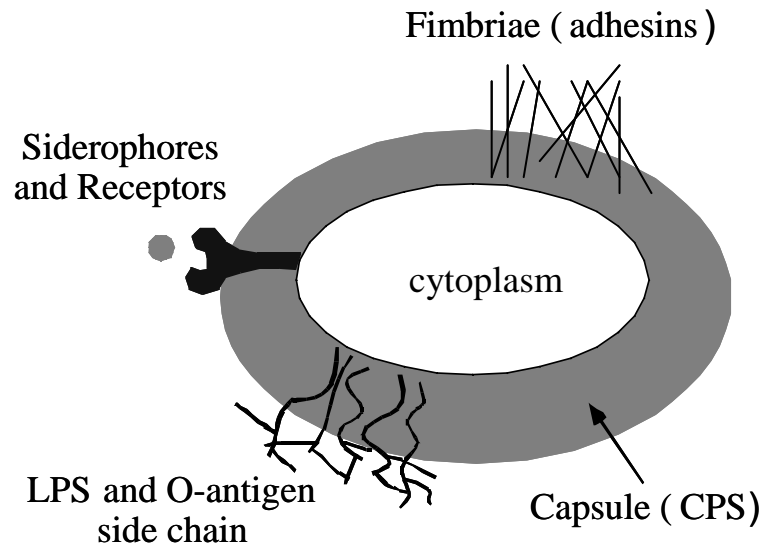
Figure I.2 *Klebsiella pneumoniae* **Virulence Factors**

Capsular Polysaccharide

Most clinical isolates of *K. pneumoniae* are encapsulated with a thick complex of acidic polysaccharide structure comprised of repeating 4-6 sugar subunits. Capsular polysaccharides (CPS) have been classified into 77 serological types, termed K-antigens. The presence of the capsule is critical for the virulence of *K. pneumoniae* [14, 31-34]. Deletion of the Orf6 gene within the CPS operon resulted in an avirulent unencapsulated *K. pneumoniae* mutant [35]. Similarly, *wabG* mutants lack cell-attached CPS and were shown to be avirulent in animal models of both UTI and pneumonia [36]. Deletion of

rmpA2, a transacting activator of CPS synthesis, resulted in decreased CPS production and reduced virulence *in vivo* [37].

The capsule inhibits phagocytosis by macrophages and neutrophils and binding of serum anti-microbial factors such as complement to the bacterial membrane. In general, the majority of clinical isolates are of the K1 or K2 serotype [38, 39]; however, this is not an absolute correlation [40]. Capsule switch mutants have been constructed using strains expressing K2 and K21a. It was found that the genetic background of virulent strains, independent of the capsule serotype, confers significant *in vivo* murine pathogenicity [14, 31]. This suggested that pathogenesis of *K. pneumoniae* is multifactorial and that capsule can only partially account for *in vivo* murine virulence. This is further supported by the fact that other capsular serotypes are equally as prevalent and virulent [41, 42] in mice.

Moreover, the degree of virulence associated with a particular capsular serotype may be related to the mannose content of the CPS. Macrophages possess lectin receptors for mannose-α-2/3 mannose. CPS containing repetitive sequences of this sugar structure is recognized by the macrophage receptors, resulting in increased phagocytosis and subsequent killing [43]. Interestingly, K2 CPS lacks this sugar repeat resulting in decreased lectin receptor-mediated phagocytosis and contributing to increased virulence of K2 serotypes [14].

In addition, encapsulated strain of *K. pneumoniae* have been shown to suppress the pulmonary inflammatory response by decreasing the production of pro-inflammatory cytokines TNFα, IFNγ and IL-6 while increasing the production of the anti-inflammatory cytokine, IL-10 [34, 44].

Lipopolysaccharide

Lipopolysaccharide (LPS) is known to play a role in bacterial pathogenesis and is the causative agent of gram-negative septic shock [45]. LPS consists of 3 subunits: a hydrophobic lipid A domain (endotoxin), a non-repeating core of oligosaccharide, and an outer, structurally diverse polysaccharide (O-antigen). There are currently 12 different O-antigen serotypes of *K. pneumoniae.* A recent study using *wbbO* mutants lacking O-antigen reported that these mutants are less virulent in a murine model of pneumonia that was partially attributed to decreased bacteremia during the course of pulmonary infection [46].

One of the primary host defense mechanisms during bacterial infection is mediated by the complement system. Activation of either the classical or alternate pathways results in activation of C3 and deposition of C3b opsonin on the bacteria. C3b formation can lead to the generation of the terminal attack complex (C5-C9) and bacterial killing. To counter this defense, pathogenic gram-negative bacteria express a thick CPS that can mask LPS and block C3 activation [47, 48]. Alternatively, only the outer O-antigen side chain of LPS may protrude through the capsule, resulting in C3 activation at a greater distance from the bacterial cell membrane, diminishing the formation of the complement attack complex [49]. Additionally, smooth LPS has been shown to activate only the alternative pathway, resulting in less C3b deposition compared to the activation of both pathways [50].

Fimbriae

Klebsiella fimbriae are non-flagellar, filamentous projections on the bacterial cell surface. These fimbriae are thought to play an important role during the early stages of bacterial adhesion to host cells. Fimbriae expressed by *Klebsiella* have been divided into two major categories based on whether their adhesive interaction can be inhibited by D-mannose. Type 1 fimbriae are mannose sensitive and bind to mannose containing trisaccharides on host epithelial cell glycoproteins. Interestingly, after mannose-dependent binding to epithelial cells, invasive, *K. pneumoniae* bacteria can turn off expression of type 1 fimbriae in order to avoid mannose-dependent binding by host phagocytic macrophages [51]. Type 3 fimbriae are resistant to D-mannose inhibition and have been shown to promote binding to endothelial cells, respiratory epithelium, and kidney epithelial cells. The gene cluster required for expression of type 3 fimbriae in *K. pneumoniae* has been cloned and shown to contain six genes termed MrkA-F [52]. The importance of type 3 fimbriae during infection is not well understood. However, a mutant of a *K. pneumoniae* virulent strain deficient in type 3 fimbriae production (gift from Dr. Steven Clegg, U. Iowa) was found to be no different in its pathogenicity compared to the parental strain (unpublished observation).

Siderophores

Iron is an essential element for bacterial growth and is procured from the host environment via the bacterial secretion of high affinity, low molecular weight iron chelators called siderophores. Enteric siderophores belong to three major groups, enterobactin, aerobactin, and yersiniabactin. A previous report indicated that

enterobactin production did not correlate with virulence [53] while transformation of an

avirulent, aerobactin negative *K. pneumoniae* strain with aerobactin cloned from a

virulent strain conferred virulence [54]. However, more recently, Lawlor et. al. showed

that *K. pneumoniae* yersiniabactin production is increased during pulmonary infection

while during *in vitro* iron-limiting growth conditions, enterobactin is produced at higher

levels when compared to yersiniabactin [55]. The discrepancies in these results can be

attributed to the complexity of these siderophores systems *in vivo* and also the lack of

definitive experiments addressing the importance of these iron acquisition systems.

Other Virulence Factors

     In addition to the above mentioned four major classifications of virulence factors,

recent studies have identified other putative genes associated with *K. pneumoniae*

pathogenicity. Outer membrane protein A (OmpA) in *K. pneumoniae* binds to human

and mouse macrophages and dendritic cells via TLR2, resulting in cytokine secretion

[56]. OmpA also binds to bronchial epithelial cells, inducing chemokine production and

neutrophil recruitment [57]. In addition, several studies have identified novel, previously

uncharacterized genes present in virulent strains of *K. pneumoniae* using signature-tagged

mutagenesis [58-60], *in vivo* expression technology [61], and PCR-based subtractive

hybridization [62, 63].

Sources of *Klebsiella pneumoniae*

Environmental Isolates

　　K. pneumoniae is ubiquitous in nature and can be isolated in large quantities from a variety of water sources: freshwater, sewage, rivers, streams, lakes and seas [64-67]. Not surprisingly, because of its abundance in natural water reservoirs, *K. pneumoniae* can also be found in the soil and in farm produce such as tomatoes, carrots, lettuce, radishes, celery and onions [64]. In a 2001 study, over 100 environmental surface water isolates of *K. pneumoniae* were found to be just as capable of expressing virulence factors as clinical isolates [41]. These factors include capsular polysaccharide, fimbriae and siderophores, which will be discussed later in this chapter. In addition, the virulence of *K. pneumoniae* environmental isolates were evaluated in murine models of UTI and intestinal colonization and found to be as virulent as strains of clinical origin [42]. These isolates colonized the gastrointestinal tract, bladder and kidneys in similar bacterial numbers as clinical isolates.

Commensals

　　K. pneumoniae is also a component of the normal microflora in several different mammals and can be isolated from the upper respiratory and gastrointestinal tract of both humans and mice [68-72]. Strains of *K. pneumoniae* causing nosocomial pneumonia have been shown to originate from the gastrointestinal tract of humans. In the 1970s, Seldon et al reported that about 50% of patients that were intestinal carriers of *K. pneumoniae* became infected by the same serotype whereas less than 10% of patients

who were not intestinal carriers succumbed to *K. pneumoniae* infection [73].

Furthermore, to determine the sequence of colonization from the stomach to lungs, the

trachea, oropharynx, stomach and rectum of patients admitted to an intensive care unit

were examined for *K. pneumoniae* colonization from 5 days post ICU admission to the

development of pneumonia. *K. pneumoniae* was found in the stomach samples prior to

tracheal colonization indicating the gastrointestinal tract as a possible source for

Klebsiella pneumonia [74].

The ubiquity of *K. pneumoniae* in nature, the infectious potential of

environmental isolates and the presence of natural reservoirs of these bacteria in the host

may explain the high frequency of opportunistic infections caused by this species.

The Mucosal Microbiota

In human adults, indigenous microorganisms colonize the skin and mucosal

surfaces of the oral cavity, upper respiratory tract, urogenital tract and much of the

gastrointestinal (GI) tract [75, 76] (Figure I.3). In the respiratory tract, the human adult

microflora of the nasal passages, or nares, reflects the microbiota of the skin with the

predominating organisms being *Staphylococcus, Corynebacterium,* and

Propionibacterium [75, 77]. This is in contrast to the distal parts of the respiratory tract,

the trachea, bronchi, and alveoli, are sterile [78]. In the mucous membranes of the oral

cavity and pharynx, the genuses *Streptococcus, Lactobacillus,* and *Haemophilus*

predominate. In the gastrointestinal tract, due to the acidity and presence of proteolytic

enzymes, the stomach is generally free of indigenous microbes with the exception of

Helicobacter pylori. In addition, the upper two-thirds of the small intestine, the

14

A

nasopharynx

oropharynx

laryngopharynx

bronchus

lung

nasal cavity

nares

trachea

B

stomach

small intestine

rectum

large
intestine
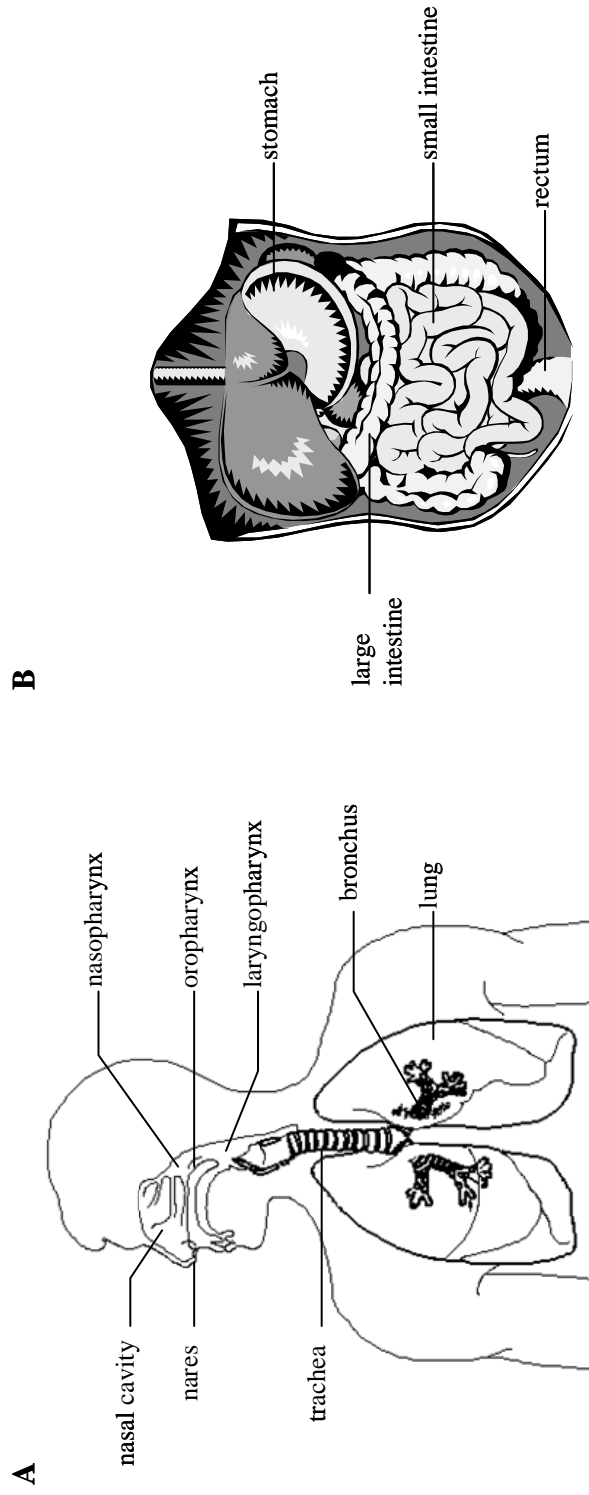
Figure I.3 The Respiratory and Gastrointestinal Tract
Certain mucosal surfaces of the upper respiratory tract (A) and the gastrointestinal tract (B) are inhabited by
indigenous microorganisms, known as the mucosal microbiota.

duodenum, jejunum and the proximal ileum, is thought to be free of microbes as well.

However, the distal ileum and the mucosal surface and lumen of the large intestine

contains about 99.9% of the human indigenous microbiota [76]. Gram-negative and

gram-positive, facultative micraerophilic and strictly anaerobic species have been

identified in these organs with the majority of them being anaerobic organisms.

Microbial populations within the host have considerable impact on host systems as well

as those of other bacterial populations.

Colonization Resistance and Probiotics

The mucosal microbiota has the capacity to either limit the growth of, or to

eliminate, certain transient microbial pathogens entering their environment via

mechanisms associated with colonization resistance. Competition for nutrients and

mucosal adhesion sites and secretion of toxic metabolic end products are some of the

mechanisms exhibited by the indigenous microbiota to suppress pathogen growth.

Interestingly, colonization resistance requires the entire microflora to function optimally.

Resistance to a particular microbial pathogen, such as *E. coli*, could not be demonstrated

in animals colonized with only one to several indigenous microbial species [79].

Potentially pathogenic microbes are present in healthy individuals as part of the

normal microflora and have the capacity to overgrow especially after hospitalization

and/or antibiotic treatment. Due to hospitalization alone, *K. pneumoniae* levels in both

fecal and oropharyngeal specimens were significantly higher after 15 days of

hospitalization and at the time of discharge compared to those levels in newly admitted

patients [80, 81]. Increases in levels of *K. pneumoniae* bacteria was also demonstrated in

16

fecal and throat specimens of patients receiving antibiotics [82-84]. This increase in potentially pathogenic microbes is clinically significant since, as stated above, pneumonia causing microbes have been shown to originate in the GI tract of hospitalized patients. Furthermore, the alteration of the normal microbiota has also been linked to rheumatoid arthritis [85], diarrhea [86], and allergy [87, 88]. Thus maintenance of the microbiota is important in preventing disease.

The use of probiotic bacteria, live microorganisms belonging to the natural flora with low or no pathogenicity, has been increasingly accepted as a means to control overgrowth of potentially pathogenic organisms. Probiotics have been defined as a "live microbial feed supplement which beneficially affects the host animal or human by improving its intestinal microbial balance" [89]. The species currently being used as probiotics include *Lactobacillus acidophilus, L. casei, Streptococcus thermophilus, Enterococcus faecalis, Bifidobacterium* species, *E. coli, Bacillus subtilis, Bacteroides* species, and *Saccharomyces boulardii*. These probiotic bacteria have been shown to control growth of various enteric pathogens such as *Salmonella typhimurium, Shigella, Clostridium difficile, Campylobacter jejuni, E. coli,* and *H. pylori* in mice [90-94]. Thus probiotics are effective tools to prevent and treat microbial infections as well as to restore and uphold a microflora that is beneficial to the host.

The Role of the Microbiota in the Mucosal Immune System

The components of the microflora interact with the immune system of the host in a variety of ways. LPS, a major surface component of all gram-negative bacteria, is a strong stimulator of the innate immune system interacting with pathogen recognition

17

receptors, CD14 and TLR4, to induce production of both reactive oxygen intermediates and secretion of inflammatory cytokines [95]. Peptidoglycan (PGN) surrounds the cytoplasmic membrane of bacteria maintaining shape and is abundant in the cell wall of gram-positive bacteria. PGN is recognized by CD14 and TLR2 and cytoplasmic proteins, Nod1 and Nod2, ultimately activating macrophages and production of NF-κB and proinflammatory mediators [96]. Immunostimulatory bacterial DNA containing CpG motifs, activates dendritic cells and macrophages to produce cytokines and expression of maturation markers through TLR9 [97]. The interaction of these components, as well as others, with the host immune system is responsible for eliciting regulatory (inhibitory) mechanisms, in addition to establishing mucosal tolerance to the abundant microbiota. This has been hypothesized to involve the cytokine signaling network, but the exact mechanisms are still unknown.

The use of germ-free (GF) and gnotobiotic animals, those with known defined microflora, has been indispensable in determining the role of commensal bacteria in the development of the mucosal immune system. GF mice that lack commensal enteric flora have fewer numbers of intra-epithelial lymphocytes and immunoglobulin A (IgA) producing cells, contain relatively small Peyer's patches and lack germinal centers [98-100]. Indigenous bacteria in the GI tract have also been shown to not elicit as great a host immune response as do various non-indigenous bacteria [76]. Secretory IgA (sIgA) can eliminate *S. typhimurium* and *Vibrio cholera* from the GI tract of mice [101, 102]; however, sIgA is unable to clear the indigenous anaerobic bacteria from the intestine despite these microbes being coated with sIgA in the feces [103]. These studies suggest

that the immune system is tolerant of the indigenous microflora through complex mechanisms that have yet to be fully elucidated.

In addition, differences between GF and conventionally reared animals (CVAs) are most significant in regions of the host where bacterial densities are normally the highest. These differences include enlargement of the cecum, shorter and few crypt cells, and lack of fecal fatty acids and metabolic breakdown of bilirubin, pancreatic enzymes, cholesterol, and steroid hormones in the GF mice [104, 105]. The gut-associated lymphoid tissue in the Peyer's patches and lamina propria of CVAs are prominent and stocked with large numbers of monocytic cells whereas in GF animals, these areas are hypocellular containing little monocytic cells [76]. Humoral and secretory responses in GF animals also develop at slower rates compared to CVAs. This suggests that GF animals are immunologically competent and that the immune system state of CVAs is a result of continual indigenous microbial antigen challenge. All of these observations support the notion that the microbiota is important to the development and maintenance of the host mucosal immune system.

To study interactions of the intestinal microflora with the host, mice with defined microflora are currently used to both simplify the microbial ecosystem and enhance reproducibility in laboratory experiments that aim to determine specific roles of certain microbes. The early work of Schaedler, Dubos and coworkers [106-108] has led to the development of mice with a defined intestinal flora consisting of eight benign commensal enteric bacteria, also known as altered Schaedler flora (ASF) mice [109] (Table I.1). This flora is proposed to be functionally similar to the normal microbiota because of their ability to restore the cecal morphology of GF mice to that of normal mice [107]. In one

Table I.1 Altered Schaedler Flora Bacterial Strains

Species	Strain	Oxygen Tolerance	Gram Staining	Morphology
Lactobacillus sp.	ASF360	Facultative anaerobe	+	rod
Lactobacillus murinus	ASF361	Facultative anaerobe	+	rod
Bacteroides distasonis	ASF519	Anaerobe	-	coccobacillus
Mucispirillum schaedleri	ASF457	Anaerobe	-	spiral-shaped
Clostridium sp.	ASF356	Extremely Oxygen Sensitive	+	tapered rod
Eubacterium plexicaudatum	ASF492	Extremely Oxygen Sensitive	+	tapered rod
Firmicutes sp.	ASF500	Extremely Oxygen Sensitive	+	tapered rod
Clostridium sp.	ASF502	Extremely Oxygen Sensitive	+	tapered rod

study, ASF mice that were colonized with either *Helicobater bilis* or *Brachyspira hyodysenteriae* in murine models of colitis were found to vary in the severity of intestinal inflammation, production of proinflammatory cytokines and antigen-specific antibody responses [110]. Their results also demonstrated that colonization with a single bacterial strain can induce immune responses to nonpathogenic resident bacteria ultimately leading to chronic intestinal inflammation. Thus the manipulation of immunologically competent, defined flora mice will be useful in determining the role of intestinal bacteria in the development and maintenance of both the host mucosal immune system and inflammatory diseases.

Objective of this Study

Initial observations indicated that 2 clinical isolates of *K. pneumoniae* differed significantly in their ability to cause disease in a murine model of pneumonia, with strain IA565 inducing no mortality even at high doses. Thus, the objective of this dissertation was to investigate mechanisms that determine mucosal tissue colonization and infection by *Klebsiella pneumoniae*.

References

1.   Ko, W.C., et al., *Community-acquired Klebsiella pneumoniae bacteremia: global differences in clinical patterns.* Emerg Infect Dis, 2002. **8**(2): p. 160-6.

2.   Richards, M.J., et al., *Nosocomial infections in medical intensive care units in the United States. National Nosocomial Infections Surveillance System.* Crit Care Med, 1999. **27**(5): p. 887-92.

3.   Bartlett, J.G., et al., *Bacteriology of hospital-acquired pneumonia.* Arch Intern Med, 1986. **146**(5): p. 868-71.

4.   De Champs, C., et al., *Factors associated with antimicrobial resistance among clinical isolates of Klebsiella pneumoniae: 1-year survey in a French university hospital.* Eur J Clin Microbiol Infect Dis, 2004. **18**: p. 18.

5.   Jong, G.M., et al., *Rapidly fatal outcome of bacteremic Klebsiella pneumoniae pneumonia in alcoholics.* Chest, 1995. **107**(1): p. 214-7.

6.   Yinnon, A.M., et al., *Klebsiella bacteraemia: community versus nosocomial infection.* Qjm, 1996. **89**(12): p. 933-41.

7.   Meyer, K.S., et al., *Nosocomial outbreak of Klebsiella infection resistant to late-generation cephalosporins.* Ann Intern Med, 1993. **119**(5): p. 353-8.

8.   Davies, J., *Inactivation of antibiotics and the dissemination of resistance genes.* Science, 1994. **264**(5157): p. 375-82.

9.   Hoffman, N.R. and F.S. Preston, Jr., *Friedlander's pneumonia. A report of 11 cases and appraisal of antibiotic therapy.* Dis Chest, 1968. **53**(4): p. 481-6.

10.   Hippenstiel, S., et al., *Lung epithelium as a sentinel and effector system in pneumonia--molecular mechanisms of pathogen recognition and signal transduction.* Respir Res, 2006. **7**: p. 97.

11.   Schurr, J.R., et al., *Central role of toll-like receptor 4 signaling and host defense in experimental pneumonia caused by Gram-negative bacteria.* Infect Immun, 2005. **73**(1): p. 532-45.

12.   Hickling, T.P., et al., *Collectins and their role in lung immunity.* J Leukoc Biol, 2004. **75**(1): p. 27-33.

13.   Ofek, I., E. Crouch, and Y. Keisari, *The role of C-type lectins in the innate immunity against pulmonary pathogens*. The biology and pathology of innate immunity mechanisms, ed. Y. Keisari and I. Ofek. 2000, New York, NY: Kluwer Academic/Plenum Publishing. 27-36.

14.   Kabha, K., et al., *Relationships among capsular structure, phagocytosis, and mouse virulence in Klebsiella pneumoniae.* Infect Immun, 1995. **63**(3): p. 847-52.

15.   Kabha, K., et al., *SP-A enhances phagocytosis of Klebsiella by interaction with capsular polysaccharides and alveolar macrophages.* Am J Physiol, 1997. **272**(2 Pt 1): p. L344-52.

16.   Kostina, E., et al., *Noncapsulated Klebsiella pneumoniae bearing mannose-containing O antigens is rapidly eradicated from mouse lung and triggers cytokine production by macrophages following opsonization with surfactant protein D.* Infect Immun, 2005. **73**(12): p. 8282-90.

17. Keisari, Y., et al., *Surfactant protein D-coated Klebsiella pneumoniae stimulates cytokine production in mononuclear phagocytes.* J Leukoc Biol, 2001. **70**(1): p. 135-41.

18. Ofek, I., et al., *Surfactant protein D enhances phagocytosis and killing of unencapsulated phase variants of Klebsiella pneumoniae.* Infect Immun, 2001. **69**(1): p. 24-33.

19. Broug-Holub, E., et al., *Alveolar macrophages are required for protective pulmonary defenses in murine Klebsiella pneumonia: elimination of alveolar macrophages increases neutrophil recruitment but decreases bacterial clearance and survival.* Infect Immun, 1997. **65**(4): p. 1139-46.

20. Lindell, D.M., et al., *Macrophage inflammatory protein 1alpha/CCL3 is required for clearance of an acute Klebsiella pneumoniae pulmonary infection.* Infect Immun, 2001. **69**(10): p. 6364-9.

21. Greenberger, M.J., et al., *Neutralization of macrophage inflammatory protein-2 attenuates neutrophil recruitment and bacterial clearance in murine Klebsiella pneumonia.* J Infect Dis, 1996. **173**(1): p. 159-65.

22. Tsai, W.C., et al., *Lung-specific transgenic expression of KC enhances resistance to Klebsiella pneumoniae in mice.* J Immunol, 1998. **161**(5): p. 2435-40.

23. Moore, T.A., et al., *Gamma delta-T cells are critical for survival and early proinflammatory cytokine gene expression during murine Klebsiella pneumonia.* J Immunol, 2000. **165**(5): p. 2643-50.

24. Laichalk, L.L., et al., *Tumor necrosis factor mediates lung antibacterial host defense in murine Klebsiella pneumonia.* Infect Immun, 1996. **64**(12): p. 5211-8.

25.   Moore, T.A., et al., *Divergent role of gamma interferon in a murine model of pulmonary versus systemic Klebsiella pneumoniae infection.* Infect Immun, 2002. **70**(11): p. 6310-8.

26.   Zeng, X., et al., *Interferon-inducible protein 10, but not monokine induced by gamma interferon, promotes protective type 1 immunity in murine Klebsiella pneumoniae pneumonia.* Infect Immun, 2005. **73**(12): p. 8226-36.

27.   Ye, P., et al., *Requirement of interleukin 17 receptor signaling for lung CXC chemokine and granulocyte colony-stimulating factor expression, neutrophil recruitment, and host defense.* J Exp Med, 2001. **194**(4): p. 519-27.

28.   Greenberger, M.J., et al., *Neutralization of IL-10 increases survival in a murine model of Klebsiella pneumonia.* J Immunol, 1995. **155**(2): p. 722-9.

29.   Strieter, R.M., J.A. Belperio, and M.P. Keane, *Host innate defenses in the lung: the role of cytokines.* Curr Opin Infect Dis, 2003. **16**(3): p. 193-8.

30.   Podschun, R. and U. Ullmann, *Klebsiella spp. as nosocomial pathogens: epidemiology, taxonomy, typing methods, and pathogenicity factors.* Clin Microbiol Rev, 1998. **11**(4): p. 589-603.

31.   Ofek, I., et al., *Genetic exchange of determinants for capsular polysaccharide biosynthesis between Klebsiella pneumoniae strains expressing serotypes K2 and K21a.* Infect Immun, 1993. **61**(10): p. 4208-16.

32.   Struve, C. and K.A. Krogfelt, *Role of capsule in Klebsiella pneumoniae virulence: lack of correlation between in vitro and in vivo studies.* FEMS Microbiol Lett, 2003. **218**(1): p. 149-54.

33.   Yeh, K.M., et al., *Serotype K1 Capsule, Rather than magA Per Se, Is Really the Virulence Factor in Klebsiella pneumoniae Strains That Cause Primary Pyogenic Liver Abscess.* J Infect Dis, 2006. **194**(3): p. 403-4.

34.   Yoshida, K., et al., *Role of bacterial capsule in local and systemic inflammatory responses of mice during pulmonary infection with Klebsiella pneumoniae.* J Med Microbiol, 2000. **49**(11): p. 1003-10.

35.   Cortes, G., et al., *Molecular analysis of the contribution of the capsular polysaccharide and the lipopolysaccharide O side chain to the virulence of Klebsiella pneumoniae in a murine model of pneumonia.* Infect Immun, 2002. **70**(5): p. 2583-90.

36.   Izquierdo, L., et al., *The Klebsiella pneumoniae wabG gene: role in biosynthesis of the core lipopolysaccharide and virulence.* J Bacteriol, 2003. **185**(24): p. 7213-21.

37.   Lai, Y.C., H.L. Peng, and H.Y. Chang, *RmpA2, an activator of capsule biosynthesis in Klebsiella pneumoniae CG43, regulates K2 cps gene expression at the transcriptional level.* J Bacteriol, 2003. **185**(3): p. 788-800.

38.   Podschun, R., *Phenotypic properties of Klebsiella pneumoniae and K. oxytoca isolated from different sources.* Zentralbl Hyg Umweltmed, 1990. **189**(6): p. 527-35.

39.   Podschun, R., et al., *Serotypes, hemagglutinins, siderophore synthesis, and serum resistance of Klebsiella isolates causing human urinary tract infections.* J Infect Dis, 1993. **168**(6): p. 1415-21.

40.   Mizuta, K., et al., *Virulence for mice of Klebsiella strains belonging to the O1 group: relationship to their capsular (K) types.* Infect Immun, 1983. **40**(1): p. 56-61.

41.   Podschun, R., et al., *Incidence of Klebsiella species in surface waters and their expression of virulence factors.* Appl Environ Microbiol, 2001. **67**(7): p. 3325-7.

42.   Struve, C. and K.A. Krogfelt, *Pathogenic potential of environmental Klebsiella pneumoniae isolates.* Environ Microbiol, 2004. **6**(6): p. 584-90.

43.   Sharon, N., *Bacterial lectins, cell-cell recognition and infectious disease.* FEBS Lett, 1987. **217**(2): p. 145-57.

44.   Yoshida, K., et al., *Protection against pulmonary infection with Klebsiella pneumoniae in mice by interferon-gamma through activation of phagocytic cells and stimulation of production of other cytokines.* J Med Microbiol, 2001. **50**(11): p. 959-64.

45.   Caroff, M., et al., *Structural and functional analyses of bacterial lipopolysaccharides.* Microbes Infect, 2002. **4**(9): p. 915-26.

46.   Shankar-Sinha, S., et al., *The Klebsiella pneumoniae O Antigen Contributes to Bacteremia and Lethality during Murine Pneumonia.* Infect Immun, 2004. **72**(3): p. 1423-1430.

47.   Cortes, G., et al., *Role of lung epithelial cells in defense against Klebsiella pneumoniae pneumonia.* Infect Immun, 2002. **70**(3): p. 1075-80.

48.   De Astorza, B., et al., *C3 Promotes Clearance of Klebsiella pneumoniae by A549 Epithelial Cells.* Infect Immun, 2004. **72**(3): p. 1767-1774.

49. Tomas, J.M., S. Camprubi, and P. Williams, *Surface exposure of the O-antigen in Klebsiella pneumoniae O1:K1 serotype strains.* Microb Pathog, 1988. **5**(2): p. 141-7.

50. Alberti, S., et al., *Analysis of complement C3 deposition and degradation on Klebsiella pneumoniae.* Infect Immun, 1996. **64**(11): p. 4726-32.

51. Maayan, M.C., et al., *Population shift in mannose-specific fimbriated phase of Klebsiella pneumoniae during experimental urinary tract infection in mice.* Infect Immun, 1985. **49**(3): p. 785-9.

52. Allen, B.L., G.F. Gerlach, and S. Clegg, *Nucleotide sequence and functions of mrk determinants necessary for expression of type 3 fimbriae in Klebsiella pneumoniae.* J Bacteriol, 1991. **173**(2): p. 916-20.

53. Miles, A.A. and P.L. Khimji, *Enterobacterial chelators of iron: their occurrence, detection, and relation to pathogenicity.* J Med Microbiol, 1975. **8**(4): p. 477-90.

54. Nassif, X. and P.J. Sansonetti, *Correlation of the virulence of Klebsiella pneumoniae K1 and K2 with the presence of a plasmid encoding aerobactin.* Infect Immun, 1986. **54**(3): p. 603-8.

55. Lawlor, M.S., C. O'Connor, and V.L. Miller, *Yersiniabactin is a virulence factor for Klebsiella pneumoniae during pulmonary infection.* Infect Immun, 2007. **75**(3): p. 1463-72.

56. Jeannin, P., et al., *Outer membrane protein A (OmpA): a new pathogen-associated molecular pattern that interacts with antigen presenting cells-impact on vaccine strategies.* Vaccine, 2002. **20**(Suppl 4): p. A23-7.

57.   Pichavant, M., et al., *Outer membrane protein A from Klebsiella pneumoniae activates bronchial epithelial cells: implication in neutrophil recruitment.* J Immunol, 2003. **171**(12): p. 6697-705.

58.   Lawlor, M.S., et al., *Identification of Klebsiella pneumoniae virulence determinants using an intranasal infection model.* Mol Microbiol, 2005. **58**(4): p. 1054-73.

59.   Maroncle, N., et al., *Identification of Klebsiella pneumoniae genes involved in intestinal colonization and adhesion using signature-tagged mutagenesis.* Infect Immun, 2002. **70**(8): p. 4729-34.

60.   Struve, C., C. Forestier, and K.A. Krogfelt, *Application of a novel multi-screening signature-tagged mutagenesis assay for identification of Klebsiella pneumoniae genes essential in colonization and infection.* Microbiology, 2003. **149**(Pt 1): p. 167-76.

61.   Lai, Y.C., H.L. Peng, and H.Y. Chang, *Identification of genes induced in vivo during Klebsiella pneumoniae CG43 infection.* Infect Immun, 2001. **69**(11): p. 7140-5.

62.   Lai, Y.C., et al., *Identification of genes present specifically in a virulent strain of Klebsiella pneumoniae.* Infect Immun, 2000. **68**(12): p. 7149-51.

63.   Lau, H.Y., S. Clegg, and T.A. Moore, *Identification of Klebsiella pneumoniae genes uniquely expressed in a strain virulent using a murine model of bacterial pneumonia.* Microb Pathog, 2007.

64. Duncan, D.W. and W.E. Razzell, *Klebsiella biotypes among coliforms isolated from forest environments and farm produce.* Appl Microbiol, 1972. **24**(6): p. 933-8.

65. Filali, B.K., et al., *Waste water bacterial isolates resistant to heavy metals and antibiotics.* Curr Microbiol, 2000. **41**(3): p. 151-6.

66. Knittel, M.D., *Occurrence of Klebisiella pneumoniae in surface waters.* Appl Microbiol, 1975. **29**(5): p. 595-7.

67. Niemi, M., M. Sibakov, and S. Niemela, *Antibiotic resistance among different species of fecal coliforms isolated from water samples.* Appl Environ Microbiol, 1983. **45**(1): p. 79-83.

68. Cangemi de Gutierrez, R., et al., *Microbial flora variations in the respiratory tract of mice.* Mem Inst Oswaldo Cruz, 1999. **94**(5): p. 701-7.

69. Drasar, B., Barrow, PS, Editors, *Intestinal Microbiology*, ed. B.S. Drasar. 1985, England: Van Nostrand Reinhold (UK) Co. Ltd.

70. Kasman, L.M., *Barriers to coliphage infection of commensal intestinal flora of laboratory mice.* Virol J, 2005. **2**: p. 34.

71. Niemela, S.I., et al., *Microbial incidence in upper respiratory tracts of workers in the paper industry.* Appl Environ Microbiol, 1985. **50**(1): p. 163-8.

72. Ostfeld, E., et al., *Bacterial colonization of the nose and external ear canal in newborn infants.* Isr J Med Sci, 1983. **19**(12): p. 1046-9.

73. Selden, R., et al., *Nosocomial klebsiella infections: intestinal colonization as a reservoir.* Ann Intern Med, 1971. **74**(5): p. 657-64.

74.   Bonten, M.J., et al., *The stomach is not a source for colonization of the upper respiratory tract and pneumonia in ICU patients.* Chest, 1994. **105**(3): p. 878-84.

75.   Hentges, D.J., *The anaerobic microflora of the human body.* Clin Infect Dis, 1993. **16 Suppl 4**: p. S175-80.

76.   Savage, D.C., *Mucosal Microbiota*. Third ed. Mucosal Immunology, ed. M.E.L. Jiri Mesecky, Jerry R McGhee, John Bienenstock, Lloyd Mayer, Warren Strober. 2005, Amsterdam: Elsevier Academic Press.

77.   Tannock, G.W., *Normal Microflora: An Introduction to Microbes Inhabiting the Human Body*. 1995, London: Chapman and Hall. 1-115.

78.   Tlaskalova-Hogenova, H., et al., *Commensal bacteria (normal microflora), mucosal immunity and chronic inflammatory and autoimmune diseases.* Immunol Lett, 2004. **93**(2-3): p. 97-108.

79.   Freter, R., et al., *Mechanisms that control bacterial populations in continuous-flow culture models of mouse large intestinal flora.* Infect Immun, 1983. **39**(2): p. 676-85.

80.   Filius, P.M., et al., *Colonization and resistance dynamics of gram-negative bacteria in patients during and after hospitalization.* Antimicrob Agents Chemother, 2005. **49**(7): p. 2879-86.

81.   Davis, T.J. and J.M. Matsen, *Prevalence and characteristics of Klebsiella species: relation to association with a hospital environment.* J Infect Dis, 1974. **130**(4): p. 402-405.

82.   Cooke, E.M., et al., *Further studies on the sources of Klebsiella aerogenes in hospital patients.* J Hyg (Lond), 1979. **83**(3): p. 391-5.

83. Pollack, M., et al., *Factors influencing colonisation and antibiotic-resistance patterns of gram-negative bacteria in hospital patients.* Lancet, 1972. **2**(7779): p. 668-71.

84. Rose, H.D. and J. Schreier, *The effect of hospitalization and antibiotic therapy on the gram-negative fecal flora.* Am J Med Sci, 1968. **255**: p. 228-36.

85. Toivanen, P., *Normal intestinal microbiota in the aetiopathogenesis of rheumatoid arthritis.* Ann Rheum Dis, 2003. **62**(9): p. 807-11.

86. Bartlett, J.G., *Narrative review: the new epidemic of Clostridium difficile-associated enteric disease.* Ann Intern Med, 2006. **145**(10): p. 758-64.

87. Kalliomaki, M. and E. Isolauri, *Role of intestinal flora in the development of allergy.* Curr Opin Allergy Clin Immunol, 2003. **3**(1): p. 15-20.

88. Noverr, M.C. and G.B. Huffnagle, *The 'microflora hypothesis' of allergic diseases.* Clin Exp Allergy, 2005. **35**(12): p. 1511-20.

89. Fuller, R., *Probiotics in man and animals.* J Appl Bacteriol, 1989. **66**(5): p. 365-78.

90. Gagnon, M., et al., *Effect of Bifidobacterium thermacidophilum probiotic feeding on enterohemorrhagic Escherichia coli O157:H7 infection in BALB/c mice.* Int J Food Microbiol, 2006. **111**(1): p. 26-33.

91. Kabir, A.M., et al., *Prevention of Helicobacter pylori infection by lactobacilli in a gnotobiotic murine model.* Gut, 1997. **41**(1): p. 49-55.

92. Martins, F.S., et al., *Screening of yeasts as probiotic based on capacities to colonize the gastrointestinal tract and to protect against enteropathogen challenge in mice.* J Gen Appl Microbiol, 2005. **51**(2): p. 83-92.

93. Ohkawara, S., et al., *Effect of oral administration of Butyrivibrio fibrisolvens MDT-1 on experimental enterocolitis in mice.* Clin Vaccine Immunol, 2006. **13**(11): p. 1231-6.

94. Rani, B. and N. Khetarpaul, *Probiotic fermented food mixtures: possible applications in clinical anti-diarrhoea usage.* Nutr Health, 1998. **12**(2): p. 97-105.

95. Van Amersfoort, E.S., T.J. Van Berkel, and J. Kuiper, *Receptors, mediators, and mechanisms involved in bacterial sepsis and septic shock.* Clin Microbiol Rev, 2003. **16**(3): p. 379-414.

96. Dziarski, R., *Recognition of bacterial peptidoglycan by the innate immune system.* Cell Mol Life Sci, 2003. **60**(9): p. 1793-804.

97. Wagner, H., *Toll meets bacterial CpG-DNA.* Immunity, 2001. **14**(5): p. 499-502.

98. Pollard, M. and N. Sharon, *Responses of the Peyer's Patches in Germ-Free Mice to Antigenic Stimulation.* Infect Immun, 1970. **2**(1): p. 96-100.

99. Shroff, K.E. and J.J. Cebra, *Development of mucosal humoral immune responses in germ-free (GF) mice.* Adv Exp Med Biol, 1995. **371A**: p. 441-6.

100. Umesaki, Y., et al., *Expansion of alpha beta T-cell receptor-bearing intestinal intraepithelial lymphocytes after microbial colonization in germ-free mice and its independence from thymus.* Immunology, 1993. **79**(1): p. 32-7.

101. Apter, F.M., et al., *Analysis of the roles of antilipopolysaccharide and anti-cholera toxin immunoglobulin A (IgA) antibodies in protection against Vibrio cholerae and cholera toxin by use of monoclonal IgA antibodies in vivo.* Infect Immun, 1993. **61**(12): p. 5279-85.

102.   Michetti, P., et al., *Monoclonal secretory immunoglobulin A protects mice against oral challenge with the invasive pathogen Salmonella typhimurium.* Infect Immun, 1992. **60**(5): p. 1786-92.

103.   van der Waaij, L.A., et al., *Direct flow cytometry of anaerobic bacteria in human feces.* Cytometry, 1994. **16**(3): p. 270-9.

104.   Falk, P.G., et al., *Creating and maintaining the gastrointestinal ecosystem: what we know and need to know from gnotobiology.* Microbiol Mol Biol Rev, 1998. **62**(4): p. 1157-70.

105.   Gustafsson, B.E., *The physiological importance of the colonic microflora.* Scand J Gastroenterol Suppl, 1982. **77**: p. 117-31.

106.   Dubos, R., et al., *Indigenous, Normal, and Autochthonous Flora of the Gastrointestinal Tract.* J Exp Med, 1965. **122**: p. 67-76.

107.   Schaedler, R.W., R. Dubs, and R. Costello, *Association of Germfree Mice with Bacteria Isolated from Normal Mice.* J Exp Med, 1965. **122**: p. 77-82.

108.   Schaedler, R.W., R. Dubs, and R. Costello, *The Development of the Bacterial Flora in the Gastrointestinal Tract of Mice.* J Exp Med, 1965. **122**: p. 59-66.

109.   Dewhirst, F.E., et al., *Phylogeny of the defined murine microbiota: altered Schaedler flora.* Appl Environ Microbiol, 1999. **65**(8): p. 3287-92.

110.   Jergens, A.E., et al., *Induction of differential immune reactivity to members of the flora of gnotobiotic mice following colonization with Helicobacter bilis or Brachyspira hyodysenteriae.* Microbes Infect, 2006. **8**(6): p. 1602-10.

Chapter II

Materials and Methods

Animals

C57BL/6J wild-type and $RAG1^{-/-}$ mice were purchased from The Jackson Laboratory and housed in specific pathogen-free conditions within the animal care facility at the University of Michigan until the day of sacrifice.

Germfree (GF) Swiss Webster mice were maintained in flexible plastic isolators in the Germfree Mouse Resource Laboratory in the Life Science Institute at the University of Michigan. GF Swiss Webster mice were co-housed with Defined Flora CB17 mice acquired from Taconic in order to develop an altered Schaedler Flora (ASF) gut microbiota. Mice were then transferred to SPF conditions until the day of sacrifice.

All experimental animal procedures were approved by the University Committee on Use and Care of Animals at the University of Michigan.

Techniques used for Murine Inoculation

Mice were anesthetized with ketamine and xylazine. For intratracheal inoculation, the trachea was exposed, and 30μl inoculum was administered via a sterile 26 gauge needle. For intranasal inoculation, mice were given a 5μL bolus of *K. pneumoniae* in each nostril followed by a 10μL flush with sterile saline in each nostril.

For intraperitoneal inoculation, a 200μL inoculum was administered via a 27 gauge needle into the peritoneum of mice. Mice were inoculated with the bacteria by oral administration with a 24-gauge feeding needle attached to a 1mL syringe. The syringe containing the bacterial suspension was mounted onto a Stepper repetitive pipette (Tridak, Brookfield, Conn.) to deliver an equal amount of suspension to each mouse. An aliquot of the inoculated bacterial suspension was serially diluted onto appropriate agar plates to determine actual dose of inoculated bacteria.

An aliquot of the inoculated *K. pneumoniae* suspension was serially diluted onto blood agar plates to determine actual dose of inoculated bacteria.

Bacterial Strains and Plasmids

Strains used in this study are listed in Table II.1. *K. pneumoniae* strain 43816 is a clinical isolate with an O1:K2 serotype (ATCC, Rockville, MD). Strain IA565 is a clinical isolate from the University of Iowa Hospitals and Clinics with a K15 serotype (K-typing performed at the Unit of Gastrointestinal Infections, Statens Serum Institut, Denmark) [1]. These strains were grown in tryptic soy broth (Difco, Detroit, MI) overnight at 37˚C. *K. pneumoniae* IA565 and its streptomycin resistant derived strain, IA565S were grown in luria broth (LB) and LB supplemented with 50μg/mL of streptomycin (Teknova, Hollister, CA) overnight at 37˚C, respectively. The plasmid, pAM401 containing a chloramphenicol resistant gene, was transformed into *K. pneumoniae* IA565 and named IA565pAM401. This strain was grown in LB containing 50μg/mL of chloramphenicol (Teknova, Hollister, CA) overnight at 37ºC. *Citrobacter rodentium* (ATCC 51459, Rockville, MD was grown in LB overnight at 37ºC. Bacterial

concentration was determined by measuring the amount of absorbance at 600 nm and compared to a predetermined standard curve. Bacteria were then diluted to the desired concentration for inoculation into mice in saline.

Plasmids used in this study are listed in Table II.2.

Lipopolysaccharide Quantification Assay

For quantification of LPS on the surface of *K. pneumoniae*, the Pyrochrome® Chromogenic Test Kit (Cape Cod, Inc, Mass.) was used and manufacturer's protocols were followed. *Limulus* amebocyte lysate (LAL) is an aqueous extract of blood cells (amebocytes) from the horseshoe crab, *Limulus polyphemus*. LAL reacts with bacterial endotoxin or lipopolysaccharide, which is a membrane component of gram negative bacteria. In the presence of LPS, factors in LAL are activated in a proteolytic cascade that results in the cleavage of a colorless artificial peptide substrate present in Pyrochrome LAL. Cleavage of this substrate liberates p-nitroaniline, which is yellow and absorbs at 405nm.

Briefly, overnight cultures of strain IA565 and 43816 grown in TSB at 37ºC were centrifuged at 5000 g for 10 minutes. 2mLs of supernatant was pulled off and set aside for the assay. The control standard endotoxin (CSE) provided in the kit was diluted to make standards at 8, 16, 25, 50, 100, 200, and 400 endotoxin units (EU)/mL. 25μL of each standard was plated in duplicate as well as IA565 and 43816 supernatants. 25μL of LPS-free reagent water (LRW) and TSB were added in only one well each. 25μL of hydrochloric acid was added to the wells and 100mL of Pyrochrome LAL. The plate was

incubated at 37ºC shaking at 125rpm for 12 minutes. 31.25µL of 50% acetic acid was added to stop the reaction and the plate was read at 405nm.

Bronchoalveolar lavage

Bronchoalveolar lavage (BAL) was performed to obtain BAL cells and fluid. The trachea was exposed and intubated using a 1.27mm OD polyethylene catheter. BAL was performed by instilling 1.6ml PBS/ 5mM EDTA. Approximately 1.5ml of lavage fluid was retrieved per mouse and cytospins were prepared from BAL cells.

Growth Curve Analysis

For *K. pneumoniae* growth in whole blood, mice were euthanized and heparinized blood was collected via cardiac puncture. In a 1mL volume of blood, approximately 5 x 10^4 CFU of *K. pneumoniae* was added. For growth in TSB, PBS and BAL fluid, approximately 10^3 CFU of *K. pneumoniae* was added in a 1mL volume. Growth via CFU analysis was performed by taking aliquots of the culture at designated time points.

For *K. pneumoniae* IA565 and IA565S growth in LB with and without streptomycin, approximately 10^8 CFU of *K. pneumoniae* was added in 50mLs of broth. Growth via CFU analysis was performed by taking aliquots of the cultures at designated time points.

Whole Lung Homogenization for CFU, Myeloperoxidase, and Cytokine Analysis

At designated time points, the mice were euthanized by inhalation of CO_2. Before lung removal, the pulmonary vasculature was perfused with 2 to 3 ml PBS/5 mM EDTA

and removed for analyses. After removal, whole lungs were homogenized using a tissue homogenizer (Biospec Products, Bartlesville, OK) in 1 ml PBS/Complete protease inhibitor cocktail (Boehringer Mannheim Biochemical, Chicago, IL). For lung CFU determination, a small aliquot of lung homogenate was serially diluted and plated on blood agar plates, incubated at 37°C and colonies counted.

Lung myeloperoxidase, MPO activity, as an indirect measurement of total neutrophil numbers, was quantified by a method as described previously [2]. Briefly, 100μL lung homogenate was mixed with 100μL MPO homogenization buffer (0.5 % hexadecyltrimethylammonium bromide and 5 mM EDTA) and vortexed. The mixture was sonicated and centrifuged at 12,000 g for 15 minutes. The supernatant was then mixed 1:15 with assay buffer and read at 490 nm. MPO units were calculated as the change in absorbance over time.

For total lung cytokine ELISA analyses, lung homogenates were sonicated briefly to ensure complete cellular disruption, then centrifuged at 1,500 g for 10 minutes. The supernatants were collected and assessed for cytokine levels by ELISA. Murine cytokines were quantified using a modification of a sandwich ELISA method [3]. This methodology allows detection of these cytokines at concentrations of 20 pg/ml and higher. Additionally, assays have been shown to be specific for the indicated murine chemokine and show no cross-reactivity with any other murine cytokines tested.

Peripheral blood CFU

For determination of peripheral blood bacterial numbers, mice were euthanized and heparinized blood was collected by cardiac puncture at the indicated time points.

Serial dilutions were plated onto blood agar plates, incubated at 37˚C and colonies counted.

Nasal Cavity and Tracheal CFU Analysis

At designated time points, mice were sacrificed by CO_2 asphyxiation and were dissected aseptically. The trachea and nasal cavity was removed and homogenized using a tissue homogenizer (Biospec Products, Bartlesville, OK) in 1 ml 1x PBS. For CFU determination, a small aliquot of the homogenates was serially diluted and plated on blood agar plates, incubated at 37˚C and colonies counted.

Gastrointestinal Tract and Fecal CFU Analysis

At designated time points, mice were euthanized by inhalation of CO_2. Excised whole organs were homogenized using a tissue homogenizer (Biospec Products, Bartlesville, OK) in 1mL 1x PBS for feces and 1mL distilled water for small and large intestine and cecum. For CFU determination, a sample of the homogenate (100μL) was serially diluted and plated on blood agar plates for IA565 CFU assessment, LB-Streptomycin agar for IA565S CFU assessment, and MacConkey agar for *Citrobacter rodentium* assessment. Plates were incubated at 37ºC and colonies counted.

***In vitro* Peritoneal Macrophage Phagocytosis Assays**

This protocol, previously described elsewhere [4, 5] was used and modified. Non-elicited peritoneal macrophages from C57BL/6J mice was isolated and plated into half-sized 96-well plates. FITC-labeled *K. pneumoniae* was opsonized by incubation in

5% mouse serum for 15-30 minutes. These bacteria were then added to the macrophage

cells in quadruplicate at a bacterium to macrophage ratio of 100:1. After incubation,

unbound bacteria were washed off and extracellular fluorescence was quenched with

trypan blue. Internalized FITC signal was then analyzed with a fluorometer (Tecan

SPECTRAFluorPlus).

To access phagocytosis via another method, non-elicited peritoneal macrophages

from C57BL/6J mice was isolated and suspended in 1mL RPMI 1640 (Invitrogen) culture

medium at a concentration of 10^6 cells/mL. *K. pneumoniae* was then added to the

macrophage cells at a bacterium to macrophage ratio of 100:1. At designated time points,

an aliquot of the suspension were spun down onto a glass slide, which was air dried,

stained with Diff-Quick, and examined under oil immersion. The initial 200 peritoneal

cells were counted to determine the number of whole intracellular bacteria in each cell.

The phagocytic index (PI) was calculated as: PI = (percent of macrophages containing at

least one bacterium) x (mean number of bacteria per positive cell).

In vivo Alveolar Macrophage Phagocytosis Assay

The protocol for alveolar macrophage *in vivo* phagocytosis has been previously

described [6]. Briefly, mice were intratracheally injected with approximately 1 x 10^6

CFU of *K. pneumoniae* at time zero. At 2 h post infection, BAL was performed to obtain

alveolar leukocytes. The lavage fluid was centrifuged at 500 *g* for 5 min and the pellet

resuspended in PBS containing 2% serum. Thirty thousand cells were then spun down

onto a glass slide, which was air dried, stained with Diff-Quick, and examined under oil

immersion. The initial 200 alveolar macrophages or polymorphonuclear cells were

counted to determine the number of whole intracellular bacteria in each cell. The

phagocytic index (PI) was calculated as described above.

In vitro Peritoneal Macrophage Killing Assays

Approximately 10^6 non-elicited, freshly isolated peritoneal macrophage cells from

C57BL/6J mice in a 1mL volume were incubated with 10^6 CFU of strain 43816 and

IA565 with and without prior incubation with 5% normal mouse serum. At 30 and 90

minutes, an aliquot of the mixture was plated for CFU.

Enzyme-Linked ImmunoSorbent Assay (ELISA)

Murine cytokines were quantified using a modification of a sandwich ELISA

method [3]. This methodology allows detection of these cytokines at concentrations of

20 pg/ml and higher. Additionally, assays have been shown to be specific for the

indicated murine chemokine and show no cross-reactivity with any other murine

cytokines tested. Human cytokines were quantified as previously described [7].

In Vivo Antibody Administration

Neutrophils were depleted *in vivo* utilizing the pan-granulocytic antibody RB6-

8C5 [8], directed against Ly-6G. Anti-Ly-6G was produced as an ascites in SCID mice

by TSD BioServices (Germantown, NY) and used at a dilution determined to deplete

both peripheral blood and resident lung neutrophils. The antibody was injected in a 0.5

ml volume intraperitoneally 18 hours prior to infection and again one day post infection.

This treatment scheme has been used to deplete neutrophils in vivo in a variety of

bacterial and fungal models. Reagent control animals for anti-Ly-6G received normal mouse serum at the same dilution used for anti-Ly-6G treatment. For survival studies, mice received injections of antibody every 48 hours post initial injection.

Mice were injected intraperitoneally either with 500µg of anti-TNFα neutralizing monoclonal antibody (clone MP6-XT3) or anti-IFNγ neutralizing monoclonal antibody (clone XmG1.2) 2 hours before infection with *K. pneumoniae*. For survival studies, mice received a second injection of antibody on day 2 post-infection.

A549 Cell Adhesion and Invasion Assays and Supernatant ELISAs

A549 cells were generously provided by Dr. Douglas A. Arenberg (University of Michigan) and were grown in RPMI 1640, with 25mM HEPES and L-glutamine (Invitrogen) supplemented with 10% fetal bovine serum, 1x penicillin, streptomycin and L-glutamine, 1x sodium pyruvate, 1x non-essential amino acids and 0.1% 2-mercaptoethanol. Cells were grown as monolayers in 100% humidity and 5% CO_2 at 37ºC. For bacterial assays, cell culture medium without penicillin/streptomycin was used. A549 cells were seeded into 24-well plates at a density of 10^5/well in a 2mL volume and incubated for 24 hours. Cells were washed 3 times with 1x phosphate buffered saline. Then 1mL of antibiotic free culture medium was added in addition to *K. pneumoniae* at a bacterium to cell ratio of 100:1. Plates were centrifuged at 1000 x g for 5 minutes.

For the adhesion assay, plates were incubated for 30-90 minutes. At each 30 minute interval, cells were washed 10X with 1x PBS. 1mL 1x trypsin and 1µL TritonX-100 was added to the wells, incubated at 37ºC for 10 minutes, and then plated for

bacterial CFU. For the invasion assay, plates were incubated after centrifugation for 60-120 minutes. At each 30 minute interval, cells were washed 3 times with 1x PBS. 1mL of 100ng/mL gentamycin containing culture medium was added to wells and incubated for 20 minutes. Cells were then washed 3 times with 1x PBS, 1mL 1x trypsin and 1μL TritonX-100 was added to the wells, incubated at 37ºC for 10 minutes, and then plated for bacterial CFU.

Supernatants of A549 cells pulsed with *K. pneumoniae* bacteria were harvested and accessed for A549 cytokine production.

MLE-12 cell Adhesion Assay and Supernatant ELISAs

MLE-12 cells were generously provided by Dr. Paul Christensen (University of Michigan) and were grown in HITES medium [RPMI 1640, with 25mM HEPES and L-glutamine (Invitrogen) supplemented with 1X insulin, transferrin, and sodium selenite solution, 50μg/mL human apo-transferrin, 0.01μM hydrocortisone, 0.01μM B-estradiol, 1X penicillin/streptomycin/L-glutamine solution, and 2% fetal calf serum]. Cells were grown as monolayers in 100% humidity and 5% CO_2 at 37ºC. For bacterial assays, HITES medium without penicillin/streptomycin was used.

MLE-12 cells were seeded into 24-well plates at a density of 10^5/well in a 2mL volume and incubated for 24 hours. Cells were washed 1 time with 1x phosphate buffered saline. Then 1mL of antibiotic free HITES medium with or without 50mg/mL of D-mannose (Sigma) was added in addition to *K. pneumoniae* at a bacterium to cell ratio of 100:1. Plates were centrifuged at 1000 x g for 5 minutes and then incubated for 2 hours. At each 15 minute interval, cells were washed 10 times with 1mL of 1x PBS,

scraped off the bottom of the well in the presence of 1mL 1x PBS and placed in a tube with 1μL TritonX-100. This solution was then plated for bacterial CFU to assess for numbers of bacteria that adhered to cells.

Supernatants of MLE-12 cells pulsed with *K. pneumoniae* bacteria for 24 hours were harvested and accessed for MLE-12 cytokine production.

Alveolar Macrophage depletion

Clodronate liposomes were obtained from Dr. Nico van Rooijen (Vrije Universiteit, The Netherlands) and have been previously described [9]. Mice were anesthetized with ketamine and xylazine and 60μL of clodronate liposomes were administered intranasally for 2 consecutive days for a total of 720ng of clodronate liposomes /mouse. Mice were allowed to rest for 1 day before bacterial infection for a total of 720ng of clodronate liposomes /mouse

Serum administration

Whole mouse blood was collected and pooled from several mice. Serum was collected and 1mL was intraperitoneally injected into *RAG1*$^{-/-}$ mice, 500μL 24 hours before bacterial challenge and 500μL 24 hours after challenge.

Administration of Dextran Sodium Sulfate (DSS)

Mice received 3% weight/volume DSS molecular weight 36,000-50,000 (ICN Biomedicals, Inc., Irvine, CA) in their drinking water *ad libitum* for 7 days.

Histology

The colon was removed, cut longitudinally and washed in 1x PBS and embedded in paraffin sections in a Swiss roll fashion. Sections were cut, mounted onto slides and stained with hematoxyline and eosine.

Nucleic Acid Isolation

Total RNA and genomic DNA was isolated from *K. pneumoniae* strain 43816 and IA565 using the Qiagen RNeasy® Mini Kit and Qiagen Genomic DNA Buffet Set and Genomic Tips (Valencia, CA). Total RNA was converted into total cDNA using Clontech's SMART™ PCR cDNA Synthesis Kit (La Jolla, CA).

Subtractive Hybridization (SH)

Clontech's PCR-Select™ Bacterial Genomic Subtraction and PCR-Select™ cDNA Subtraction Kit protocols were performed on both genomic DNA and total cDNA from strain IA565 and 43816 according to manufacturer's protocols. To further enrich for uniquely expressed sequences, PCR-Select™ Differential Screening Kit (Clontech) was carried out on end products obtained from the subtraction kits.

Cloning of Subtractive Hybridization Products

Blunt ended cloning of SH products were performed using Stratagene's PCR-Script™ Amp Electroporation-Competent Cell Cloning Kit (La Jolla, CA) as per manufacturer's protocols.

Restriction Enzyme Digests

Enzymes used in this study were purchased from New England BioLabs (Ipswich, MA) and are listed in Table II.3.

Polymerase Chain Reaction (PCR)

PCR primers used in this study are listed in Table II.4 as well as the details of PCR conditions for each. Primers were ordered from Sigma-Genosys (St. Louis, MO). PCR reactions were carried out using the GeneAmp 9700 PCR Thermal Cycler (Applied Biosystems, Foster City, CA) and the Platinum® Taq DNA Polymerase PCR Kit from Invitrogen (Carlsbad, CA). Platinum® Taq DNA Polymerase High Fidelity is an enzyme mixtures composed of recombinate Taq DNA polymerase, *Pyrococcus species* GB0D polymerase, and Platinum® Taq antibody. *Pyrococcus species* GB-D polymerase possesses proofreading ability via its 3' to 5' exonuclease activity. The antibody inhibits polymerase activity until incubation at 94ºC. After amplification, the PCR products were separated on, depending on size, a 0.3 to 2% agarose gel containing ethidium bromide (0.3mg/mL [0.003%]). Bands were visualized via UV transillumination and photographed using the Gel Logic 100 Image Analysis System (Kodak, New Haven, CT).

Allelic Exchange Technique using pLD55

A similar method used in this study has been described elsewhere [10]. A 907bp fragment of the UreF gene and a 927bp fragment of the FimC gene in *K. pneumoniae* 43816 were cloned via PCR using gene specific primers. The resulting fragments were cloned using Stratagene's PCR-Script™ Amp Electroporation-Competent Cell Cloning

Kit (La Jolla, CA) [cloned products are denoted, pFimC and pUreF). An internal

fragment was removed from each cloned gene: pFimC, digested with BlpI and BseRI,

removed a 155bp internal fragment, and pUreF, digested with Bpu10I and BlpI, removed

a 117bp internal fragment. These products are denoted as pFimCΔ and pUreFΔ. The

internal fragments were replaced with a kanamycin resistant cassette resulting in the

products pFimCΔK and pUreFΔK. The fragments containing the insertionally

inactivated genes, FimCΔK and UreFΔK into the *pir*-dependent vector pLD55 [11].

Lambda Red Recombinase Technique

        This method has been described elsewhere [12]. Briefly, a pair of primers

containing 40 nucleotides of the 3' and 5' ends of the FimC gene were generated, P1 H1-

FimC and P2 H2-FimC. The primers contain the P1 and P2 sites flanking a kanamycin

resistant cassette so PCR amplification of the kanamycin resistance gene on the plasmid,

pKD4 can be performed. This PCR product was named fimCΔKan^R. pKD78, a

temperature sensitive plasmid containing the lambda red genes under an arabinose

inducible promoter and a chloramphenicol resistance gene, was transformed into *K.*

pneumoniae 43816, denoted HL078. HL078 was grown in the presence of arabinose and

harvested for use for electroporation. The linear PCR product fimCΔKan^R was

electroporated into HL078 cells and grown at the non-permissive temperature, 37ºC.

Transformants containing the chromosomally integrated fimCΔKan^R fragment were

analyzed for successful recombination.

Construction of a Long Linear UreF Gene Fragment Disrupted with the Kanamycin Resistant Cassette

Primers V and VII-P1 contains 383bp of the 5' end of the UreF gene in *K. pneumoniae* 43816 and 20 nucleotides of the P1 site upstream of the kanamycin resistant cassette on the pKD4 plasmid. Primers VI and VIII-P2 contains 651bp of the 3' end of the UreF gene in *K. pneumoniae* 43816 and 20 nucleotides of the P2 site downstream of the kanamycin resistant cassette on the pKD4 plasmid. A diagram of the desired product is depicted in Figure IV.23. The 403bp product and 671bp product was generated via PCR of strain 43816 genomic DNA. These products were then used as PCR primers to attempt to amplify the kanamycin cassette on the pKD4 plasmid via the P1 and P2 ends of those fragments.

Temperature Sensitive Plasmid Mutagenesis Technique

A pair of primers, with Acc65I restriction sites, containing 40 nucleotides of the 3' and 5' ends of the FimC gene were generated, P1 H1-FimC and P2 H2-FimC. The primers contain the P1 and P2 sites flanking a kanamycin resistant cassette so PCR amplification of the kanamycin resistance gene on the plasmid, pKD4 can be performed. This fragment, fimCΔKan^R, and the plasmid, pKD78, were digested with Acc65I and then ligated together. The resulting plasmid was then transformed into *K. pneumoniae* 43816. The transformant was grown overnight in LB containing 50μg/mL of chloramphenicol (Teknova) at the permissive temperature of 30ºC. An aliquot of this suspension was then inoculated into LB media (1:100 dilution) and grown at 37ºC for 2 days. A serial dilution of this culture was then plated on LB-chloramphenicol plates.

One robust colony was picked and inoculated into 10mLs of LB media and grown at 30ºC. This solution was back diluted twice daily for 2 days. An aliquot of these cultures was then serially diluted and plated on LB agar. These colonies were then patched onto LB-chloramphenicol plates and accessed for drug-sensitivity. Those that were chloramphenicol sensitive were analyzed for fimCΔKan^R integration via PCR.

Allelic Exchange Technique using pKAS32 and pWM91

Two pairs of primers, with NotI restriction sites, containing 40 nucleotides of the 3' and 5' ends of the FimC and UreF gene were generated, P1 H1-FimC and P2 H2-FimC and P1 H1-UreF and P2 H2-UreF. The primers contain the P1 and P2 sites flanking a kanamycin resistant cassette so PCR amplification of the kanamycin resistance gene on the plasmid, pKD4 can be performed. These NotI digested fragments, FimCΔKan^R and UreFΔKan^R, were cloned into the NotI digested plasmid, pKAS32 [13] forming plasmids 101 and 102. In addition the NotI digested UreFΔKan^R fragment was cloned into the NotI digested plasmid, pWM91 [11] forming plasmid 103. Those plasmids were transformed into the *pir*-dependent *E. coli* strain 47084 forming HL101, HL102 and HL103. Cultures of the recipient *K. pneumoniae* strains 43816 and 43816S and the donor strains HL101, HL102 and HL103 were grown in LB, LB-streptomycin, and LB-kanamycin/ampicillin cultures, respectively. 1.5mL of each culture were spun down at 300g for 5 minutes, resuspended in 1mL of the original medium and placed in a 125mL flask containing 29mL of LB media. The cultures were then shaken at 130rpm for 2 hours and 37ºC. 0.5-5mL culture aliquots of 43816 and HL103, 43816S and HL101, and 43816S and HL102 were mixed and filtered onto a 0.45μm filter disk, named A, B and C,

respectively. Filter disks were placed onto LB agar plates and incubated at 37ºC for 3-16

hours. Disks were then placed in 50mL conical tubes containing 10mL of 1x PBS,

scratched with a glass rod and vigorously vortexed. 100mL from the tube containing

disks A and B were plated onto LB-streptomycin/kanamycin plates. 100mL from tube

containing disk C was plated onto LB-kanamycin/sucrose plates. Transconjugants were

analyzed for incorporation of the FimCΔKan^R and UreFΔKan^R fragments via PCR

analysis.

Statistical analyses

Statistical significance was determined using the unpaired, two-tailed student t

test, ANOVA for multiple group comparisons using the Student-Newman-Keuls post-

test, and Fisher's Exact Test. Calculations were performed using InStat 3 (GraphPad

Software, San Diego, CA). Statistical analyses of survival curves were performed by the

Log Rank Test using the Prism 3 software program (GraphPad Software).

Table II.1 Bacterial Strains Used in this Study

Strain	Description	Source
K. pneumoniae		
43816	Clinical Isolate, O1:K2 serotype	ATCC
43816S	Streptomycin derivative of strain 43816	This study
HL078	43816 containing pKD78	This study
IA565	Clinical Isolate, K15 serotype	Lau et al, 2007
IA565S	Streptomycin derivative of strain IA565	This study
IA565pAM401	Strain IA565 containing the chloramphenicol resistance conferring plasmid, pAM401	This study
Citrobacter rodentium		
51459	Strain used to induced murine colitis	ATCC
E coli		
47084	RP4-2*tet*:Mu-1*kan*::Tn7-integrant uidA(ΔMlu1)::*pir+ recA1* leu-63::IS*10 creC*510 *hsdR17 endA1 zbf-5 thi*	ATCC
BW19335	Strain containing pWM91	*E. coli* Genetic Stock Center, CT
BW21038	Strain containing pLD55	*E. coli* Genetic Stock Center, CT
BW26949	Strain containing pKD78	*E. coli* Genetic Stock Center, CT
VJ737	Strain containing pKAS32	DiRita Lab
HL101	47084 with plasmid 101	This study
HL102	47084 with plasmid 102	This study
HL103	47084 with plasmid 103	This study

52

Table II.2 Plasmids Used in this Study

Plasmid		Description	Source
Plasmids			
	pWM91	*oriR6K$_g$, ori$_{fl(+)}$, lacZa, MCS*(SK), *oriT$_{RP4}$ [sacB]$_{subtilis}$, bla*(ampicillin resistance)	Isolated from BW19335
	pLD55	*oriR6K$_g$, ori$_{fl(+)}$, tetR, MCS*(SK), *oriT$_{RP4}$, tetA, bla-1*(ampicillin resistance)	Isolated from BW21038
	pKD78	*araBp-gam-bet-exo, repA101*(ts), *oriR101, cat* (chloramphenicol resistance gene)	Isolated from BW26949
	pKAS32	*oriR6K, oriT, MCS, rpsL, bla-1*(ampicillin resistance)	Isolated from VJ737
	101	UreFΔKan^R fragment ligated into pKAS32	This study
	102	FimCΔKan^R fragment ligated into pKAS32	This study
	103	UreFΔKan^R fragment ligated into pWM91	This study
	pKD4	*oriR6K$_g$, kan*(kanamycin resistance), *bla*(ampicillin resistance)	Mobley Lab
pPCR-Script Amp SK(+)		*pUC ori, ori$_{fl(+)}$, lacZ, MCS, bla*(ampicillin resistance)	Stratagene
	pFimC	FimC gene fragment ligated into pPCR-Script Amp SK(+)	This study
	pUreF	UreF gene fragment ligated into pPCR-Script Amp SK(+)	This study
	pEntA	EntA gene fragment ligated into pPCR-Script Amp SK(+)	This study

Table II.3 Restriction Enzymes Used in Various Methods

Methods and Restriction Enzymes used in each	DNA digested	Digestion Protocol
Subtractive Hybridization		
RsaI	*K. pneumoniae* genomic DNA; total cDNA	90min, 37°C, 1x RsaI buffer, 10 units for 1μg DNA
Allelic Exchange using pLD55		
BamHI	pKD4	30min, 37°C, 1x BSA, BamHI buffer, 20 units for 1mg DNA
NotI Acc65I	pFimC, pUreF, pEntA, pFimCDK, pUreFDK, pEntADK	1 hour, 37°C, 1x BSA, NEBuffer #3, 10 units for 1.2-4mg DNA
BlpI BseRI	pFimC	1 hour, 37°C, 1x BSA, NEBuffer #2, 10 units for 10mg DNA
Bpu10I BlpI	pUreF	1 hour, 37°C, SEBuffer K, 10 units for 10mg DNA 1 hour, 37°C, NEBuffer #4, 10 units for 10mg DNA
BsbI SphI	pEntA	1 hour, 37°C, 1x BSA, NEBuffer #2, 20 units for 10mg DNA
TS Plasmid Mutagenesis Protocol		
Acc65I	pKD78, fimC::Kan	1.5 hours, 37°C, 1x BSA, NEBuffer #3, 10 units for 5mg DNA
Allelic Exchange using pWM91 and pKAS32		
NotI	pWM91, pKAS32, ureF::Kan, fimC::Kan	1 hour, 37°C, 1x BSA, NEBuffer #3, 10 units for 3mg DNA

Table II.4 Primers Used in this Study

Methods and Primers used in each	Primer Sequence (5' to 3')	PCR Cycling Parameters
Subtractive Hybridization		
Nested Primer 1	TCGAGCGGCCGCCCGGGCAGGT	Clontech Protocol
Nested Primer 2R	AGCGTGGTCGCGGCCGAGGT	Clontech Protocol
23S rRNA Forward	AAATTAGCGGATGACTTGTGGC	Clontech Protocol
23S rRNA Reverse	GACTTTGGGACCTTAGCTGGC	Clontech Protocol
T7	GTAATACGACTCACTATAGGGC	30 cycles: 94°C 1min, 54°C 2min, 72°C 2min
T3	AATTAACCCTCACTAAAGGG	"
PCR Confirmation of Differentially Expressed Sequences		
C142-2.1	TCGGTGGATCAGGTAGTGG	95°C 1min; 30 cycles 94°C 30s, 54.4°C 30s, 72°C 1min; hold at 4°C
C142-2.2	ATGGGGGAAGAGATTGAAAC	"
C160-1.1	CGGCGTCGTGGCGTTTAGCA	95°C 1min; 30 cycles 94°C 30s, 58.6°C 30s, 72°C 1min; hold at 4°C
C160-1.2	TTCGCGGCCAAAATCGGTCAG	"
C163-1.1	AACCCCGCCTCCCTCAGTCG	95°C 1min; 30 cycles 94°C 30s, 61.2°C 30s, 72°C 1min; hold at 4°C
C163-1.2	CGCCACCTCCTCCCAGCAGA	"
C164-2.1	TGGGGCTATAAACAGGGGGATGC	95°C 1min; 30 cycles 94°C 30s, 58.6°C 30s, 72°C 1min; hold at 4°C
C164-2.2	AGCGCCACCGGGGATTTCTA	"
C186-2.1	CACCAGCAGCGGCCAGCAAAAAGTA	95°C 1min; 30 cycles 94°C 30s, 61.2°C 30s, 72°C 1min; hold at 4°C
C186-2.2	GCGATCCGAATGTGGCGAAGAAAT	"
C202-2.1	GCGCGGCACCGAAGGCAATAAT	"
C202-2.2	GCCCGGCGCAGGTACGATAGAAGAT	"

Table II.4 Primers Used in this Study (cont.)

Methods and Primers used in each	Primer Sequence (5' to 3')	PCR Cycling Parameters
C211-1.1	TGCGCAGCCAGGGAAAAGTCTAAC	95°C 1min; 30 cycles 94°C 30s, 58.6°C 30s, 72°C 1min; hold at 4°C
C211-1.2	GCCGGTGTCGCTGCCAAAAA	"
C218-2.1	TCAGGCCTGCATCATCTCGTATCA	"
C218-2.2	TTTCGCCGCGGCAATCAGTTC	"
C234-1.1	GGCCGCATTAACGACTTCTCCTT	"
C234-1.2	GTCGCCAACGCCATCGCTATT	"
C237-1.1	ACGCCGGTAGCCGCCTTCAG	95°C 1min; 30 cycles 94°C 30s, 58.6°C 30s, 72°C 1min; hold at 4°C
C237-1.2	GTCGCGGCCGAGGTGACGAT	"
C246-1.1	TCCTCGCCATCTTTCGCTGTCTAC	95°C 1min; 30 cycles 94°C 30s, 55.9°C 30s, 72°C 1min; hold at 4°C
C246-1.2	CCTGCTCCGGGGTCAACTCG	"
C249-1.1	CGCCGCCACCAGCTTCTGAAT	95°C 1min; 30 cycles 94°C 30s, 58.6°C 30s, 72°C 1min; hold at 4°C
C249-1.2	GTTTTGGCGGCGTCCTGAACG	"
C255-2.1	ACCCTTTTACGCCCGCATTGAACG	95°C 1min; 30 cycles 94°C 30s, 61.2°C 30s, 72°C 1min; hold at 4°C
C255-2.2	GGAGAGCGCTTTTGACCCACACG	"
C256-2.1	CAGCCCACCTACGCACCAGAGC	95°C 1min; 30 cycles 94°C 30s, 58.6°C 30s, 72°C 1min; hold at 4°C
C256-2.2	GAAGGGAGCGCATTAGTTCAGCAGT	"
C274-2.1	CCCGCCGTCAGGTTGTAGTAATCC	95°C 1min; 30 cycles 94°C 30s, 61.2°C 30s, 72°C 1min; hold at 4°C
C274-2.2	CCGCCCGGGCAGGTAAAATG	"
C284-2.1	AAAGCGGGCATATCGGGTCAGC	95°C 1min; 30 cycles 94°C 30s, 58.6°C 30s, 72°C 1min; hold at 4°C
C284-2.2	ACGGCGGTTTCATTCTCATAAGC	"
C297-1.1	CGAAGCCGGCCTGGTCTACAAG	"
C297-1.2	CCCGCGCCTGGTTATCGTT	"

56

Table II.4 Primers Used in this Study (cont.)

Methods and Primers used in each	Primer Sequence (5' to 3')	PCR Cycling Parameters
C312-2.1	TTCCGTAGCAATTTATCCGTCACA	95°C 1min; 30 cycles 94°C 30s, 55.9°C 30s, 72°C 1min; hold at 4°C
C312-2.2	GCGCGTCTTTTATTGGTCATCTCT	"
C321-2.1	CGCGCTAACCCTGAATAAT	95°C 1min; 30 cycles 94°C 30s, 58.6°C 30s, 72°C 1min; hold at 4°C
C321-2.2	TCTACGCGAAGTGGGATGAA	"
C328-2.1	CCAGGAGCGCACGCAGAAGGTC	95°C 1min; 30 cycles 94°C 30s, 61.2°C 30s, 72°C 1min; hold at 4°C
C328-2.2	CCGCCCGGGCAGGTCACG	"
C348-2.1	CAGGCGGCGGCATCGGCATCATC	95°C 1min; 30 cycles 94°C 30s, 64.2°C 30s, 72°C 1min; hold at 4°C
C348-2.2	GCCGCTCCACCACCCCGCTCTC	"
C366-2.1	CCCCTTCCGCTGCGCCTTCAATC	95°C 1min; 30 cycles 94°C 30s, 61.2°C 30s, 72°C 1min; hold at 4°C
C366-2.2	ACGCCGGCAAATCCACCTTCATCC	"
C391-2.1	TCGTTCCGGGTGCTTCTCAGGTTTG	95°C 1min; 30 cycles 94°C 30s, 58.6°C 30s, 72°C 1min; hold at 4°C
C391-2.2	GCAGGTACTTCCGGCACGACATCT	"
C392-1.1	TCCGCGCCTGATTAAGCAAGAAC	95°C 1min; 30 cycles 94°C 30s, 61.2°C 30s, 72°C 1min; hold at 4°C
C392-1.2	CGCGCGCGAAGCAGTGC	"
C402-2.1	GATTTGCGGTGGCCTTTCTGAT	95°C 1min; 30 cycles 94°C 30s, 58.6°C 30s, 72°C 1min; hold at 4°C
C402-2.2	TGCCCGGCGTCTACCACCAG	"
C407-1.1	TCTCAGGGGGTCCAGCATCCAT	"
C407-1.2	CACCTCTGACATTTTCGCCACCAC	"
C418-2.1	GTGAGTTGCGGGCGTGGGTTATC	"
C418-2.2	ATTTACCGGCGCCGTTCTCACC	"
C431-2.1	CTTTGTCGCCATTGCCGTCAGC	95°C 1min; 30 cycles 94°C 30s, 61.2°C 30s, 72°C 1min; hold at 4°C
C431-2.2	GGCGTCCGCAACCTACCGTAACTCC	"

Table II.4 Primers Used in this Study (cont.)

Methods and Primers used in each	Primer Sequence (5' to 3')	PCR Cycling Parameters
C440-1.1	GGGGCTGCCGCTGTGTAAAA	95°C 1min; 30 cycles 94°C 30s, 58.6°C 30s, 72°C 1min; hold at 4°C
C440-1.2	GGTCGCGGCCGAGGTTC	"
C448-1.1	CCGCCCGCGCCTCTTCATCCATC	95°C 1min; 30 cycles 94°C 30s, 64.2°C 30s, 72°C 1min; hold at 4°C
C448-1.2	GGCGTTCACCACCGGCGTMC	"
C451-2.1	AGGTGGGTAATGGTCTGGTTCTGC	95°C 1min; 30 cycles 94°C 30s, 58.6°C 30s, 72°C 1min; hold at 4°C
C451-2.2	CTTCGCCCCGCTTTCGTGAT	"
C469-2.1	GCTGCCGCCGATCCTCACCTTTCA	95°C 1min; 30 cycles 94°C 30s, 64.2°C 30s, 72°C 1min; hold at 4°C
C469-2.2	CCGGGGGCAGCAGCGTATTCACC	"
C479-1.1	NTACGGCCCCAGTTCACCAT	95°C 1min; 30 cycles 94°C 30s, 55.9°C 30s, 72°C 1min; hold at 4°C
C479-1.2	CAGGCCGATAGCGATGATGAGAAA	"
C482-1.1	AGCCGGAAATACCACCACCCAACT	95°C 1min; 30 cycles 94°C 30s, 58.6°C 30s, 72°C 1min; hold at 4°C
C482-1.2	ATAACCCGGCAGACAGGCAATCAC	"
C500-2.1	CGCCGCCAGGACGACGAAGCAGA	95°C 1min; 30 cycles 94°C 30s, 61.2°C 30s, 72°C 1min; hold at 4°C
C500-2.2	GAAAACCCGGAGATCAGCCAGACC	"
C518-2.1	TCGCTGGTGGGGACGAACTTCA	95°C 1min; 30 cycles 94°C 30s, 58.6°C 30s, 72°C 1min; hold at 4°C
C518-2.2	ATATCGCCGGAGGGGAGCATCA	"
C529-2.1	TTGCCGGACCGTAACCTATTG	"
C529-2.2	CTACGGCTGGGAGAAAACCTG	"
C544-2.1	TTGCGTATTTCATGGCCTGTCTCG	"
C544-2.2	GGTTGCAGCGCCCGAATAATC	"
C553-1.1	GGTGCGCCAGCCCCTCTTT	"
C553-1.2	CCGCCGCATATCGTGTGGAAAAA	"

Table II.4 Primers Used in this Study (cont.)

Methods and Primers used in each	Primer Sequence (5' to 3')	PCR Cycling Parameters
C561-1.1	NGGGGCGCTGGATTATCTGGTTA	95°C 1min; 30 cycles 94°C 30s, 61.2°C 30s, 72°C 1min; hold at 4°C
C561-1.2	CCTGCATCGCCGGGCTGTC	"
C587-1.1	CGCTATCCTGGCCGTTTCTCT	95°C 1min; 30 cycles 94°C 30s, 58.6°C 30s, 72°C 1min; hold at 4°C
C587-1.2	GTAGCCGCCTTCGTCACCAA	"
C595-2.1	GCCGCGCCAGCCATCGTT	"
C595-2.2	GTTAGCCCGGACATCATCAGC	"
C612-1.1	AAGGGCGAGTAGAGCAAAAACAGG	"
C612-1.2	GCCGAGGTACGCGACAAACGAT	"
C622-2.1	TAGGCGCGTTTAAACTCGGTCAGG	95°C 1min; 30 cycles 94°C 30s, 61.2°C 30s, 72°C 1min; hold at 4°C
C622-2.2	CCGCCCGGGCAGGTGTC	"
C639-1.1	CCTTGGGCGGTCTACTTTCTCT	95°C 1min; 30 cycles 94°C 30s, 58.6°C 30s, 72°C 1min; hold at 4°C
C639-1.2	CTCCATCGCCCGGTTACAGC	"
C682-2.1	GAGGCGCGGAAAGGACAGAAAG	95°C 1min; 30 cycles 94°C 30s, 55.9°C 30s, 72°C 1min; hold at 4°C
C682-2.2	CCGCCCGGGCAGGTATGA	"
C710-2.1	CCGAATGGCTCACAATAGAAAAT	"
C710-2.2	NAGGCCCGGATGCGATAGT	"
C721-2.1	CACGCCGCCCCTGGTCAAAT	95°C 1min; 30 cycles 94°C 30s, 58.6°C 30s, 72°C 1min; hold at 4°C
C721-2.2	GGGCAGGTACGGCAGCAACATAAA	"
C730-1.1	ATTCCCACCACGCCGGCTTTTGAC	95°C 1min; 30 cycles 94°C 30s, 61.2°C 30s, 72°C 1min; hold at 4°C
C730-1.2	GGTGCGTTTGGCCCGGTAGACATT	"
C734-1.1	CAGCAATACGCAGGGAATGACG	95°C 1min; 30 cycles 94°C 30s, 58.6°C 30s, 72°C 1min; hold at 4°C
C734-1.2	CCCCTGGAATATTGGCAAGATG	"

Table II.4 Primers Used in this Study (cont.)

Methods and Primers used in each	Primer Sequence (5' to 3')	PCR Cycling Parameters
C778-2.1	CCCCGCCGGCGGAGATGAAAAC	95°C 1min; 30 cycles 94°C 30s, 64.2°C 30s, 72°C 1min; hold at 4°C
C778-2.2	CCGCCCGGGCAGGTCCACAA	"
C780-2.1	CCAGCGGCCTTCGGTGTCTTTCTC	95°C 1min; 30 cycles 94°C 30s, 58.6°C 30s, 72°C 1min; hold at 4°C
C780-2.2	CCTTTGCTGGCGTGGGTGATGTTAA	"
C805-2.1	CAACTGCCTGAACATAACCTCTG	95°C 1min; 30 cycles 94°C 30s, 55.9°C 30s, 72°C 1min; hold at 4°C
C805-2.2	CCAAGCGGCGACAATCC	"
C813-1.1	ACACCGCCATCGATCCCTCCTACG	95°C 1min; 30 cycles 94°C 30s, 64.2°C 30s, 72°C 1min; hold at 4°C
C813-1.2	ACGCCGCGGTCAGCCCAGAAT	"
C883-2.1	CCAGCCAGCGCCCTTTTATGTG	95°C 1min; 30 cycles 94°C 30s, 55.9°C 30s, 72°C 1min; hold at 4°C
C883-2.2	TGGCTCTATCGGTTCGGCTTTACG	"
G171-1.1	GGGCGAGGGCGGAGGGATAG	95°C 1min; 30 cycles 94°C 30s, 60.3°C 30s, 72°C 1min; hold at 4°C
G171-1.2	GCGGCCGAGGTACCATTCACG	"
G176-2.1	CATTGCCGGCGCCCTT-FCTC	95°C 1min; 30 cycles 94°C 30s, 59.6°C 30s, 72°C 1min; hold at 4°C
G176-2.2	GCAGCGCCACCCAACCAG	"
G180-2.1	CAATCGCAGCGCCAAACTGTTGTT	95°C 1min; 30 cycles 94°C 30s, 60.3°C 30s, 72°C 1min; hold at 4°C
G180-2.2	AGGTACCGCCGGGGACCCTCTC	"
G190-2.1	GCGGTTGGAATACGGCGATGCT	"
G190-2.2	TTACCGGCTTTCACCCCAATGTCA	"
G206-1.1	TGAGCGCAGAGCAAAGGAATGT	95°C 1min; 30 cycles 94°C 30s, 56.5°C 30s, 72°C 1min; hold at 4°C
G206-1.2	NTGGGGGATGACGGATGTAG	"
G212-2.1	AACACCACCGGCCTCATAGGT	95°C 1min; 30 cycles 94°C 30s, 57.6°C 30s, 72°C 1min; hold at 4°C
G212-2.2	CAGCGGGGATGTGGTGTGGAG	"

Table II.4 Primers Used in this Study (cont.)

Methods and Primers used in each	Primer Sequence (5' to 3')	PCR Cycling Parameters
G222-1.1	AGAAGCGACATAAACGGGGAAAAT	95°C 1min; 30 cycles 94°C 30s, 56.5°C 30s, 72°C 1min; hold at 4°C
G222-1.2	CTGGGGGATATGAAGCGTCTGAAC	"
G238-1.1	TCAGGCGAGGCACTACCAACATCA	95°C 1min; 30 cycles 94°C 30s, 60.3°C 30s, 72°C 1min; hold at 4°C
G238-1.2	GGCGGCACCGGCTCTTTACTACG	"
G253-2.1	GGTGGCTTAGAACTCGACATTTGA	95°C 1min; 30 cycles 94°C 30s, 58.4°C 30s, 72°C 1min; hold at 4°C
G253-2.2	GGGGGCGCTGCAGGTATTTC	"
G255-2.1	GCTCCGCCGACGCCATCAAA	95°C 1min; 30 cycles 94°C 30s, 60.3°C 30s, 72°C 1min; hold at 4°C
G255-2.2	CCGCCCGGCCAGGTACGAGTTA	"
G387-2.1	CCGCTATTCAGGTGGGGATTGGTC	95°C 1min; 30 cycles 94°C 30s, 59.6°C 30s, 72°C 1min; hold at 4°C
G387-2.2	GGGCGGCGCTCAGGATAGTCAT	"
G434-2.1	ATGCCCGCCGGACTTTACA	95°C 1min; 30 cycles 94°C 30s, 51.7°C 30s, 72°C 1min; hold at 4°C
G434-2.2	TCCCCGCTACTGGCTGAA	"
G451-2.1	CGGTCGGCGGCACAAAGA	95°C 1min; 30 cycles 94°C 30s, 58.4°C 30s, 72°C 1min; hold at 4°C
G451-2.2	TCAGGCGACAATGGGAATCA	"
G464-2.1	TACCTGCCCGATACCACCACCTGA	"
G464-2.2	ACGCCCCGCCAACGATGAAC	"
G465-1.1	GGTCGCCTGAGTCTCTGGTAAAAG	95°C 1min; 30 cycles 94°C 30s, 56.5°C 30s, 72°C 1min; hold at 4°C
G465-1.2	TCCTGGCTGAAGTGGTGAACGA	"
G505-1.1	ATCATTTGCCGGAAGCCGTTTGTTA	"
G505-1.2	GCGCTGAAATTAGCCACCGAAATAC	"
G538-1.1	TCTTTCGCCGCCTGGTGGAG	95°C 1min; 30 cycles 94°C 30s, 60.3°C 30s, 72°C 1min; hold at 4°C
G538-1.2	CAGAGGAGCGAGGTGGATGAGAAT	"

61

Table II.4 Primers Used in this Study (cont.)

Methods and Primers used in each	Primer Sequence (5' to 3')	PCR Cycling Parameters
G542-2.1	GAATGCCGCCGCCGACTG	95°C 1min; 30 cycles 94°C 30s, 58.4°C 30s, 72°C 1min; hold at 4°C
G542-2.2	NGATGCCGCCGTTGAGAAAG	"
G579-2.1	NGGCGCGGGGTTAAGCATCATT	"
G579-2.2	CAGTGGGGTGGCGGAAGC	"
G591-2.1	ACGCCGACGCCGATCACCATC	95°C 1min; 30 cycles 94°C 30s, 59.6°C 30s, 72°C 1min; hold at 4°C
G591-2.2	TTATTATCGCGCTGGCTTTTGTGG	"
G598-2.1	GCAAGACCTGAAAGCCCAACACTG	95°C 1min; 30 cycles 94°C 30s, 55.4°C 30s, 72°C 1min; hold at 4°C
G598-2.2	ACGAGCGGCT(TAATACCCTTTCA	"
G629-2.1	GGGCCGGCCATGACAGGGTATTC	95°C 1min; 30 cycles 94°C 30s, 60.3°C 30s, 72°C 1min; hold at 4°C
G629-2.2	CGCAGCGCATAACGGTTGAAGT	"
G645-2.1	ATCGCGGGTTAAAATACAGTTCAG	95°C 1min; 30 cycles 94°C 30s, 55.4°C 30s, 72°C 1min; hold at 4°C
G645-2.2	CTTCAGTCGAGCAGGGAGTTCAC	"
G674-2.1	TCGACGAGCCTGGACTGATTTTC	"
G674-2.2	CACGCCAACATTGTCTCCTATTCC	"
G693-1.1	ACGTCGCGCTGGTTGAGGTTATTA	95°C 1min; 30 cycles 94°C 30s, 58.4°C 30s, 72°C 1min; hold at 4°C
G693-1.2	ATGTGGTCGCGTTTGATGAAGTGG	"
G696-1.1	CCACCAGCGCTTTTCCTCCATTC	"
G696-1.2	AT(CCCGGCTTGCGCTTTGATTAT	"
G700-2.1	GGGGGCGAATGATGTAGATGAA	95°C 1min; 30 cycles 94°C 30s, 55.4°C 30s, 72°C 1min; hold at 4°C
G700-2.2	ATTGCGCCAGTTGGATTTATTGTC	"
G705-1.1	CCTGACGGCTTTGGGTTCG	95°C 1min; 30 cycles 94°C 30s, 57.6°C 30s, 72°C 1min; hold at 4°C
G705-1.2	CTAAATCCGCCGGTGCTGACATA	"

Table II.4 Primers Used in this Study (cont.)

Methods and Primers used in each	Primer Sequence (5' to 3')	PCR Cycling Parameters
Allelic Exchange using pLD55		
Kleb UreF 1	TGACCCTTTGGCCAGCTGCCGTTCG	95°C 1min; 30 cycles 94°C 30s, 63.6°C 30s, 72°C 1min; last cycle 94°C 1min, 63.6°C 30s, 72°C 1min; hold at 4°C
Kleb UreF 2	ACCACCGCCAGCTGCCAGGTATCG	"
Kleb FimC 1	TGCCCGGCTGTCATTGCTTCTGGT	"
Kleb FimC 2	TACCGCGGACCGACGACGCTAAAT	"
Kleb EntA 1	CTTCCAGTCGGGTGTAGATGATGC	"
Kleb EntA 2	CGTGATGCTGGCGAAGAACC	"
T7	see above	see above
T3	see above	see above
Lambda Red Recombinase Method		
P1-H1 FimC	CGGCAACCTAAATGATCCAGTCCATATTTCCGATGTGACAGTGTAGGCTGGAGCTGCTTC	94°C 1min; 25 cycles 94°C 30s, 55°C 30s, 68°C 2min; hold at 4°C
P2-H2 FimC	CAGGACAACACCGGTGAGCAGACAACAAGGAGATAATGTTGAGAAATGGGAATTAGCCATGGTCC	"
PCR Test FimC1	AAAAGCGGGGGTTAAAATAGAGGT	94°C 5min; 35 cycles 94°C 30s, 59.9°C 30s, 68°C 2:15min; hold at 4°C
PCR Test FimC2	ACGGCGTGGCTGATGGA	"
Gam1	ACCCCCTTTCCTGTTTTCCTAATC	94°C 5min; 30 cycles 94°C 30s, 57.7°C 30s, 68°C 1min; hold at 4°C
Gam2	CCTGGTTGGTGAGCAATGGTTTC	"
V	CGGTGATTGGCGAAAACCTTCA	**For PCR Cycles attempted with various combinations of the primers listed; please see results section**
VI	TGGTTGACGTTGGGCTGGATG	"
VII-P1	GAAGCAGCTCCAGCCTACACCATAACGTTCTCTTAAGTCAGC	"
VIII-P2	GGACCATGGCTAATTCCCATAGGTAGCGCCATGATC	"

63

Table II.4 Primers Used in this Study (cont.)

Methods and Primers used in each	Primer Sequence (5' to 3')	PCR Cycling Parameters
TS Plasmid Mutagenesis Protocol		
P1-H1 FimC Acc65I	GGTACCCGGCAACCTAAATGATCCAGTCCATATTTCCGATGTGACAGTGTTAGGCTGGAGCTGCTTC	94°C 1min; 25 cycles 94°C 30s, 55°C 30s, 68°C 2min; hold at 4°C
P2-H2 FimC Acc65I	GGTACCCAGGACAACACGGTGAGCCAGACAAGGAGTAATGTGAGAAATGGGAATTAGCCATGGTCC	"
PCR Test FimC1	see above	see above
PCR Test FimC2	see above	see above
Gam1	see above	see above
Gam2	see above	see above
kt	GCGGTCCGCCACACCCAGCC	94°C 5min; 35 cycles 94°C 30s, 67°C 30s, 72°C 1min; hold at 4°C
k2	CGGTGCCCTGAATGAACTGC	"
Allelic Exchange using pWM91 and pKAS32		
NotI-UreA-P1	GCGGCCGCGCGGCCTCGAAGCTCAACTATCCGGAGTCCGTGGCCCTCCATGTGTAGGCTGGAGCTGCTTC	94°C 1min; 25 cycles 94°C 30s, 55°C 30s, 68°C 2min; hold at 4°C
NotI-UreA-P2	GCGGCCGCCGTCCGGGAAGGTGGCTTCGACCTGGATATCCGGGATCAATGGGAATTAGCCATGGTCC	"
NotI-FimC-P1	GCGGCCGCCGGCAACCTAAATGATCCAGTCCATATTTCCGATGTGACAGTGTTAGGCTGGAGCTGCTTC	"
NotI-FimC-P2	GCGGCCGCCAGGACAACACGGTGAGCAGACAAGGAGATAATGTGAGAAAATGGGAATTAGCCATGGTCC	"
T7	see above	see above
T3	see above	see above
PCR Test FimC1	see above	see above
PCR Test FimC2	see above	see above
V	see above	94°C 5min; 35 cycles 94°C 30s, 59.9°C 30s, 68°C 2:15min; hold at 4°C
VI	see above	"

References

1.   Lau, H.Y., S. Clegg, and T.A. Moore, *Identification of Klebsiella pneumoniae genes uniquely expressed in a strain virulent using a murine model of bacterial pneumonia.* Microb Pathog, 2007. **42**(4): p. 148-55.

2.   Remick, D.G., et al., *Role of tumor necrosis factor-alpha in lipopolysaccharide-induced pathologic alterations.* Am J Pathol, 1990. **136**(1): p. 49-60.

3.   Greenberger, M.J., et al., *Neutralization of IL-10 increases survival in a murine model of Klebsiella pneumonia.* J Immunol, 1995. **155**(2): p. 722-9.

4.   Aronoff, D.M., C. Canetti, and M. Peters-Golden, *Prostaglandin E2 inhibits alveolar macrophage phagocytosis through an E-prostanoid 2 receptor-mediated increase in intracellular cyclic AMP.* J Immunol, 2004. **173**(1): p. 559-65.

5.   Wan, C.P., C.S. Park, and B.H. Lau, *A rapid and simple microfluorometric phagocytosis assay.* J Immunol Methods, 1993. **162**(1): p. 1-7.

6.   Ojielo, C.I., et al., *Defective phagocytosis and clearance of Pseudomonas aeruginosa in the lung following bone marrow transplantation.* J Immunol, 2003. **171**(8): p. 4416-24.

7.   Christensen, P.J., et al., *Characterization of the production of monocyte chemoattractant protein-1 and IL-8 in an allogeneic immune response.* J Immunol, 1993. **151**(3): p. 1205-13.

8.   Hestdal, K., et al., *Characterization and regulation of RB6-8C5 antigen expression on murine bone marrow cells.* J Immunol, 1991. **147**(1): p. 22-8.

9.   van Rooijen, N. and E. van Kesteren-Hendrikx, *"In vivo" depletion of macrophages by liposome-mediated "suicide".* Methods Enzymol, 2003. **373**: p. 3-16.

10.   Shankar-Sinha, S., et al., *The Klebsiella pneumoniae O Antigen Contributes to Bacteremia and Lethality during Murine Pneumonia.* Infect Immun, 2004. **72**(3): p. 1423-1430.

11.   Metcalf, W.W., et al., *Conditionally replicative and conjugative plasmids carrying lacZ alpha for cloning, mutagenesis, and allele replacement in bacteria.* Plasmid, 1996. **35**(1): p. 1-13.

12.   Datsenko, K.A. and B.L. Wanner, *One-step inactivation of chromosomal genes in Escherichia coli K-12 using PCR products.* Proc Natl Acad Sci U S A, 2000. **97**(12): p. 6640-5.

13.   Skorupski, K. and R.K. Taylor, *Positive selection vectors for allelic exchange.* Gene, 1996. **169**(1): p. 47-52.

Chapter III

Lack of *in vivo* Pathogenicity of *K. pneumoniae* strain IA565

and its Role as a Murine Commensal

Introduction

Background of Strains Used in this Study

Animal models have proven extremely useful in determining host: pathogen interactions during *K. pneumoniae* infection. As described in the first chapter, IFNγ, IP-10, IL-17 and TNFα play an important role in mediating lung antibacterial host responses during *K. pneumoniae* infection as well as the influx of PMNs into the lungs and the action of resident alveolar macrophages. However, the majority of these studies utilized a single clinical isolate of *K. pneumoniae*, strain 43816. This is the prototypical virulent strain used in a variety of different studies to determine the host mechanisms of pulmonary bacterial clearance.

Strain 43816 is of the O1:K2 serotype and was originally isolated from a cancer patient in the 1970s. However, because of inconsistent strain designations, it is unclear whether strain 43816 was a blood, wound, urinary tract or pulmonary isolate. For strain IA565, the O-antigen serotype is unknown, but via PCR, IA565 was found not to express the O1 antigen (unpublished data). Strain IA565 has a K15 capsular serotype and was originally isolated from the tracheal aspirate of a hospitalized patient. It is unclear why

the patient was admitted to the University of Iowa Hospitals and Clinics as the patient's history is unavailable.

Both strain 43816 and IA565 express the prototypical virulence factors associated with *K. pneumoniae* pathogenicity; being capsule, LPS, and type 1 and 3 fimbriae. Of these three, capsule is perhaps the most well studied virulence factor. As stated before, via construction of capsule switch mutants, the genetic background of virulent strains and not the capsule serotype was shown to confer significant *in vivo* murine pathogenicity [1, 2]. This suggested that pathogenesis of *K. pneumoniae* is multifactorial and that capsule can only partially account for *in vivo* murine virulence.

Inflammatory Bowel Disease: Role of Commensal Bacteria and Current Murine Models

As alluded to earlier, the mucosal immune system is a highly specific anti-inflammatory mechanism responsible for mucosal tolerance. A break in mucosal tolerance leading to inappropriate immune responses to commensal bacteria is hypothesized to be an important contributing factor to inflammatory bowel disease (IBD). IBD refers to two chronic diseases that cause inflammation of the intestine: ulcerative colitis (UC) and Crohn's disease.

In murine models of IBD, described below, several studies have shown that the driving force of intestinal inflammation is the mucosal microbiota [3-5]. Mice that develop inflammatory disease in specific-pathogen free conditions do not do so in GF environments. In addition, inflammation is alleviated when mice are treated with antibiotics that rid the mucosa of certain classes of microbes [6]. Current models of IBD involve treatment with mucosal-injuring agents (dextran sodium sulfate, DSS), alteration

of murine cytokine function (IL-10 and IL-2 deficient mice), alteration of T-cell function (T cell receptor α and β knockout mice), and infection with enteric pathogens (*Citrobacter rodentium*) [7, 8].

C. rodentium is a commonly used murine model pathogen for human enteropathogenic *E. coli* (EPEC) infections as well as IBD. The characteristic histopathological feature of attaching and effacing (A/E) lesions within the intestinal mucosa seen during EPEC infections are indistinguishable from those caused by *C. rodentium*. Mice infected with *C. rodentium* displays crypt hyperplasia, loss of goblet cells and mixed inflammatory cell infiltration of the mucosa and submucosa with lymphocytes, macrophages, neutrophils and mast cells [8].

DSS is a sulfated polysaccharide commonly used to induce colitis in rodents. The *in vivo* action of DSS is currently not well understood, but it is thought that DSS is toxic to colonic crypt epithelium and acts directly on these cells to induce inflammation. DSS was first introduced in 1990 as a reliable model of acute UC in mice that resembled the human manifestation of UC [9]. The stages of DSS induced colitis, within the first several days of administration, were histologically examined and it was determined that many architectural changes occur first such as crypt loss not associated with inflammation [10].

Objective

Clinical isolate IA565 was used in a well established murine model of acute bacterial pneumonia to investigate the induction of host anti-bacterial responses to this organism and to determine the factors that control lung growth. In addition, mucosal

colonization of strain IA565 in the upper respiratory and gastrointestinal tract of wild-type, germ-free and defined flora mice was performed to determine the mechanisms responsible for colonization at those sites. The ability of strain IA565 to change and respond to the inflammatory environment of the gastrointestinal tract was also investigated using the DSS and *C. rodentium* models of IBD described above. The results from this study elucidate the mechanisms controlling mucosal tissue colonization and infection by *K. pneumoniae*, which is the primary objective of this project.

Results

Lack of mortality in IA565 infected mice

To determine the pathogenicity of strain IA565 and 43816, C57BL/6J mice were intratracheally (IT), intraperitoneally (IP) and intravenously (IV) inoculated with strain IA565 and IT and IV inoculated with strain 43816 (Figure III.1). The LD_{50} dose for strain 43816 in the systemic IV model and the pneumonia IT model is approximately 5 x 10^4 and 5 x 10^3 CFU/mL, respectively. This corresponded to the survival curves shown in Figure III.1. Strain IA565 was given to mice at about 1-2 log CFU doses higher than the LD_{50} dose for strain 43816. However, at these high doses of strain IA565, mice displayed 0% mortality (Figure III.1). These survival curves indicate an apparent lack of pathogenicity of strain IA565 is a murine model of bacterial pneumonia.

Rapid pulmonary clearance of IA565 infected mice

To determine whether the observed lack of mortality correlated with the rapid clearance of strain IA565 bacteria from the lungs, C57BL/6J mice were intratracheally inoculated with 3 x 10^5 CFU of IA565 and 43816 and analyzed 24 hours post infection (Figure III.2). Mice infected with strain 43816 displayed high bacterial load in both the lungs and blood (Figure III.2A). In contrast, bacterial CFU in the lungs and blood from the IA565 infected mice were below the limit of detection by 24 hours post infection. These results suggest that the lack of mortality in IA565 infected mice is due to the rapid clearance of this strain from the lungs.
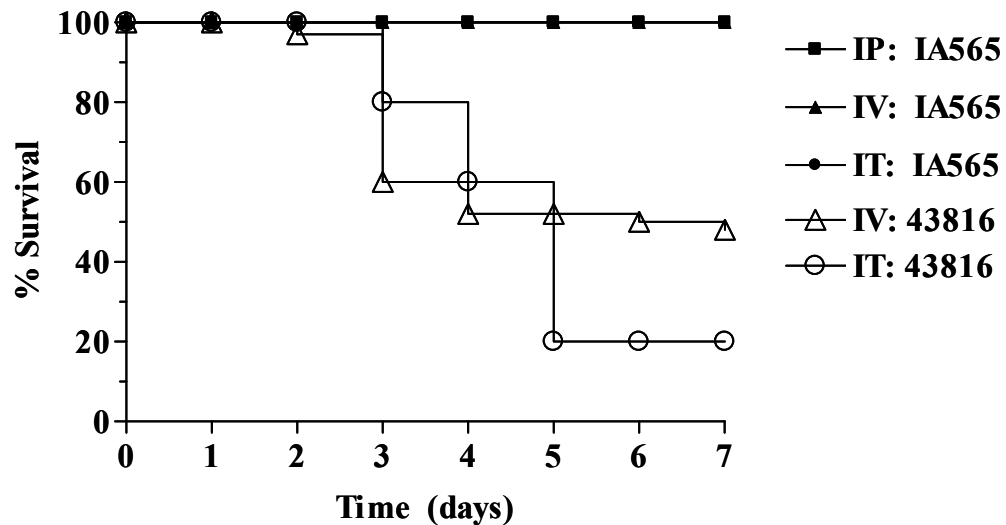
Figure III.1 Survival of *K. pneumoniae* Inoculated C57BL/6J Mice
For IA565 inoculation, C57BL/6J mice were intraperitoneally (IP) injected with
7.8 x 10^5 CFU in a 200μL volume, intravenously (IV) injected with 2 x 10^5 and
2 x 10^6 CFU in 500μL volumes, and intratracheally (IT) injected with 5 x 10^3,
5 x 10^4 and 5 x 10^5 CFU in 30μL volumes. n = 4-6 mice per dose and route
of infection. For 43816 inoculation, C56BL/6J mice were IV injected with
8 x 10^4 CFU in a 500μL volume and IT injected with 9.8 x 10^3 CFU in a 30μL
volume. n = 5-9 mice per route of infection. Survival was monitored over a
course of 7 days.

Figure III.2 Day 1 Harvest of IA565 and 43816 Intratracheally Infected mice
Bacterial burden, chemokine induction, and MPO activity following intratracheal
infection with strain IA565 or 43816. Mice were infected with 3 x 10^5 CFU of
strain IA565 or 43816 and analyzed 24 hours post infection. (A) Bacterial
numbers for the lungs are for the entire tissue, while bacterial numbers for the
blood are per mL of blood. (B) Chemokine production was assessed from total
lung homogenates by ELISA. (C) Lungs were also assessed for MPO activity.
Units are expressed as a change in absorbance over time. Data are presented as
mean ± SEM and were generated from two independent experiments with 4-5
animals per group. *, $p < 0.001$. n.d., no data. LOD, limit of detection.

A
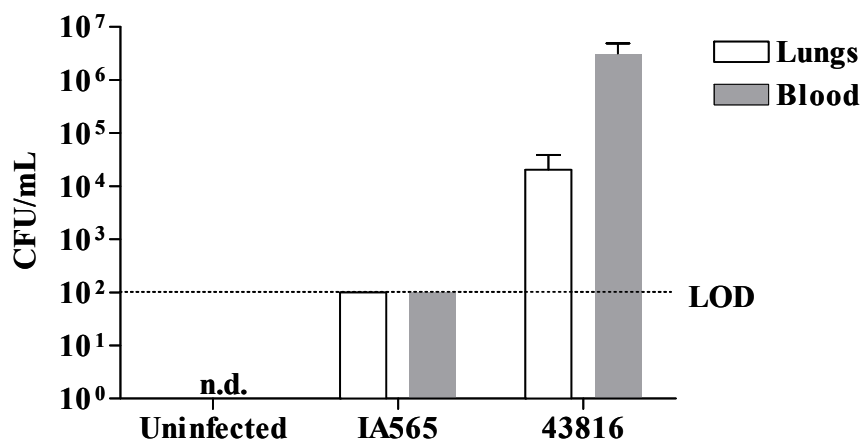
B
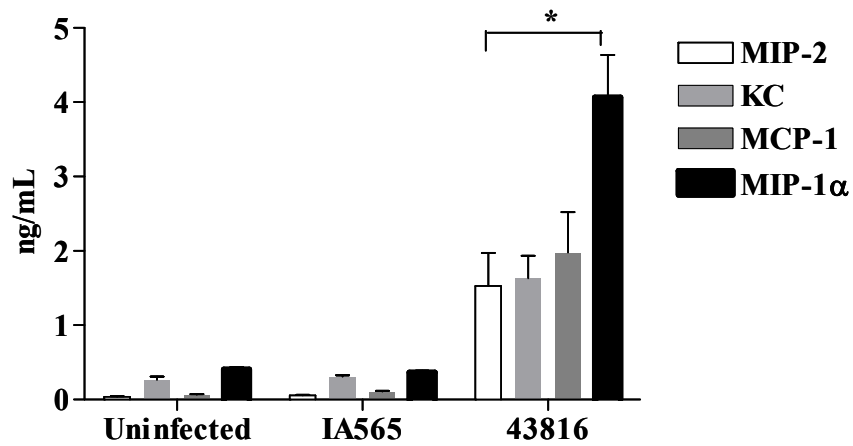
C
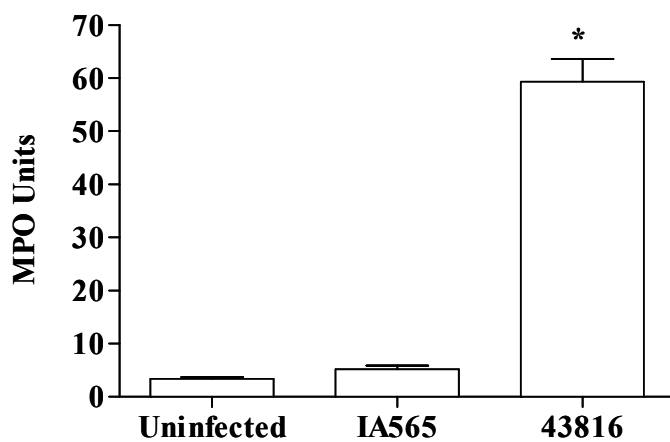
Lack of significant chemokine induction and neutrophil recruitment in the lungs of IA565

infected mice

To determine if the rapid clearance of strain IA565 resulted from enhanced

neutrophil and/or macrophage recruitment into the pulmonary airspace, lung

homogenates were analyzed for the production of chemokines responsible for recruiting

these cell types 24 hours post inoculation (Figure III.2B). The neutrophil recruiting

chemokines, MIP-2 and KC were significantly increased in the lungs of strain 43816

infected mice. MCP-1, capable of recruiting circulating monocytes was also significantly

increased in the lungs of these mice. Correlating with increased MIP-2 and KC,

myeloperoxidase (MPO) activity, an indirect measurement of neutrophil numbers, in the

lungs of 43816 infected mice was significantly elevated compared to uninfected control

animals. In contrast, lung homogenates from IA565 infected mice contained baseline

levels of MIP-2, KC and MCP-1 and MPO levels were essentially equal to those seen in

uninfected controls (Figure III.2C). These data indicate that, at this time point, IA565

infected mice do not display enhanced neutrophil and macrophage recruitment into the

pulmonary airspace.

Kinetics of chemokine induction and bacterial clearance during IA565 infection

Since cytokine levels and MPO levels were at baseline levels by 24 hours post

inoculation, IA565 infected mice were analyzed at earlier time points to determine

whether a rapid but transitory immune response was responsible for the rapid clearance

of this strain. Mice were challenged with $2x\ 10^5$ CFU of strain IA565 and analyzed at 2,

12, and 24 hours post infection. Significant bacterial clearance is seen within 2 hours

post infection and decreased by 10-fold at 12 hours post inoculation with no detectable levels by 24 hours (Table III.1). Interestingly, a transitory but significant increase in the production of MIP-2 and KC was noted at 2 hours post infection which suggests that a rapid influx of neutrophils very early during the course of infection may contribute to the rapid bacterial clearance observed.

Kinetics of bacterial clearance and chemokine induction in neutrophil-depleted mice IA565 infected mice

Neutrophils were depleted *in vivo* by intraperitoneal inoculation of an anti-Ly6G monoclonal antibody 18 hours prior to intratracheal inoculation of strain IA565 to determine their contribution during *K. pneumoniae* IA565 infection. Surprisingly, these neutrophil depleted mice displayed 100% survival even at high doses (Figure III.3) indicating that neutrophils are not required for survival of IA565 infected mice.

To determine the kinetics of bacterial clearance from the lungs, neutrophil depleted mice were analyzed 2, 6, 12, 24 and 48 hours post infection (Table III.2). A delay in bacterial clearance was seen in the lungs of neutrophil depleted IA565 infected mice as compared to wild-type infected untreated animals. By 24 hours post infection, lungs in the anti-Ly6G treated animals contained approximately 5×10^4 CFU. However, by 48 hours post infection, 70% of the animals treated with IA565 contained no detectable bacteria while the remaining 30% contained only 100-300 bacteria. MPO activity was measured to confirm neutrophil depletion. At the later time points, 12 and 24 hours post infection, MPO activity was at or below baseline levels seen in uninfected control animals. However, at 2 hours post infection, the MPO activity in these mice was

Table III.1 Kinetics of Lung Bacterial Clearance, Neutrophil Recruitment, and Chemokine Induction in Wild-Type Infected Mice[a]

	Lung CFU[b] (log 10)	MPO Activity (U/mL)	ELISA[c] (pg/mL)			
			MIP-2	KC	MCP-1	MIP-1α
Uninfected	n.d.	2.68 ± 0.4	46 ± 6	218 ± 29	96 ± 13	288 ± 38
2 hr	3.80 ± 0.09	5.33 ± 0.4[+]	732 ± 80*	1,230 ±110*	96 ± 10	536 ± 40*
12 hr	2.89 ±0.12	5.23 ± 0.7[+]	147 ± 20*	324 ± 20*	162 ± 20*	369 ± 30
24 hr	<LOD	5.18 ± 0.7[+]	56 ± 10	305 ± 20[+]	106 ± 10	366 ± 20

[a]Mice were intratracheally inoculated with 2×10^5 CFU of strain IA565 and analyzed at the indicated time points.
[b]Bacterial burden from the lung were determined as described in Materials and Methods. Limit of detected is 2 (log 10) CFU.
[c]Chemokine induction was assessed by ELISA as described in Materials and Methods.
Data were obtained from 2-3 independent experiments with 5 mice per group. LOD, limit of detection.
*, $p < 0.01$; [+], $p < 0.05$ (compared to uninfected control levels).
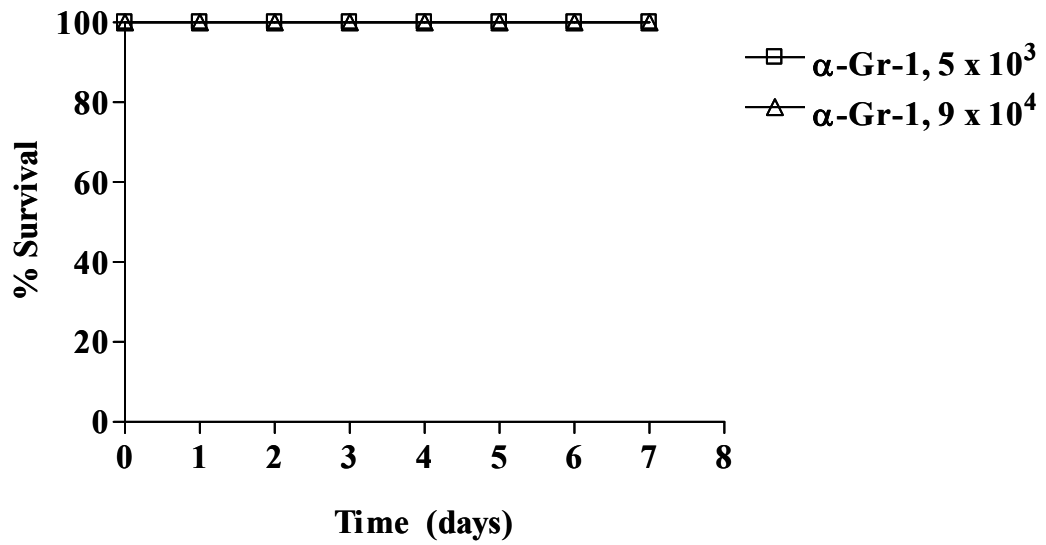
Figure III.3 Lack of Mortality in IA565 Infected Neutrophil-Depleted Mice
Mice were intratracheally inoculated with 5×10^3 and 9×10^4 CFU of strain IA565 and overall survival was determined for 7 days post infection. Survival curves were generated with 5 mice per group per dose.

Table III.2 Kinetics of Lung Bacterial Clearance, Neutrophil Recruitment, and Chemokine Induction in Neutropenic Mice[a]

	Lung CFU[b] (log 10)	MPO Activity (U/mL)	ELISA[c] (pg/mL)			
			MIP-2	KC	MCP-1	MIP-1α
Uninfected	n.d.	2.68 ± 0.4	46 ± 6	218 ± 29	96 ± 13	288 ± 38
2 hr	4.02 ± 0.19	5.33 ± 0.4*	1,120 ± 200*	839 ± 120*	426 ± 60*	356 ± 30
6 hr	3.71 ± 0.10	n.d.	422 ± 40*	485 ± 40*	405 ± 30*	511 ± 90+
12 hr	3.64 ± 0.18	1.91 ± 0.2	200 ± 20*	440 ± 30*	1,050 ± 240*	320 ± 30
24 hr	4.47 ± 0.27	2.13 ± 0.1	110 ± 10*	300 ± 20*	840 ± 80*	260 ± 20
48 hr	2.32 ± 0.16	n.d.	48 ± 10	249 ± 10*	247 ± 40*	365 ± 20

[a]Mice were intratracheally inoculated with 2×10^5 CFU of strain IA565 and analyzed at the indicated time points.
[b]Bacterial burden from the lung were determined as described in Materials and Methods and represent those from the entire tissue. Limit of detection is 2 (log 10) CFU.
[c]Chemokine induction was assessed by ELISA as described in Materials and Methods.
Data were obtained from 2-3 independent experiments with 5 mice per group. n.d., no data.
*, $p < 0.01$; +, $p < 0.05$ (compared to uninfected levels).

significantly higher than wild type baseline levels (Table III.2, $p < 0.01$). This correlated

with the same transitory increase in MIP-2 and KC seen in wild-type infected animals

(Table III.1), peaking at 2 hours post infection before returning to baseline levels by 48

hours. Interestingly, there was a delayed yet significant induction of MCP-1 with levels

peaking at 12 hours post infection and remaining elevated thru 24 hours before

decreasing to near baseline levels by 48 hours (Table III.2). These data suggest that there

is delayed recruitment of monocytes in response to neutrophil deficiency, resulting in

delayed but eventual clearance of bacteria from the lungs.

Kinetics of bacterial clearance and chemokine induction in alveolar macrophage-depleted IA565 infected mice

Since the lack of neutrophils did not increase IA565 bacterial burden in the lungs

or induce mortality in these mice, the role of AMϕs during IA565 pulmonary infection

was investigated. AMϕs were depleted *in vivo* by intranasal inoculation of clodronate

liposomes. In addition, both neutrophils and AMϕs were depleted to determine if lack of

these two important phagocytic cells will induce mortality in IA565 infected mice (Figure

III.4). Surprisingly, these AMϕ depleted and AMϕ and neutrophil depleted IA565

infected mice displayed 100% survival indicating that both neutrophils and AMϕs are not

required for survival of IA565 infected mice.

To determine the kinetics of bacterial clearance from the lungs, neutrophil

depleted and AMϕ plus neutrophil depleted mice were analyzed 12, 24, 48, and 72 hours

post IA565 infection at a dose of 10^6 CFU (Figure III.5A). In addition, lung cytokine

levels were also assessed for production of MIP-2, KC, MCP-1 and MIP-1α (Figure
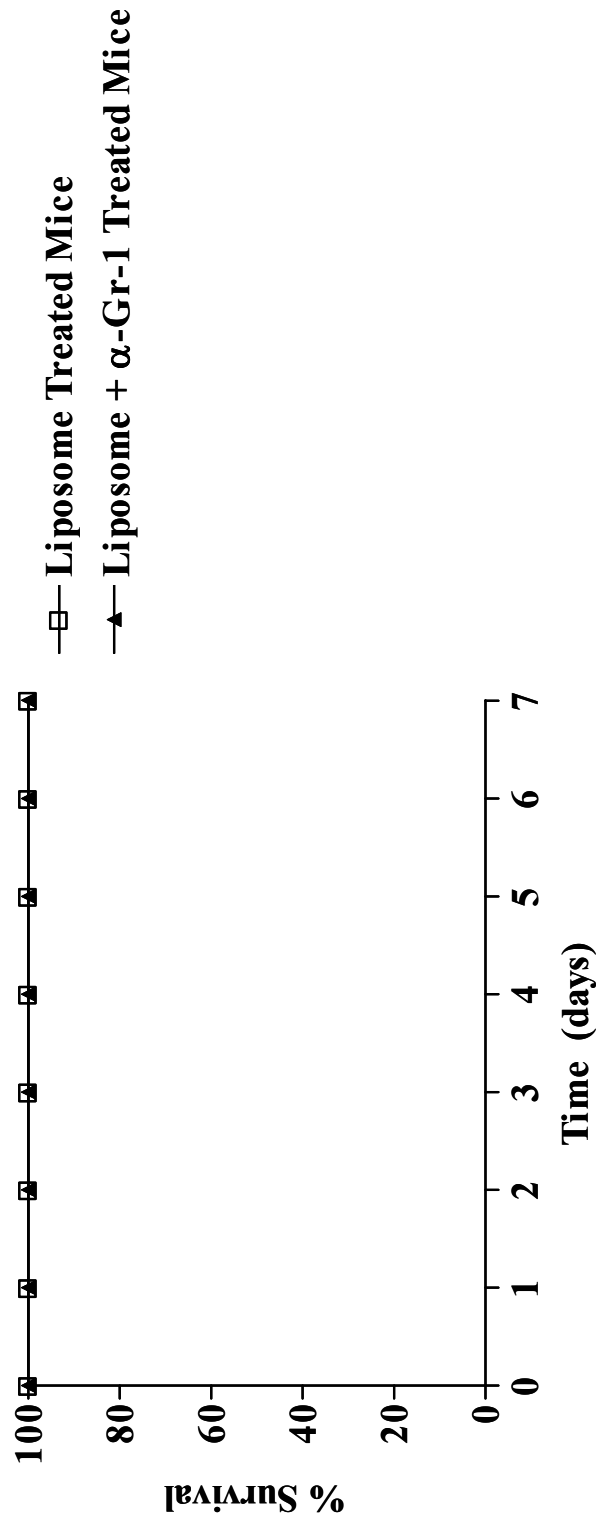
Figure III.4 Survival of IA565 infected Alveolar Macrophage and Neutrophil Depleted Mice αGr-1 and clodronate liposome treated mice were intranasally inoculated with 4×10^5 CFU of strain IA565 and overall survival was determined for 7 days post infection. Survival curve was generated with 5 mice per group.

Figure III.5 Bacterial Burden and Chemokine Induction in IA565 Infected Immunocompromised Mice

Mice were infected with 1.4 x 10^6 CFU of strain IA565 and analyzed at the indicated timepoints. White bars, wild-type infected mice, grey bars, neutrophil depleted mice, and black bars, neutrophil and alveolar macrophage depleted mice. (A) Bacterial burden from the lung of infected animals are for the entire tissue. The dotted line represents the limit of detection.
 (B) Chemokine production was assessed from total lung homogenates by ELISA. The dotted line represents the amount of cytokine levels in the lungs of uninfected control animals: 2pg/mL for MIP-2, 208pg/mL for KC, 12pg/mL for MCP-1, and 6pg/mL for MIP-1α. Data were generated from one experiment with 3 mice per group.

A
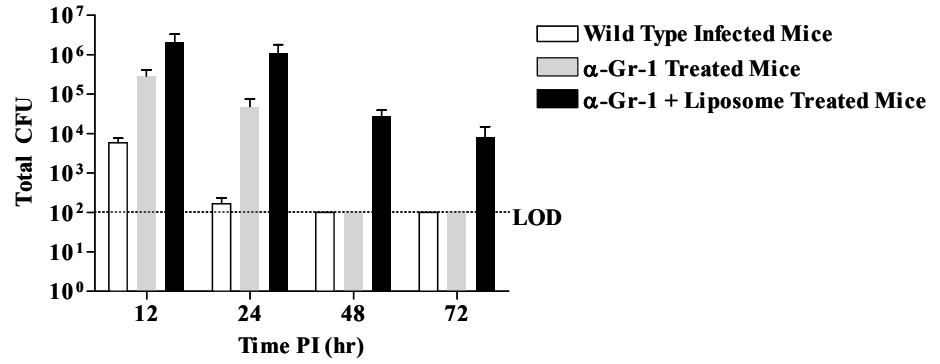
B
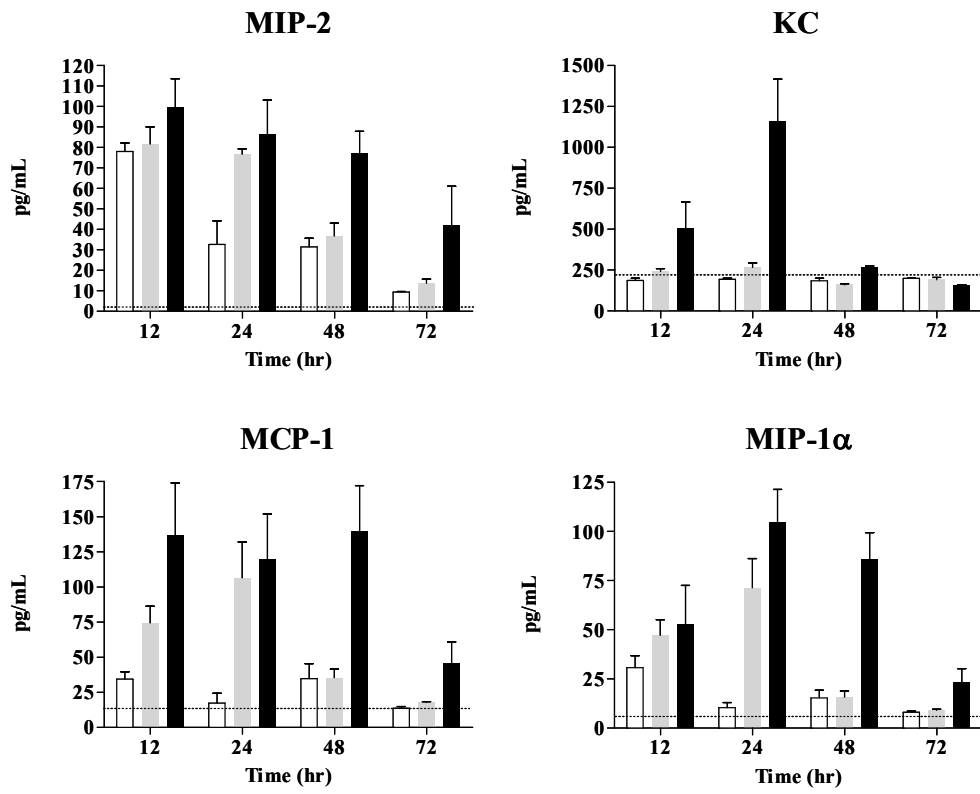
III.5B). Mice depleted of neutrophils plus AMϕs had higher levels of bacteria in the lungs

compared to the wild-type and neutrophil depleted mice at all time points analyzed. By

48 and 72 hours post infection, the wild-type and neutrophil depleted mice, respectively,

no longer had detectable levels of CFU in the lung. Interestingly, the AMϕs and

neutrophil depleted mice still had high levels of CFU by 72 hours post infection (Figure

III.5A) suggesting that these cell types combined play an important role for the rapid

clearance of strain IA565 from the lungs.

In addition, the levels of MIP-2 and MCP-1 correlated quite well with bacterial

CFU in the lungs remaining high at 12 hours post infection for wild-type animals and

high at 12-48 hours for neutrophil depleted mice and AMϕ and neutrophil depleted mice

(Figure III.5B). Wild-type infected animals produced basal levels of KC, MCP-1 and

MIP-1α at these time points. Production of these cytokines in the other infected mouse

groups were high at earlier time points, but decreased at the later time points.

Bacterial clearance in T and B cell, AMϕ, and neutrophil deficient IA565 infected mice

To determine if the presence of natural antibodies play a role in IA565 clearance,

RAG1$^{-/-}$ mice, with and without αGr-1 plus clodronate liposome treatment, were infected

with 8 x 10^5 CFU of strain IA565 and sacrificed at 4 days post infection (Figure III.6).

Day 4 lung CFU levels in the neutrophil and AMϕ depleted mice were slightly above the

limit of detection and the majority of the *RAG1*$^{-/-}$ untreated mice had no detectable CFU

in the lungs. However, CFU levels in the *RAG1*$^{-/-}$ treated mice were slightly higher than

those in both the infected *RAG1*$^{-/-}$ untreated mice and wild-type treated mice suggesting

that the absence of neutrophils, AMϕs and T and B cells result in delayed clearance of

IA565 from the lungs at this time point (Figure III.6). However, the levels were not statistically significant.

Furthermore, to determine whether or not the function of T and B cells in the clearance of IA565 is due to the production and presence of natural antibodies in the lungs, $RAG1^{-/-}$ treated mice were intraperitoneally (IP) injected with 1mL of wild type uninfected serum (Figure III.6). IP administration of normal, non-immunized wild-type mouse serum into infected $RAG1^{-/-}$ treated mice seemed to increase IA565 CFU levels in the lungs suggesting that natural antibodies present in the serum of mice do not play a role in IA565 clearance (Figure III.6, $p = 0.03$). However, the outlier in the $RAG1^{-/-}$ treated group may be contributing to the statistical significance observed. In addition, these observations may not be biologically significant as the lung CFU levels in these animals were near the limit of detection and animals displayed no mortality. Thus, clearance of strain IA565 from the lungs of these animals is not due to the presence of natural antibodies.

Lack of mortality in TNFα and IFNγ depleted IA565 infected mice

As stated in the previous chapter, the proinflammatory cytokines TNFα and IFNγ are essential for host defense during pulmonary *K. pneumoniae*. To determine the contributions of each during *K. pneumoniae* IA565 infection, mice were injected intraperitoneally with an anti-TNFα and an anti-IFNγ neutralizing monoclonal antibody 2 hours before intratracheal infection with strain IA565 (Figure III.7). Surprisingly, these TNFα and IFNγ neutralized mice displayed 100% survival even at high doses indicating that these cytokines are not required for the survival of IA565 infected mice.
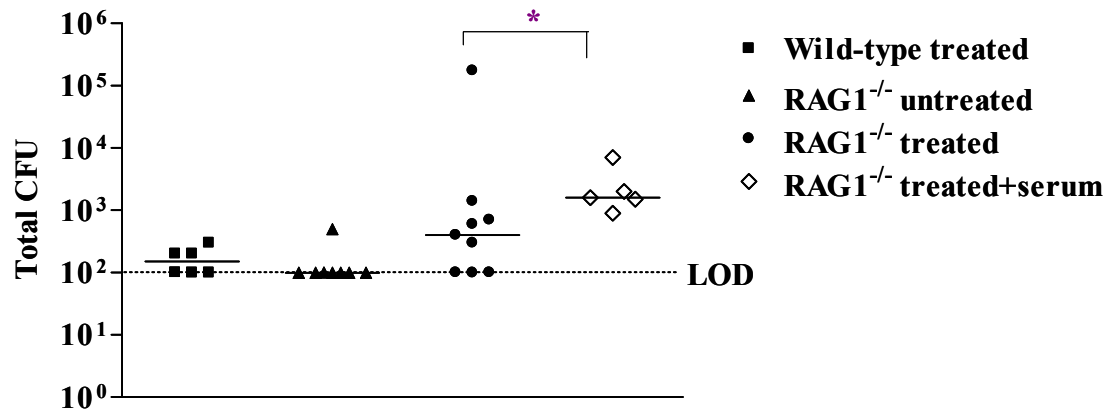
Figure III.6 Day 4 Lung CFU in IA565 Infected *RAG1⁻ᐟ⁻* Mice
Mice were intranasally inoculated with 7.8×10^5 CFU of strain IA565. Lungs were harvested at day 4 post infection. Treated mice were given αGr-1 to deplete neutrophils and clodronate lipsomes to deplete alveolar macrophages. Serum was given as described in Materials and Methods. Data are from two independent experiments with 5-8 mice per group. Bars in each group represent the median value of CFU numbers. LOD, limit of detection.
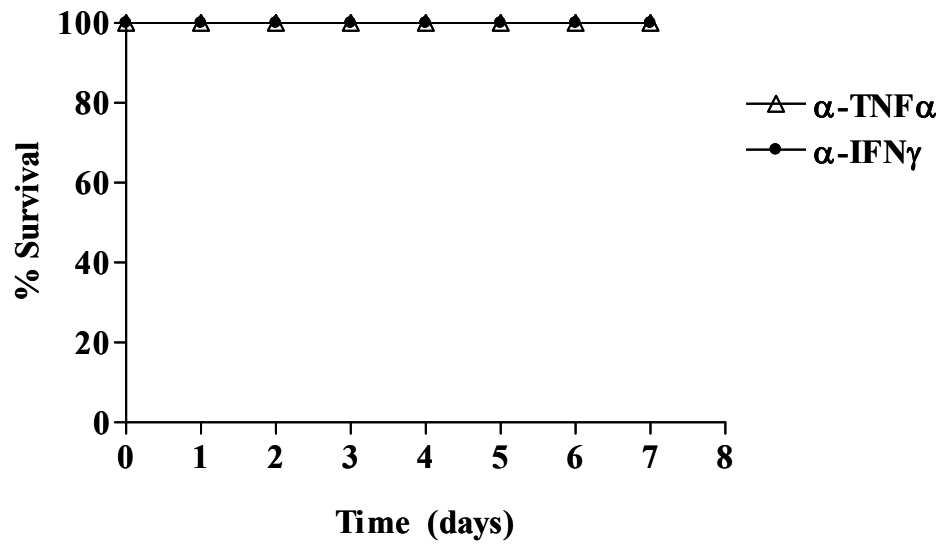
Figure III.7 Survival of IA565 Infected TNFα and IFNγ Depleted Mice
Mice were intratracheally inoculated with 5 x 10^3 and 9 x 10^4 CFU of strain
IA565 and overall survival was determined for 7 days post infection. Survival
curves were generated with 5 mice per group per dose.

In vitro growth characterizations of K. pneumoniae strain IA565

Although *K. pneumoniae* strain 43816 and IA565 are clinical isolates and express the prototypical virulence factors associated with *K. pneumoniae* pathogens, the *in vivo* characterization of strain IA565 indicates that it is avirulent, rapidly cleared, and elicits little to no host responses in the lungs. Therefore, any *in vitro* differences existing between the two that could explain the dissimilarity in *in vivo* pathogenicity were investigated.

To determine if any growth differences in culture media exist between strain IA565 and 43816 to account for the lack of pathogenicity of IA565, growth in rich tryptic soy broth (TSB), phosphate buffered saline (PBS), mouse whole blood (WB), and cell-free bronchoalveolar lavage fluid (BALs) was determine for both strains (Figure III.8). Growth in BALs fluid would address the question of whether or not surfactant and/or other non-cellular lung proteins can affect growth. In addition, growth in whole blood addresses the question of whether or not complement can alter their growth. In PBS media, strain IA565 and 43816 did not grow, with the bacteria remaining viable. Conversely, in mouse whole blood, TSB and cell-free BAL fluid, both strains grew equally well indicating that there are no growth defects, i.e. biochemical defects, associated with either strain and that non-cellular host innate defense components in the lungs and blood do not alter growth of these strains as well.
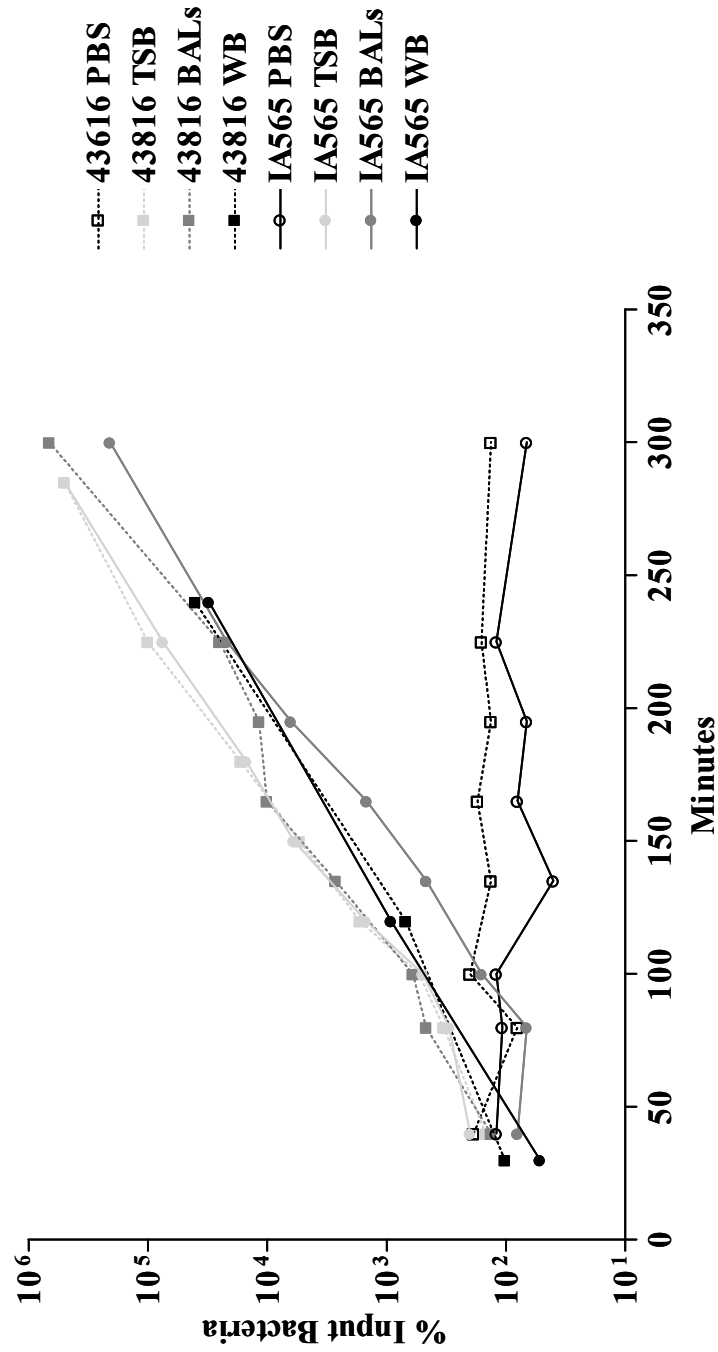
Figure III.8 Growth of IA565 and 43816 in Various Media
In 1mL TSB, 750 CFU of strain 43816 and 500 CFU of strain IA565 was inoculated. In 750μL of 1x PBS and BALs fluid, 750 CFU of strain 43816 and IA565 was inputted. In 1mL of mouse whole blood isolated via cardiac punction, 6.1 x 10^4 CFU of strain 43816 and 5.5 x 10^4 CFU of strain IA565 was inoculated. Each culture was incubated at 37°C while shaking at 125rpm and at 30-40 minute intervals, an aliquot was taken and plated for CFU.

Lipopolysaccharide quantification of strain 43816 and IA565

As stated earlier, even though the capsular serotypes for both strains are different, studies have shown that the capsule alone does not confer pathogenicity. Therefore, the relative amount of LPS, another major virulence factor, on both strains was quantified using a *Limulus* amebocyte lysate (LAL) assay (Figure III.9). LAL is an aqueous extract of blood cells (amebocytes) from the horseshoe crab, *Limulus polyphemus*. Figure III.9A illustrates the standard curve generated in this assay using known amounts of LPS. The concentration is expressed as endotoxin units (EU)/mL and corresponds to the measured OD at 405nm. Supernatants from overnight cultures of both strains (plated in duplicate), LPS-free reagent water (LRW) and TSB were used in this assay (Figure III.9B). The negative control, LRW, did not react to Pyrochrome LAL as indicated by low absorbance in contrast to TSB, which had an OD of 0.504. It was not surprising to detect LPS reactivity in TSB medium since the broth contains bacterial lysate. The mean absorbance for IA565 and 43816 culture supernatants were 0.852 and 0.848, respectively. Even with subtracting out the absorbance from the TSB control, there is still significant LPS reactivity in the culture supernatants of these strains. However, there were no significant differences between the two strains suggesting that lack of LPS does not account for the *in vivo* pathogenicity differences observed between IA565 and 43816.

A

Std	Conc	Mean Abs OD	Replicates Abs OD	Well
1.000	8.000		0.164	E1
1.000	8.000	0.146	0.128	E2
2.000	16.000		0.235	A11
2.000	16.000	0.280	0.325	A12
3.000	25.000		0.343	A9
3.000	25.000	0.353	0.353	A10
4.000	50.000		0.612	A7
4.000	50.000	0.604	0.595	A8
5.000	100.000		0.737	A5
5.000	100.000	0.748	0.753	A6
6.000	200.000		0.773	A3
6.000	200.000	0.772	0.773	A4
7.000	400.000		0.790	A1
7.000	400.000	0.780	0.773	A2

$Y = (A-D)/(1+(X/C)^B) + D$
$A = 0.124, B = 2.065, C = 31.83, D = 0.789, 50\% = 0.456$

B

Sample	Dilution	Mean Abs OD
IA565	1.000	
IA565	1.000	0.852
KP	1.000	
KP	1.000	0.848
LRW	1.000	6.100E-02
TSB	1.000	0.504

Figure III.9 LAL assay for *K. pneumoniae* LPS Quantification
The supernatants of overnight cultures of strain IA565 and 43816 grown in TSB at 37°C
were used in this assay and incubated with Pyrochrome LAL. (A) The curve generated
from serial dilutions of known amounts of LPS. The units of concentration is given as
endotoxin units per mL (EU/mL). (B) The mean absorbance at 405nm of IA565 and
43816 culture supernatants, LPS-free reagent water (LRW), and tryptic soy broth
(TSB).

In vitro peritoneal macrophage phagocytosis of K. pneumoniae strain IA565 and 43816

To assess the ability of strain IA565 and 43816 to be phagocytosed by macrophages, an *in vitro* phagocytosis assay was performed on freshly isolated, non-elicited peritoneal macrophages (PMφs) from B6 mice (Figure III.10). PMφs were incubated with opsonized, FITC-labeled IA565 or 43816 bacteria for 30 minutes at a bacterium to macrophage ratio of 100:1. Values were expressed as relative fluorescence units calculated based on fluorescent standards. In one experiment, phagocytosis of strain IA565 and 43816 was essentially equivalent while in the other experiment phagocytosis of strain IA565 was slightly higher than strain 43816 (Figure III.10, p = 0.04).

An additional *in vitro* PMφ killing experiment was done with IA565 and 43816 bacteria with or without prior incubation in 5% normal mouse serum. Incubation in mouse serum was performed to address the question of whether or not opsonized bacteria would be killed more efficiently by these cell types. Briefly, in one experiment, bacterial cells were incubated for 30 and 90 minutes in wells with and without PMφs at a cell to bacterial ratio of 1:1. This experiment was repeated, but bacteria were incubated with 5% normal mouse serum before addition to PMφs in culture (Figure III.11). At 30 minutes post incubation, the presence of PMφs did not seem to affect the viability of bacteria in culture. This was also the case with opsonized bacteria. However, after 90 minutes in culture, non-opsonized 43816 did not grow as vigorously in the presence of PMφs than without suggesting that the PMφs were phagocytosing 43816 cells. Surprisingly, at 90 minutes post-incubation, non-opsonized IA565 grew better in the presence of PMφs than in culture alone. Incubation of opsonized 43816 and IA565 with PMφs resulted in
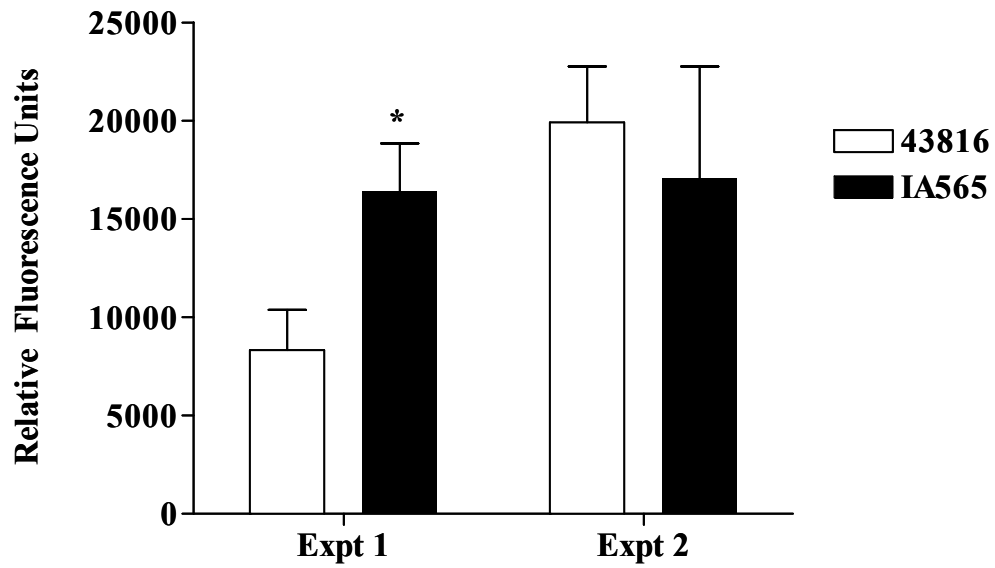
Figure III.10 *In Vitro* **Peritoneal Macrophage Phagocytosis of FITC-labeled 43816 and IA565 Bacteria**
Non-elicited peritoneal macrophages from C57BL/6J mice were isolated and cultured 1:100 with opsonized FITC-labeled bacteria in duplicates for each experiment. *, p = 0.04.
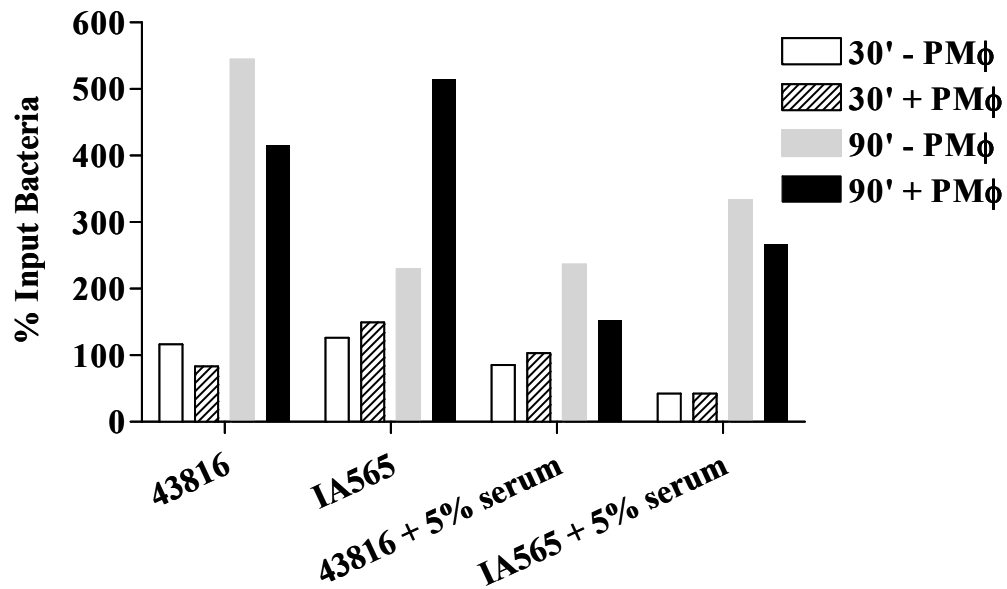
Figure III.11 *In Vitro* **Peritoneal Macrophage Killing Assay**
Freshly isolated, non-elicited PMϕs from C57BL/6J mice
were incubated with 10^6 CFU of IA565 or 43816 at a bacteria to cell
ratio of 1:1. Bacterial cells were also incubated in 5% normal mouse
serum before addition to PMϕs. Data were obtained from one
experiment and are represented as a percentage of input bacteria
calculated from the number of bacteria that grew out of the aliquot
taken at 30 and 90 minutes post incubation divided by the total
bacteria added at 0 minutes.

inhibition of growth when compared to wells containing opsonized bacteria alone.

Cytospin slides were prepared from PMϕs incubated with strain IA565 and 43816 at a bacterium to cell ratio of 100:1. Cells were harvested at 30, 45-60 and 90 minutes post co-incubation from 2 independent experiments. A total of 400 peritoneal macrophages were counted and the numbers of intracellular, phagocytosed bacteria were determined. This was done to calculate the PMϕ phagocytic index (PI) for each strain (Table III.3). The PI index for strain IA565 is higher than that for strain 43816; however, there was no statistical significance indicating that the difference in *in vivo* pathogenicity of these two strains cannot be correlated with these *in vitro* data.

In vivo alveolar macrophage phagocytosis of K. pneumoniae strain IA565 and 43816

Because of the inconsistencies in the above mentioned *in vitro* experiments and the use of a less relevant cell type (PMϕ) to study pulmonary pathogens, an *in vivo* pulmonary phagocytosis assay was performed to address the susceptibility or resistance to alveolar macrophage (AMϕ) phagocytosis of both strains. BALs were performed 2 hours post intratracheal inoculation with 10^5 and 10^6 CFU of strain 43816 and IA565 and 4 hours post inoculation with 10^6 CFU of strain 43816 and IA565. Cytospin slides were prepared (Table III.4) with Figure III.12 showing a representative image of strain 43816 and IA565 phagocytosed by AMϕs. The calculated PI index for strain IA565 was significantly higher than that for strain 43816, but only at 2 hours post inoculation at the high dose and not at the lower dose. Furthermore, at 4 hours post inoculation, both strains had similar PI indexes. This suggests that resistance to phagocytosis early on

Table III.3 Peritoneal Macrophage *In Vitro* Phagocytosis Data[a]

| Strain used | Time Point | # macrophages with ≥ 1 bacteria (total) | % macrophages with ≥ 1 bacteria | # of cells with | | | Mean # of bacteria/ cell | Phagocytic Index [b](PI) |
				1-2 bacteria	3-6 bacteria	≥ 7 bacteria		
43816	**30'**	8 (379)	2.10	8	-	-	1.00	2.10
	45'-60'	14 (377)	3.70	14	-	-	1.00	3.70
	90'	9 (380)	2.40	9	-	-	1.00	2.40
IA565	**30'**	55 (385)	14.30	38	15	2	3.50	50.05
	45'-60'	62 (383)	16.20	30	20	12	3.98	64.48
	90'	70 (379)	18.50	40	18	12	3.48	64.38

[a] *K. pneumoniae* strain IA565 and 43816 were added to non-elicited peritoneal macrophages and cytospins were prepared as described in Materials and Methods.

[b] PI index = (percent of macrophages containing at least one bacterium) x (mean number of bacteria per positive cell).

Table III.4 Alveolar Macrophage *In Vivo* Phagocytosis: Lung CFU and PI index[a]

Time point and Dose	Strain	Total Lung CFU (log)[b]	% Total CFU in BAL fluid	% Total CFU in Lungs	# macrophages with ≥1 bacteria	% macrophages with ≥1 bacteria	# of cells with			Mean # of bacteria/cell	Phagocytic Index (PI)
							1-2 bacteria	3-6 bacteria	≥7 bacteria		
2hr											
2.8×10^5	43816	5.3 (0.1)	93.3 (0.6)	6.7 (0.6)	2.4 (1.2)	1.2 (0.6)	2.2 (1.2)	0.2 (0.2)	-	1.1 (0.5)	2.1 (1.0)
1.4×10^5	IA565	4.6 (0.1)*	80.8 (4.5)	19.2 (4.5)	4.0 (1.8)	2.0 (0.9)	3.8 (1.6)	0.2 (0.2)	-	1.0 (0.3)	2.9 (1.4)
2hr											
1.4×10^6	43816	6.2 (0.04)	92.4 (0.9)	7.7 (0.9)	14.7 (2.2)	7.6 (1.0)	11.5 (1.6)	2.9 (0.6)	0.3 (0.2)	2.1 (0.2)	16.4 (2.7)
1.4×10^6	IA565	5.8 (0.1)**	87.8 (1.2)*	12.2 (1.2)	29.1 (1.7)	14.6 (0.9)	18.1 (1.7)	9.0 (0.9)	2.0 (0.4)	2.8 (0.2)	40.4 (2.0)**
4hr											
1.1×10^6	43816	6.4 (0.1)	93.2 (1.7)	6.8 (1.7)	20.8 (4.9)	16.8 (2.6)	6.25 (1.6)	9.0 (2.0)	5.5 (2.2)	4.9 (0.9)	88.1 (24.8)
1.3×10^6	IA565	5.5 (0.2)*	85.8 (1.5)*	14.2 (1.5)	20.6 (3.3)	14.0 (2.2)	4.8 (1.5)	7.0 (1.1)	8.8 (1.5)	6.4 (0.6)	93.5 (20.8)

[a]BAL cells were isolated from mice 2–4 hours post intratracheal inoculation with either strain IA565 or 43816 as described in Materials and Methods.
[b]Bacterial burden from the lung were determined as described in Materials and Methods and represent those from the entire tissue.
Data from the 2 hour timepoint at 10^6 dose are from 2 independent experiments with 9-10 animals per group. The remaining data are from one experiment with 4-5 animals per group. Data are presented as the mean (SEM).
*, $p < 0.04$; **, $p < 0.001$

97
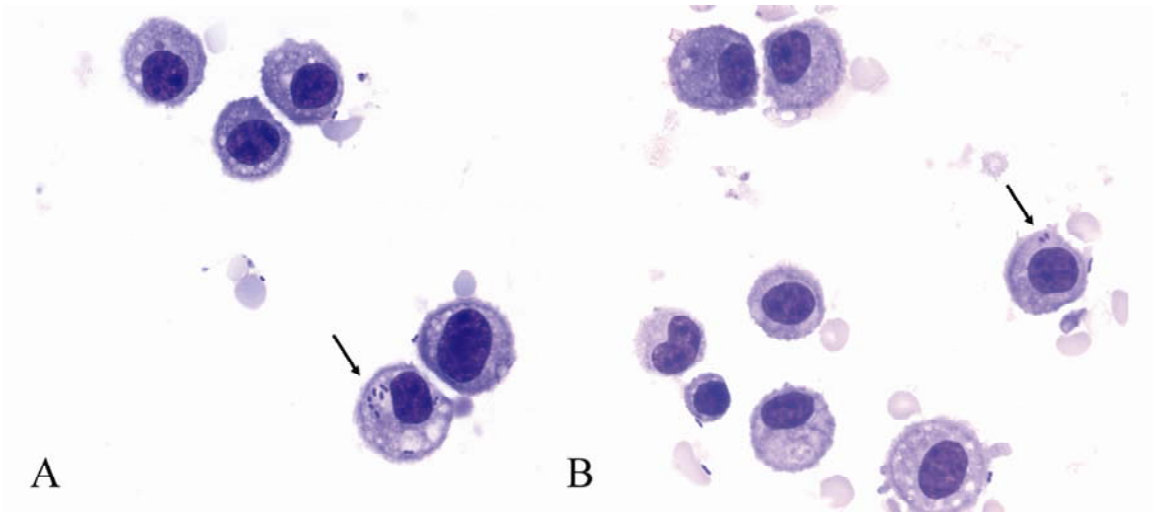
Figure III.12 *In Vivo* **Alveolar Macrophage Phagocytosis of** *K. pneumoniae*
Representative images of the cytospins are shown for strain IA565 (A) and
43816 (B) infected mice at 400X. Arrows point to bacterial cells contained
within the alveolar macrophages.

during infection likely contributes to the virulence of strain 43816. Conversely, the enhanced early phagocytosis and clearance of strain IA565 may explain its avirulence in the murine host. Interestingly, at all the time points, the lung CFU in IA565 inoculated animals was significantly lower than in 43816 infected animals.

BAL supernatants were also analyzed for protein cytokine levels of MIP-2, KC, MIP-1α, MCP-2 and TNFα (Table III.5). Although, no significant cytokine level differences were seen in the BAL fluid from these infected mice.

Collectively, these results suggest that although AMϕ enhanced phagocytosis of strain IA565 may contribute to its rapid clearance, other factors are most likely playing a role in its avirulence.

Adherence and invasion of 43816 and IA565 into type II alveolar epithelial cell lines

Since the enhanced phagocytosis of strain IA565 seems to only partially account for lack of virulence, lung epithelial adherence and invasion, as other host mechanisms responsible for IA565 avirulence, were explored. One of the key steps in bacterial pathogenesis is intimate attachment to host cell surfaces. Because the bronchial and lung epithelium comprises a large surface area and can be a primary target during lung infection, these are ideal cell types to use to assess the role of epithelial cells during *K. pneumoniae* pathogenesis. The A549 and MLE-12 cell lines are both well differentiated epithelial cells with many of the characteristics of type II alveolar pneumocytes, including surfactant production and expression of differentiated cell markers [11-13].

In this study, the human, A549, and murine, MLE-12, type II lung epithelial cell lines were used in *in vitro* adhesion and invasion assays to determine if there are any

99

**Table III.5 Alveolar Macrophage *In Vivo* Phagocytosis*:*
BAL Supernatant ELISA[a]**

Time point and Dose	Strain	MIP-2	KC	MIP-1α	MCP-1	TNFα
2hr						
	control	-	-	-	0.063 (.001)	-
2.8 x 10^5	**43816**	0.573 (0.3)	-	0.008 (0.002)	0.076 (0.002)	0.142 (0.02)
1.4 x 10^5	**IA565**	0.684 (0.2)	0.401 (0.2)	0.030 (0.01)	0.078 (0.005)	0.335 (0.1)
2hr						
	control	-	-	-	0.058 (0)	n.d.
1.4 x 10^6	**43816**	0.307 (0.1)	0.064 (0.03)	0.047 (0.01)	0.079 (0.002)	n.d.
1.4 x 10^6	**IA565**	0.327 (0.09)	0.031 (.03)	0.032 (0.01)	0.075 (0.01)	n.d.
4hr						
	control	-	-	-	0.063 (0.001)	-
1.1 x 10^6	**43816**	1.002 (0.2)	1.626 (0.2)	++	0.131 (0.007)	1.118 (0.2)
1.3 x 10^6	**IA565**	0.868 (0.05)	1.144 (0.3)	0.555 (0.3)	0.198 (0.03)	0.542 (0.2)

[a]BAL fluid was isolated from mice 2-4 hours post intratracheal inoculation and protein ELISAs were performed as described in Materials and Methods. Data from the 2 hour time point at 10^6 dose are from 2 independent experiments with 9-10 animals per group. The remaining data are from one experiment with 4-5 animals per group.
Data are presented as mean (SEM) in ng/mL.
n.d. = no data. ++ = levels were above the upper limit of the standard curve.

differences between strains IA565 and 43816 to account for their *in vivo* virulence.

IA565 and 43816 bacteria were incubated with A549 and MLE-12 cells and adhesion

was assessed after short incubation times and vigorous washing to remove loosely

adhered bacteria (Figure III.13). For bacterial invasion assays using A549 cells, a similar

method was performed, but after vigorous washing, cells were incubated with

gentamycin, to kill extracellular bacteria, and then lysed to release the intracellular

bacteria (Figure III.14).

There were no significant differences in adherence and invasion of IA565 and

43816 bacteria into A549 cells (Figure III.13A and Figure III.14). Similar adherence and

invasion properties of IA565 and 43816 are not surprising since both are human clinical

isolates. One would assume that since both are able to cause human respiratory disease,

they would also behave the same way *in vitro* using a human cell line. On the other hand,

if the *in vivo* pathogenicity of both strains were different in humans, the adherence and

invasion data would contradict that observation and illustrate the disconnect between *in

vivo* and *in vitro* modeling. However, the pathogenicity of each strain in humans is

unknown.

In Figure III.13B, there is a trend for a greater adherence of IA565 bacteria to

MLE-12 cells when compared to 43816 bacteria. No statistics could be run because there

were too few data points from the two experiments. However, this trend could explain

the virulence associated with strain 43816. Although adherence is an important step

during pathogenesis, binding to epithelial cells and triggering an immune response would

not be a desired effect if immune evasion was a virulence strategy. Therefore, the

enhanced ability of strain IA565 to adhere to MLE-12 cells could promote their detection

A

B
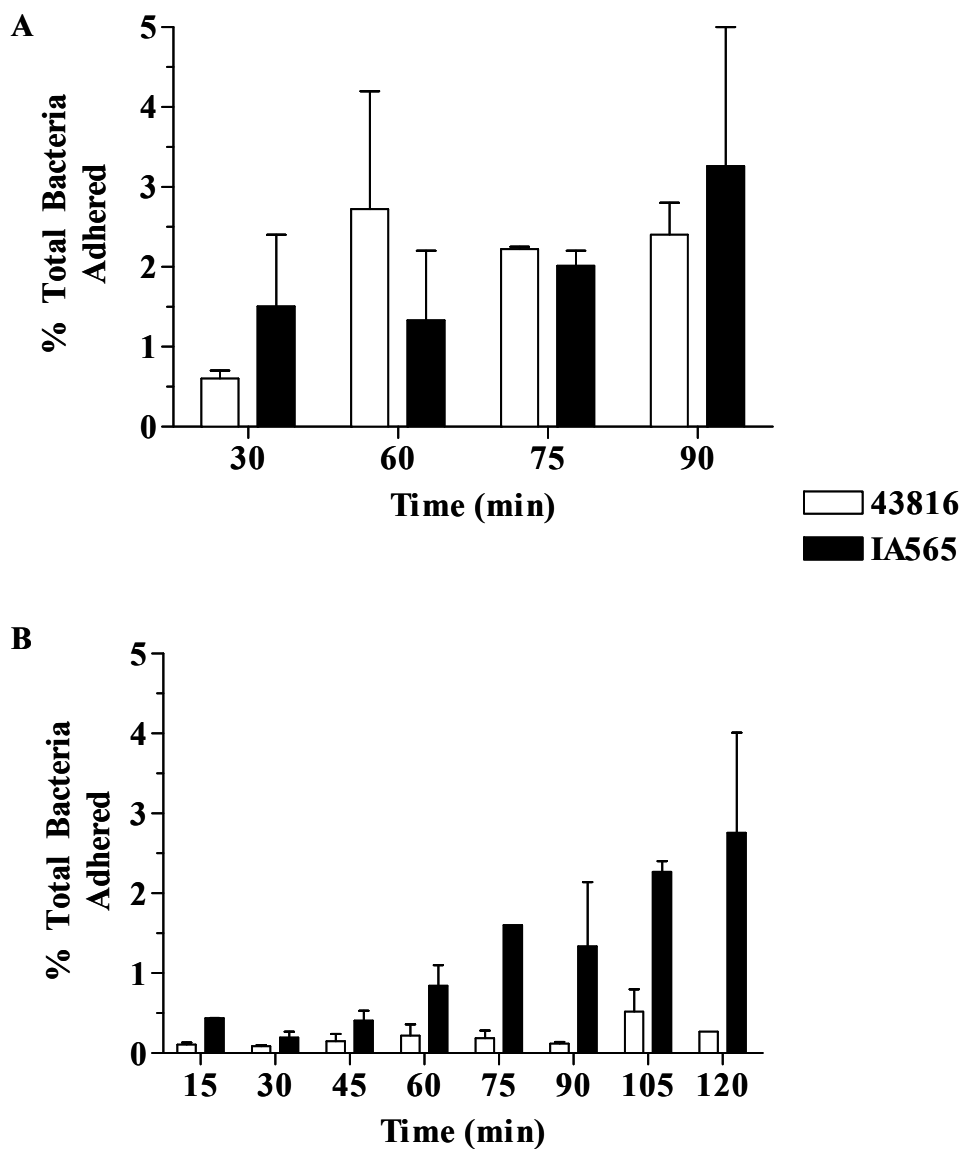
Figure III.13 Adherence of IA565 and 43816 to A549 and MLE-12 cells
A549 (A) and MLE-12 (B) cell monolayers were exposed
to IA565 and 43816 bacteria at a cell to bacteria ratio of about 1:100.
At various times post co-incubation, the cells were vigorously washed,
trypsinized (A549) or scrapped (MLE-12) and lysed. An aliquot of this
suspension was plated and bacteria CFU after treatment was determined.
Data are presented as a percent of total bacteria that adhered and are
from two independent experiments.
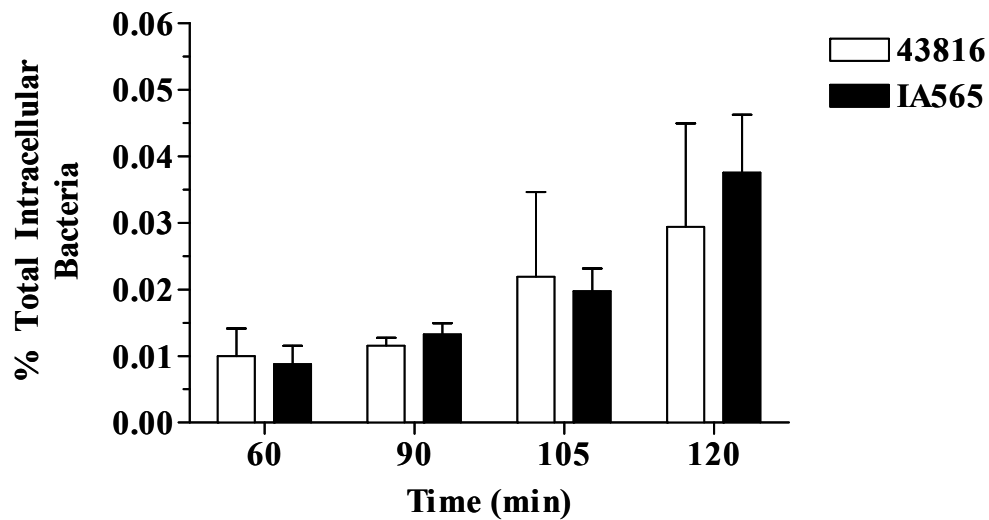
Figure III.14 Invasion of 43816 and IA565 bacteria into A549 cells
A549 cell monolayers were exposed to IA565 and 43816 bacteria
at a cell to bacteria ratio of about 1:100. At various times post co-incubation,
the cells were vigorously washed, incubated with gentamycin, trypsinized,
and lysed. An aliquot of this suspension was plated and bacteria CFU after
treatment was determined. Data are presented as a percent of total bacteria that
adhered and are from two independent experiments.

and rapid activation of the immune response to phagocytose and clear this organism from the murine host.

Cytokine levels in the supernatants of these cultures were also analyzed via ELISA to detect any differences between IA565 and 43816 induced cytokine production in these cells. Supernatants of MLE-12 cells incubated with IA565 and 43816 bacteria were harvested at 3, 6 and 12 hours post co-incubation (Table III.6). Levels of MIP-2, KC, TNFα, IL-10 or IL-12 were not detected. And of those cytokines that were detected, MCP-1, RANTES, and IP-10, no significant differences were observed. Supernatants of A549 cells incubated with IA565 and 43816 bacteria were harvested at 6 and 24 hours post co-incubation (Figure III.15). There were no significant differences in the levels of IL-8, RANTES, and MCP-1 in the supernatant of A549 cells cultured with 43816 and IA565 bacteria (Figure III.15A, B and C, respectively).

Effect of D-mannose on adherence to MLE-12 cells and survival of IA565 and 43816 infected mice

As stated in the previous chapter, type 3 fimbriae binding to cell surfaces are not inhibited by mannose whereas type 1 fimbrial mediated binding is mannose-sensitive. To determine the potential contribution of type 1 fimbriae during *K. pneumoniae* adherence to MLE-12 cells, two independent adherence assays were carried out with or without the presence of D-mannose (Figure III.16A and B). In the first experiment, strain IA565 adherence to MLE-12 cells was inhibited with the addition of D-mannose at 120 minutes post incubation (Figure III.16A). However, this trend was not seen in the second experiment and at 45 and 75 minutes post incubation, addition of D-mannose increased

Table III.6 Supernatant Cytokine Analysis of MLE-12 Cells
Cultured with *K. pneumoniae*[a]

Time point	Sample	bacteria to cell ratio	MCP-1	RANTES	IP-10
3hr	control		0.08 (0.01)	-	-
	43816	1:1	0.216 (0.03)	-	0.003 (0.003)
		100:1	0.200 (0.02)	-	0.005 (0.003)
	IA565	1:1	0.195 (0.004)	-	0.006 (0.01)
		100:1	0.167 (0.03)	0.016 (0.02)	0.024 (0.01)
6hr	control		0.120 (0.01)	0.067 (0.01)	0.013 (0.001)
	43816	1:1	0.198 (0.01)	0.091 (0.006)	0.046 (0.01)
		100:1	0.197 (0.01)	0.107 (0.01)	0.064 (0.02)
	IA565	1:1	0.194 (0.03)	0.121 (0.01)	0.071 (0.002)
		100:1	0.152 (0.02)	0.081 (0.005)	0.065 (0.01)
12hr	control		0.109 (0.02)	0.140 (0.02)	0.031 (0.002)
	43816	1:1	0.157 (0.01)	0.232 (0.01)	0.113 (0.001)
		100:1	0.201 (0.04)	0.257 (0.01)	0.209 (0.02)
	IA565	1:1	0.113 (0.003)	0.319 (0.02)	0.122 (0.004)
		100:1	0.120 (0.005)	0.240 (0.01)	0.163 (0.01)

[a] Supernatants were harvested from MLE-12 cells incubated with strain IA565 and 43816 as described in Materials and Methods. For control samples, wells were in duplicates and experimental samples were plated in triplicates. Data are presented as mean (SEM) in ng/mL and are from one experiment.
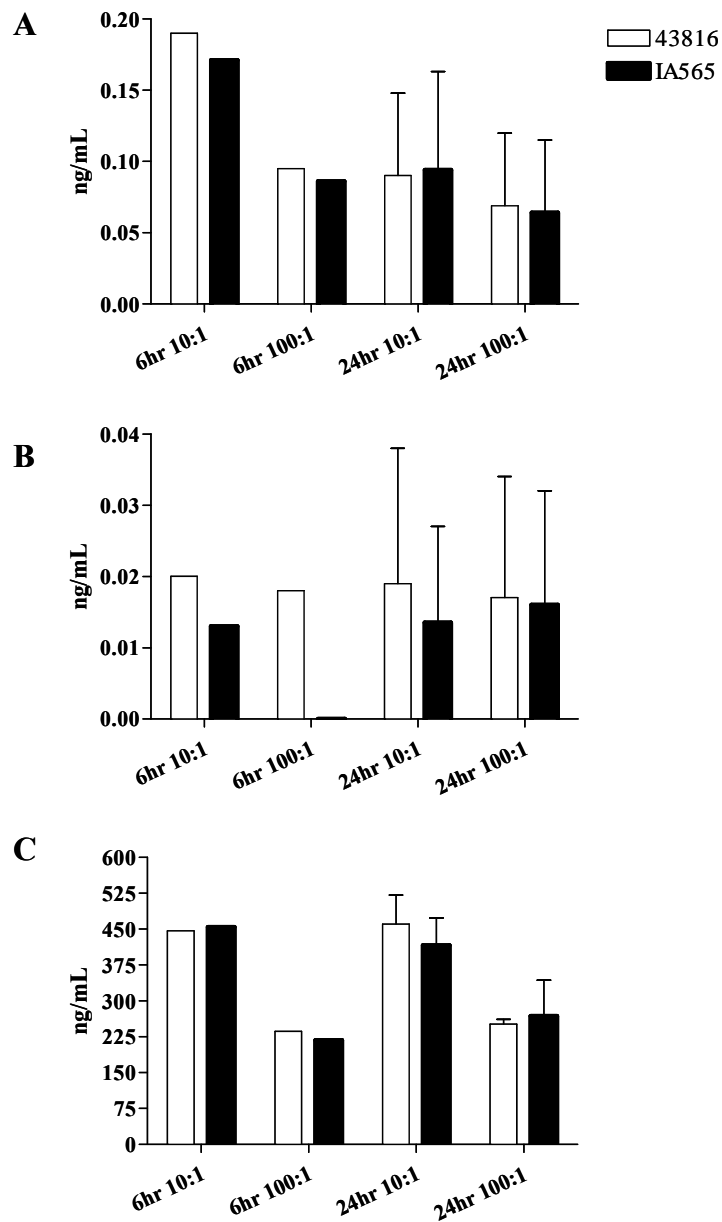
Figure III.15 Supernatant Cytokine Analysis of A549 Cells Cultured with *K. pneumoniae*

Supernatants were harvested from A549 cells incubated with strain IA565 and 43816 at a bacterium to cell ratio of 10:1 and 100:1 at 6 and 12 hour time points. Levels of IL-8 (A), RANTES (B) and MCP-1 (C) are shown. Experimental samples were plated in duplicate. Data are from two independent experiments.

Figure III.16 Effect of D-Mannose on *In Vitro* Adherence and *In Vivo* Survival
MLE-12 cell monolayers were exposed to IA565 and 43816 bacteria at a cell to bacteria ratio of about 1:100 (A) and 1:500 (B) in duplicates. D-mannose at a concentration of 50mg/mL was added. At various times post co-incubation, the cells were vigorously washed, scraped of the culture dish and lysed. Bacterial CFU after treatment was determined. Data are presented as a percent of total bacteria that adhered. (C) C57BL/6J mice were intranasally inoculated with 8 x 10^3 CFU of strain 43816 and 8 x 10^5 CFU of strain IA565 at day 0. Mice were intranasally injected with 15µL of 1mM D-mannose at day 1, 2, and 3 post infection. Data are from one experiment with 4 animals per group.
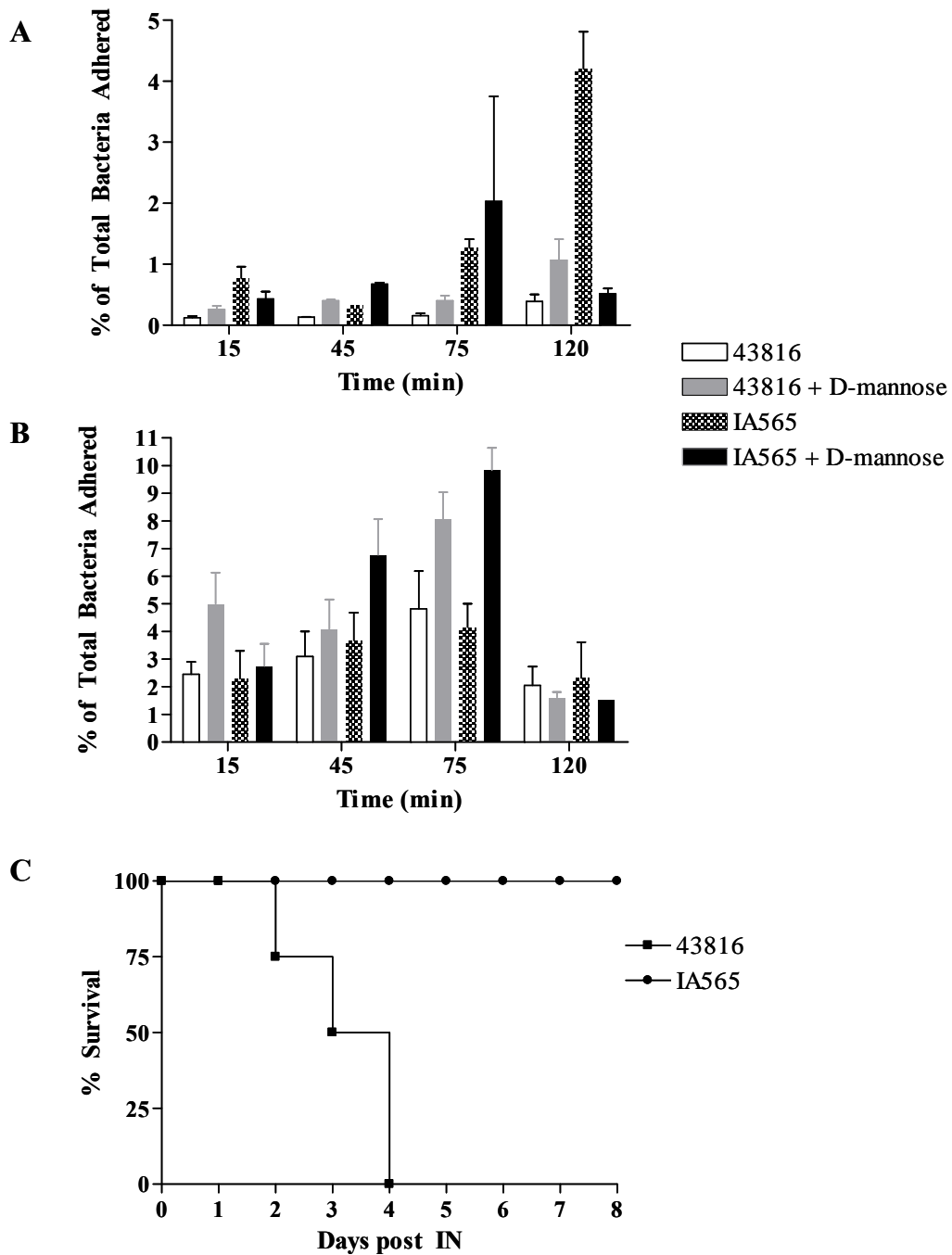
IA565 adherence (Figure III.16B). These data suggest that IA565 and 43816 binding to MLE-12 cells is type 1 fimbriae independent.

To determine if D-mannose will alter the outcome of infection, C57BL/6J mice were intranasally infected with 8 x 10^3 CFU of 43816 and 8 x 10^5 CFU of strain IA565 and were intranasally given 15μL of 1mM D-mannose at day 1, 2 and 3 post infection (Figure III.16C). Addition of D-mannose did not change the outcome of disease for 43816 infected animals (LD_{100}) and IA565 infected animals (LD_0). If during 43816 infection a decrease in mortality was observed, D-mannose would presumably be blocking or inhibiting a virulence trait. If an increase in mortality was seen in IA565 infected animals, D-mannose would presumably serve a function that allows strain IA565 to cause disease. However, it is possible that the amount of D-mannose given was not enough to observe any biological phenotypes. Thus, D-mannose did not alter the outcome of infection in these mice.

Strain IA565 stably colonizes the nasal cavity of wild-type and immunocompromised mice

Since *K. pneumoniae* strain IA565 is rapidly cleared from the lungs of mice, its ability to colonize the mucosal surfaces of the nasal cavity was investigated. C57BL/6J wild-type untreated, neutrophil, and AMϕ and neutrophil depleted mice were intranasally inoculated with 1.4 x 10^6 CFU of strain IA565. Bacterial CFU levels in the nasal cavity were assessed at 12, 24, 48 and 72 hours post inoculation (Figure III.17A). At each time point, the levels of strain IA565 CFU in the immunocompromised mice were slightly
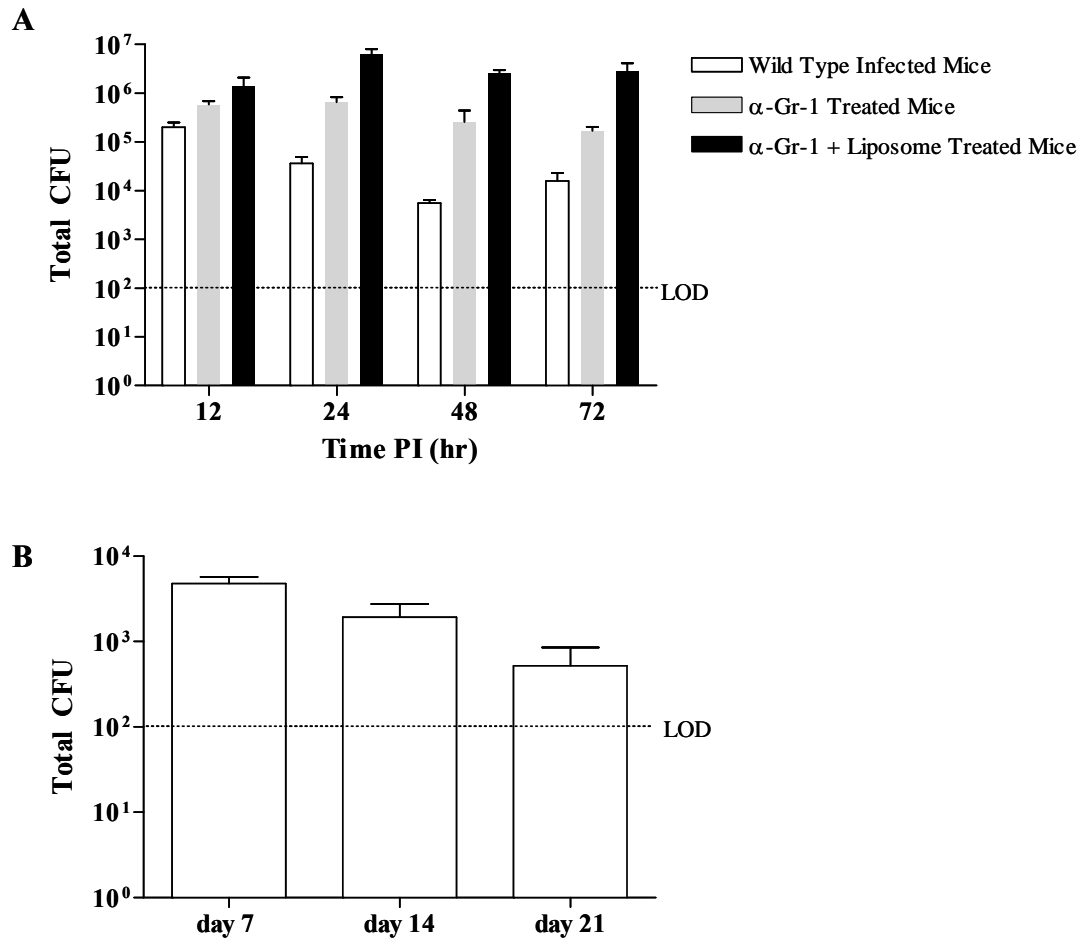
Figure III.17 Nasal Cavity CFU of IA565 Infected Wild-Type and Immunocompromised Mice

Wild-type, neutrophil, and AMφ and neutrophil depleted C57BL/6J mice (A) were intranasally inoculated with 1.4 x 10^6 CFU of strain IA565 and the nasal cavity was harvested at the indicated time points for CFU. Data were generated from one experiment with 3 mice per group. C57BL/6J mice (B) were inoculated with 10^6 CFU of strain IA565 and the nasal cavity CFU was determined. Data were generated from two independent experiments for a total of 10 mice per group. Nasal cavity bacterial numbers are for the entire organ. LOD, limit of detection.

higher than wild type untreated mice. However, this was not statistically significant

because of the small number of data points. In addition, for each group at each time

point, the CFU levels remained constant indicating that strain IA565 not only colonizes

the nasal cavity of immunocompetent and immunocompromised mice at similar levels,

this colonization is stable showing no decrease in bacterial numbers 3 days post

inoculation.

To determine how long strain IA565 can be detected in the nasal cavity,

C57BL/6J wild-type mice were intranasally inoculated with 10^6 CFU of strain IA565.

Bacterial levels were determined at week 1, 2 and 3 post challenge (Figure III.17B).

Surprisingly, there are still significant levels of IA565 in the nasal cavity even at 3 weeks

post inoculation suggesting that IA565 colonizes this site both stably and persistently.

Strain IA565 stably colonizes the nasal cavity of germ-free mice

Because immunodeficiency did not significantly affect the ability of strain IA565

to colonize the nasal cavity, Swiss Webster germ-free (GF) mice were intranasally

challenged with this strain to determine whether the absence of the normal mucosal

microbiota in the upper respiratory tract would alter IA565 colonization. Figure III.18

shows the CFU levels of strain IA565 at day 1, 7, and 21 post intranasal challenge in

C57BL/6J, Swiss Webster, and Swiss Webster GF mice. Although the CFU levels at day

21 were lower than day 1 levels of each group, there are still significant amounts of

IA565 bacteria in the nasal cavity even at 3 weeks post inoculation. Furthermore, similar

to the results obtained from the immunodeficient mice; bacterial levels were not

statistically different between the wild-type and GF mice. These data suggest that, unlike
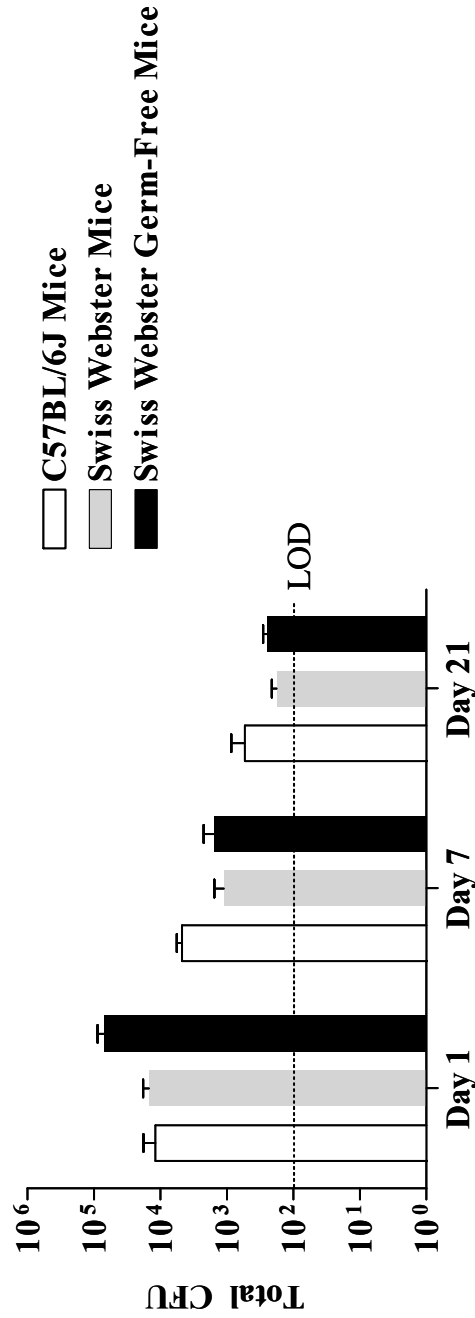
Figure III.18 IA565 Nasal Cavity Colonization in Wild-Type and Germ Free Mice
C57BL/6J, Swiss Webster, and Swiss Webster germ free mice were intranasally inoculated with 10^6 CFU of strain IA565 and the nasal cavity was harvested at the indicated time points for CFU. Data were generated from two independent experiments with 4-10 mice per group. Nasal cavity bacterial numbers are for the entire organ. LOD, limit of detection.

the lungs, strain IA565 is not rapidly cleared from the nasal cavity and can stably and

persistently colonize this organ in immunocompetent, immunodeficient and germ-free

mice. Thus, upper respiratory tract colonization of strain IA565 is unaffected by host

innate defenses and presence of the normal microbiota.

Generation of antibiotic resistant strains of IA565 to examine GI tract colonization

From the previous data, strain IA565 exhibits commensal behavior. Because the

GI tract houses more than 99% of the normal microflora, the ability of strain IA565 to

colonize this area was determined. Strain IA565S, a streptomycin resistant derivative of

IA565, and strain IA565pAM401, IA565 transformed with pAM401 containing a

chloramphenicol resistance gene, were generated to easily culture out and quantify GI

tract colonization of these strains. C57BL/6J mice were pretreated with cephoperazone, a

broad-spectrum antibiotic, for 4 days in their drinking water and then given normal water

for 24 hours. These mice were then orally gavaged with 10^7 CFU of IA565pAM401 and

IA565S on 2 consecutive days (day 0 and 1). The small and large intestine and cecum

were harvested at day 2 and 7 to determine GI tract CFU (Figure III.19). For both strains,

the CFU levels dropped about 3-5 logs from day 2 to day 7 post gavage. However,

IA565pAM401 day 7 GI tract CFU levels seemed to decrease more so than day 7 levels

of IA565S from their respective day 2 levels. This greater difference in bacterial

numbers of IA565pAM401 was attributed to the absence of selective pressure to keep the

chloramphenicol resistance marker. Since the acquired streptomycin resistance of strain

IA565S is due to a chromosomal mutation and has been shown to be stable and difficult

to eliminate [14], IA565S was used for the remainder of these studies. Figure III.20
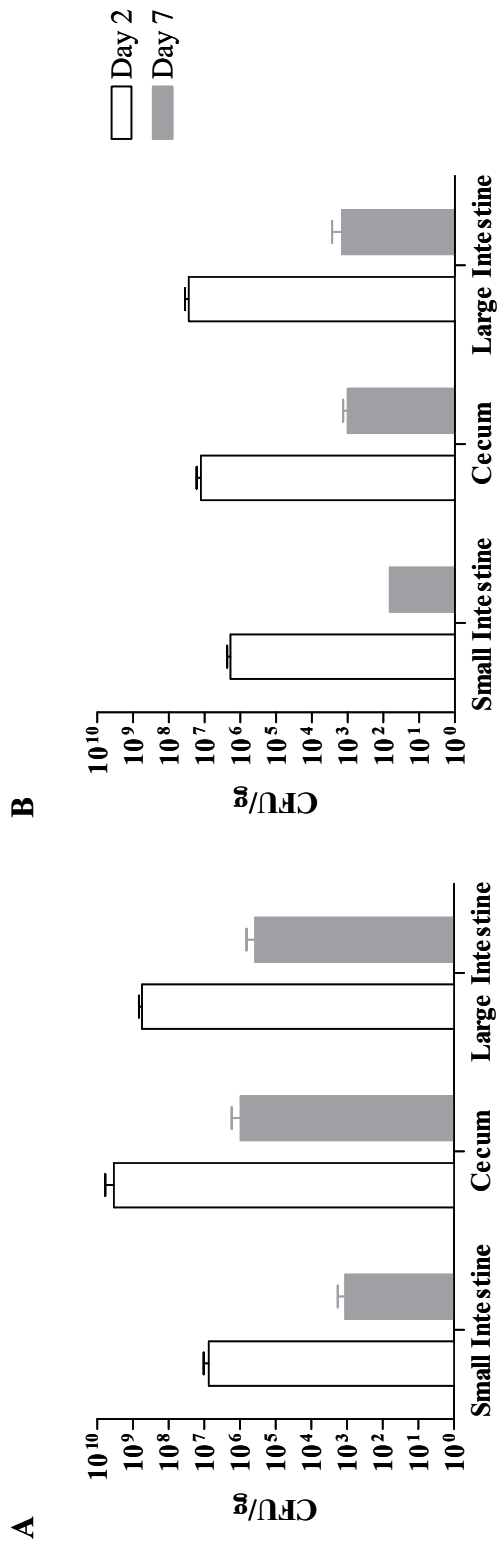
Figure III.19 Gastrointestinal Tract CFU of Mice Infected with Antibiotic Resistant Strains of IA565 C57BL/6J mice were orally gavaged with 10^7 CFU of strain IA565S (A) and IA565pAM401 (B) for two consecutive days after 4 days of cephoperazone treatment. On day 2 and day 7 post initial gavage, the small and large intestine and cecum were harvested for CFU analysis. Data were generated from one experiment with 3 mice per group.
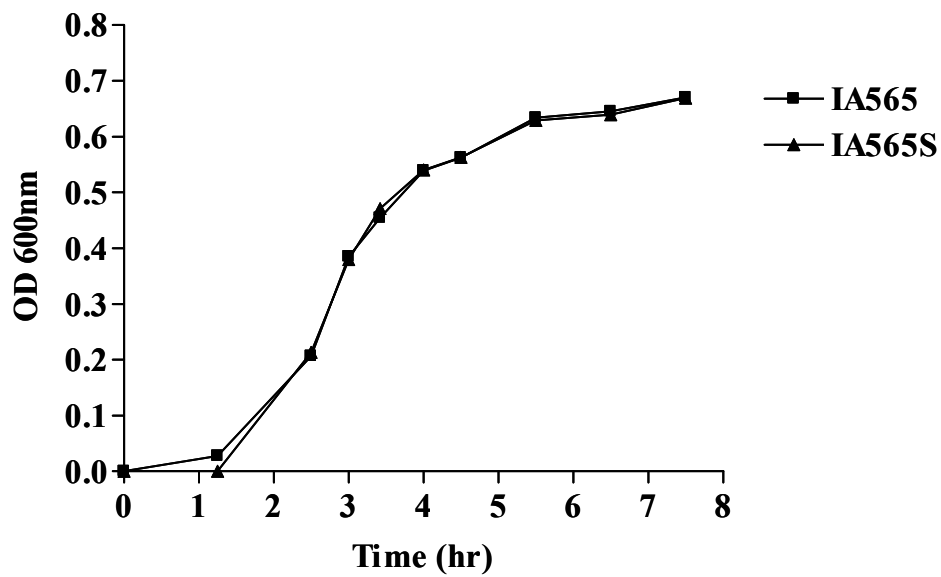
Figure III.20 Growth Curve of IA565 and IA565S
In 50mLs of LB medium, 10^8 CFU of strain IA565 and IA565S was inoculated and incubated at 37ºC while shaking at 125rpm. Aliquots were taken and plated for CFU approximately every hour.

shows an identical growth curve of both IA565 and IA565S indicating no growth defects in this derivative.

Gastrointestinal tract colonization of wild-type mice with strain IA565S

To determine the ability of IA565S to colonize the GI tract for longer periods of time, C57BL/6J mice were orally gavaged twice with 10^7 CFU of strain IA565S for 2 consecutive days after cephoperazone treatment. The GI tract CFU levels were assessed at days 6, 13, and 20 post gavage (Figure III.21). IA565S bacterial CFU were similar for each organ analyzed at each time point suggesting that this strain can both stably and persistently colonize the GI tract of mice.

Gastrointestinal tract colonization of germ-free and gnotobiotic mice with strain IA565S

Since upper respiratory tract colonization of strain IA565 is not affected by the absence of the normal microbiota, strain IA565S GI tract colonization of GF mice was determined to see if the colonization of this mucosal site is also independent of the normal flora. Swiss Webster wild-type and GF mice were intranasally inoculated with 10^6 CFU of strain IA565S. GI tract CFU levels were analyzed at day 7 and day 21 post challenge (Figure III.22). Unlike in the nasal cavity (Figure III.18), the absence of the mucosal microbiota significantly increases the colonization levels of strain IA565S in the GI tract (Figure III.22, white and black bars at each time point in each organ, p < 0.0001). The GI tract CFU in GF mice were about 10^4-10^6 fold higher than those levels in conventionally reared animals. These data suggest that the presence of the microflora in wild-type mice suppresses the growth of strain IA565S.

116
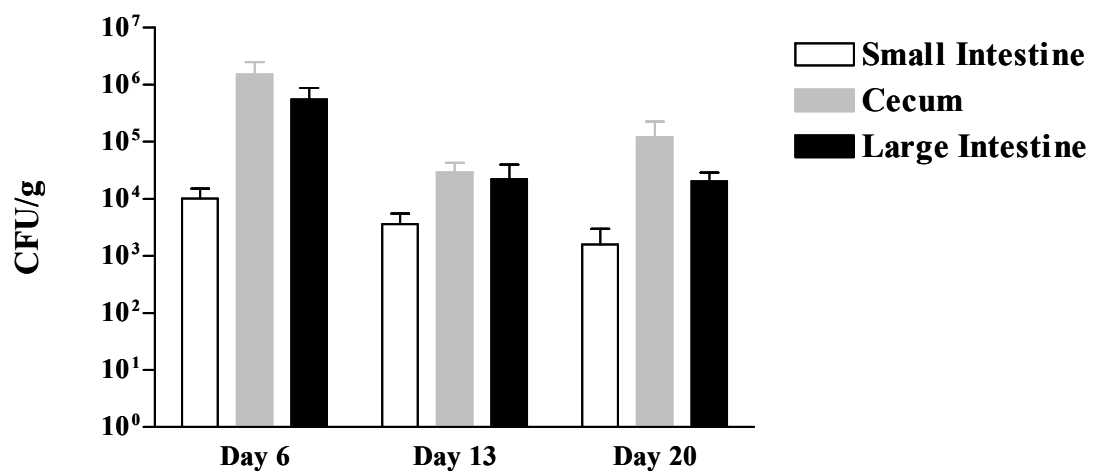
Figure III.21 Long Term IA565S Gastrointestinal Tract Colonization in Mice
C57BL/6J mice were orally gavaged with 10^7 CFU of strain IA565S for two consecutive days after 4 days of cephoperazone treatment. On day 6, 13, and 20 post initial gavage, the small and large intestine and cecum were harvested for CFU analysis. Data were generated from one experiment with 4 mice per group.
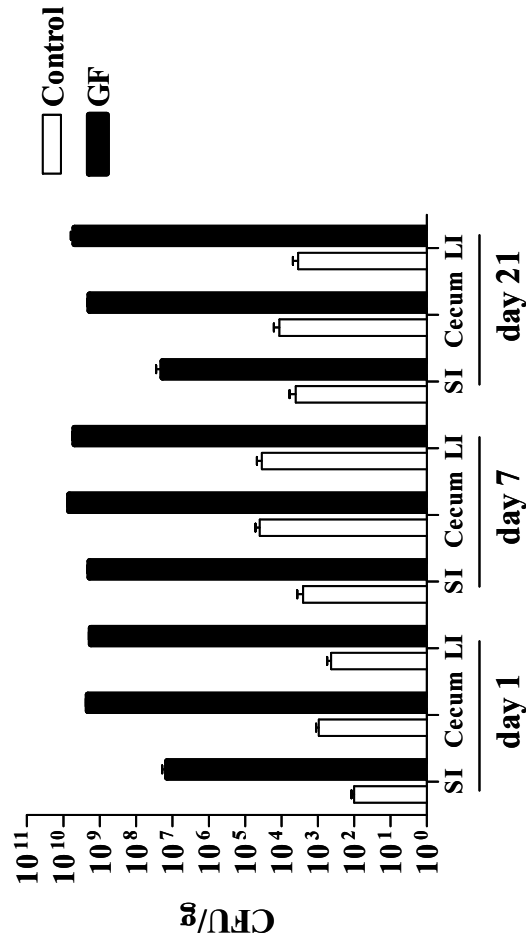
Figure III.22 IA565S GI Colonization of Swiss Webster Wild-Type and Germ Free Mice
Swiss Webster wild-type and germ free mice were intranasally inoculated with 10^6 CFU of
strain IA565S. Data were generated from 2 independent experiments with 10 mice per group.
GI organs were harvested on day 1, 7 and 21 post inoculation and assessed for CFU. SI, small
intestine; LI, large intestine.
p < 0.0001; Control mice vs GF mice.

Furthermore, Swiss Webster mice containing only the 8 strains of the altered

Schaedler flora (ASF) were orally gavaged 3 times with 10^6 CFU of strain IA565S (day

0, 2, and 4). IA565S bacterial levels in the GI tract were analyzed at day 7, 14 and 21

post gavage (Figure III.23). Interestingly, not only were bacterial CFU levels in each

organ at each time point significantly higher in the ASF mice than wild-type mice ($p <$

0.05), IA565S CFU levels fell between those recorded for the GF and wild-type mice.

Collectively, these data suggest that IA565S can both stably and persistently

colonize the GI tract of mice. However, the level of IA565S colonization is dictated by

the number of commensals in the gut. That is, there seems to be an indirectly

proportional relationship between IA565S colonization and normal levels of the gut

microflora.

Disease progression during murine colitis is unaffected in the presence of IA565

Data thus far indicate that strain IA565 can stably and benignly colonize the GI

tract of mice. As stated in Chapter I, there are commensals in the GI tract that are known

to be probiotic benefiting the host in maintaining overall good health and even alleviating

symptoms associated with IBD. To assess the probiotic potential of IA565S during

intestinal inflammation, two different murine models of colitis, induced by dextran

sodium sulfate treatment and *Citrobacter rodentium* infection, were used and progression

of disease was monitored. Figure III.24 A and B shows the experiment set-up used in the

C. rodentium and DSS model, respectively. Both DSS and *C. rodentium* treated mice

developed diarrhea at day 3-4 post treatment with the former treatment being both severe

and bloody. The oral gavage of strain IA565S into these treated mice did not reduce or
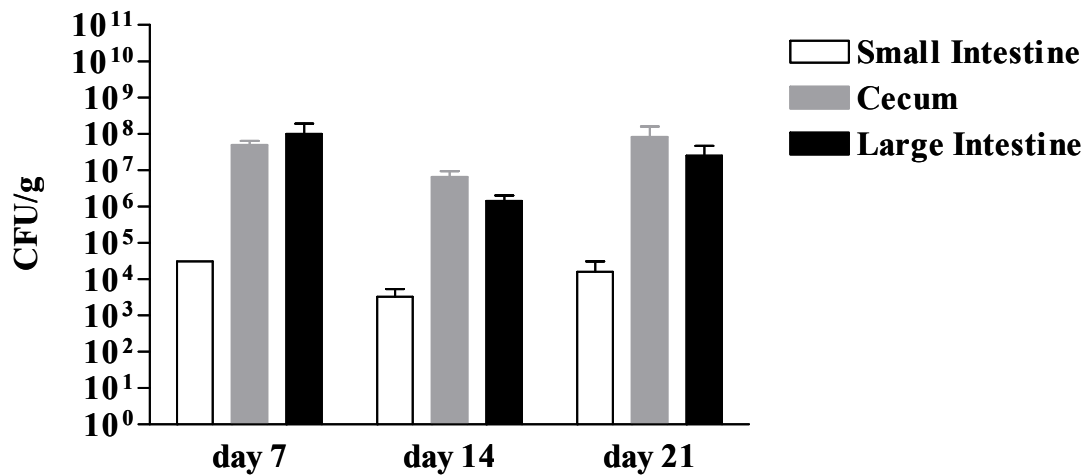
Figure III.23 IA565S GI Colonization of Swiss Webster ASF Mice
Altered Schaedler flora Swiss Webster mice were orally gavaged with 10^6 CFU of
strain IA565S at day 0, 2 and 4. Data were generated from one experiment with 2
mice per group. GI organs were harvested on day 7, 14 and 21 post inoculation
and assessed for CFU. SI, small intestine; LI, large intestine.
$p < 0.05$: Control mice vs ASF mice, except for SI on day 21.

A

gavage IA565S
10^8-10^{10} CFU

-2 -1 0 1 2 5 7 9 11 13 14

gavage
C. rodentium
10^8 CFU

collect fecal pellets

harvest GI tract for CFU

Groups:
1. IA565S alone
2. *C. rodentium* alone
3. IA565S + *C. rodentium*

B

gavage IA565S
10^8-10^9 CFU

-2 -1 0 1 2 4 6 7

Day 0-7
3% DSS in
water *ad libitum*

harvest GI tract for CFU

Groups:
1. IA565S alone
2. 3% DSS alone
3. IA565S + 3% DSS
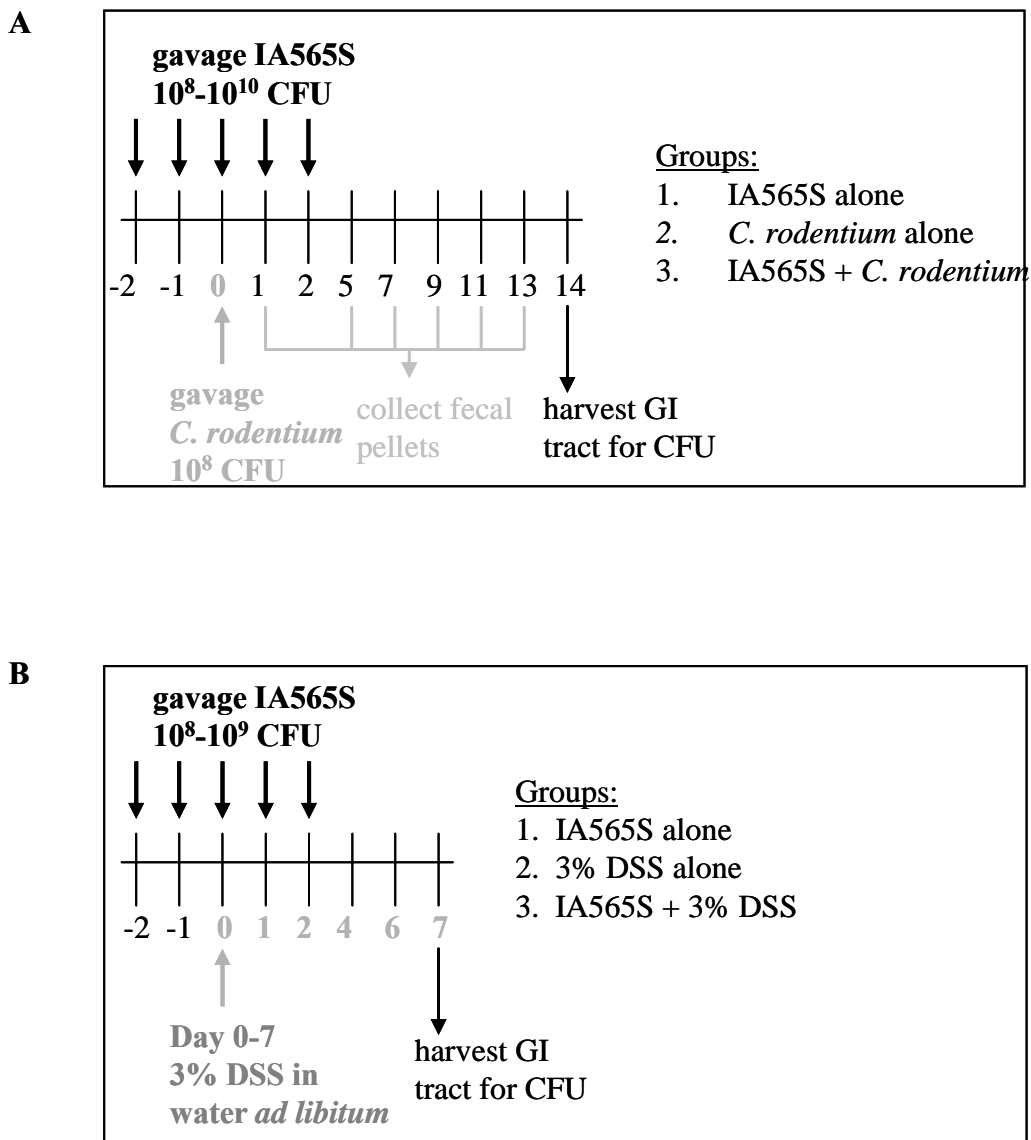
Figure III.24 Experimental Setups for Induction of Murine Colitis
Setup for *Citrobacter rodentium* (A) and 3% dextran sodium sulfate, DSS (B) induced intestinal inflammation and IA565S inoculation.

eliminate diarrhea. In addition, colons were removed for histological analysis from these mice to visualize the degree of inflammation induced (Figure III.25). The colons of both wild-type (Figure III.25A) and IA565S alone mice (Figure III.25B) display characteristics of a normal colonic mucosa with the crypts being straight, well-defined, and sitting on the muscularis mucosae. Thus, strain IA565 colonizes the GI tract very well and the host does not show signs of gastrointestinal damage indicating that strain IA565 behaves like a commensal.

No differences were noted in the *C. rodentium* alone (Figure III.25C) and IA565S and *C. rodentium* (Figure III.25D) groups. The colons from both groups displayed heavy inflammatory cell infiltrate (black arrowhead) and colonic hyperplasia (overall denser staining compared to wild-type and IA565S alone). Characteristic of *C. rodentium* induced inflammation, there is significant loss of crypt morphology with elongation (double headed arrows) and mucosal thickening (box) indicating an overall strong inflammatory response. Pretreatment with IA565S also did not affect the histological outcome of DSS treatment. DSS alone (Figure III.25E) and IA565S and DSS treated (Figure III.25F) mice were similar in that both colons exhibited inflammatory cell infiltrate (black arrowheads), severe submucosal edema (line with arrow), and crypt destruction and elongation (double headed arrows). DSS treated mice also displayed more structural damage compared to *C. rodentium* infected mice already indicating significant differences in induced inflammation between these 2 colitis models.

In the DSS model, C57BL/6J mice were orally gavaged with strain IA565S with or without 3% DSS administration. Another group of mice were given 3% DSS only. The weight of these mice was recorded (Figure III.26). The average weight of IA565S

122

Figure III.25 Representative Colon Histology of Mice with Induced Colitis

Swiss rolls displaying the normal colonic mucosa were prepared from wild-type (A) and IA565S gavaged mice (B). Colon tissue for *C. rodentium* (C) and *C. rodentium* and IA565S (D) treated mice were taken at 14 days post *C. rodentium* inoculation. Colon tissue for 3% DSS (E) and 3% DSS and IA565S (F) treated mice were prepared at 7 days post 3% DSS treatment. Double-headed arrows show crypt destruction and elongation (⟷). The box highlights mucosal thickening (☐). Black arrows indicate edema (⟶). Black arrowheads indicated leukocyte infiltrate (▼). Images on the left are at 40X magnification and images on the right at 100X magnification.
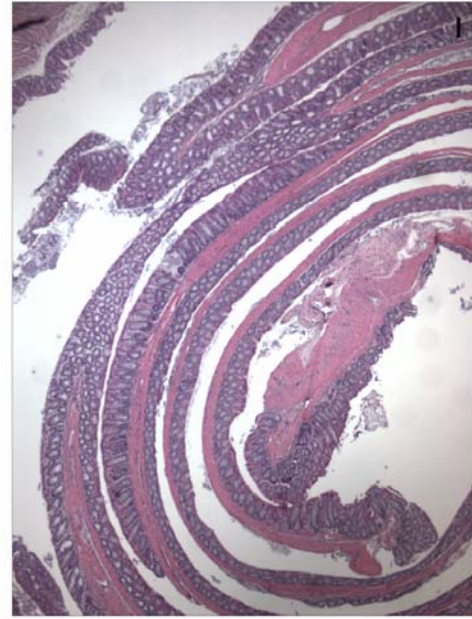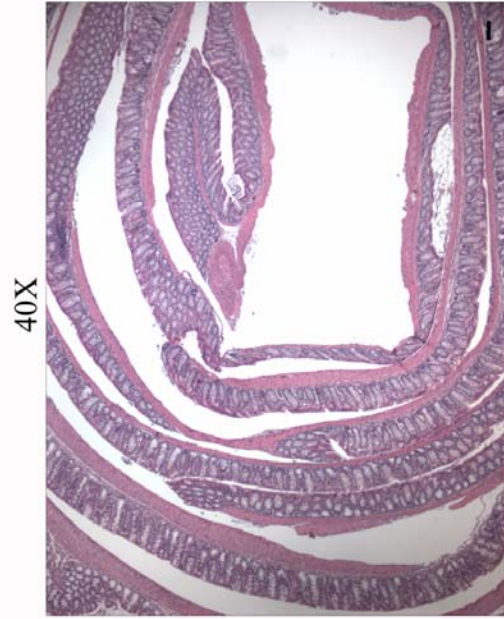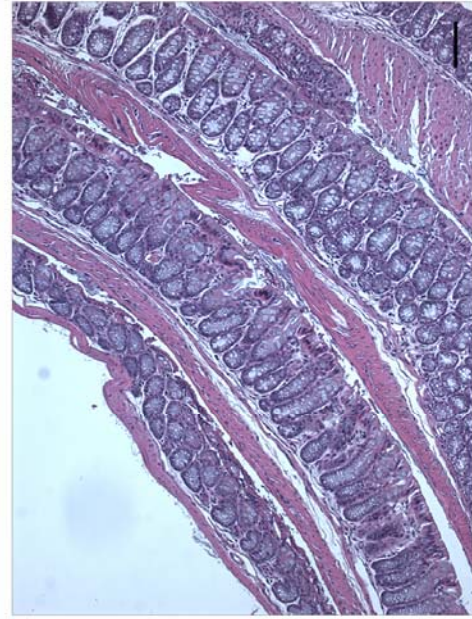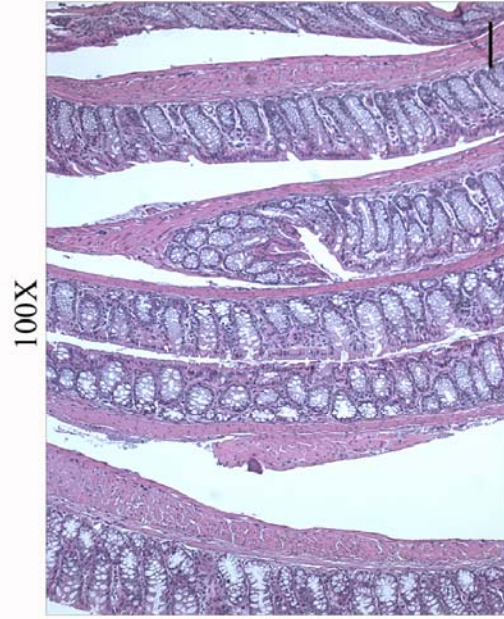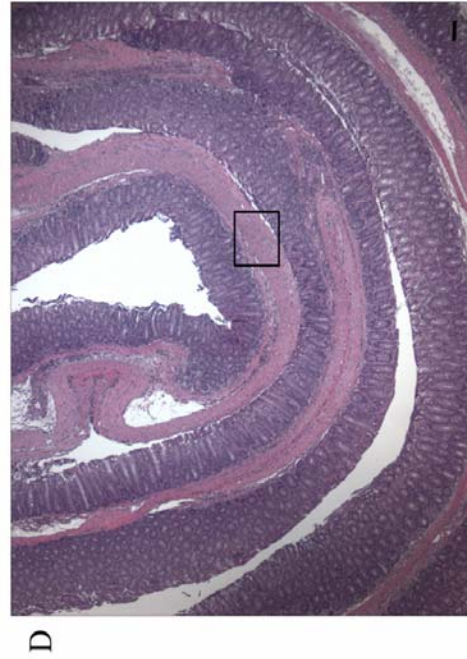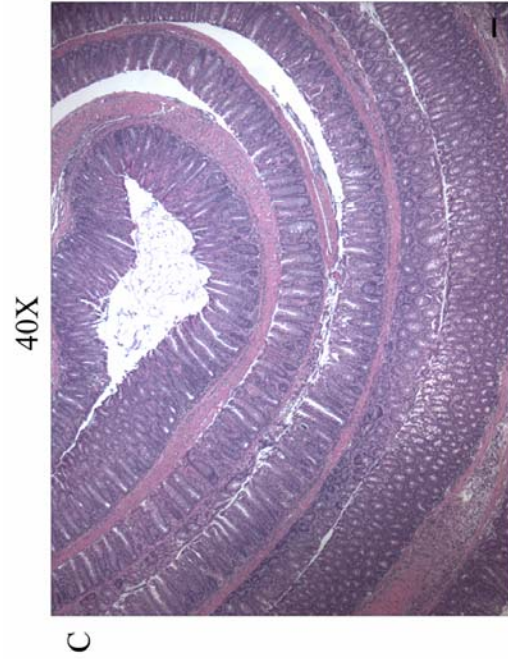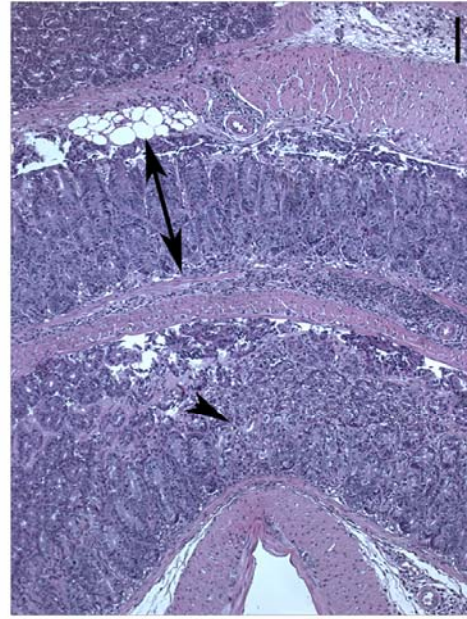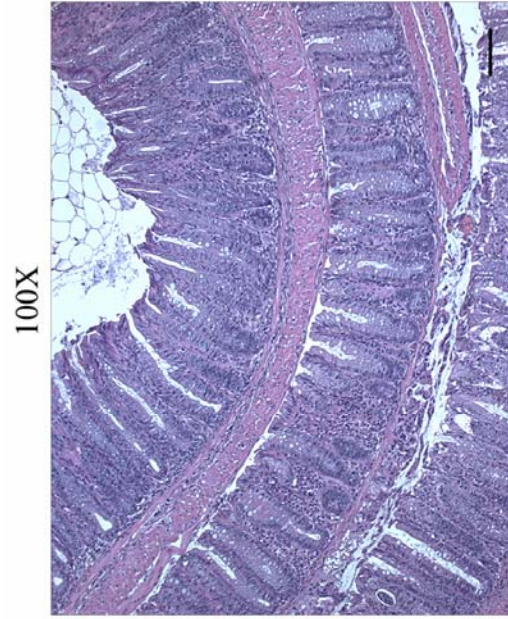
100X
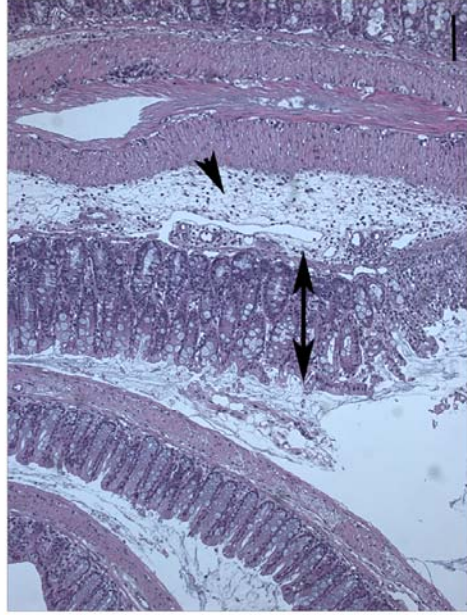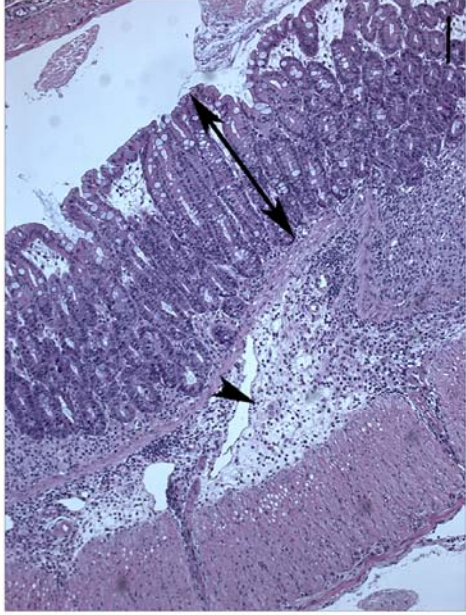
40X
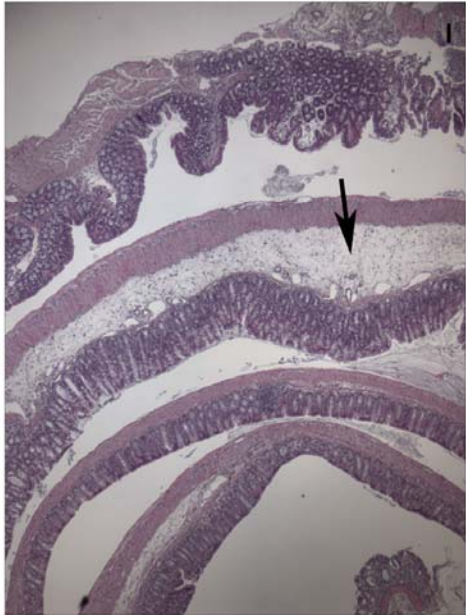
E
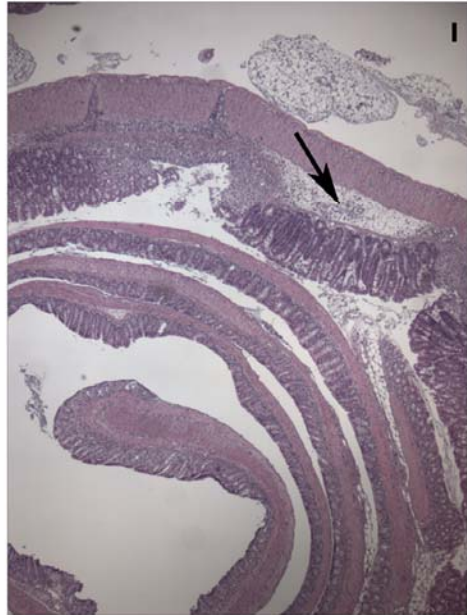
F
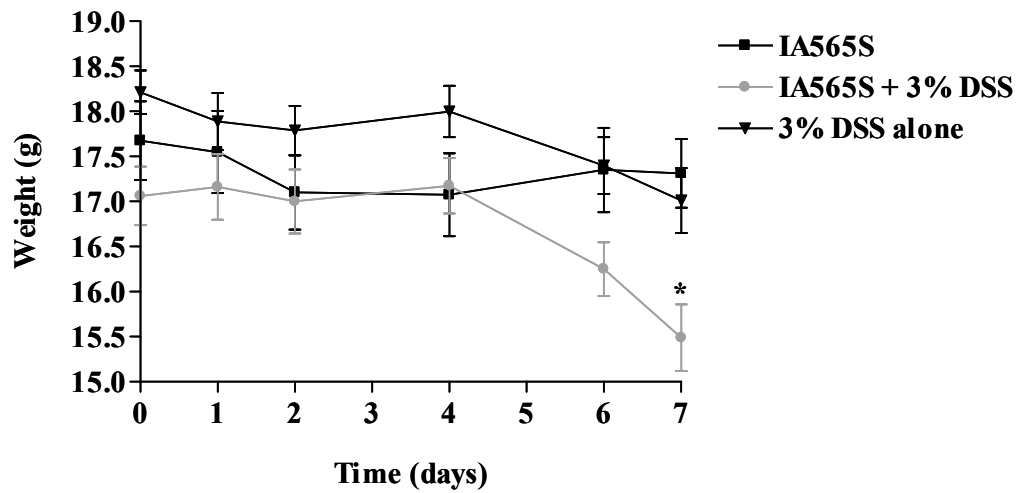
Figure III.26 Weight of IA565S Infected DSS-Treated Mice
Mice given 3% DSS with or without IA565S treatment were
weighed once a day for 7 days post DSS treatment. Data were
generated from 2 independent experiments with 8 mice per group.
*, $p < 0.005$.

and DSS treated mice were found to be significantly lower than that of the other groups

(p < 0.005). However, as stated before, IA565S treatment did not reduce diarrhea or

intestinal inflammation (Figure III.25F) suggesting that the difference in weight may be

statistically significant but not biologically significant.

Collectively, these results indicate that strain IA565S cannot alleviate or prevent

any of the disease manifestations during these models of murine colitis.

Alteration of gastrointestinal colonization of strain IA565 during murine colitis

To assess the potential alteration of IA565S GI tract colonization during intestinal

inflammation induced by DSS treatment and *C. rodentium* infection, fecal pellets and GI

tracts were collected and analyzed for IA565S CFU levels. For the *C. rodentium* model,

C57BL/6J mice were orally gavaged with strain IA565S alone, *C. rodentium* alone, or

IA565S and *C. rodentium*. Fecal pellets from these mice were collected to indirectly

assess for CFU levels of both IA565S and *C. rodentium* in the GI tract (Table III.7).

IA565S fecal CFU numbers in the IA565S alone group were at constant levels of around

10^3-10^4 CFU/g feces. IA565S fecal CFU levels in the IA565S and *C. rodentium* group

were also constant from day 1-7, decreased dramatically at day 9 and day 11, and then

jumped back from undetectable amounts to levels around 10^4 CFU/g feces. The amounts

of *C. rodentium* bacteria in the *C. rodentium* alone and the IA565S and *C. rodentium*

group peaked at day 9 and day 5, respectively at around 10^7 CFU/g before returning to

around 10^4-10^5 CFU/g feces. These mice were sacrificed at day 14 and GI tract organs

were harvested for CFU analysis (Figure III.27). The bacterial levels of IA565S in both

the IA565S alone and IA565S and *C. rodentium* group were similar for each of the

Table III.7 Fecal CFU of *Citrobacter rodentium* Infected Mice[a]

Timepoint	IA565S alone	*C. rodentium* alone	IA565S and *C. rodentium* treated group	
			IA565S CFU	*C. rodentium* CFU
Day 1	$2.3 \times 10^4 \pm 1.3 \times 10^4$	$3.0 \times 10^3 \pm 2.1 \times 10^3$	$4.0 \times 10^4 \pm 3.7 \times 10^4$	$8.2 \times 10^3 \pm 3.9 \times 10^3$
Day 5	$6.8 \times 10^3 \pm 3.6 \times 10^3$	$6.1 \times 10^4 \pm 1.8 \times 10^4$	$4.1 \times 10^4 \pm 3.9 \times 10^4$	$1.5 \times 10^7 \pm 7.6 \times 10^6$
Day 7	$8.2 \times 10^3 \pm 3.7 \times 10^3$	$1.2 \times 10^7 \pm 5.7 \times 10^6$	$4.3 \times 10^4 \pm 3.4 \times 10^4$	$3.7 \times 10^6 \pm 1.5 \times 10^6$
Day 9	$2.4 \times 10^4 \pm 1.8 \times 10^4$	$2.0 \times 10^7 \pm 9.0 \times 0^6$	238 ± 238	$4.1 \times 10^6 \pm 3.7 \times 10^6$
Day 11	$3.3 \times 10^4 \pm 3.0 \times 10^4$	$1.3 \times 10^7 \pm 7.7 \times 10^6$	0 ± 0	$1.9 \times 10^5 \pm 8.5 \times 10^4$
Day 13	$1.1 \times 10^4 \pm 1.1 \times 10^4$	$2.1 \times 10^5 \pm 1.6 \times 10^5$	$1.1 \times 10^4 \pm 1.1 \times 10^4$	$1.3 \times 10^4 \pm 8.4 \times 10^3$

[a]Fecal pellets were collected from mice infected with *C. rodentium* with or without IA565S treatment as described in Materials and Methods.
Data were generated from 2 independent experiments with 8 mice per group. Date are presented as mean CFU ± SEM.
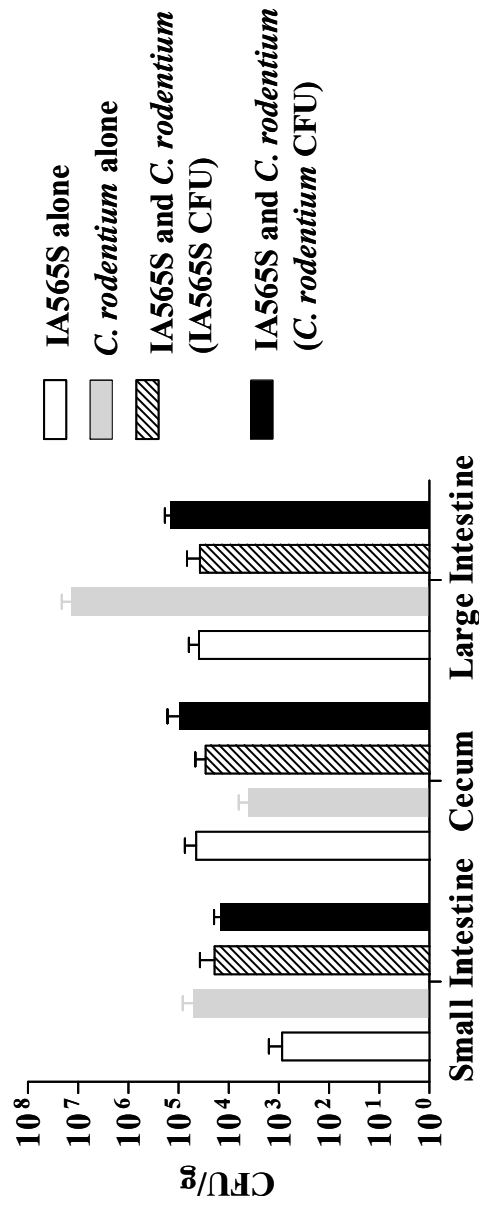
Figure III.27 IA565S and *C. rodentium* Gastrointestinal CFU in Mice with Colitis
Mice infected with *C. rodentium* with or without IA565S treatment were sacrificed at day 14 post *C. rodentium* infection. GI organs were harvested and assessed for bacterial CFU. Data were generated from 2 independent experiments with 8 mice per group.

organs (white and hatched bars). And, except for the large intestine CFU of the *C. rodentium* alone group, similar bacterial levels of *C. rodentium* were also seen for the *C. rodentium* alone and IA565S and *C. rodentium* group. The increase in the large intestinal C. rodentium CFU levels were only seen in one of the two experiments. In the second experiment, similar bacterial levels of *C. rodentium* were seen for both the *C. rodentium* alone and IA565S and *C. rodentium* group. Fecal pellet CFU titers at day 13 of each group seemed to correlate with the day 14 large intestinal CFU levels except for the *C. rodentium* alone group. The large intestinal CFU for that group was around 10^7 CFU/g whereas the fecal pellet CFU was around 10^5 CFU/g. Thus, *C. rodentium* induced intestinal inflammation did not alter IA565S GI tract colonization.

In the DSS model, C57BL/6J mice were orally gavaged with strain IA565S with or without 3% DSS administration. Another group of mice were given 3% DSS only. Fecal pellets were collected and analyzed for CFU (Figure III.28A). There were no differences observed in the fecal pellet IA565S CFU levels in either group at each of the time points (Figure III.28A). At day 7 post DSS treatment, the GI tract organs were harvested for CFU analysis. Interestingly, day 7 GI tract IA565S CFU levels between the IA565S alone and IA565S and DSS treated group were significantly different (Figure III.28B, $p < 0.0005$). With DSS treatment, the GI tract colonization of strain IA565S increases dramatically in contrast to colonization levels during *C. rodentium* infection (Figure III.27).

Collectively, these data indicate that DSS induced, but not *C. rodentium* induced, intestinal inflammation significantly alters the gastrointestinal colonization ability of *K. pneumoniae* strain IA565.

A
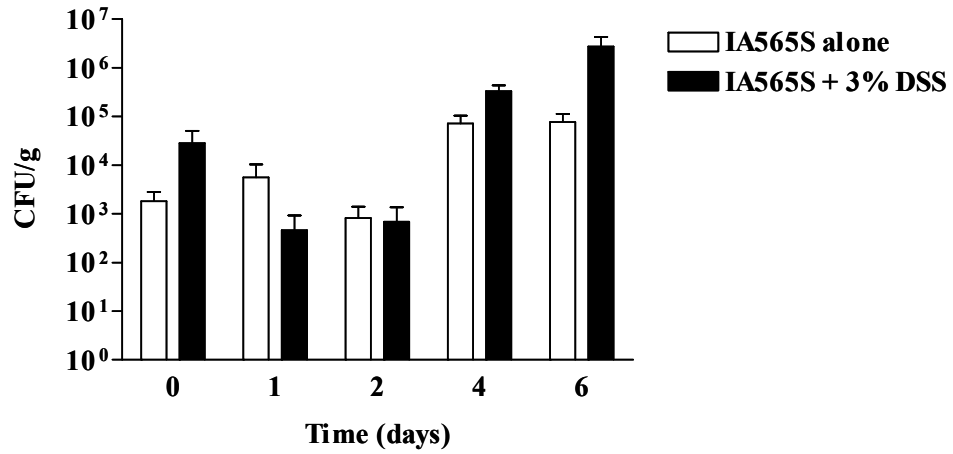
B
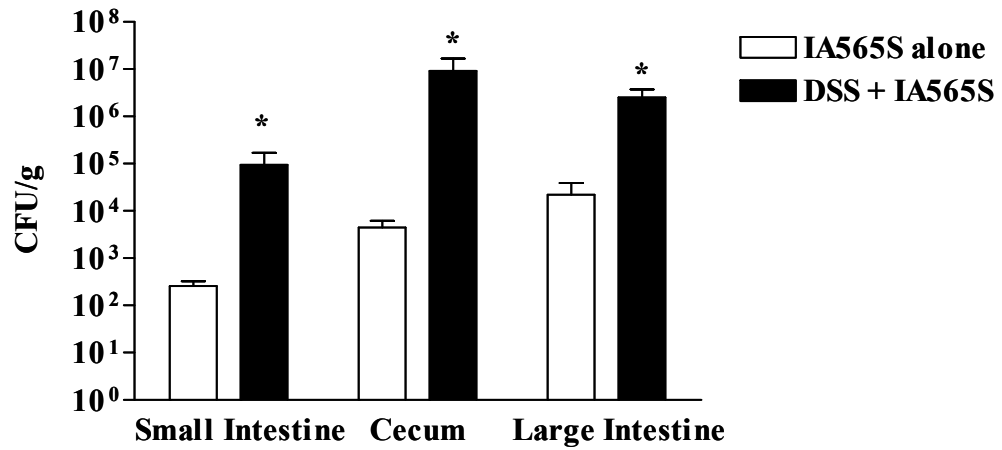
Figure III.28 Fecal Pellet and GI Tract CFU in IA565S Infected DSS-Treated Mice
Mice were given 3% DSS with or without IA565S treatment. Fecal pellets were collected and analyzed for IA565S CFU once a day for 7 days post DSS treatment (A). At day 7, animals were sacrificed and GI organs were harvested for IA565S CFU (B). Data were generated from 2 independent experiments with 8 mice per group. *, $p < 0.005$.

Discussion

Mechanisms determining lung colonization and infectious outcome of strain IA565

In culture, strain 43816 and IA565 both grow equally well in tryptic soy broth, phosphate buffered saline, mouse whole blood and bronchoalveolar lavage fluid (Figure III.8). However, when these strains are used in a murine model of acute bacterial pneumonia, the dissimilarity in pathogenesis is extreme. Murine challenge with strain IA565 induces no mortality and is very rapidly cleared from the lungs with low levels of chemokine induction (Figure III.2). Astonishingly, this is also observed in IA565-challenged mice that are depleted of TNFα, IFNγ, neutrophils, alveolar macrophages, and T and B cells (Figure III.4, 6-7). Conversely, during *K. pneumoniae* 43816 pulmonary infection, the lack of pro-inflammatory cytokines and innate phagocytic cells leads to significant increases in bacterial burden and mortality.

Strain 43816 may just also be an atypical pathogenic strain of *K. pneumoniae*. It is most commonly used in murine models of pneumonia because of its virulence. There have been comparative studies performed using various *K. pneumoniae* isolates in murine models of pneumonia. Specifically, Yadav et al. noticed a difference in the rate of clearance and level of persistence in the lungs between two *K. pneumoniae,* K2 strains, 43816 and B5055 [15]. Strain 43816 persisted longer in the host with higher levels of CFU in the lungs compared to strain B5055. In another study, a rat model was also established which displays classical symptoms for *K. pneumoniae* pneumonia found in humans using clinical isolates with two varying serotypes [16]. These strains displayed differences in their ability to establish chronic lobar pneumonia with only one causing

significant lung pathology, further emphasizing the *K. pneumoniae* strain specificity

associated with establishing respiratory tract infections. The point being that the

biological readouts, i.e., high bacterial loads and significant mortality, associated with

strain 43816 respiratory infection is not common to or representative of all *K.*

pneumoniae strains.

It is possible that within the lung environment, strain 43816 harbors a genetic

factor, absent in strain IA565, which confers some growth advantage and thus enabling

strain 43816 to cause disease. Several such factors have been described in other

pulmonary pathogens. In *Cryptococcus neoformans*, glucosylceramide (GlcCer) is a

glycosphingolipid located on the fungal cell surface. Using a *C. neoformans* GlcCer

mutant, this molecule was found to be critical for *C. neoformans* growth in the

extracellular but not the intracellular environment of the lung [17]. GlcCer was shown to

facilitate fungal cell cycle progression during growth in neutral/alkaline pH

environments, such as the lung alveolar spaces [17]. In addition, a defect in the Nox-2

gene in Group B *Streptococcus (*GBS), which encodes for a H_2O-forming NADH

oxidase, reduced virulence by only affecting aerobic growth of this mutant [18].

Anaerobic growth of the *nox2* mutant was indistinguishable from the wild-type GBS

strain. These studies show that even genetic factors involved in various metabolic

functions can play an important role in the virulence of pulmonary pathogens.

The inability of strain IA565 to grow in the lung even in extremely

immunosuppressive conditions could be attributed to the lack of metabolic factors that

would otherwise enable it to grow in the specialized environment of the alveolar space.

Another possibility is that non-cellular components of the lung are restricting IA565

growth. Surfactant, defensins, complement, lysozyme, lactoferrin, and cathelicidins are a few of many airway secretion components involved in innate antimicrobial defenses [19]. A vast majority of those compounds serve as opsonins facilitating and enhancing phagocytosis. However, since during the absence of phagocytic cells, strain IA565 is still unable to grow and persist in the lungs, it is unlikely that opsonins play a significant role in its avirulence (Figure III.4 and III.5).

In this study, using a well established murine model of acute bacterial pneumonia, IA565 does not cause respiratory disease because it is unable to grow and persist in the lung environment. The host factors identified in this study that are not responsible for this lack of growth are the proinflammatory cytokines, TNFα and IFNγ, neutrophils, alveolar macrophages and T and B cells. In the absence of these factors, strain IA565 is still unable to grow to high titers and persist in the pulmonary airspace. Thus, either some genetic property of strain IA565 is inhibiting lung growth or other innate immunity factors within the lung is prohibiting IA565 growth in this compartment.

Mechanisms determining mucosal tissue colonization of strain IA565

In normal, healthy animals, lungs are kept sterile by effective host defense mechanisms with bacteria generally confined to the upper respiratory tract [20]. Intranasal instillation of *K. pneumoniae* strain IA565 is immediately cleared in the lungs by phagocytes of the innate defense system. However, this strain is able to stably and persistently colonize the nasal cavity of wild-type mice out to 3 weeks post inoculation. Furthermore, mice that are depleted of neutrophils and alveolar macrophages displayed the same levels of IA565 CFU in the nasal cavities as wild-type mice with these

immunodeficient mice displaying no pulmonary disease manifestations (Figure III.17). Thus, in the lung, an area of the host that is normally colonized by bacteria both poorly and sparsely, strain IA565 is unable to take advantage of the induced deficiencies in the host defense mechanisms to establish a pulmonary infection. This suggests that strain IA565 lacks virulence mechanisms to cause disease. However, this strain is capable of colonizing the upper respiratory tract where other microbes are normally confined to in healthy animals. These results, coupled with the fact that *K. pneumoniae* is part of the normal flora of both humans and mice, indicate that *K. pneumoniae* strain IA565 may behave more like a commensal organism than an opportunistic pathogen.

Since the gastrointestinal tract houses more than 99% of the normal microflora, the ability of strain IA565 to colonize this mucosal site was investigated. In wild-type mice orally and intranasally instilled with a streptomycin resistant derivative of IA565, IA565S, significant bacterial titers of this strain can be found in the GI tract even at 3 weeks post inoculation (Figure III.21). Thus this strain is also able to stably and, most importantly, benignly colonize the GI tract of mice.

Furthermore, in the absence of the normal microbiota, the colonization levels of this strain increases in the gut, but remains the same in the nasal cavity as compared to CFU levels in wild-type mice (Figure III.18 and III.22). There are several possibilities to explain this interesting observation. First, some bacterial genetic factor could be limiting IA565 nasal cavity growth, giving the impression that nasal cavity colonization is independent of the microbiota. Variation in oxygen tolerance of anaerobes is reported to be related to superoxide dismutase levels, an enzyme that neutralizes superoxide radicals generated from molecular oxygen [21]. *K. pneumoniae* is a facultative anaerobe but

growth in the presence of high oxygen levels could be limiting growth in the nasal cavity

of both wild-type and germ-free mice, imposing a colonization threshold for this

bacterium. Second, the nasal cavity and the GI tract are 2 very different environments

with their own defined niches for bacterial colonization. Many microbes have been

shown to monocolonize the GI tract at levels of 10^8-10^9 CFU/g intestinal tissue [22-24].

And, although the CFU levels of the normal microbiota are not quantifiable because of

culturing limitations, these studies suggest that the GI tract is capable of accommodating

a certain maximum load of microbial CFU. This may not be the case in the nasal cavity.

It has been reported that certain terminal carbohydrate structures in the mucin of the

murine nasal cavity can dictate susceptibility to bacterial colonization [25]. Thus, nasal

cavity colonization, even in the absence of normal flora, can be limiting and adhesion

sites not as accessible or promiscuous as the GI tract.

      Interestingly, IA565S colonization of altered Schaedler flora (ASF) mice was not

as robust as in GF mice, but was more so than wild-type, conventionally reared mice

(Figure III.23). It is important to mention that the data from the ASF experiment were

generated from one experiment with 2 mice at each time point. Nonetheless, the

variations between each of the mice were minimal and CFU levels were found to be

statistically significant when compared to those of wild-type and GF mice. This suggests

that at least one of the ASF strains has the ability to either actively limit IA565S

colonization via secretion of inhibitory compounds; passively do so by minimizing

available adhesion sites and/or available nutrients; or a combination of both.

      The 8 murine commensal strains colonizing ASF mice are listed in Table I.1. Not

much work has been done with *Mucispirillum schaedleri* (ASF457), *Eubacterium*

plexicaudatum (ASF492), and *Firmicutes sp.* (ASF500). However, *Lactobacillus* species have long been known to secrete a variety of antimicrobial compounds including organic acids, hydrogen peroxide and bacteriocins, bioactive peptides with bactericidal effects on other microbes [26, 27]. In one study, *L. murinus*, isolated from rat feces, was grown in culture and secreted compounds were purified and found to inhibit *in vitro* growth of many enteric pathogens including *E. coli, Enterococcus faecalis, Salmonella typhimurium,* and *Shigella sonnei* [28]. A *Clostridium* species, isolated from conventional mice, was orally given to gnotobiotic mice followed by *Shigella flexneri* inoculation. This limited *S. flexneri* growth to below limits of detection in the GI tract [29]. Furthermore, culture filtrates of *Bacteroides distasonis* was shown to inhibit polymorphonuclear cell chemotaxis and migration *in vitro* [30]. Thus, 5 of the 8 ASF strains (ASF360, ASF361, ASF356, ASF519 and ASF 502) are likely candidates in limiting strain IA565S growth either by inhibiting host functions, secreting antimicrobial products or by some other mechanism of colonization resistance.

Because strain IA565 can colonize the GI tract so stably and in such high titers in wild-type and GF mice without causing sickness, its ability to elicit health benefits during murine colitis was examined. The use of probiotics in murine models of colitis has been previously described. In *Citrobacter rodentium* induced colitis, administration of *Bacillus subtilis* spores, *Lactobacillus rhamnosus*, and *L. acidophilus* attenuated the effect of *C. rodentium* in those mice as measured by decreased CFU levels in the colon and decreased enteropathology in the colonic tissue [31-34]. In models of dextran sodium sulfate (DSS) induced colitis, mice orally given DSS and *E. coli* Strain Nissle 1917 resulted in alleviation of body weight loss and colonic damage when compared to

mice treated with DSS only [35, 36]. However, oral administration of strain IA565S did not prevent or reduce diarrhea, weight loss or intestinal inflammation in these *C. rodentium* and DSS treated mice (Figure III.25 and III.26) indicating that strain IA565 does not behave like a probiotic in these models.

Interestingly, IA565S GI CFU levels in DSS treated mice were significantly higher than those in DSS only treated mice (Figure III.28B). In contrast, *C. rodentium* infection did not alter IA565S CFU titers in the GI tract (Figure III.27). This may be attributed to the inherent differences in initiation of inflammation during DSS and *C. rodentium* induced colitis.

During self-limiting *C. rodentium* intestinal infections, there is heavy inflammatory cell infiltration of the mucosa and submucosa with lymphocytes, macrophages, neutrophils and mast cells [8]. T and B cells have been shown to mediate much of the tissue pathology observed during *C. rodentium* infection [37]. The T-lymphocytes present during inflammation are in environments of high IFNγ, TNFα, and IL-12 levels and are, thus, Th1 polarized [38]. In addition, keratinocyte growth factor, responsible for epithelial cell proliferation, is upregulated on the mucosal epithelium during *C. rodentium* infection [38]. This observation is consistent with the crypt cell hyperplasia seen during *C. rodentium* infection. The increase in epithelial cell proliferation leads to a significant increase in crypt depth and is proposed to facilitate host shedding of infected cells [39]. *C. rodentium* induced hyperplasia is reversible with the crypt cells and length returning to normal after the bacteria is cleared.

In contrast, DSS treatment immediately destroys intestinal crypt cells before the presence of inflammation [10] resulting in colonic mucosal permeability to luminal

bacteria or bacterial products. DSS-induced inflammation is not dependent on T, B, or NK cells as mice deficient in these cell types still develop colitis [40, 41]. DSS was found to be toxic to epithelial cells causing injury [41, 42] as well as to inhibit colonic epithelial cell proliferation [43, 44]. Furthermore, normal interaction between intestinal lymphocytes and epithelial cells may be disrupted since DSS can aggregate T cells *in vitro* on extracellular matrix plates [42].

The intestinal epithelial cell layer plays a vital role in mucosal tolerance and immunity [45]. Commensal bacteria and their products are usually denied access to the mucosa via the epithelial cell barrier which consists of mucin glycoproteins, antimicrobial peptides and secretory IgA [46]. In IBD patients and murine models of IBD, there is primary epithelial cell defects leading to permeability [10, 47] as well as the requirement of T cells to maintain the chronic inflammatory state [48]. Thus, the intestinal epithelium may be involved in regulating mucosal T cells. The significant increase in IA565S colonization during DSS-induced inflammation may be due to epithelial cell damage not present during *C. rodentium* induced inflammation. This cell damage results in uncontrolled mucosal permeability to microbes and unregulated T cell responses that create an environment conducive to IA565 intestinal overgrowth.

Collectively, these data indicate that *K. pneumoniae* strain IA565 is truly a murine commensal organism colonizing the upper respiratory and gastrointestinal tract in stable and persistent levels. This strain does not behave like probiotic organism eliciting beneficial and alleviative effects during murine models of IBD. However, its growth can be affected by intestinal epithelial cell damage when mucosal tolerance to the microbiota is dysregulated.

Moreover, the presence of the normal microbiota in the GI tract can suppress growth of strain IA565, whereas in the microbiota in the nasal cavity has no effect on IA565 colonization in that mucosal site. During non-specific inflammation generated during DSS treatment, IA565 growth is increased suggesting that the dysregulation of inflammatory processes has a direct effect on commensal GI growth. This is further supported by the fact that during specific inflammatory processes generated towards the self-limiting, enteric pathogen, *C. rodentium*, the GI colonization of IA565 is unaffected. Thus, the results from this study shed light on the mechanisms regulating mucosal tissue colonization of strain IA565.

These studies are the first to characterize host responses to *K. pneumoniae* strain IA565, a murine commensal, in a pneumonia model and to identify host mechanisms modulating its growth in two distal mucosal sites.

References

1. Kabha, K., et al., *Relationships among capsular structure, phagocytosis, and mouse virulence in Klebsiella pneumoniae.* Infect Immun, 1995. 63(3): p. 847-52.

2. Ofek, I., et al., *Genetic exchange of determinants for capsular polysaccharide biosynthesis between Klebsiella pneumoniae strains expressing serotypes K2 and K21a.* Infect Immun, 1993. 61(10): p. 4208-16.

3. Rath, H.C., et al., *Different subsets of enteric bacteria induce and perpetuate experimental colitis in rats and mice.* Infect Immun, 2001. 69(4): p. 2277-85.

4. Sartor, R.B., *Colitis in HLA-B27/beta 2 microglobulin transgenic rats.* Int Rev Immunol, 2000. 19(1): p. 39-50.

5. Strober, W., I.J. Fuss, and R.S. Blumberg, *The immunology of mucosal models of inflammation.* Annu Rev Immunol, 2002. 20: p. 495-549.

6. Brimnes, J., et al., *Enteric bacterial antigens activate CD4(+) T cells from scid mice with inflammatory bowel disease.* Eur J Immunol, 2001. 31(1): p. 23-31.

7. Hendrickson, B.A., R. Gokhale, and J.H. Cho, *Clinical aspects and pathophysiology of inflammatory bowel disease.* Clin Microbiol Rev, 2002. 15(1): p. 79-94.

8. Eckmann, L., *Animal models of inflammatory bowel disease: lessons from enteric infections.* Ann N Y Acad Sci, 2006. 1072: p. 28-38.

9. Okayasu, I., et al., *A novel method in the induction of reliable experimental acute and chronic ulcerative colitis in mice.* Gastroenterology, 1990. 98(3): p. 694-702.

10. Cooper, H.S., et al., *Clinicopathologic study of dextran sulfate sodium experimental murine colitis.* Lab Invest, 1993. 69(2): p. 238-49.

11. Foster, K.A., et al., *Characterization of the A549 cell line as a type II pulmonary epithelial cell model for drug metabolism.* Exp Cell Res, 1998. 243(2): p. 359-66.

12. Ikeda, K., et al., *Immortalization of subpopulations of respiratory epithelial cells from transgenic mice bearing SV40 large T antigen.* Am J Physiol, 1994. 267(3 Pt 1): p. L309-17.

13. Yavlovich, A., M. Tarshis, and S. Rottem, *Internalization and intracellular survival of Mycoplasma pneumoniae by non-phagocytic cells.* FEMS Microbiol Lett, 2004. 233(2): p. 241-6.

14. Enne, V.I., et al., *Assessment of the fitness impacts on Escherichia coli of acquisition of antibiotic resistance genes encoded by different types of genetic element.* J Antimicrob Chemother, 2005. 56(3): p. 544-51.

15. Yadav, V., et al., *Induction & resolution of lobar pneumonia following intranasal instillation with Klebsiella pneumoniae in mice.* Indian J Med Res, 2003. 118: p. 47-52.

16. Domenico, P., W.G. Johanson, Jr., and D.C. Straus, *Lobar pneumonia in rats produced by clinical isolates of Klebsiella pneumoniae.* Infect Immun, 1982. 37(1): p. 327-35.

17. Rittershaus, P.C., et al., *Glucosylceramide synthase is an essential regulator of pathogenicity of Cryptococcus neoformans.* J Clin Invest, 2006. 116(6): p. 1651-9.

18. Yamamoto, Y., et al., *The Group B Streptococcus NADH oxidase Nox-2 is involved in fatty acid biosynthesis during aerobic growth and contributes to virulence.* Mol Microbiol, 2006. 62(3): p. 772-85.

19. Mason, C.M. and S. Nelson, *Pulmonary host defenses and factors predisposing to lung infection.* Clin Chest Med, 2005. 26(1): p. 11-7.

20. Wilson, R., R.B. Dowling, and A.D. Jackson, *The biology of bacterial colonization and invasion of the respiratory mucosa.* Eur Respir J, 1996. 9(7): p. 1523-30.

21. Tally, F.P., et al., *Superoxide dismutase in anaerobic bacteria of clinical significance.* Infect Immun, 1977. 16(1): p. 20-5.

22. Bohn, E., et al., *Host gene expression in the colon of gnotobiotic interleukin-2-deficient mice colonized with commensal colitogenic or noncolitogenic bacterial strains: common patterns and bacteria strain specific signatures.* Inflamm Bowel Dis, 2006. 12(9): p. 853-62.

23. Rask, C., et al., *A full flora, but not monocolonization by Escherichia coli or lactobacilli, supports tolerogenic processing of a fed antigen.* Scand J Immunol, 2005. 61(6): p. 529-35.

24. Schroder, R., R. Blatz, and K. Linde, *Modulating the microbial colonization of the gastrointestinal tract by oral administration of defined Escherichia coli strains. III. Lipopolysaccharide-specific IgA in the intestine after oral administration of Escherichia coli.* Acta Microbiol Hung, 1990. 37(3): p. 263-7.

25.   Ueno, K., Y. Hanamure, and M. Ohyama, *Differences in terminal carbohydrate structures of sialomucin in the murine nasal cavity.* Eur Arch Otorhinolaryngol, 1994. 251(2): p. 119-22.

26.   Klaenhammer, T.R., *Genetics of bacteriocins produced by lactic acid bacteria.* FEMS Microbiol Rev, 1993. 12(1-3): p. 39-85.

27.   Vesterlund, S., et al., *Staphylococcus aureus adheres to human intestinal mucus but can be displaced by certain lactic acid bacteria.* Microbiology, 2006. 152(Pt 6): p. 1819-26.

28.   Nardi, R.M., et al., *Purification and molecular characterization of antibacterial compounds produced by Lactobacillus murinus strain L1.* J Appl Microbiol, 2005. 99(3): p. 649-56.

29.   Ducluzeau, R., et al., *Antagonistic effect of extremely oxygen-sensitive clostridia from the microflora of conventional mice and of Escherichia coli against Shigella flexneri in the digestive tract of gnotobiotic mice.* Infect Immun, 1977. 17(2): p. 415-24.

30.   Rotstein, O.D., et al., *A Bacteroides by-product inhibits human polymorphonuclear leukocyte function.* Arch Surg, 1986. 121(1): p. 82-8.

31.   Chen, C.C., et al., *Preinoculation with the probiotic Lactobacillus acidophilus early in life effectively inhibits murine Citrobacter rodentium colitis.* Pediatr Res, 2005. 58(6): p. 1185-91.

32.   D'Arienzo, R., et al., *Bacillus subtilis spores reduce susceptibility to Citrobacter rodentium-mediated enteropathy in a mouse model.* Res Microbiol, 2006. 157(9): p. 891-7. Epub 2006 Sep 26.

33.   Johnson-Henry, K.C., et al., *Amelioration of the effects of Citrobacter rodentium infection in mice by pretreatment with probiotics.* J Infect Dis, 2005. 191(12): p. 2106-17. Epub 2005 May 11.

34.   Varcoe, J.J., et al., *Prophylactic feeding of Lactobacillus acidophilus NCFM to mice attenuates overt colonic hyperplasia.* J Food Prot, 2003. 66(3): p. 457-65.

35.   Kamada, N., et al., *Nonpathogenic Escherichia coli strain Nissle1917 prevents murine acute and chronic colitis.* Inflamm Bowel Dis, 2005. 11(5): p. 455-63.

36.   Schultz, M., et al., *Preventive effects of Escherichia coli strain Nissle 1917 on acute and chronic intestinal inflammation in two different murine models of colitis.* Clin Diagn Lab Immunol, 2004. 11(2): p. 372-8.

37.   Vallance, B.A., et al., *Mice lacking T and B lymphocytes develop transient colitis and crypt hyperplasia yet suffer impaired bacterial clearance during Citrobacter rodentium infection.* Infect Immun, 2002. 70(4): p. 2070-81.

38.   Higgins, L.M., et al., *Citrobacter rodentium infection in mice elicits a mucosal Th1 cytokine response and lesions similar to those in murine inflammatory bowel disease.* Infect Immun, 1999. 67(6): p. 3031-9.

39.   Sherman, M.A. and D. Kalman, *Initiation and resolution of mucosal inflammation.* Immunol Res, 2004. 29(1-3): p. 241-52.

40.   Axelsson, L.G., et al., *Dextran sulfate sodium (DSS) induced experimental colitis in immunodeficient mice: effects in CD4(+) -cell depleted, athymic and NK-cell depleted SCID mice.* Inflamm Res, 1996. 45(4): p. 181-91.

41.   Dieleman, L.A., et al., *Dextran sulfate sodium-induced colitis occurs in severe combined immunodeficient mice.* Gastroenterology, 1994. 107(6): p. 1643-52.

42. Ni, J., S.F. Chen, and D. Hollander, *Effects of dextran sulphate sodium on intestinal epithelial cells and intestinal lymphocytes.* Gut, 1996. 39(2): p. 234-41.

43. Chen, Y. and M. Grisham, *Dextran Sodium (DSS)-induces colitis in rats by enhancing mucosal permeability: Effects of sulfasalazine.* Gastroenterology, 1994. 106: p. 663.

44. Tessner, T.G., et al., *Prostaglandins prevent decreased epithelial cell proliferation associated with dextran sodium sulfate injury in mice.* Gastroenterology, 1998. 115(4): p. 874-82.

45. Yu, Y., S. Sitaraman, and A.T. Gewirtz, *Intestinal epithelial cell regulation of mucosal inflammation.* Immunol Res, 2004. 29(1-3): p. 55-68.

46. Mahida, Y.R. and V.E. Rolfe, *Host-bacterial interactions in inflammatory bowel disease.* Clin Sci (Lond), 2004. 107(4): p. 331-41.

47. Hollander, D., *Intestinal permeability, leaky gut, and intestinal disorders.* Curr Gastroenterol Rep, 1999. 1(5): p. 410-6.

48. Tlaskalova-Hogenova, H., et al., *Involvement of innate immunity in the development of inflammatory and autoimmune diseases.* Ann N Y Acad Sci, 2005. 1051: p. 787-98.

Chapter IV

Identification of Putative Virulence Factors in a Pathogenic Strain of *K. pneumoniae* using a PCR-based Subtractive Hybridization Approach

Introduction

K. pneumoniae strain 43816 is an extremely virulent murine pathogen while *K. pneumoniae* strain IA565 exhibits commensal behavior. To identify the genetic factors that allow *K. pneumoniae* strain 43816 to cause disease, a PCR-based suppressive subtractive hybridization (SSH) technique was performed.

Subtractive hybridization has been used to identify pathogenicity islands, mobile genetic elements and differences in virulence gene expression in a variety of different pathogens including *Salmonella* spp [1, 2], *E. coli* [3, 4], *H. pylori* [5], and *K. pneumoniae* [6]. Employing the same PCR-based SSH technique used in this study, uniquely expressed *K. pneumoniae* sequences were found to be highly homologous to the *Bordetella pertussis* BvgAS gene [6]. BvgAS encodes a two-component signal transduction system that has been shown to play an important role in pathogenesis [7, 8]. The BvgS homologue in *K. pneumoniae*, KvgS, was mutated via introduction of an internal deletion and the resulting mutant was found to be as virulent as the parental strain in a mouse peritonitis model [9].

The major problems associated with subtractive hybridization are the difficulty in isolating a complete spectrum of differentially represented clones as well as full length clones. PCR-based SSH yields only small cDNA or genomic fragments making it hard to determine how many different clones are represented in the subtraction products. However, with the increase in DNA sequencing of microbial genomes and those procedures becoming more efficient, it may be possible to analyze those short fragments using microbial genome chips thus circumventing the aforementioned problems.

In this technique, the nucleic acid population from which one wants to isolate unique sequence (the tester) is hybridized to complementary nucleic acids that are believed to lack sequences of interest (the driver). Higher concentrations of driver nucleic acid must be present during the hybridization step as it dictates the speed of the reannealing reaction. Using single-stranded driver sequences is most efficient since the concentration of driver only slightly decreases as driver-tester duplexes are formed. Over time, driver-driver hybrids will compete with the reaction decreasing concentrations of driver sequences and reducing subtraction efficiency [10]. After tester and driver populations are allowed to hybridize, driver-tester hybrids and unhybridized driver are removed constituting the subtraction step. The tester-tester sequences remaining can be enriched using many positive selection methods, all of which require the tester population to be pretreated or labeled in some way before hybridization occurs.

Tester nucleic acid can be initially treated with the Klenow fragment of DNA polymerase I in the absence of nucleotides to trim the 3' ends. This is followed by addition of deoxynucleotide thiotriphosphates to protect the tester-tester end products and not tester-driver and unhybridized driver sequences from exonuclease activity [11].

Alternatively, the tester population is prepared by restriction endonuclease digestion to generate sticky ends while driver sequences are not. After hybridization, the reaction mixture is combined with DNA ligase and a vector with the corresponding sticky ends to clone only tester-tester duplexes efficiently. The positive selection method used in this study involved the ligation of specific primer binding sites to the ends of tester sequences to allow exponential amplification of tester-tester hybrids and only linear amplification of tester-driver duplexes.

In this study, using PCR-based genomic DNA and cDNA SSH, 9 DNA sequences unique to pathogenic *K. pneumoniae* strain 43816 were identified and found to be highly homologous to enteric bacterial genes regulating iron uptake, fimbrial-mediated adhesion, energy production and conversion, transcriptional regulation, signal transduction, restriction endonuclease activity and membrane transport.

Results

Identification of uniquely expressed sequences present in strain 43816

To identify the presence of putative virulence factors in the pathogenic strain of

K. pneumoniae 43816, a PCR-based suppressive subtractive hybridization (SSH)

technique was used to enrich for DNA sequences present in strain 43816 but not the

nonpathogenic IA565 strain (Figure IV.1). This approach can identify genomic DNA

differences as well as gene expression differences using synthesized cDNA from total

RNA. Clontech's PCR-Select™ Bacterial Genome Subtraction and PCR-Select™ cDNA

Subtraction kit protocols were performed on both genomic DNA and total cDNA from

strain IA565 and 43816 (Figure IV.1, Step A). DNA fragments obtained from both

subtractions were cloned (Figure IV.1, Step B) and then used in a differential screening

protocol to help minimize the background of high non-differentially expressed sequences

present in the subtraction mixture (Figure IV.1, Step C).

In step A, genomic and cDNA from strain 43816 and IA565 were isolated and

RsaI-digested. 43816 sequences were subdivided into 2 portions and each was ligated to

either Adaptor 1 or Adaptor 2R. Two hybridizations were performed and the

differentially expressed sequences were PCR amplified using primers complementary to

the adaptor sequences. Step A for both the cDNA and genomic SSH is shown in Figure

IV.2 and IV.3, respectively.

Total RNA or genomic DNA,
(total nucleic acid, NA)

ds tester NA
ds driver NA

Rsa1-digestion

Tester NA with Adaptor 1

Tester NA with Adaptor 2R

driver NA in excess

First Hybridization

NAs unique to tester, self-hybridization

differentially expressed tester NA

NAs common to driver and tester

NAs unique to driver, self-hybridization

Second Hybridization
(generate templates for PCR amplification from differentially expressed sequences)

Fill in ends
Exponentially amplify

A

pPCR-Script Amp SK(+)
3.0 kb
f1 (+) ori
lacZ
Kpn I
MCS
Sac I
P lac
pUC ori
ampicillin

+

B

PCR bacterial colonies from transformation experiment to confirm presence of NA in vector

C

Array PCR products on nylon membranes to generate NA dot blots

Probe with ^{32}P-dCTP labeled NAs from tester population

Figure IV.1 Suppressive Subtractive Hybridization Protocol
Modified from BD Clontech Manual. The protocol is broken up into step A-C and are referred to later on in the Results Section.
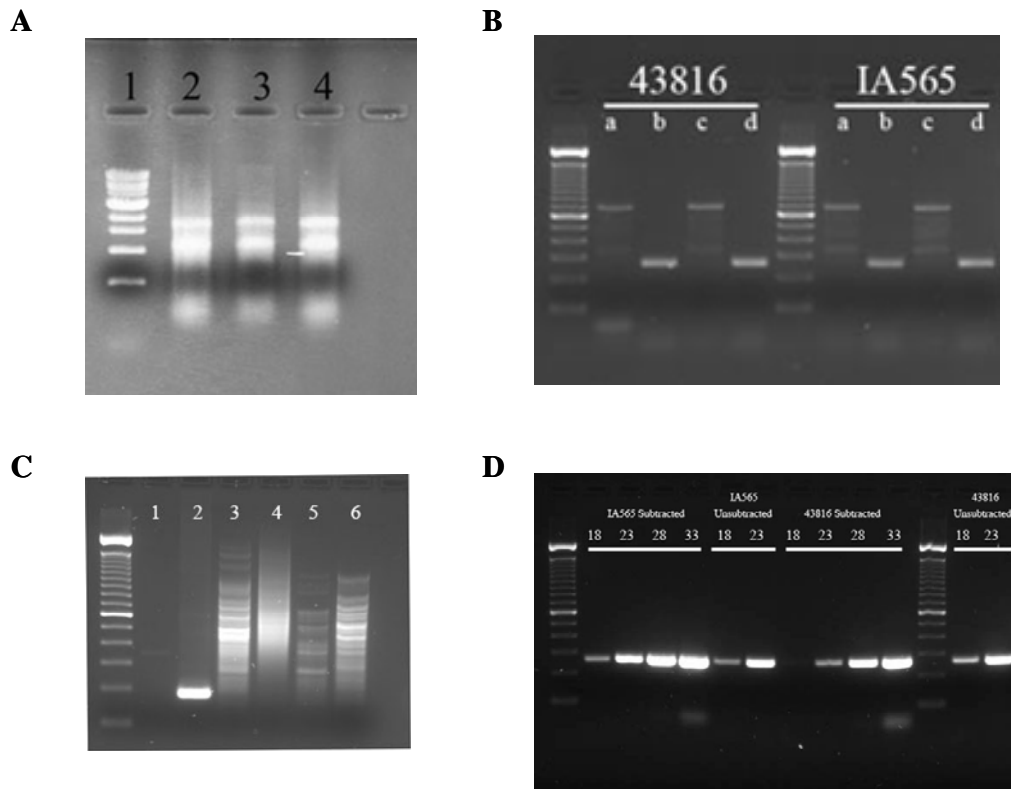
Figure IV.2 cDNA Subtractive Hybridization Step A

A. Total RNA Isolation. Lane 1, 1Kb ladder; Lane 2 and 3, strain 43816; and Lane 4, strain IA565. The major bands represent 16S and 23S rRNA, 1.5Kb and 2.9Kb respectively.

B. cDNA Adaptor Ligation Efficiency. Unmarked lanes, 100bp ladder, Lanes:
    a: Adaptor 1 ligated cDNA template with 23S Forward and PCR primer 1 primers
    b: Adaptor 1 ligated cDNA template with 23S Forward and Reverse primers
    c: Adaptor 2R ligated cDNA template with 23S Forward and PCR primer 2 primers
    d: Adaptor 2R ligated cDNA template with 23S Forward and Reverse primers
    23S Forward and Reverse primer amplicons = 273bp.

C. cDNA Subtraction Results. 100bp ladder, Lane 1, 1R control, 340bp; Lane 2, 2R control, 200bp; Lane 3, 43816 "unique cDNA"; Lane 4, 43816 unsubtracted; Lane 5, IA565 "unique cDNA"; Lane 6, IA565 unsubtracted.

D. PCR Analysis of Subtraction Efficiency using 23S Primers. 100bp ladder, 273bp amplicon. PCR cycles 18, 23, 28 and 33.

Figure IV.3 Genomic DNA Subtractive Hybridization Step A

A. Genomic DNA Isolation. Lane 1, 1Kb ladder; Lane 2 and 3, strain 43816; and Lane 4 and 5, strain IA565.
B. RsaI-digestion. Lane 1 and 2, *E. coli* control digested DNA; Lane 3, 43816 undigested; Lane 4, 43816 digested; Lane 5, IA565 undigested; and Lane 6, IA565 digested
C. DNA Adaptor Ligation Efficiency. Unmarked lanes, 100bp ladder, Lanes:
    a: Adaptor 1 ligated DNA template with 23S Forward and PCR primer 1 primers
    b: Adaptor 1 ligated DNA template with 23S Forward and Reverse primers
    c: Adaptor 2R ligated DNA template with 23S Forward and PCR primer 2 primers
    d: Adaptor 2R ligated DNA template with 23S Forward and Reverse primers
    23S Forward and Reverse primer amplicons = 273bp.
D. DNA Subtraction Results. 100bp ladder, Lane 1, *E. coli* kit control subtracted DNA; Lane 2, 43816 "unique DNA" #1; Lane 3, IA565 "unique DNA" #1; Lane 4, 43816 unsubtracted DNA; Lane 5, IA565 unsubtracted.DNA; Lane 6, 43816 "unique DNA" #2; Lane 7, IA565 "unique DNA" #2; Lane 8, *E. coli* subtracted DNA; Lane 9, 43816 unsubtracted DNA; Lane 10, IA565 unsubtracted DNA; Lane 11, *E. coli* unsubtracted DNA.
E. PCR Analysis of Subtraction Efficiency using 23S Primers. 100bp ladder, 273bp amplicon. PCR cycles 18, 21, 24 and 27. Subtracted and unsubtracted #1 refers to 43816 and subtracted and unsubtracted #2 refers to IA565.

155
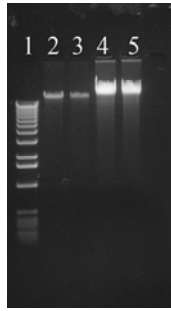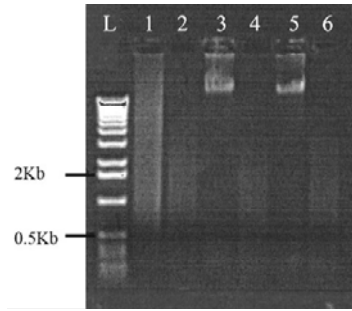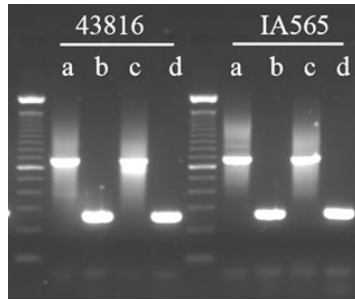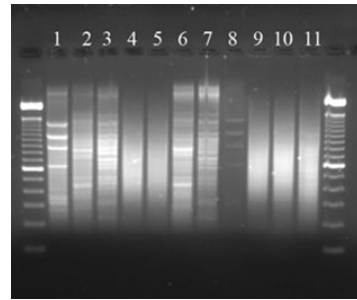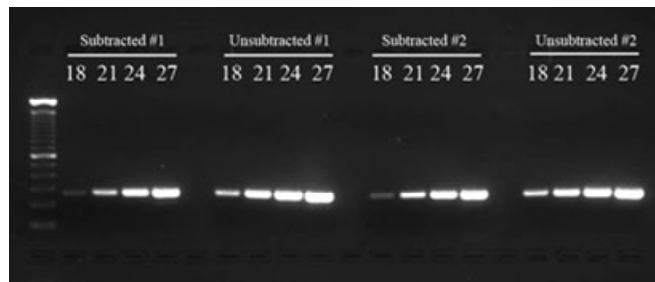
Adaptor ligation efficiency was performed to verify that at least 25% of the DNA has adaptors on both ends. This was done by comparing the amplification signal of the 23S rRNA DNA to that of the PCR product generated using an adaptor primer and one of the 23S rRNA DNA primers. Signal from the latter should be at least 25% of the former (Figure IV.1C and IV.2B). This was indeed the case for each of the subtractions.

Analysis of subtraction efficiency was done using 23S rRNA DNA primers (Figure IV.2D and IV.3E). The presence or increased intensity of the PCR product in the subtracted samples should happen during later PCR cycles compared to the unsubtracted samples. For both genomic and cDNA subtractions in the 18 PCR cycles lane, there is little to no 23S DNA amplification from the 43816 subtracted samples compared to the unsubtracted samples. This indicates that the subtraction was successful in eliminating a common gene between strains 43816 and IA565.

The subtraction products from both forward subtractions, where 43816 is the tester, and the reverse subtractions, where IA565 is the tester, were run on a gel. The banding patterns for Figure IV.2C, Lanes 3 versus 5 and for Figure IV.3D, Lanes 6 versus 7, are visually very different indicating a large population of differentially expressed sequences between the 2 strains.

The 43816 subtraction products were cloned (Figure IV.1, Step B). For the cDNA subtraction, 889 clones were obtained and for the genomic subtraction, 709 clones were obtained. Bacterial colony lysate PCR was performed on the cDNA (Figure IV.4) and genomic DNA (Figure IV.5) clones to determine both presence and size of the subtraction product insert.

Figure IV.4 cDNA Subtractive Hybridization Step B
43816 subtraction products were cloned and bacterial transformant colony lysate PCR was performed using T3 and T7 primers flanking the cloning site. Clones #: A, C101-148; B, C149-176; C, C177-232; D, C233-280; E, C281-334; F, C335-385; G, C389-442; H, C443-496; I, C497-550; J, C551-604; K, C605-658; L, C659-712; M, C713-766; N, C767-820; O, C821-874; and P, C875-889.
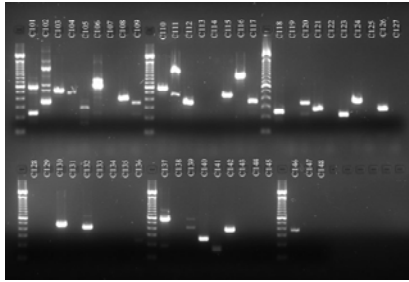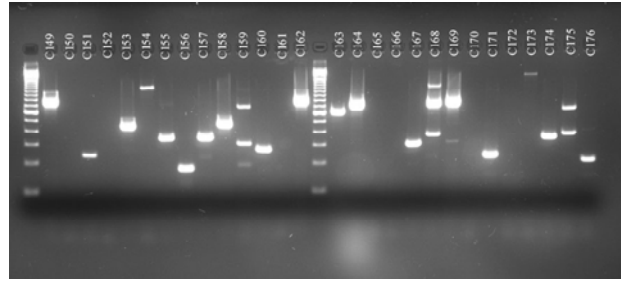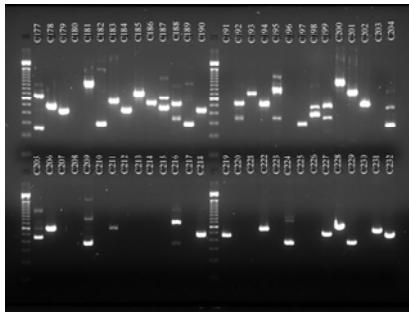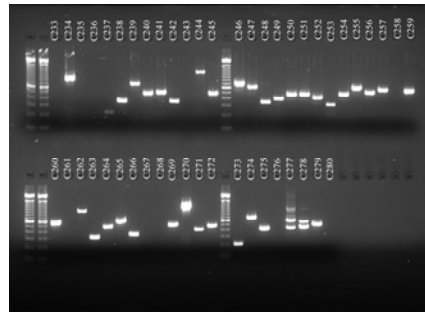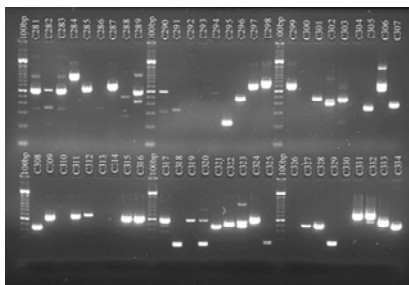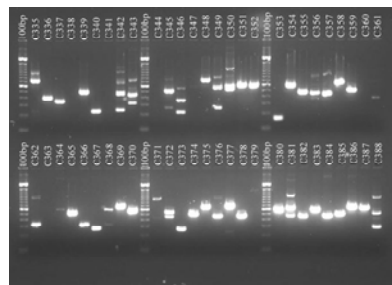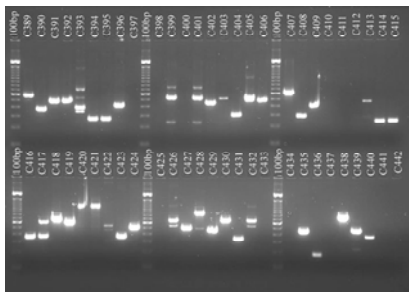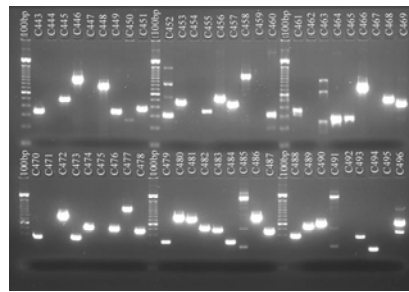
I
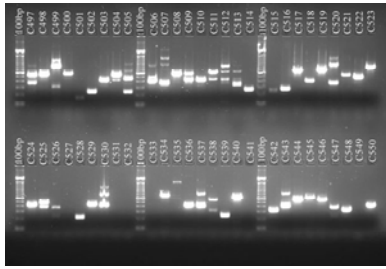
J
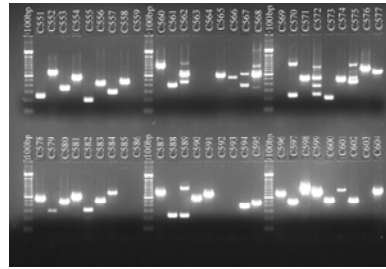
K
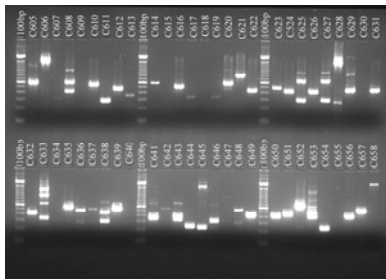
L
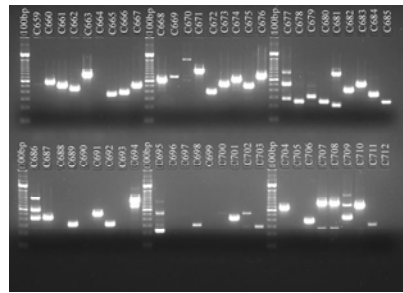
M
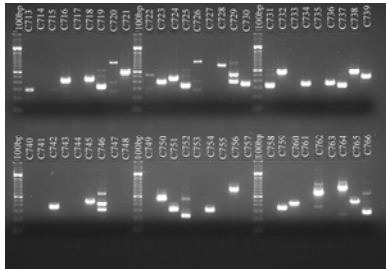
N
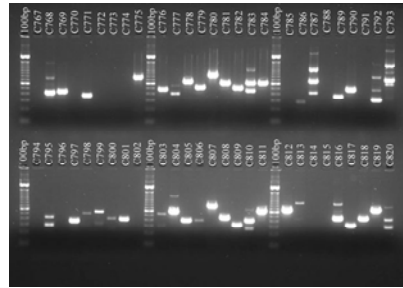
O
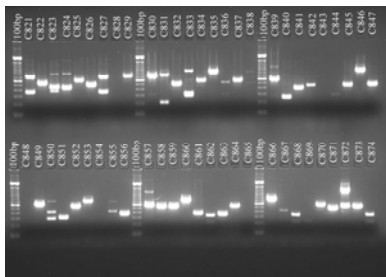
P
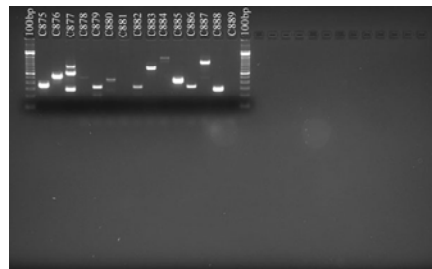
Figure IV.5 Genomic DNA Subtractive Hybridization Step B
43816 subtraction products were cloned and bacterial transformant
colony lysate PCR was performed using T3 and T7 primers flanking
the cloning site. Clones #: A, G101-154; B, G155-190; C, G191-246;
D, G247-302; E, G303-355; F, G356-409; G, G410-463; H, G464-
517; I, G518-571; J, G572-625; K, G626-679; and L, G680-709.

I
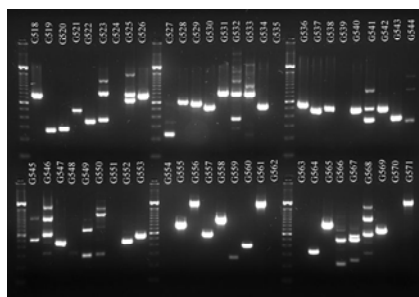
J
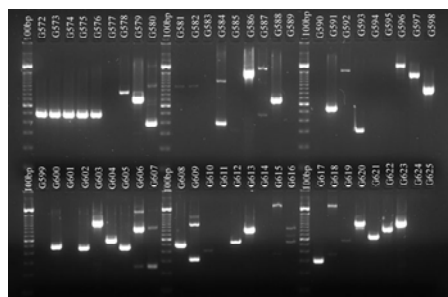
K
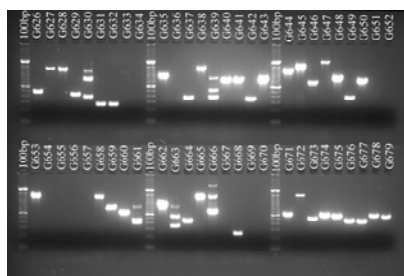
L
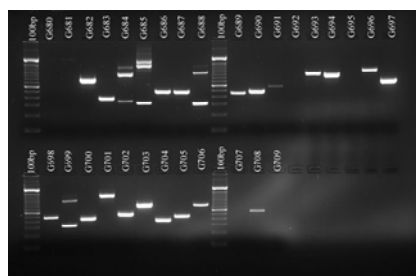
Differential screening on cloned products from SSH technique

Of the 889 clones obtained from the cDNA subtraction, 437 clones were found to contain an insert. Of the 709 clones obtained from the genomic DNA subtraction, 352 clones were found to contain an insert. Clones were grown in cultures and about 1-2μL of each culture were spotted in duplicate onto nylon membranes. A differential screening protocol (Figure IV.1, Step C) was performed to help minimize the background of non-differentially expressed sequences present in the subtraction mixture.

For the cDNA subtraction method, clones were spotted on 4 membranes which were incubated in the presence of radioactively labeled total 43816 cDNA, total IA565 cDNA, 43816 subtraction products (IA565 as driver) and IA565 subtraction products (43816 as driver) (Figure IV.6). Clones were considered to be differentially expressed if hybridization to only 43816 subtracted and unsubtracted probes occurred and if hybridization to only 43816 subtracted products occurred. If hybridization occurs with all probes, clones that hybridized to the 43816 subtracted products with a greater than 5-fold intensity were considered to be differentially expressed. Of the 437 clones analyzed, 284 of those cloned sequences were considered to be differentially expressed.

For the genomic subtraction method, clones were spotted onto 2 membranes which were then incubated in the presence of radioactively labeled total 43816 genomic DNA and total IA565 genomic DNA (Figure IV.7). Clones that only hybridized to 43816 genomic DNA were considered to be 43816 specific sequences. Of the 709 clones analyzed, 107 of those cloned sequences were found to be uniquely present in strain 43816 and absent in IA565.

Figure IV.6 cDNA Subtractive Hybridization Step C
PCR products of cloned 43816 subtraction products were arrayed on
nylon membranes and probed with ^{32}P-dCTP labeled 43816
subtraction products (upper left hand corner), IA565 subtraction
products (upper right hand corner), total 43816 cDNA (lower left hand
corner), and total IA565 cDNA (lower right hand corner).
A, Clones C103-443; B, Clones C445-780; and C, Clones C781-888.

C

1. C781-888 dot blot image:

FS

RS

1-C

2-C
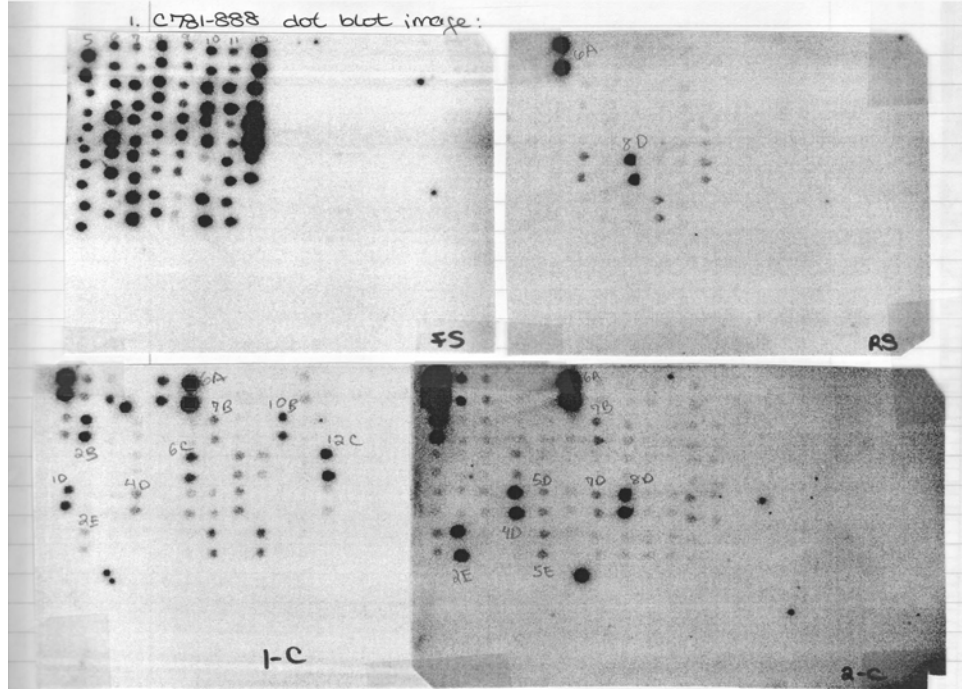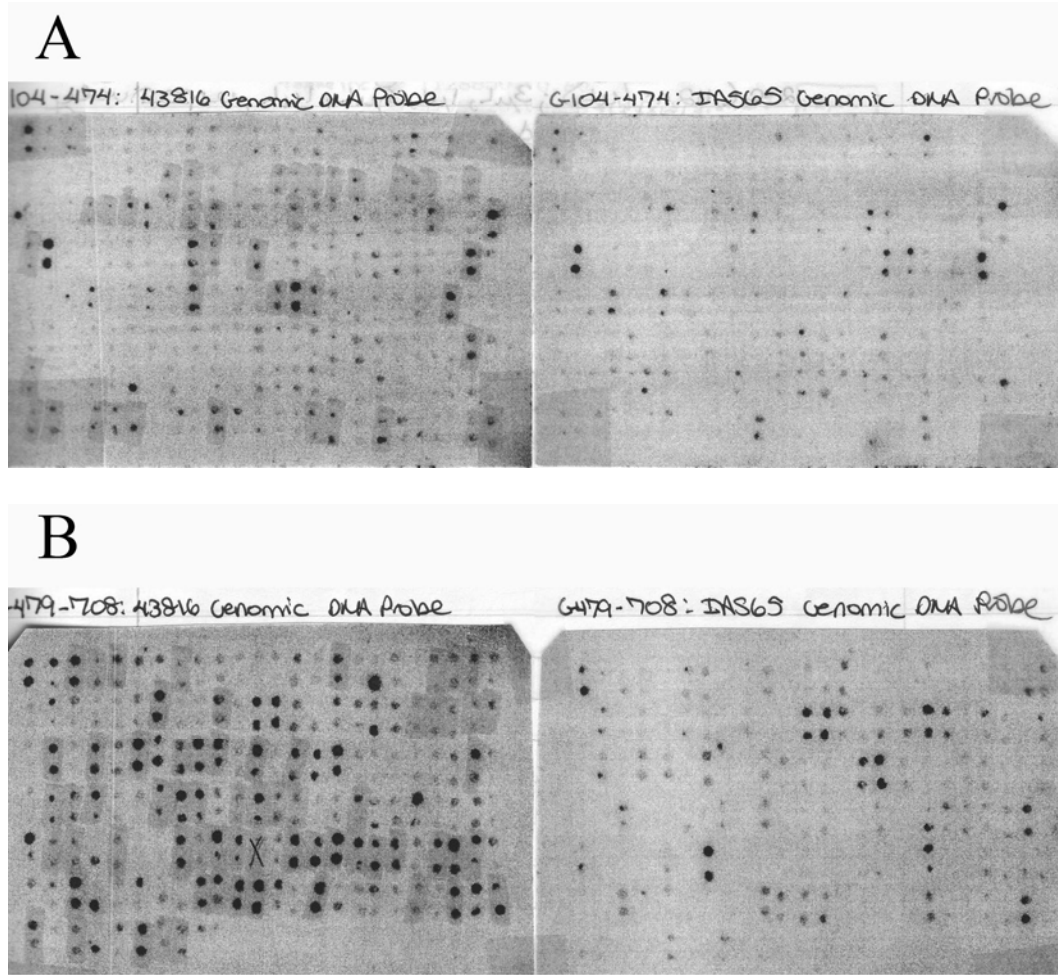
Figure IV.7 Genomic DNA Subtractive Hybridization Step C
PCR products of cloned 43816 subtraction products were arrayed on
nylon membranes and probed with ^{32}P-dCTP labeled 43816 total
genomic DNA (left) and IA565 total genomic DNA (right).
A, Clones G104-474 and B, Clones G479-708.

Identification of sequence homologies to cloned inserts from differential screening

The 284 and 107 differentially expressed cloned subtraction products from the cDNA subtraction and the genomic subtraction, respectively, were submitted to the University of Michigan DNA Sequencing Core. Homologies to microbial genes were determined using the National Center for Biotechnology Information (NCBI) microbial genome database BLAST search engine. The microbial genomes searched were Proteobacteria under the gamma subdivision of *Enterobacteriales*, which include the genera *Buchnera, Candidatus, Enterobacter, Erwinia, Escherichia, Klebsiella, Salmonella, Serratia, Shigella, Wigglesworthia,* and *Yersinia*. The results are shown in Table IV.1. Using the BLAST search results, clones were grouped into categories: KC, homologies to various Klebsiella contigs belonging to strain MGH78578; MH, multiple homologies to various bacteria; NSSF, no significant similarities found; and Sanger, homologies to the Sanger database of sequenced genomes. KC and NSSF categorized sequences were also used in a BLASTx search to obtain more sequence information. BLASTx searches the protein database using a translated nucleotide query.

Table IV.1 BLAST and BLASTx Results for Differentially Expressed Sequences[a]

Clone #	Category	% Identity	Homology to	Comments	BLASTx	% Identity	Results
C110	KC	93	Contig 1580	same as C137, C370, C732, C738	2		percentage homologies too low
C116	MH	74	S. enterica subsp. Enterica serovar Typhi str. CT18 = hypothetical protein	same as C262, C846			
C118	MH	95	E. coli O157:H7 = rrlE, rrlA, rrlC, rrlD, rrlG, rrlH, rrlB, 23S ribosomal RNA				
C130	KC	99, 88	Contig 652, 221		2	79	E. coli = D-serine dehydratase transcriptional activator
C132	KC	97	Contig 998		2	96	S. flexneria 2a str. 2457T = putative structural protein
C137	KC	93	Contig 1580	same as C110, C370, C732, C738	1		Score / e values too high
C142	KC	96	Contig 1474	same as C672	2	60	S. typhimurium LT2 = putative transcriptional regulator
C146	NSSF	60	Y. peudotuberculosis IP 32953 = multidrug efflux pump, permease/ATPase domains				
C153	NSSF	97	K. pneumoniae = maltoporin				
C154	KC	96	Contig 1527, TIGR_198628		1	65	K. pneumoniae = hypthetical protein
C155	KC	96	Contig 1690	same as C337	2	88	E. coli CFT073 = hypothetical protein yieG
C160	KC	97	Contig 876		1	82	E. coli K12 = umuC, SOS mutagenesis and repair

Table IV.1 BLAST and BLASTx Results for Differentially Expressed Sequences (cont.)[a]

Clone #	Category	% Identity	Homology to	Comments	BLASTx	% Identity	Results
C162	NSSF	62	S. flexneri 2a str. 2457T = putative DNA helicase				
C163	KC	98	Contig 855	same as C247, C354, C383, C784, C825	2	76	S. enterica CT18 = L-rhamnose operon regulatory protein
C164	MH	87	E. coli CFT073 = ybiT, hypothetical ABC transporter ATP-binding protein	same as C481, C591, C596			
C167	KC	99	Contig 1618		1	60	Burkholderia cepacia R1808 = permeases of major facilitator superfamily
C179	KC	97	Contig 623	same as C190, C503	2	43	S. enterica CT18 = possible ATP-binding protein
C181	KC	97	Contig 279		2		Score / e values too high
C183	KC	97	Contig 1329	same as C319	2		No significant similarities found
C185	NSSF	~20-40	percentage homologies too low				
C186	KC/MH	93, 82	Contig 1398, S. typhimurium LT2 = sbp, sulfate transport protein				
C190	KC	97	Contig 623	same as C179, C503	1	41	S. enterica CT18 = possible ATP-binding protein
C193	KC	95	Contig 1635	same as C239, C299, C430	2	73	S. enterica CT18 = hypothetical protein STY4650
C194	KC	93	Contig 309		2	74	S. flexneria 2a str. 2457T = putative protease maturation protein
C200	NSSF	67	S. enterica ATCC 9150 = putative phage gene				
C201	MH	98, 85	Contig 1639, E. coli K12 = glnA, glutamine synthetase	same as C287, C386			

Table IV.1 BLAST and BLASTx Results for Differentially Expressed Sequences (cont.)[a]

Clone #	Category	% Identity	Homology to	Comments	BLASTx	% Identity	Results
C202	KC	98	Contig 1071	same as C483, C790	1	92	S. flexneri str. 301 = putative LYSR-type transcriptional regulator
C211	MH	99, 80	Contig 1351, S. typhi. LT2 = fldA, flavodoxin 1; ybfE, put. SOS response protein				
C218	KC	97	Contig 710	same as C355, C378, C574, C580, C597	2	92	S. enterica ATCC 9150 = 2-amino-3-ketobutyrate coenzyme A ligase
C219	KC	100	Contig 1432		1	95	S. flexneri str. 301 = hypothetical protein
C222	KC	93	Contig 1681	same as C257	1	72	P. luminescens TT01 = hypothetical protien plu3262
C227	KC	97	Contig 1554	same as C240	1	66	E. coli CFT073 = protein elaC
C234	KC	96	Contig 1342		1	76	K. pneumoniat IA565 = type 1 fimbrial protein precursor
C237	KC	95	Contig 1575		1	91	E. coli O157:H7 = L-1,2-propanediol oxidoreductase
C238	NSSF	~20-40	percentage homologies too low				
C239	KC	95	Contig 1635	same as C193, C299, C430	2	73	S. enterica CT18 = conserved hypothetical protein yjhP
C240	KC	97	Contig 1554	same as C227	2	65	S. enterica ATCC 9150 = putative hydrolase
C244	KC	96	Contig 1721	same as C458, C477	2	63	E. coli O157:H7 = orf, hypothetical protein
C245	NSSF	61	E. coli = stbA, plasmid stable inheritance protein				
C246	MH	98, 81	Contig 964, S. enterica CT18 = putative exported protein				

Table IV.1 BLAST and BLASTx Results for Differentially Expressed Sequences (cont.)[a]

Clone #	Category	% Identity	Homology to	Comments	BLASTx	% Identity	Results
C247	KC	98	Contig 855	same as C163, C354, C383, C784, C825	1	79	S. enterica CT18 = L-rhamnose operon regulatory protein
C249	MH	98, 87	Contig 824, S. typhimurium LT2 = aceA. Isocitrate lyase				
C252	KC	96	Contig 1212		2		Score / e values too high
C253	MH/NSSF	93, 92	Contig 1621, S. typhimurium LT2 = ahpC, alkyl hydroperoxide reductase C22 subunit	same as C780			
C255	MH	98, 85	Contig 1250, S. enterica CT18 = mltD, membrabe-bound lytic murein transglycosylase D	same as C352			
C256	NSSF	48	Erwinia caratovora SCRI1043 = putative exported lipase				
C257	KC	93	Contig 1681	same as C222	1	72	P. luminescens TT01 = hypothetical protien plu3262
C259	NSSF	35	Bacteriophage E8498 = ORF10a				
C262	MH	74	S. enterica subsp. Enterica serovar Typhi str. CT18 = hypothetical protein	same as C116, C846			
C264	MH	91, 89	Contig 1419, E. coli K12 = deaD, cold-shock DeaD box ATP-dependent RNA helicase	same as C382, C776			
C265	KC	98, 99, 100	Contig 1688, 1247, 1425	same as C308, C331, C457, C840; similar to C296	1	100	K. pneumoniae = ORFA
C269	MH	96	Y. pestis biovar Med. str. 91001 = virB4, type IV secretory pathway protein	same as C616, C779			

Table IV.1 BLAST and BLASTx Results for Differentially Expressed Sequences (cont.)[a]

Clone #	Category	% Identity	Homology to	Comments	BLASTx	% Identity	Results
C270	MH/NSSF	97	E. coli O157:H7 = hypothetical lipoprotein				
C271	MH	93, 94	Contig 870, E. coli K12 = rplT, 50S ribosomal subunit protein L20				
C272	KC	96	Contig 1709		2	68	Y. pestis 91001 = putative sugar ABC transporter
C274	KC	96	Contig 945		2	90	E. coli K12 = yigO, ubiquinone/menaquinone biosynthesis methyltransferase
C275	NSSF	33	V. cholera N16961 = secA-related protein				
C279	MH	92, 98, 90	Contig 475, 355, E coli K12 = pnp, polynucleotide phosphorylase, RNA DNA synthesis	same as C427			
C284	NSSF	65	Y. pestis biovar Med. str. 91001 = putative aldo/keto reductase				
C287	MH	98, 85	Contig 1639, E. coli K12 = glnA, glutamine synthetase	same as C201, C386			
C291	NSSF/MH	96, 89	Contig 860, E. coli K12 = ordL, probable oxidoreductase				
C296	MH/KC	98, 99, 100	Contig 1688, 1247, 1425; rrl genes, 23S ribosomal RNA	similar to C265, C308, C331, C457, C840			
C297	KC	95, 97	Contig 1453, 335	same as C369, C375	1	66	E. coli O157:H7 = putative iron compound receptor
C298	NSSF	74	S. flexneri 2a str. 2457T = putative integrase				

173

Table IV.1 BLAST and BLASTx Results for Differentially Expressed Sequences (cont.)[a]

Clone #	Category	% Identity	Homology to	Comments	BLASTx	% Identity	Results
C299	KC	95	Contig 1635	same as C193, C239, C430	2	73	S. enterica CT18 = hypothetical protein STY4650
C307	KC	97	Contig 951		1	53	E. carotovora SCRI1043 = putative raffinose permease
C308	KC	98, 99, 100	Contig 1688, 1247, 1425	same as C265, C331, C457, C840; similar to C296	1	100	K. pneumoniae = ORFA
C309	MH	98, 83	Contig 1544, S. enterica CT18 = possible membrane transport protein	same as C351			
C311	KC	98, 99, 97	Contig 1688, 794, TIGR_198628	same as C545, C577, C849; similar to C435, C473, C558	2	99	K. pneumoniae = OrfB
C312	KC	97	Contig 1399		2	80	B. fungorum LB400 = anaerobic dehydrogenase, typically selenocysteine-containing
C315	NSSF	95	K. pneumoniae = virulence protein S				
C316	NSSF	98	K. pneumoniae = virulence protein S				
C319	KC	97	Contig 1329	same as C183	1		No significant similarities found
C321	NSSF	91	K. pneumoniae = maltoporin				
C322	NSSF		score/e value too high				
C328	KC/NSSF	94	Contig 1551	same as C476	2	79	S. enterica ATCC 9150 = RND family, multidrug transport protein, acriflavin resistance protein F
C331	KC	98, 99, 100	Contig 1688, 1247, 1425	same as C265, C308, C457, C840; similar to C296	2	99	K. pneumoniae = OrfA
C336	Sanger	80	Sanger_218493	same as C409, C841			

Table IV.1 BLAST and BLASTx Results for Differentially Expressed Sequences (cont.)[a]

Clone #	Category	% Identity	Homology to	Comments	BLASTx	% Identity	Results
C337	KC	96	Contig 1690	same as C155	2	87	E. coli CFT073 = yieG, hypothetical protein
C339	NSSF		score/e value too high				
C340	KC	95	Contig 1029	same as C588	1	77	E. coli O157:H7 = bacitracin resistance; possibly phosphorylates undecaprenol
C348	MH	97, 90	Contig 1623, S. typhimurium LT2 = oadB/dcoB, oxaloacetate decarboxylase beta chain	same as C534, C584, C829			
C351	MH	98, 83	Contig 1544, S. enterica CT18 = possible membrane transport protein	same as C309			
C352	MH	98, 85	Contig 1250, S. enterica CT18 = mltD, membrabe-bound lytic murein transglycosylase D	same as C255			
C354	KC	98	Contig 855	same as C163, C247, C383, C784, C825	2	80	S. enterica CT18 = L-rhamnose operon regulatory protein
C355	KC	97	Contig 710	same as C355, C378, C574. C580, C597	2	92	S. enterica ATCC 9150 = 2-amino-3-ketobutyrate coenzyme A ligase
C358	NSSF		percentage homologies too low				
C359	NSSF		percentage homologies too low				
C366	MH	98, 85	Contig 1500, E. coli CFT073 = yhbZ, hypothetical GTP-binding protein	same as C404, C484			
C369	KC	95, 97	Contig 1453, 335	same as C297, C375	1	66	E. coli CFT073 = putative iron compound receptor
C370	KC	93	Contig 1580	same as C110, C137, C732, C738	1		Score / e values too high
C374	MH	97	Contig 1500, Salmonella genomes unanotated	same as C385, C522			

175

Table IV.1 BLAST and BLASTx Results for Differentially Expressed Sequences (cont.)[a]

Clone #	Category	% Identity	Homology to	Comments	BLASTx	% Identity	Results
C375	KC	95, 97	Contig 1453, 335	same as C297, C369	1	66	E. coli CFT073 = putative iron compound receptor
C378	KC	97	Contig 710	same as C218, C355, C574, C580, C597	2	92	S. enterica ATCC 9150 = 2-amino-3-ketobutyrate coenzyme A ligase
C380	NSSF	46	P. luminescens TT01 = hypothetical protein				
C382	MH	91, 89	Contig 1419, E. coli K12 = deaD, cold-shock DeaD box ATP-dependent RNA helicase	same as C264, C776			
C383	KC	98	Contig 855	same as C163, C247, C354, C784, C825	2	80	S. enterica CT18 = L-rhamnose operon regulatory protein
C385	MH	97	Contig 1500, Salmonella genomes unanotated	same as C374, C522			
C386	MH	98, 85	Contig 1639, E. coli K12 = glnA, glutamine synthetase	same as C201, C287			
C389	MH	99, 80	Contig 1351, S. typhi. LT2 = fldA, flavodoxin 1; ybtE, put. SOS response protein	same as C211, C546, C837			
C391	MH	96	S. typhimurium LT2 = Mrr, putative restriction endonuclease	same as C602			
C392	KC	98	Contig 1152, TIGR_198628		1	99	K. pneumoniae = MdcA, malonate decarboxylase, alpha subunit
C396	KC	97	Contig 609	same as C760	1	87	S. enterica ATCC 9150 = proline dipeptidase
C402	MH	90, 94, 87	Contig 1111, 1141; E. coli CFT073 = lepA, GTP-binding protein				

Table IV.1 BLAST and BLASTx Results for Differentially Expressed Sequences (cont.)[a]

Clone #	Category	% Identity	Homology to	Comments	BLASTx	% Identity	Results
C404	MH	98, 85	Contig 1500, E. coli CFT073 = yhbZ, hypothetical GTP-binding protein	same as C366, C484			
C406	MH	99, 96	Contig 1500, E. coli EDL933 = rplU, 50S ribosomal subunit				
C407	MH	97, 83	Contig 1527, S. typhimurium LT2 = sgaT, putative PTS enzyme II				
C409	Sanger	80	Sanger_218493	same as C336, C841			
C413	KC	98, 96	Contig 1409, 1418		1	73	K. oxytoca = xynT, xyloside permease
C414	NSSF	42	E. coli = periplasmic chaperone precursor				
C415	NSSF	42	E. coli = periplasmic chaperone precursor				
C418	KC/MH	98, 85	Contig 1687, E. coli K12 = mglA, ATP-binding comp. of methyl-galactoside transport+taxis				
C420	MH	93; 85	Contig 1494, 1247, 1570; S. enterica CT18 = yjgA, hypothetical protein	same as C421			
C421	MH	93; 85	Contig 1494, 1247, 1570; S. enterica CT18 = yjgA, hypothetical protein	same as C420			
C424	NSSF	55	Burkholderia pseudomallei K96243 = putative phage terminase				
C427	MH	92, 98, 90	Contig 475, 355, E coli K12 = pnp, polynucleotide phosphorylase, RNA DNA synthesis	same as C279			

177

Table IV.1 BLAST and BLASTx Results for Differentially Expressed Sequences (cont.)[a]

Clone #	Category	% Identity	Homology to	Comments	BLASTx	% Identity	Results
C429	KC	95	Contig 1510	same as C453	2	57	E. coli CFT073 = hypothetical protein
C430	KC	95	Contig 1635	same as C193, C239, C299	2	73	S. enterica CT18 = hypothetical protein STY4650
C431	KC	91	Contig 1165	same as C443	2	95	K. pneumoniae = OmpK35 porin
C435	KC	98, 99; 97	Contig 1688, 794, TIGR_198628	same as C473, C558; similar to C311, C545, C577, C849	1	100	K. pneumoniae = OrfB
C438	NSSF	53	Methyloccoccus capsulatus str. Bath = glycosyl transferase, group 2 family protein				
C440	MH	98, 82	Contig 1402, P. luminescens TT01 = cbiP, cobyric acid synthase				
C443	KC	91	Contig 1165	same as C431	1	98	K. pneumoniae = OmpK35 porin
C445	KC	96	Contig 1493		2		percentage homologies too low
C446	KC	98	Contig 1140	same as C560	2		percentage homologies too low
C448	MH	95, 98; 82	Contig 1404, 841; E. coli EDL933 = ybbA, put. ATP-binding component of transport system	same as C604			
C451	KC	98	Contig 1213		2	74	K. pneumoniae = lacZ, beta-galactosidase
C453	KC	95	Contig 1510	same as C429	2	57	S. enterica SC-B67 = hypothetical protein SC4162
C456	KC	98, 96	Contig 1441, 1387	same as C864, C876	2	83	E. coli O157:H7 = putative hydrolase

Table IV.1 BLAST and BLASTx Results for Differentially Expressed Sequences (cont.)[a]

Clone #	Category	% Identity	Homology to	Comments	BLASTx	% Identity	Results
C457	KC	98, 99, 100	Contig 1688, 1247, 1425	same as C265, C308, C331, C840; similar to C296	1	100	K. pneumoniae = OrfA
C458	KC	96	Contig 1721	same as C244, C458	2	66	E. coli CFT073 = hypothetical lipoprotein ydcL precursor
C466	NSSF	37	Erwinia caratovora SCRII043 = putative acyltransferase				
C469	KC	96	Contig 1212		2	44	Y. pestis 91001 = putative membrane protein
C472	NSSF	37	Erwinia caratovora SCRII043 = putative acyltransferase				
C473	KC	98, 99; 97	Contig 1688, 794, TIGR_198628	same as C435, C558; similar to C311, C545, C577, C849	2	100	K. pneumoniae = OrfB
C476	KC/NSSF	94	Contig 1551	same as C328	1	79	S. enterica ATCC 9150 = RND family, multidrug transport protein, acriflavin resistance protein F
C477	KC	96	Contig 1721	same as C244, C458	2	68	S. flexneri str. 2457T = hypothetical protein S1495
C478	KC	98	Contig 1495		2	52	B. pseusomallei K96243 = putative histidine-binding periplasmic protein precursor
C479	MH	98, 96; 85	Contig 1647, S. typhimurium LT2 = nuoA, NADH dehydrogenase I chain A	same as C751, C754, C817			
C480	NSSF	50	Methyloccocus capsulatus str. Bath = glycosyl transferase, group 2 family protein				
C481	MH	87	E. coli CFT073 = ybiT, hypothetical ABC transporter ATP-binding protein	same as C164, C591, C596			

Table IV.1 BLAST and BLASTx Results for Differentially Expressed Sequences (cont.)[a]

Clone #	Category	% Identity	Homology to	Comments	BLASTx	% Identity	Results
C482	KC	99	Contig 1135		1	80	E. coli O157:H7 = alpha-ketoglutarate permease
C483	KC	98	Contig 1071	same as C202, C790	1	91	S. flexneri str. 301 = putative LYSR-type transcriptional regulator
C484	MH	98, 85	Contig 1500, E. coli CFT073 = yhbZ, hypothetical GTP-binding protein	same as C366, C404			
C486	NSSF	48	Methyloccocus capsulatus str. Bath = glycosyl transferase, group 2 family protein				
C500	MH	98, 89	Contig 1656, E. coli K12 = fdoH/I, formate dehydrogenase-O, Fe-S/cytochrome B556 subunit	same as C590			
C503	KC	97	Contig 623	same as C179, C190	1	40	S. enterica CT18 = possible ATP-binding protein
C508	NSSF	92	K. pneumoniae = unknown				
C517	NSSF		percentage homologies too low				
C518	MH	89	E. coli CFT073 = iroN, siderophore receptor				
C519	NSSF	74	S. flexneri 2a str. 2457T = putative integrase				
C522	MH	97	Contig 1500, Salmonella genomes unanotated	same as C374, C385			
C529	NSSF	87	S. enterica ATCC 9150 = antimicrobial peptide resistance and lipid A acylation protein				
C534	MH	97, 90	Contig 1623, S. typhimurium LT2 = oadB/dcoB, oxaloacetate decarboxylase beta chain	same as C348, C584, C829			

Table IV.1 BLAST and BLASTx Results for Differentially Expressed Sequences (cont.)[a]

Clone #	Category	% Identity	Homology to	Comments	BLASTx	% Identity	Results
C536	NSSF	34	V. cholera N16961 = secA-related protein				
C542	KC	98	Contig 1071		2	87	S. enterica ATCC 9150 = hypothetical protein SPA3102
C544	KC	97	Contig 675		2	51	S. enterica ATCC 9150 = putative membrane protein
C545	KC	98, 99; 97	Contig 1688, 794, TIGR_198628	same as C311, C577, C849; similar to C435, C473, C558	2	99	K. pneumoniae = OrfB
C546	MH	99, 80	Contig 1351, S. typhi. LT2 = fldA, flavodoxin 1; ybfE, put. SOS response protein	same as C211, C389, C837			
C552	MH	98, 85	Contig 792, E. coli EDl933 = rpsO, 30S ribosomal subunit protein S15				
C553	MH	85	E. coli EDL933 = putative aminotransferase				
C554	KC	90	Contig 1105		2		Score / e value too high
C558	KC	98, 99; 97	Contig 1688, 794, TIGR_198628	same as C435, C473; similar to C311, C545, C577, C849	1	99	K. pneumoniae = OrfB
C560	KC	1140	Contig 1140	same as C446	2	41	A. tumefaciens str. C58 = GGDEF family protein
C561	KC	96	Contig 1503		1	74	K. oxytoca = hydG, hydrogenase regulatory protein
C571	KC	97	Contig 1457		1		No significant similarities found
C574	KC	97	Contig 710	same as C218, C355, C378, C580, C597	2	92	S. enterica ATCC 9150 = 2-amino-3-ketobutyrate coenzyme A ligase

181

Table IV.1 BLAST and BLASTx Results for Differentially Expressed Sequences (cont.)[a]

Clone #	Category	% Identity	Homology to	Comments	BLASTx	% Identity	Results
C576	NSSF	74	S. flexneri 2a str. 2457T = putative integrase				
C577	KC	98, 99; 97	Contig 1688, 794, TIGR_198628	same as C311, C545, C849; similar to C435, C473, C558	2	96	K. pneumoniae = OrfB
C578	NSSF	31	Bacteriophage E8498 = ORFl0a				
C580	KC	97	Contig 710	same as C218, C355, C378, C574. C597	1	88	S. enterica ATCC 9150 = 2-amino-3-ketobutyrate coenzyme A ligase
C581	NSSF	44	E. coli O157:H7 = orf, hypothetical protein				
C582	KC	95	Contig 1092		1	63	Y. pestis 91001 = putative lipoprotein
C583	MH	99, 93	Contig 1007, S. typhimurium LT2 = rpsB, 30S ribosomal unit protein S2				
C584	MH	97, 90	Contig 1623, S. typhimurium LT2 = oadB/dcoB, oxaloacetate decarboxylase beta chain	same as C348, C534, C829			
C587	MH	92	E. coli CFT073 = eno, enolase	same as C599, C866			
C588	KC	95	Contig 1029	same as C340	2	86	D. hafniense DCB-2 = COG1968: uncharacterized bacitracin resistance protein
C590	MH	98, 89	Contig 1656, E. coli K12 = fdoH/I, formate dehydrogenase-O, Fe-S/cytochrome B556 subunit	same as C500			
C591	MH	87	E. coli CFT073 = ybiT, hypothetical ABC transporter ATP-binding protein	same as C164, C481, C596			

Table IV.1 BLAST and BLASTx Results for Differentially Expressed Sequences (cont.)[a]

Clone #	Category	% Identity	Homology to	Comments	BLASTx	% Identity	Results
C594	NSSF	56	E coli = stbA, stable plasmid inheritance protein A				
C595	KC	98	Contig 1576		2	83	E. coli O157:H7 = mlc, putative NAGC-like transcriptional regulator (imported)
C596	MH	87	E. coli CFT073 = ybiT, hypothetical ABC transporter ATP-binding protein	same as C164, C481, C591			
C597	KC	97	Contig 710	same as C218, C355, C378, C574, C580	2	92	S. enterica ATCC 9150 = 2-amino-3-ketobutyrate coenzyme A ligase
C598	NSSF	59	E coli CFT073 = hypothetical protein				
C599	MH	92	E. coli CFT073 = eno, enolase	same as C587, C866			
C600	MH	99, 100; 82	Contig 1595, 1510, S. enterica CT18 = gltP, proton glutamate symport protein	same as C661, C667			
C602	MH	96	S. typhimurium LT2 = Mrr, putative restriction endonuclease	same as C391			
C604	MH	95, 98; 82	Contig 1404, 841; E. coli EDL933 = ybbA, put. ATP-binding component of transport system	same as C448			
C606	MH/NSSF	95, 91	Contig 1599, E coli CFT073 and Y. 32953 = between two genes				
C610	KC	98	Contig 226	same as C657	2		Score / e value too high
C611	KC	98	Contig 635		1	68	S. enterica ATCC 9150 = protein-export membrane protein

Table IV.1 BLAST and BLASTx Results for Differentially Expressed Sequences (cont.)[a]

Clone #	Category	% Identity	Homology to	Comments	BLASTx	% Identity	Results
C612	MH/KC	96, 79	Contig 1021, S. enterica CT18 = corE, put. Cytochrome c-type biogenesis protein				
C616	MH	96	Y. pestis biovar Med. str. 91001 = virB4, type IV secretory pathway protein	same as C269, C779			
C621	MH	89	S. typhimurium LT2 = thrS, threonine tRNA synthase				
C622	MH	94, 83	Contig 693, S. typhimurium LT2 = ldcC, lysine decarboxylase	same as C624, C626, C632, C650, C656, C701			
C623	MH	99, 86	Contig 83, S. typhimurium LT2 = yidC, putative preprotein translocase subunit				
C624	MH	94, 83	Contig 693, S. typhimurium LT2 = ldcC, lysine decarboxylase	same as C622, C626, C632, C650, C656, C701			
C626	MH	94, 83	Contig 693, S. typhimurium LT2 = ldcC, lysine decarboxylase	same as C622, C624, C632, C650, C656, C701			
C631	MH	93	Y. pestis biovar Med. str. 91001 = virB4, type IV secretory pathway protein	same as C631, C718, C724			
C632	MH	94, 83	Contig 693, S. typhimurium LT2 = ldcC, lysine decarboxylase	same as C622, C624, C626, C650, C656, C701			
C635	KC	98	Contig 821		2	85	E. coli O157:H7 = orf, hypothetical protein
C639	KC	97	Contig 438		1	86	S. enterica ATCC 9150 = aerobic respiration control sensor protein

Table IV.1 BLAST and BLASTx Results for Differentially Expressed Sequences (cont.)[a]

Clone #	Category	% Identity	Homology to	Comments	BLASTx	% Identity	Results
C649	KC	97	Contig 1339		2	100	K. aerogenes = unnamed protein product
C650	MH	94, 83	Contig 693, S. typhimurium LT2 = ldcC, lysine decarboxylase	same as C622, C624, C626, C632, C656, C701			
C651	NSSF		percentage homologies too low				
C656	MH	94, 83	Contig 693, S. typhimurium LT2 = ldcC, lysine decarboxylase	same as C622, C624, C626, C632, C650, C701			
C657	KC	98	Contig 226	same as C610	2		Score / e value too high
C661	MH	99, 100; 82	Contig 1595, 1510, S. enterica CT18 = gltP, proton glutamate symport protein	same as C600, C667			
C663	NSSF	48	Methyloccoccus capsulatus str. Bath = glycosyl transferase, group 2 family protein				
C665	NSSF/KC	92	Contig 1332		2	65	E. carotovora SCRI1043 = hypothetical protein ECA2766
C667	MH	99, 100; 82	Contig 1595, 1510, S. enterica CT18 = gltP, proton glutamate symport protein	same as C600, C661			
C668	NSSF	44	E. coli O157:H7 = orf, hypothetical protein				
C671	NSSF	66	S. enterica ATCC 9150 = putative phage gene				
C672	KC	96	Contig 1474	same as C142	1	62	S. typhimurium LT2 = putative NtrC family transcriptional regulator, ATPase domain
C674	NSSF	44	E coli O157:H7 = orf, hypothetical protein				

Table IV.1 BLAST and BLASTx Results for Differentially Expressed Sequences (cont.)[a]

Clone #	Category	% Identity	Homology to	Comments	BLASTx	% Identity	Results
C675	NSSF		percentage homologies too low				
C676	NSSF		percentage homologies too low				
C679	NSSF	73	Pseudomonas fluorescens PfO-1 = arginase/agmatinase/formimionoglutamate hydrolase				
C682	NSSF	88	K. pneumoniae = PagO, similar to PagO from S. typh., predicted interal membrane protein				
C683	NSSF	74	S. flexneria 2a str. 2457T = putative integrase				
C685	MH	95, 87	Contig 1630, E. coli EDL933 = ilvG, amino acid biosynthesis, isoleucine				
C689	KC	97	Contig 1619	same as C692	1	84	E. coli CFT073 = yhiR, hypothetical protein
C692	KC	97	Contig 1619	same as C689	1	84	E. coli CFT073 = yhiR, hypothetical protein
C698	KC	96	Contig 1355		2	83	S. enterica ATCC 9150 = phosphoribosylglycinamide formyltransferase 2
C701	MH	94, 83	Contig 693, S. typhimurium LT2 = ldcC, lysine decarboxylase	same as C622, C624, C626, C632, C650, C656			
C710	KC	97	Contig 1701		2	58	P. putida = putative LysR-type transcriptional regulator
C713	MH	98, 85	Contig 1414, E. coli EDL933 = mtlA, mannitol specific enzyme, transport of small molecules	similar to C883			

Table IV.1 BLAST and BLASTx Results for Differentially Expressed Sequences (cont.)[a]

Clone #	Category	% Identity	Homology to	Comments	BLASTx	% Identity	Results
C716	NSSF	96	K. pneumoniae = ORF12				
C718	MH	93	Y. pestis biovar Med. str. 91001 = virB4, type IV secretory pathway protein	same as C631, C724			
C721	KC	99	Contig 313		2	49	E. tarda = fimbrial chaperon protein
C723	NSSF		no similarities found				
C724	MH	93	Y. pestis biovar Med. str. 91001 = virB4, type IV secretory pathway protein	same as C631, C718			
C730	KC	97	Contig 1701	same as C110, C137, C370, C738	1	62	B. anthracis A2012 = alcohol dehydrogenase, short chain
C732	KC	93	Contig 1580		2		percentage homologies too low
C734	NSSF	80	Y. pseudotuberculosis IP 32953 = urease alpha subunit, UreC				
C738	KC	93	Contig 1580	same as C110, C137, C370, C732	2		percentage homologies too low
C739	KC	98	Contig 1725	same as C745	1	58	K. pneumoniae = acid phosphatase
C745	KC	98	Contig 1725	same as C739	1	58	K. pneumoniae = acid phosphatase
C751	MH	98, 96; 85	Contig 1647, S. typhimurium LT2 = nuoA, NADH dehydrogenase I chain A	same as C479, C754, C817			
C754	MH	98, 96; 85	Contig 1647, S. typhimurium LT2 = nuoA, NADH dehydrogenase I chain A	same as C479, C751, C817			
C760	KC	97	Contig 609	same as C396	1	87	S. enterica ATCC 9150 = proline dipeptidase

Table IV.1 BLAST and BLASTx Results for Differentially Expressed Sequences (cont.)[a]

Clone #	Category	% Identity	Homology to	Comments	BLASTx	% Identity	Results
C765	KC	99	Contig 1382		2	70	B. mallei ATCC 23344 = naphthalene 1,2-dioxygenase system ferredoxin component
C769	MH	98, 87	Contig 1669, S. enterica CT18 = dam, DNA adenine methylase				
C771	KC	99	Contig 1723		2	41	P. luminescens TTO1 = hypothetical protein plu2159
C775	MH	99, 81	Contig 886, S. typhimurium LT2 = yrdC, putative dsRNA-binding protein				
C776	MH	91, 89	Contig 1419, E. coli K12 = deaD, cold-shock DeaD box ATP-dependent RNA helicase	same as C264, C382			
C778	NSSF/KC	98	Contig 1259		2	84	E. coli CFT073 = glyceraldehyde 3-phosphate dehydrogenase A
C779	MH	96	Y. pestis biovar Med. str. 91001 = virB4, type IV secretory pathway protein	same as C269, C616			
C780	MH	93, 92	Contig 1621, S. typhimurium LT2 = ahpC, alkyl hydroperoxide reductase C22 subunit	same as C253			
C784	KC	98	Contig 855	same as C163, C247, C354, C383, C825	2	80	S. enterica CT18 = L-rhamnose operon regulatory protein
C790	KC	98	Contig 1071	same as C202, C483	2	93	S. flexneri str. 2457T = putative LYSR-type transcriptional regulator
C797	KC	94	Contig 1711		2	65	R. metallidurans CH34 = ethanolamine ammonia-lyase, large subunit

Clone #	Category	% Identity	Homology to	Comments	BLASTx	% Identity	Results
C801	KC	97	Contig 1549		1	91	S. enterica CT18 = B12-dependent homocysteine-N5-methyltetrahydrofolate transmethylase
C805	MH	98, 83	Contig 1569, E. coli EDL933 = perM, putative permease				
C807	NSSF	48	Methyloccoccus capsulatus str. Bath = glycosyl transferase, group 2 family protein				
C813	MH/NSSF	97, 79	Contig 1703, S. typhimurium LT2 = treC, trehalose-6-phosphate hydrolase				
C817	MH	98, 96; 85	Contig 1647, S. typhimurium LT2 = nuoA, NADH dehydrogenase I chain A	same as C479, C751, C754			
C818	KC	98	Contig 1592		2	90	E. coli O157:H7 = DNA biosynthesis; DNA primase
C819	KC	97	Contig 1636		2	58	S. avermitilis MA-4680 = hypothetical protein
C825	KC	98	Contig 855	same as C163, C247, C354, C383, C784	1	80	S. enterica CT18 = L-rhamnose operon regulatory protein
C826	NSSF	74	S. flexneria 2a str. 2457T = putative integrase				
C829	MH	97, 90	Contig 1623, S. typhimurium LT2 = oadB/dcoB, oxaloacetate decarboxylase beta chain	same as C348, C534, C584			
C837	MH	99, 80	Contig 1351, S. typhii. LT2 = fldA, flavodoxin 1; ybfE, put. SOS response protein	same as C211, C389, C546			
C840	KC	98, 99, 100	Contig 1688, 1247, 1425	same as C265, C308, C331, C457; similar to C296	1	100	K .pneumoniae = OrfA

Table IV.1 BLAST and BLASTx Results for Differentially Expressed Sequences (cont.)[a]

Clone #	Category	% Identity	Homology to	Comments	BLASTx	% Identity	Results
C841	Sanger	80	Sanger_218493	same as C336, C409			
C845	NSSF	64	Y pestis str. 91001 = putative vitamin B12 receptor protein				
C846	MH	74	S. enterica subsp. Enterica serovar Typhi str. CT18 = hypothetical protein	same as C116, C262			
C849	KC	98, 99, 97	Contig 1688, 794, TIGR_198628	same as C311, C545, C577; similar to C435, C473, C558	2	99	K. pneumoniae = OrfB
C859	MH	97, 96	Contig 817, E. coli CFT073 = rplO, 50S ribosomal protein L15				
C864	KC	98, 96	Contig 1441, 1387	same as C456, C876	1	77	S. flexneri str. 2457T = putative hydrolase
C866	MH	92	E. coli CFT073 = eno, enolase	same as C587, C599			
C876	KC	98, 96	Contig 1441, 1387	same as C456, C864	1	82	S. flexneri str. 2457T = putative hydrolase
C883	MH	97, 87	Contig 1414, E. coli CFT073 = mtlA, mannitol specific enzyme, transport of small molecules	similar to C713			
C885	MH	91, 81	Contig 368, E coli K12 = argG, amino acid biosynthesis, arginine				
C887	MH	97, 78	Contig 1558, S. enterica CT18 = hypothetical protein				
C888	NSSF	58	E. coli CFT073 = hypothetical protein c4512				
G160	KC	98	Contig 1688	same as G441	1	98	K. pneumoniae = OrfB
G164	KC	95	Contig 951		2	47	E. coli = putative protein

190

Table IV.1 BLAST and BLASTx Results for Differentially Expressed Sequences (cont.)[a]

Clone #	Category	% Identity	Homology to	Comments	BLASTx	% Identity	Results
G171	KC	98	Contig 649		2	94	S. enterica ATCC 9150 = regulatory protein
G174	KC	97	Contig 831		2	64	S. enterica CT18 = hypothetical protein STY4676
G175	MH	89	E. coli CFT073 = prlA, preprotein translocase subunit; rpl0, ribosome				
G176	NSSF	67	Y. pestis biovar Mediaevails str. 91001 = putative urea transporter				
G177	MH	92	S. typhimurium LT2 = putative DNA repair ATPase	same as G626			
G179	NSSF	67	Y. pestis biovar str. 91001 = hypothetical protein YP3563				
G180	KC	98	Contig 1616	same as G637	2	95	K. pneumoniae = citrate lyase gamma-subunit
G187	NSSF		percentage homologies too low				
G190	KC	99	Contig 1053		2	42	S. enterica ATCC 9150 = putative transcriptional regulator
G200	KC	97	Contig 557		1	64	Y. pseudotuberculosis IP 32953 = hypothetical protein YPTB3823
G203	NSSF		percentage homologies too low				
G206	NSSF	70	Y. pestis biovar str. 91001 = putative membrane protein				
G212	KC	97	Contig 1408	same as G505	2	62	Y. pestis 91001 = putative solute-binding periplasmic protein of ABC transporter

Table IV.1 BLAST and BLASTx Results for Differentially Expressed Sequences (cont.)[a]

Clone #	Category	% Identity	Homology to	Comments	BLASTx	% Identity	Results
G215	NSSF		percentage homologies too low				
G222	KC	89	Contig 1549		1	81	S. enterica ATC 9150 = putative membrane protein
G233	NSSF		percentage homologies too low				
G237	KC	96	Contig 1688, 1425, 1247		2	98	K. pneumoniae = OrfA
G238	NSSF	62	Y. pseudotuberculosis IP 32953 = putative membrane protein				
G253	NSSF	52	E. carotovora SCRI1043 = putative aminotransferase				
G255	KC	95	Contig 1413		2	68	K. pneumoniae = IutA
G261	NSSF	92	S. enterica CT18 = putative hydrolase				
G289	MH	86	S. flexneri 2a str. 2457T = slpA, translation and modification; lytB, regulator				
G320	TIGR	88	TIGR_198628				
G325	KC	98	Contig 1000		2		percentage homology too low
G326	NSSF	55	Xylella fastidiosa Dixon = Type IV secretory pathway, TrbL components				
G344	KC	94	Contig 1394		2	59	Y. pseudotuberculosis IP 32953 = hypothetical protein YPTB1499
G387	NSSF	61	Y. pseudotuberculosis IP 32953 = urease accessory protein, UreF				
G391	NSSF	70	Bacteriophage HK97 = putative prohead protease gp4				

Table IV.1 BLAST and BLASTx Results for Differentially Expressed Sequences (cont.)[a]

Clone #	Category	% Identity	Homology to	Comments	BLASTx	% Identity	Results
G432	KC	98	Contig 608	same as G675	2	85	V. vulnificus CMCP6 = yjgF, putative translation initiation inhibitor
G434	NSSF	41	S. typhimurium LT2 = putative transcriptional regulator				
G438	NSSF	84	Enterobacteria phage HK022 = gp9				
G439	KC	98	Contig 1625	same as G451, G682 and G703	2		percentage homology too low
G441	KC	98	Contig 1688	same as G160	1	100	K. pnaeumoniae = OrfB
G451	KC	98	Contig 1625	same as G439, G682, and G703	2	39	E. coli K12 = putative permease
G464	KC/MH	83	Contig 1544, S. enterica = possible membrane transport protein				
G465	MH	91	S. typhimurium LT2 = putative inner membrane/cytoplasmic protein	same as G521, G540			
G467	NSSF	41	P. luminescens TTO1 = hypothetical protein plu0791				
G473	NSSF		score/e value too high				
G474	NSSF		score/e value too high				
G479	NSSF		score/e value too high				
G481	NSSF		percentage homologies too low				
G482	MH	87	E. coli O157:H7 = hypothetical protein	same as G586			
G485	KC	99	Contig 1652		2	70	E. coli = hemolysin F
G494	NSSF		no significant similarity found				

193

Table IV.1 BLAST and BLASTx Results for Differentially Expressed Sequences (cont.)[a]

Clone #	Category	% Identity	Homology to	Comments	BLASTx	% Identity	Results
G503	KC	100	Contig 417		2	45	Y. pestis 91001 = putative L-xylolose kinase
G504	KC	90	Contig 1180	same as G536	2		percentage homology too low
G505	KC	96	Contig 1408	same as G212	1	63	Y. pseudotuberculosis IP 32953 = putative ABC transporter, periplasmic iron binding protein
G518	NSSF	67	E coli K12 = multidrug resistance protein Y				
G521	MH	91	S. typhimurium LT2 = putative inner membrane/cytoplasmic protein	same as G465, G540			
G536	KC	90	Contig 1180	same as G504	1	37	E. coli K12 = putative protease
G537	KC	96	Contig 1571		2	97	K. pneumoniae = unnamed protein product, h ypothetical protein in tonB 3' region
G538	KC	98	Contig 859		2	48	E. coli O157:H7 = putative transcriptional activator
G540	MH	91	S. typhimurium LT2 = putative inner membrane/cytoplasmic protein	same as G465, G521			
G542	KC	99	Contig 1584		2	94	S. enterica CT18 = isocitrate dehydrogenase
G547	KC	99, 97	Contig 1688, 794, TIGR_198628	same as G664, G676	1	99	K. pneumoniae = OrfB
G552	KC	87	Contig 1226		1	96	K. pneumoniae = Orf3, hypothetical 55.8 kDa protein in CPS region
G555	NSSF	62	uncultured eubacterium pIE1115 = putative DNA helicase				

Table IV.1 BLAST and BLASTx Results for Differentially Expressed Sequences (cont.)[a]

Clone #	Category	% Identity	Homology to	Comments	BLASTx	% Identity	Results
G557	KC	98	Contig 1605		1	55	S. enterica ATCC 9150 = putative serine transporter
G558	NSSF	63	E coli CFT073 = hypothetical protein c4755				
G561	NSSF	66	Y. pestis 91001 = putative membrane protein				
G565	MH	80	S. paratyphi A unfinished fragement				
G579	NSSF	65	E coli CFT073 = protein hdeA precursor				
G586	MH	88	E. coli O157:H7 = hypothetical protein	same as G482			
G588	MH	83	E. coli CFT073 = ybaU/ppiD, peptidyl-prolyl cis-trans isomerase D				
G591	KC	98, 100	Contig 1391, 608		2	65	V. vulnificus CMP6 = Na+/proline symporter
G597	NSSF		percentage homologies too low				
G598	NSSF	39	S. enterica ATCC 9150 = putative fimbrial usher protein				
G602	NSSF		percentage homologies too low				
G603	NSSF		percentage homologies too low				
G604	MH	99	Contig 1232, short stretches of homologies to other enterics				
G605	NSSF		percentage homologies too low				
G613	NSSF	40	S. enterica ATCC 9150 = putative fimbrial usher protein				

Table IV.1 BLAST and BLASTx Results for Differentially Expressed Sequences (cont.)[a]

Clone #	Category	% Identity	Homology to	Comments	BLASTx	% Identity	Results
G626	MH	92	S. typhimurium LT2 = putative DNA repair ATPase	same as G177			
G627	NSSF		percentage homologies too low				S. enterica ATCC 9150 = putative transport system periplasmic binding protein
G629	KC	97	Contig 397		2	64	
G635	KC	97	Contig 1689		2		percentage homology too low
G637	KC	97	Contig 1616	same as G180	2	100	K. pneumoniae = citrate lyase gamma-subunit
G638	MH	82	Y. pestis biovar Mediaevails str. 91001 = virB6, Type IV secretion pathway protein				
G640	KC	100	Contig 1288	same as G650	2		percentage homology too low
G643	NSSF		percentage homologies too low				
G644	NSSF		percentage homologies too low				
G645	NSSF	70	E. coli = type I fimbrial chaperone				
G646	NSSF	61	Y. pseudotuberculosis IP 32953 = urease accessory protein, UreF				
G648	NSSF		percentage homologies too low				
G650	KC/NSSF	97	Contig 1288	same as G640	1		percentage homology too low
G653	NSSF	88	Enterobacteria phage HK022 = gp9				
G658	NSSF		percentage homologies too low				
G664	KC	99, 97	Contig 1688, 794, TIGR_198628	same as G547, G676	1	99	K. pneumoniae = OrfB
G674	NSSF	96	K. pneumoniae = virulence protein S				

196

Table IV.1 BLAST and BLASTx Results for Differentially Expressed Sequences (cont.)[a]

Clone #	Category	% Identity	Homology to	Comments	BLASTx	% Identity	Results
G675	KC	98	Contig 608	same as G432	2	85	V. vulnificus CMCP6 = yjgF, putative translation initiation inhibitor
G676	KC	99, 97	Contig 1688, 794, TIGR_198628	same as G547, G664	1	99	K. pneumoniae = OrfB
G677	KC	96, 99, 100	Contig 1688, 1247, 1425		2	88	K. pneumoniae OrfA
G682	KC	97	Contig 1625	same as G439, G451, G703	2	38	M. degradans 2-40 = Na+/melibose symporter and related transporters
G690	NSSF	56	Y. pseudotuberculosis IP 32953 = multidrug efflux pump, permease/ATPase domains				
G693	MH	94	S. typhimurium LT2 = putative ATP-dependent Lon protease				
G696	MH	78	S. enterica, S. typhimurium LT2 = iroN				
G697	NSSF		percentage homologies too low				
G700	NSSF	69	E coli K12 = outer membrane protein, export and assembly of type I fimbriae				
G703	KC	98	Contig 1625	same as G439, G451, G682	2	38	M. degradans 2-40 = Na+/melibose symporter and related transporters
G704	KC	96	Contig 1606		1	80	E. coli K12 = conserved hypothetical protein, phosphate-like domain
G705	MH	92	S. typhimurium LT2 = putative restriction endonuclease				

[a]Cloned subtractive hybridization products were sequenced and inputted into the National Center for Biotechnology Information (NCBI) website. All sequences were used in a BLAST search which searches the database using a nucleotide query. Categories each clone was grouped into are KC, homologies to various Klebsiella contigs belonging to strain MGH78578; MH, multiple homologies to various bacteria; NSSF, no significant similarities found; and Sanger, homologies to the Sanger database of sequenced genomes. KC and NSSF sequences were used in a BLASTx search to obtain more sequence information. BLASTx searches the protein database using a translated nucleotide query.

PCR confirmation for unique expression of sequences in strain 43816

Sequence specific primers were generated from 54 out of the 284 differentially expressed sequences from the cDNA subtraction and 27 out of the 107 unique sequences from the genomic DNA subtraction. These sequences were chosen for further analysis because of their homologies to enteric genes that could potentially play a role in virulence. They were grouped into 7 categories: regulatory proteins (RP); metabolic genes (M); protein secretion (P); antimicrobial, antibiotic, or stress resistance related (R); iron related (I); type I fimbrial associated proteins (T); and those with miscellaneous functions (Misc). Total cDNA from 43816 and IA565 served as PCR templates for amplification using the 54 sets of primers and genomic 43816 and IA565 DNA served as PCR templates for the amplification using the 27 sets of primers. The results are listed in Table IV.2.

A representative agarose gel image from this PCR confirmation experiment is shown using genomic 43816 and IA565 DNA for only 10 out of the 27 primer sets (Figure IV.8). 43816 sequence uniqueness were confirmed when a band was present using 43816 genomic DNA as template and absent using IA565 genomic DNA. For analysis of the sequences obtained from the cDNA subtraction, using 15 and 25 PCR amplification cycles for each primer set did not yield a difference in band intensity for the total cDNA templates. Therefore, 43816 differentially expressed sequences could only be confirmed when a band was present using 43816 cDNA as template and absent using IA565 cDNA. The results from the subtractive hybridization are listed in Table IV.3.

Table IV.2 Results of PCR Confirmation for Genomic and cDNA Subtraction[a]

Group[b]	Description	Clone #	Amplicon	43816 bands	IA565 bands
RP	2-amino-3-ketobutyrate coenzyme A ligase: Part of Lrp regulon; leucine response regulatory protein which controls trxn of a # of genes in E. coli	C218	278	1 band: ~300bp	1 band: ~300bp
M	aceA, isocitrate lyase: Required for fatty acid utilization via the glyoxylate shunt; essential for Salmonella persistence during chronic infection	C249	171	1 band: ~200bp	1 band: ~200bp
R	Acriflaving resistance protein F: Provides resistance to variety of antimicrobial agents in E. coli	C328	198	2 faint bands: ~700, ~300bp	4 faint bands: ~1500, ~700, ~450, ~300bp
RP	aerobic respiration control sensor protein: Global regulator of aerobic genes	C639	365	1 band: ~400bp	1 band: ~400bp
R	ahpC, alkyl hydroperoxide reductase C22, subunit: Protects against reactive nitrogen intermediates; detoxification of hydrogenperoxides	C780	431	1 band: ~400bp	1 band: ~400bp
M	alcohol dehydrogenase: catalyzes the removal of hydrogen from a substrate and the transfer of the hydrogen to an acceptor in an oxidation-reduction reaction	C730	263	No band	1 band: ~300bp
M	alpha-ketoglutarate permease: Constitutively expressed proton symporter	C482	191	1 faint band: ~200bp	1 band: ~200bp
R	antimicrobial peptide resistance and lipid A acylation protein	C529	152	1 band: ~150bp	1 band: ~150bp

199

Table IV.2 Results of PCR Confirmation for Genomic and cDNA Subtraction[a] (cont.)

Group[b]	Description	Clone #	Amplicon	43816 bands	IA565 bands
M	cbiP, cobyric acid synthase: Cobyric acid is a pathway intermediate for cobalamin biosynthesis conversion to cobinamide (makes heme and other important heme molecules)	C440	254	2 faint bands: ~500, ~350bp	2 faint bands: ~500, ~350bp
M	citrate lyase gamma subunit: Catalyzes Mg^{2+}-dependent cleavage of citrate to acetate and oxaloacetate; reactions represents initial step of all known bacterial citrate fermentation pathways	G180	412	3 bands: ~400bp, ~600bp, ~800bp	3 bands: ~400bp, ~600bp, 1Kb+
M	corE, putative cytochrome c-type biogenesis protein: Cytochrome-c plays key roles in aerobic and anaerobic respiration	C612	237	1 faint band: ~250bp	1 band: ~250bp
M	eno, enolase: Glycolytic enzyme, metabolic breakdown of glucose and other sugars that releases energy in the form of ATP; also helps to recruit plasminogen to bacteria → chews up ECM	C587	316	1 band: ~300bp	1 band: ~300bp
M	fdoH/I, formate dehydrogenase-O, Fe-S/cytochrome B556 subunit: Involved in aerobic and anaerobic respiration	C500	269	1 band: ~250bp	1 band: ~250bp
M	glyceraldehydes 3-phosphate dehydrogenase A: gapC, recruits plasminogen to cell surface, glycolytic enzyme	C778	551	No band	No band
R	hdeA precursor: head encodes a periplasmic protein involved in acid resistance	G579	456	2 bands: ~1kb, ~500bp	2 bands: ~1kb, ~900bp, smear 500-1kb

Table IV.2 Results of PCR Confirmation for Genomic and cDNA Subtraction[a] (cont.)

Group[b]	Description	Clone #	Amplicon	43816 bands	IA565 bands
M	hydG: Hydrogenase regulatory protein → regulates hydrogenase 3, which is involved in fermentative hydrogen production	C561	157	1 band: ~150bp	2 bands: ~450, ~150bp
I	iroN	C518	277	1 faint band: ~250bp	No band
		G696	354	1 band: ~350bp	No band
M	Isocitrate dehydrogenase: Controls flow of isocitrate through the glyoxylate bypass pathway which bypasses the CO_2 evolving steps of the Krebs cycle	G542	192	1 band: ~200bp, smear 300-1kb+	1 band: ~200bp, smear 300-1kb+
I	IutA	G255	260	2 bands: ~300, ~700	2 bands: ~300, ~700
M	L-1,2-propanediol oxidoreductase: Dissiminates L-fucose; functions furing fermentative growth to regenerate NAD from NADH	C237	159	Multiple bands: 10	Multiple bands: 9
RP	L-rhamnose operon regulatory protein: L-rhamnose is component of LPS core, several O antigen polysaccarhides and cell surface surfact of P. aeruginosa	C163	536	1 band: ~500bp	1 band: ~500bp
M	LacZ	C451	219	1 faint band: ~200bp	

201

Table IV.2 Results of PCR Confirmation for Genomic and cDNA Subtraction[a] (cont.)

Group[b]	Description	Clone #	Amplicon	43816 bands	IA565 bands
M	ldcC, lysine decarboxylase: Has to do with growth	C622	367	1 band: ~200bp	2 bands: ~400, ~200bp
P	LepA, GTP-binding protein: Cytoplasmic membrane bound; involved in protein secretion	C402	246	1 band: ~250bp	1 band: ~250bp
P	Maltoporin: Sugar pore	C321	220	1 band: ~200bp	1 band: ~200bp
M	MdcA: Malonate decarboxylase alpha subunit; catalyze conversion of malonate plus H+ to acetate and water; metabolic pathway	C392	263	1 band: ~300bp	1 band: ~300bp
P	MglA, ATP-binding component of methyl_galactoside transport and taxis: Part of active transport system	C418	274	1 band: ~250bp	1 band: ~250bp
RP	Mlc: Putative NAGC-like transcriptional regulator; global regulator acting as transcriptional repressor for several genes and operons in E. coli (ie sugar metabolizing enzymes and uptake systems)	C595	243	1 band: ~250bp	1 band: ~250bp
M	mltD: Membrane bound lytic murein transglycosylase D; cleaves bonds in murein layer to create sites for insertion for new material in this macromolecule surrounding cell	C255	524	2 bands: ~150, ~500bp	2 bands: ~150, ~500bp
P	mtlA, mannitol specific enzyme, transport of small molecules	C883	426	1 band: ~400bp	1 band: ~400bp

Table IV.2 Results of PCR Confirmation for Genomic and cDNA Subtraction[a] (cont.)

Group[b]	Description	Clone #	Amplicon	43816 bands	IA565 bands
P	Na+/proline symporter	G591	256	4 bands: ~250, ~350, ~450, ~800bp	Multiple bands none at ~250bp
M	nuoA, NADH dehydrogenase I chain A: One of 14 nuo genes to encode subunits of type I NADH dehydrogenase, key component of the respiratory chain	C479	225	No band	No band
P	**oadB / dcoB, oxaloacetate decarboxylase beta chain: Membrane bound biotin containing enzyme that pumps sodium**	**C348**	**346**	**1 band: ~350bp**	**No band**
P	OmpK35 porin: Used by antibiotics to get into cell; loss of porin contributes to resistance to antibiotics	C431	235	1 band: ~250bp	1 band: ~250bp
Misc	PagO	C682	342	2 bands: faint ~400bp, strong ~700bp	4 bands: ~350, ~400, ~700, ~900bp
P	Possible membrane transport protein	G464	450	2 bands: ~450, ~650bp	5 bands: ~450, ~600, ~650, ~1kb, ~1kb+
M	Putative aldo/keto reductase: AKR enzymes comprise functionally diverse gene family which catalyze NADPH-dependent reduction of a variety of carbonyl compounds	C284	544	3 bands: ~375, ~450, ~600bp	2 faint bands: ~700, ~900bp

203

Table IV.2 Results of PCR Confirmation for Genomic and cDNA Subtraction[a] (cont.)

Group[b]	Description	Clone #	Amplicon	43816 bands	IA565 bands
M	Putative aminotransferase: Catalyze transfer of amino group between an alpha amino acid and usually a specific carbon on a keto acid	C553	194	1 band: ~200bp	1 band: ~200bp
		G253	495	1 band: ~500bp	1 band: ~1kp
R	Putative ATP-dependent Lon protease: Eliminator of stress-damaged proteins; involved in SOS response	G693	415	1 band: ~400bp	multiple bands: ~300bp, several @ ~1kb+
P	Putative exported protein	C246	554	No band	1 band: ~550bp
		C256	358	1 band @ ~350bp, 3 faint bands: ~400, ~450, ~500bp	2 bands: ~500, ~650bp
Misc	putative inner membrane / cytoplasmic protein	G465	248	1 band: ~250bp	4 bands: ~700, ~750, 2 @ ~1kb+
I	Putative iron compound receptor	C297	563	No band	No band
RP	**Putative LYSR-type transcriptional regulator: LTTRs large family of transcriptional regulators; involved in regulation of diverse range of cellular processes including CO$_2$ fixation, oxidative stress; and virulence**	C202	338	1 band: ~350bp	1 band: ~350bp
		C710	482	**1 band: ~500bp**	**No band**

Table IV.2 Results of PCR Confirmation for Genomic and cDNA Subtraction[a] (cont.)

Group[b]	Description	Clone #	Amplicon	43816 bands	IA565 bands
Misc	Putative membrane protein	C469	198	No band	No band
		C544	376	1 band: ~350bp	1 band: ~350bp
		G206	484	1 band: ~500bp	3 bands: ~350, ~650, 1kb+
		G222	130	1 band: ~150bp	1 faint band @ 150bp, 2 bands ~1kb+
		G238	458	1 band: ~500bp	2 bands ~1kb+
P	Putative permease: Functions as channel for transport of a specific molecules in and out of cell	C805	223	3 bands: ~200, ~250, ~500	4 bands: ~200, ~250, ~550, ~750
		G451	438	2 bands: ~450, ~500bp	Smear ~500bp - 1kb+
Misc	**Putative restriction endonuclease: Catalyze hydrolysis of bonds between nucleic acids in interior of a DNA or RNA molecule**	**G705**	**150**	**2 bands: ~100, ~150bp**	Smear ~400bp - 1kb
		C391	**335**	**1 band: ~300bp**	**No band**

Table IV.2 Results of PCR Confirmation for Genomic and cDNA Subtraction[a] (cont.)

Group[b]	Description	Clone #	Amplicon	43816 bands	IA565 bands
P	Putative solute-binding periplasmic protein of ABC transporter	G212	161	1 band: ~200bp multiple bands	1 band: ~200bp multiple bands
P	Putative transport system periplasmic binding protein	G629	255	1 band: ~300bp	1 band: ~300bp
RP	Putative transcriptional regulator/activator	C142	190	1 band: ~200bp	1 band: ~200bp
		G190	324	2 bands: ~300, ~500bp	3 bands: ~300, ~500, ~900bp
		G434	395	1 band: ~400bp	2 bands: ~900bp, ~1kb+
		G538	231	3 bands: ~200, ~700, 1kb+	2 bands: ~200, 1kb+
P	Putative urea transporter	G176	438	2 band: ~200, 400bp	Multiple bands: ~200, 800, 900, 1kb
RP	Regulatory protein	G171	166	2 bands: ~200, ~800bp	2 bands: ~200, ~800bp

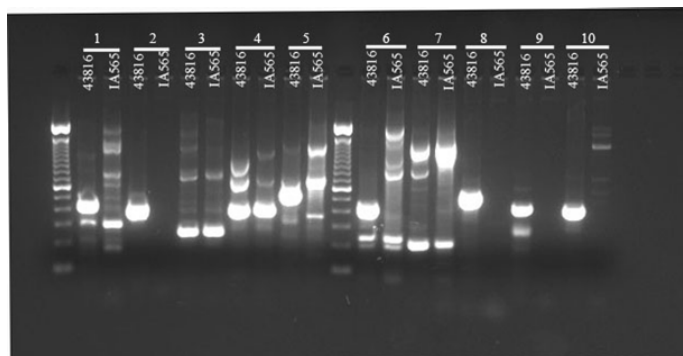## Table IV.2 Results of PCR Confirmation for Genomic and cDNA Subtraction[a] (cont.)

Group[b]	Description	Clone #	Amplicon	43816 bands	IA565 bands
P	sbp: Sulfate transport protein	C186	361	1 band: ~350bp	1 band: ~350bp
P	sgaT, putative PTS enzyme II: Uptake of ascobrate sugar	C407	480	3 bands: ~400, 500, 510bp	3 bands: ~400, 500, 510bp
R	treC, trehalose-6-phosphate hydrolase: Protects against environment stress	C813	373	1 band: ~400bp	1 band: ~400bp
T	Type 1 fimbrial associated proteins	C234	423	1 band: ~400bp	1 band: ~400bp
		C721	370	1 band: ~400bp	1 band: ~400bp
		G598	425	1 band: ~400bp	No band
		G645	452	1 band: ~450bp	Multiple bands: ~500, 550, 800, 1kb+
		G700	394	1 band: ~400bp	No band
R	UmuC: Involved in SOS response	C160	172	2 bands: ~175, ~900bp	1 band: ~175bp

Table IV.2 Results of PCR Confirmation for Genomic and cDNA Subtraction[a] (cont.)

Group[b]	Description	Clone #	Amplicon	43816 bands	IA565 bands
P	ureC, urease alpha subunit	C734	195	1 band: ~200bp	1 faint band: ~200bp
P	ureF, urease accessory protein	G387	474	2 bands: ~350bp, ~500bp	3 bands: ~350, ~650bp, 1kb+
Misc	**Virulence protein S**	**G674**	**513**	**1 band: ~500bp**	**No band**
P	ybbA, putative ATP-binding component of transport system	C448	425	1 band: ~400bp	1 band: ~400bp
R	ybfE, putative SOS response protein	C211	213	1 band: ~200bp	1 band: ~200bp
P	**ybiT, hypothetical ABC transporter ATP-binding protein**	**C164**	**367**	**1 band: ~400bp**	**No band**
Misc	yhbZ, hypothetical GTP-binding protein	C366	173	1 band: ~150bp	1 band: ~150bp
M	yigO: Ubiquinone/menaquinone biosynthesis methyltransferase involved in respiratory electron transport chain	C274	443	No band	No band

[a]PCR primers to a subset of the cloned subtractive hybridization products were generated and PCR was performed on total genomic DNA or cDNA for confirmation. Clones highlighted in bold are uniquely expressed cDNAs in strain 43816 or unique genomic DNA sequences in strain 43816.
[b]Groups represent: RP, regulatory proteins (7), M, metabolic genes (21), P, protein secretion (19), R, antimicrobial, antibiotic, or stress resistance (8), I, iron related (4), T, type I fimbrial associated proteins (1), and Misc, miscellaneous (6).

Figure IV.8 Representative Gel of PCR Confirmation Results for Genomic DNA Subtraction
PCR primers to a subset of the cloned subtractive hybridization products were generated and PCR was performed on total genomic DNA or cDNA for confirmation. This is one of the gels showing results using genomic DNA as a template. In each group, 43816 wells are on the left and IA565 wells are on the right.
Group 1: Clone G693 that has high homology to a putative ATP-dependent Lon protease
Group 2: Clone G696, that has high homology to iroN
Group 3: Clone G255, that has high homology to IutA
Group 4: Clone G180, that has high homology to the citrate lyase gamma subunit
Group 5: Clone G387, that has high homology to ureF
Group 6: Clone G176, that has high homolgoy to a putative urea transporter
Group 7: Clone G538, that has high homolgoy to a putative transcriptional regulator/activator
Group 8: Clone G674, that has high homolgoy to Virulence Protein S
Group 9: Clone G598, that has high homolgoy to the putative fimbrial usher protein, sthB
Group 10: Clone G700, that has high homolgoy to fimD

209

Table IV.3 K. pneumoniae strain 43816 Differentially Expressed Genes Identified in this Study

Accession no.	Homologous gene	(accession no.)	% Identity	Predicted Protein
DQ211084[a]	E. coli iroN	(NP_753164)	89[c]	siderophore receptor
DQ211085[b]	S. typhimurium iroN	(NP_461704)	78[c]	siderophore receptor
DQ211086[b]	S. typhimurium sthB	(NP_463449)	59[d]	putative fimbrial usher protein
DQ211087[b]	E. coli fimD	(NP_418737)	69[d]	outer membrane protein, export and assembly of type 1 fimbriae
DQ211088[b]	K. pneumoniae KvgS	(CAB61240)	96[d]	sensor protein KVGS precursor; virulence protein S
DQ211089[a]	E. coli ybiT	(NP_752836)	87[c]	hypothetical ABC transporter ATP binding protein
DQ211090[a]	S. typhimurium dcoB	(NP_459747)	90[c]	oxaloacetate decarboxylase beta chain
DQ211091[a]	P. putida Orf350	(NP_863090)	58[d]	putative LysR-type transcriptional regulator
DQ211092[a]	S. typhimurium Mrr	(NP_463349)	96[c]	putative restriction endonuclease

[a]Obtained from cDNA SSH
[b]Obtained from genomic DNA SSH
[c]Nucleotide sequence homology
[d] Protein sequence homology

Discussion

Using a PCR-based suppressive subtractive hybridization technique, 9 DNA sequences present in *K. pneumoniae* strain 43816 and absent or less expressed in strain IA565 were identified (Table IV.3). While the role that each of these genes potentially play in *K. pneumoniae* virulence is currently unknown, one can speculate based on the current understanding of the function of each gene in other bacterial species.

In both the genomic DNA and cDNA SSH technique, sequences DQ211084 and DQ211085 specific for the pathogenic strain 43816 were homologous to *iroN* from both *S. typhimurium* and *E. coli*. Iron acquisition via secretion of low molecular weight, high affinity iron chelators termed siderophores has been well documented as a virulence trait in many enteric bacteria [12]. Clinical and environmental isolates of *K. pneumoniae* have been shown to secrete the siderophores, enterochelin (enterobactin) [13, 14]. In *E. coli*, *iroN* was recently found to be the siderophore receptor for enterobactin. Additionally, *iroN* was shown to be a virulence factor in a murine model of urinary tract infection [15]. Our findings suggest a putative iron-dependent mechanism for the pathogenicity observed for strain 43816 in our model of bacterial pneumonia.

Sequences DQ211086 and DQ211087 obtained from the genomic DNA SSH technique were homologous to gene products involved in type I fimbriae formation in both *S. typhimurium* and *E. coli*, *sthB* and *fimD*, respectively. Because *K. pneumoniae* is an extracellular pathogen, a critical step in the infectious process is adherence to host mucosal surfaces. Adherence properties are mediated by fimbrial adhesions. *Klebsiella spp*. can produce type 1 and/or type 3 fimbrial adhesions [16]. The majority of clinical

respiratory isolates of *K. pneumoniae* reportedly express type 3 fimbriae [17], suggesting the importance of this fimbrial type in virulence. However, a previously constructed mini-Tn5 transposon mutant strain of *K. pneumoniae* 43816 defective in expression of type 3 fimbriae [18] was equally virulent following intratracheal inoculation as the parental 43816 strain. This suggests that *in vivo* pathogenicity of strain 43816 is not dependent upon type 3 fimbriae expression. However, the role of *K. pneumoniae* type 1 fimbriae expression in pathogenesis is unknown. Our findings suggest that type 1 fimbriae may play a role in *K. pneumoniae* pathogenicity in our model of acute bacterial pneumonia.

Sequence DQ211088 had high nucleotide sequence homology to *K. pneumoniae* gene *kvgS* which was also previously identified by Lai et. al. as a *K. pneumoniae* virulent strain specific sequence [6]. The group identified the virulent strain-specific sequence as having high homology to *bvgAS*, a two-component signal transduction system in *Bordetella pertussis* previously identified as a virulence factor [8]. They subsequently identified the sequence as gene *kvgAS*, a two-component system found in *K. pneumoniae* with homologies to the *bvgAS* system [9]. The role of the *kvgAS* system in *K. pneumoniae* virulence could not be established in their mouse peritonitis model since the pathogenicity of a *kvgS* deletion mutant was comparable to that of its parental strain. However, the role *kvgS* plays in our model of bacterial pneumonia is open to further investigation.

Four sequences obtained from the cDNA SSH technique were homologous to genes found in *Pseudomonas*, *Salmonella* and *E. coli* involved in energy production and conversion (DQ211090), transcriptional regulation (DQ211091), restriction endonuclease

212

activity (DQ211092), and membrane transport (DQ211089). The possible involvement of these genes and their putative functions in *K. pneumoniae in vivo* pathogenicity remains to be established.

The genetic differences in our *K. pneumoniae* strains and their role in establishing pneumonia may be extremely useful in determining bacterial factors involved in the disease initiation and progression. They may also aid in providing insight into the genetic mechanisms enabling *K. pneumoniae* to be an effective opportunistic pathogen. In addition, these sequences highlight the genetic differences between a *K. pneumoniae* opportunistic pathogen and a commensal organism. It is interesting that the majority of the sequences identified in this study are not classically thought of as virulence factors. These include proteins involved in transcriptional regulation, membrane transport, restriction endonuclease activity and energy production and conversion. Yet these gene sequences were differentially expressed in the *K. pneumoniae* strain that can colonize the lungs and not in the commensal IA565 strain.

As a model for *K. pneumoniae* virulence versus commensalism, opportunistic pathogens can cause disease in a two-pronged approach depicted in Figure IV.9. First, expression of the non-classically associated virulence factors allows persistence/survival in areas of the host that are normally microbe-free, such as the lung. Second, the expression of the classical virulence-associated factors, such as iroN and type I fimbriae genes, enable these organisms to grow and thus cause disease in that environment. For strain 43816, persistence and survival is achieved by expression of genes that enable this bacteria to cope with the inhospitable environment of the lung: high oxygen levels, presence of reactive oxygen species, low pH, and presence of innate immune defenses.
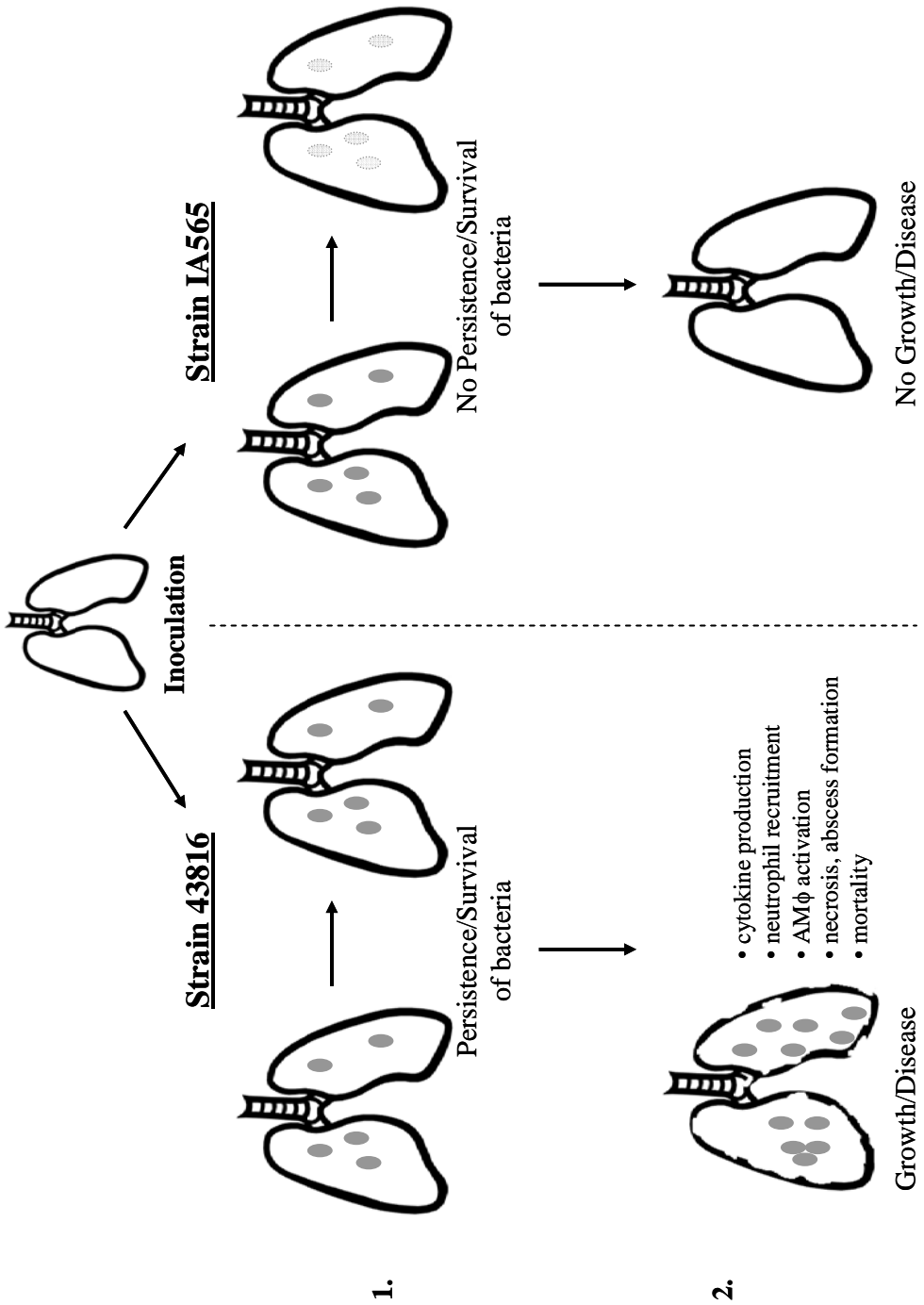
Figure IV.9 Model of *K. pneumoniae* Virulence Versus Commensalism

The subsequent growth of the bacteria and disease progression is due to the expression of classically associated virulence factors such as fimbriae for epithelial binding and capsule for immune evasion. In contrast, strain IA565 lacks these types of factors and can only proliferate in mucosal sites that are normally inhabited by various microbes. Thus, *K. pneumoniae* commensals are not genetically equipped to persist and grow in the lung environment.

Collectively, these results suggest that there are various mechanisms controlling commensal colonization at different mucosal sites such as the microflora and inflammatory processes. Furthermore, inherent properties of commensals and opportunistic pathogens dictate their ability to cause infection independent of the immune state of the host.

References

1. Emmerth, M., et al., *Genomic subtraction identifies Salmonella typhimurium prophages, F-related plasmid sequences, and a novel fimbrial operon, stf, which are absent in Salmonella typhi.* J Bacteriol, 1999. **181**(18): p. 5652-61.

2. Morrow, B.J., J.E. Graham, and R. Curtiss, 3rd, *Genomic subtractive hybridization and selective capture of transcribed sequences identify a novel Salmonella typhimurium fimbrial operon and putative transcriptional regulator that are absent from the Salmonella typhi genome.* Infect Immun, 1999. **67**(10): p. 5106-16.

3. Bogush, M.L., et al., *Identification and localization of differences between Escherichia coli and Salmonella typhimurium genomes by suppressive subtractive hybridization.* Mol Gen Genet, 1999. **262**(4-5): p. 721-9.

4. Janke, B., et al., *A subtractive hybridisation analysis of genomic differences between the uropathogenic E. coli strain 536 and the E. coli K-12 strain MG1655.* FEMS Microbiol Lett, 2001. **199**(1): p. 61-6.

5. Akopyants, N.S., et al., *PCR-based subtractive hybridization and differences in gene content among strains of Helicobacter pylori.* Proc Natl Acad Sci U S A, 1998. **95**(22): p. 13108-13.

6. Lai, Y.C., et al., *Identification of genes present specifically in a virulent strain of Klebsiella pneumoniae.* Infect Immun, 2000. **68**(12): p. 7149-51.

7.   Bock, A. and R. Gross, *The BvgAS two-component system of Bordetella spp.: a versatile modulator of virulence gene expression.* Int J Med Microbiol, 2001. **291**(2): p. 119-30.

8.   Boucher, P.E. and S. Stibitz, *Synergistic binding of RNA polymerase and BvgA phosphate to the pertussis toxin promoter of Bordetella pertussis.* J Bacteriol, 1995. **177**(22): p. 6486-91.

9.   Lai, Y.C., et al., *Identification and characterization of KvgAS, a two-component system in Klebsiella pneumoniae CG43.* FEMS Microbiol Lett, 2003. **218**(1): p. 121-6.

10.   Sagerstrom, C.G., B.I. Sun, and H.L. Sive, *Subtractive cloning: past, present, and future.* Annu Rev Biochem, 1997. **66**: p. 751-83.

11.   Zeng, J., R.A. Gorski, and D. Hamer, *Differential cDNA cloning by enzymatic degrading subtraction (EDS).* Nucleic Acids Res, 1994. **22**(21): p. 4381-5.

12.   Payne, S.M., *Iron and virulence in the family Enterobacteriaceae.* Critical Reviews in Microbiology, 1988. **16**(2): p. 81-111.

13.   Podschun, R., et al., *Incidence of Klebsiella species in surface waters and their expression of virulence factors.* Appl Environ Microbiol, 2001. **67**(7): p. 3325-7.

14.   Tarkkanen, A.M., et al., *Fimbriation, capsulation, and iron-scavenging systems of Klebsiella strains associated with human urinary tract infection.* Infect Immun, 1992. **60**(3): p. 1187-92.

15.   Russo, T.A., et al., *IroN functions as a siderophore receptor and is a urovirulence factor in an extraintestinal pathogenic isolate of Escherichia coli.* Infect Immun, 2002. **70**(12): p. 7156-60.

16. Podschun, R. and U. Ullmann, *Klebsiella spp. as nosocomial pathogens: epidemiology, taxonomy, typing methods, and pathogenicity factors.* Clin Microbiol Rev, 1998. **11**(4): p. 589-603.

17. Hornick, D.B., et al., *Fimbrial types among respiratory isolates belonging to the family Enterobacteriaceae.* J Clin Microbiol, 1991. **29**(9): p. 1795-800.

18. Langstraat, J., M. Bohse, and S. Clegg, *Type 3 fimbrial shaft (MrkA) of Klebsiella pneumoniae, but not the fimbrial adhesin (MrkD), facilitates biofilm formation.* Infect Immun, 2001. **69**(9): p. 5805-12.

Chapter V

Discussion and Future Directions

Klebsiella pneumoniae Mutagenesis

In the previous chapter, several uniquely expressed sequences were found in the virulent *K. pneumoniae* strain 43816. The generation of targeted gene deletion mutants was attempted to determine the role FimC and UreF, a type I fimbrial chaperone protein and urease accessory protein, plays during *K. pneumoniae* mediated pulmonary infection. However, using various techniques, strain 43816 mutants were unable to be generated. The details of this attempt are described below.

Rationale for Choosing Targeted Genes

To identify other possible virulence factors in *K. pneumoniae*, 25 pairs of primers were generated from *E. coli* sequences encoding *entA-F*, enterobactin synthesis genes; *fhuA*, ferrichrome receptor; *fhuE*, rhodoturulic acid receptor; *fecA*, ferric citrate receptor; *fepA*, siderophores receptor, *iucA-D*, aerobactin synthesis; *ureF*, urease accessory protein; and *fimC*, *sthE*, and *sthB*, type I fimbrial proteins. Strain 43816 and IA565 genomic DNA was used as template and PCR results are shown in Figure V.1. Gene sequences that were found to be present in strain 43816 and absent in strain IA565 were *iroN*, *ureF*, a urea transporter sequence, *sthE*, *fimC*, *sthB*, *emrY* and *entA* (Figure V.1B). Both *iroN* and *sthB* were sequences identified in the subtractive hybridization technique and were

Figure V.1 PCR of 43816 and IA565 Genomic DNA using *E. coli* Generated Primers PCR was performed on template genomic DNA from strain 43816 and IA565 (A) using primers generated from a varity of *E. coli* genomic DNA sequences (B). 4, PCR using 43816 DNA as template. I, PCR using IA565 DNA as template. +, correct amplicon detected. -, no product or wrong product detected.
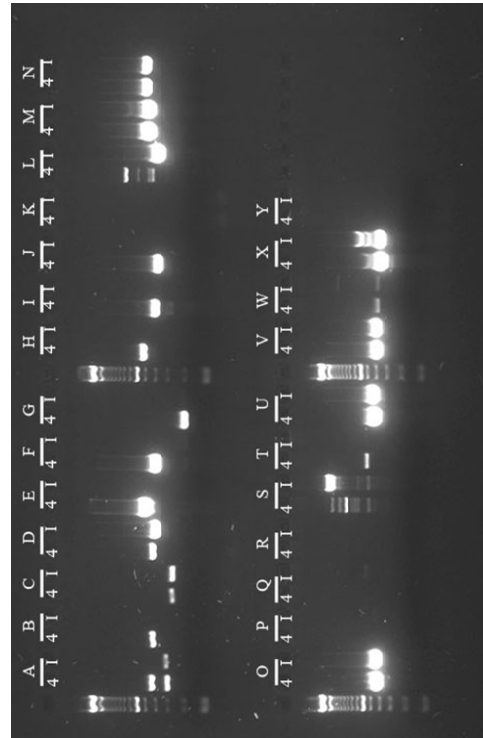
B

	Genes Tested via PCR	amplicon (bp)	43816 DNA	IA565 DNA
A	Lon Stress Protein	415	+	+
B	iroN	418	+	-
C	IutA, aerobactin R	260	+	+
D	hemolysin	418	+	+
E	UreF, urease acc. pr.	567	+	-
F	Urea Transporter	438	+	-
G	SthE, maj. Fim. sub.	206	+	-
H	FimC, chap. protein	537	+	-
I	SthB, fim. usher pr	425	+	-
J	EmrY, drug resis.	408	+	-
K	FhuE, rhodoturulic acid R	436	-	-
L	FecA, ferric citrate R	423	+	+
M	FepA, siderphore receptor	518	+	+
N	Aerobactin R	516	+	+
O	FhuA, ferrichrome R	473	+	+
P	IucA, aerobactin synthesis	554	-	-
Q	IucB, aerobactin synthesis	542	-	-
R	IucC, aerobactin synthesis	490	-	-
S	IucD, aerobactin synthesis	436	+	+
T	EntA, enterobactin synthesis	497	+	-
U	EntB, enterobactin synthesis	480	+	+
V	EntC, enterobactin synthesis	433	+	+
W	EntD, enterobactin synthesis	409	+	+
X	EntE, enterobactin synthesis	401	+	+
Y	EntF, enterobactin synthesis	402	-	-

A

221

previously confirmed to be exclusively present in strain 43816 (Table IV.3). However, for constructing *K. pneumoniae* mutants, the UreF and FimC genes were targeted for insertional inactivation with a kanamycin resistance cassette. The urease and type I fimbriae operon has been sequenced in *E. coli* and were found to be present with 60-80% nucleotide homology in the *K. pneumoniae* MGH 78578 strain (Figure V.2 and V.3). Thus, because these genes were sequenced and sequences flanking the targeted site are known, ureF and fimC were targeted for deletion.

Introduction to allelic exchange approaches used

Suicide Vectors:

Similar techniques performed in this study were previously used to mutagenize *K. pneumoniae* strains 43816 [1, 2], LM21 [3], and CG43 [4]. These studies used conditionally replicative plasmids, or suicide vectors, that allow construction of mutations and propagation in a bacterial host able to replicate them. Plasmids carrying the R6Kγ DNA origin, like in pWM91, pLD55, and pKAS32 used in this study, depend on the *pir* gene product for replication. In addition, bacterial hosts harboring these plasmids usually contain conjugation genes, called transfer or *tra* genes, which encode a surface appendage, the pilus. This is essential for recognition and mating-pair formation with the potential recipient cell [5]. *E. coli* strain 47084 is Tra+ due to the chromosomally integrated RP4 fragment [6]. In this study, *E. coli* strain 47084, carrying suicide plasmids with various disrupted *K. pneumoniae* genes, was bacterially conjugated to the recipient 43816 strain for horizontal transfer of these DNA sequences. The
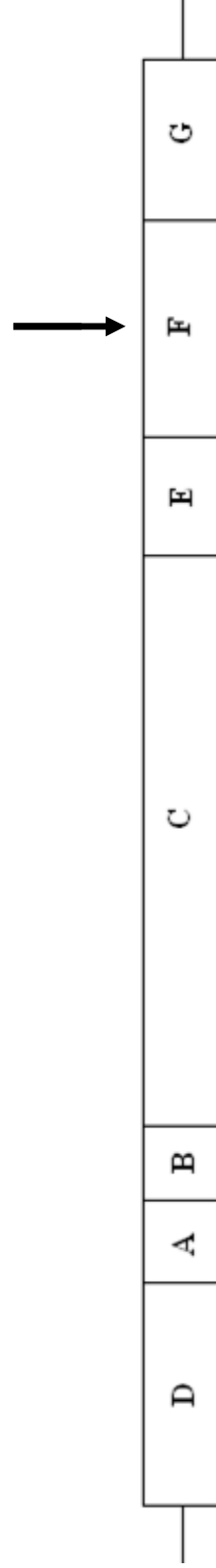
Figure V.2 Urease Operon of *K. pneumoniae* strain MGH 78578
Arrow represents gene targeted for deletion. Urease is a trimeric protein $(\alpha\beta\gamma)_3$
UreD, accessory protein (207 amino acids, 1027bp)
UreA, urease subunit γ (100 amino acids, 303bp)
UreB, urease subunit β (106 amino acids, 321bp)
UreC, urease subunit α (567 amino acids, 1704bp)
UreE, accessory protein (158 amino acids, 477bp)
UreF, accessory protein (224 amino acids, 675bp)
UreG, accessory protein (205 amino acids, 618bp)

223

Figure V.3 Type I Fimbriae Operon of *K. pneumoniae* strain MGH 78578
Arrow represents gene targeted for deletion.
FimB, regulatory protein (200 amino acids, 603bp)
FimE, regulatory protein (198 amino acids, 597bp)
FimA, A chain precursor (201 amino acids, 606bp)
FimI, fimbrin-like protein (179 amino acids, 540bp)
FimC, chaperone protein (241 amino acids, 726 bp)
FimD, outer membrane usher protein (878 amino acids, 2637bp)
FimF, protein precursor (177 amino acids, 534bp)
FimG, protein precursor (167 amino acids, 504bp)
FimH, protein precursor (303 amino acids, 912bp)

recipients were then grown under certain conditions that select for the allelic replacement of the mutated genes with their wild-type counterparts.

The suicide vectors pWM91 and pKAS32 both contain a counterselectable marker that further identifies the generation of *K. pneumoniae* mutants. The plasmid, pKAS32 contains the *rpsL* gene which encodes for ribosomal protein S12. A streptomycin resistant derivative of *K. pneumoniae* strain 43816, 43816S, was generated as a suitable recipient cell to use in this mutant selection method. When *rpsL* is expressed from pKAS32 in 43816S, the gene product assembles into ribosomes and confers a streptomycin sensitive phenotype. Selection for streptomycin resistance enables identification of transconjugants that have excised the plasmid sequences [7]. This type of method was used to generate the *K. pneumoniae* CG43 *kvgS* mutant [4]. The *sacB* gene on pWM91 when expressed in strain 43816 confers sucrose sensitivity, thus the subsequent ability to grow on sucrose plates provides another counterselectable marker to screen for *K. pneumoniae* mutants [6].

Lambda Red Recombinase System:

Three genes of the bacteriophage lambda (λ) have been used to induce DNA recombination events with as little as 40 nucleotides of shared sequence. The three genes of the λ red system are exo, gam (γ), and bet (β). The *exo* gene encodes an exonuclease which digests the 5'-end of double-stranded DNA, the β product binds to single-stranded DNA and promotes strand annealing, and the γ protein binds to and inhibits bacterial RecBCD enzyme [8]. Expression of plasmid encoded Red genes in bacterial cells is able to facilitate recombination between the bacterial chromosome and linear dsDNA molecules exogenously introduced via electroporation [9].

Allelic exchange using suicide vectors introduced via bacterial conjugation

   K. pneumoniae strain 43816 FimC and UreF sequences were amplified using

primers generated from *K. pneumoniae* specific sequences (Figure V.4) and cloned into

pPCR-Script Amp SK(+) generating pFimC and pUreF. PCR amplification of the cloned

insert was performed using the T3 and T7 primers flanking the cloning site (Figure V.5A)

as well as excision of the inserts via restriction enzyme digests with NotI and Acc65I

(Figure V.5B) to confirm cloning of the desired FimC and UreF genes. The kanamycin

resistance gene from pUC4K was removed via PstI digestion and 155bp and 100bp sized

internal fragments were removed from pFimC and pUreF, respectively (Figure V.6) to

generate pFimCΔ and pUreFΔ. The kanamycin cassette was ligated into the pFimCΔ and

pUreFΔ vector and then excised via restriction enzyme digest with NotI and Acc65I

(Figure V.7A). The excised fragments, FimCΔK and UreFΔK, had predicted sizes of

about 2Kb. However, Figure V.7A shows 2 bands at 3Kb and 2.5Kb. The 3Kb band

represents the vector and the 2.5Kb band represents the FimCΔK and UreFΔK fragments.

Since the fragment sizes were about 500bp larger than expected, pUreFΔK was submitted

for sequencing and it was found that there was an approximately 500bp repeat of the 3'

end of the kanamycin cassette within the disrupted genes. This is depicted in Figure

V.7B. Despite this, the FimCΔK and UreFΔK fragments were cloned into the pLD55

suicide vector.

   Primers were generated containing a NotI restriction enzyme recognition site, 40

nucleotides homologous to either FimC or UreF genes, and P1 or P2 sequences flanking

the kanamycin resistance cassette in pKD4 (Table II.4). Using pKD4 as template, the

primers were used to construct FimCΔKan^R and UreFΔKan^R, insertionally inactivated
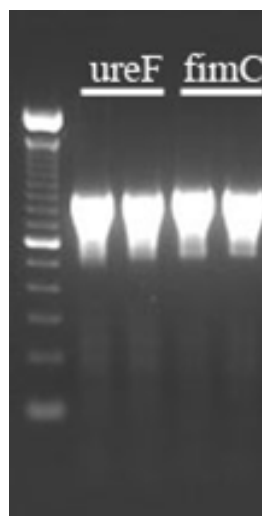
Figure V.4 Amplification and Isolation of *K. pneumoniae* strain 43816 FimC and UreF Sequences
Primers were generated towards *K. pneumoniae* FimC and UreF sequences and amplified in strain 43816. Expected sizes were 927bp and 907bp for FimC and UreF, respectively. 100bp ladder is shown on the far left hand side.
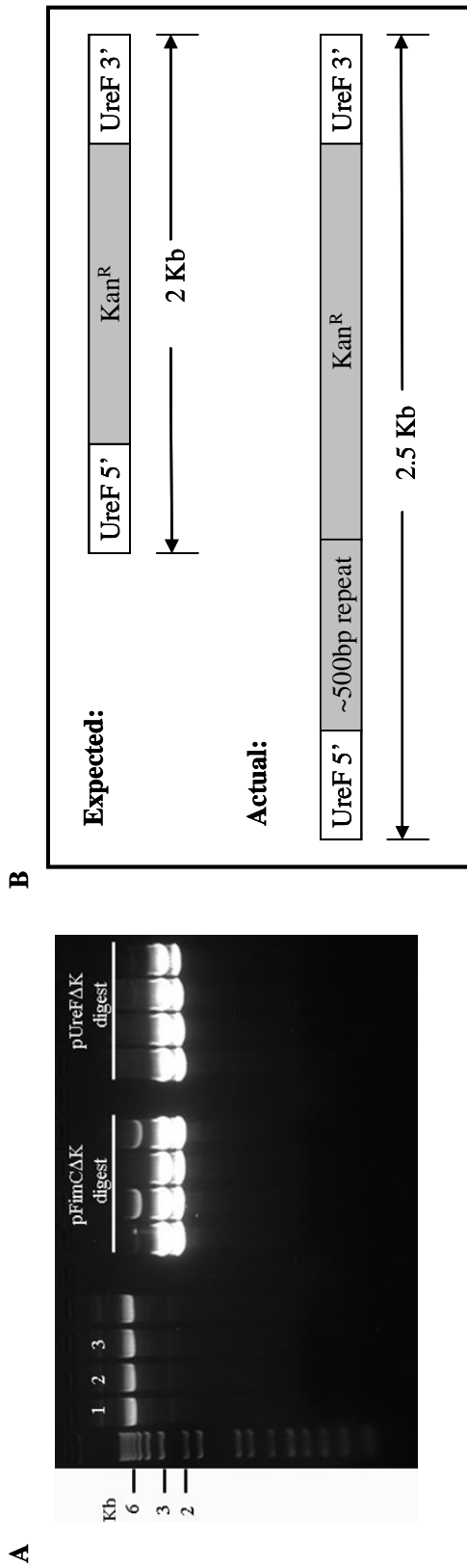
A

B
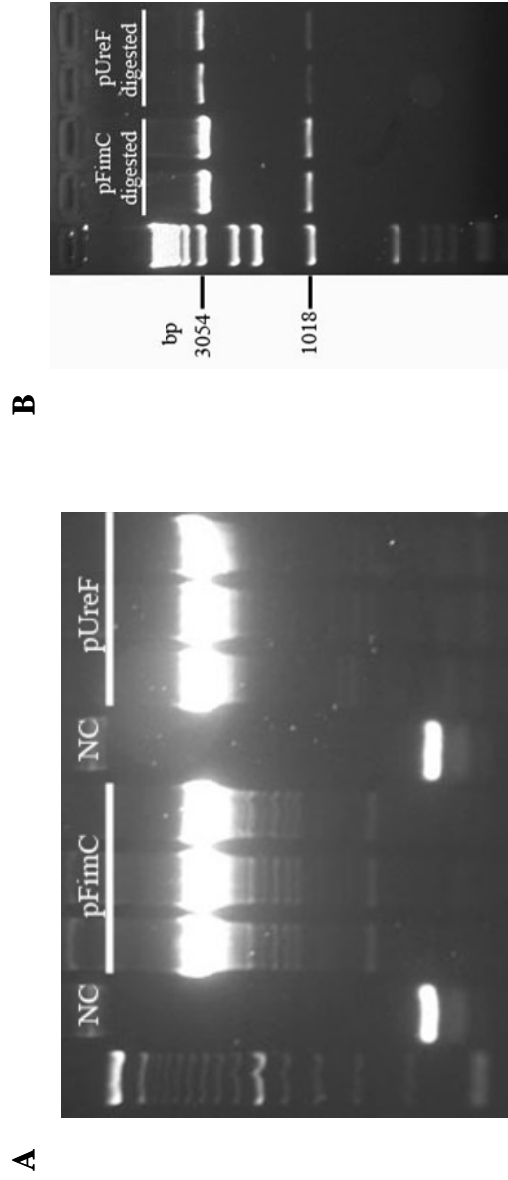
Figure V.5 Confirmation of Cloned FimC and UreF Genes
Genes were cloned into pPCR-Script Amp SK(+) Vector and plasmids were isolated from bacterial transformants. T3 and T7 primers flanking the cloning site were used to amplify the cloned gene to confirm insertion (A). NC lane represents the amplicon of an empty vector. These cloned genes were also digested with NotI and Acc65I, unique restriction sites flanking the cloning site. The 3Kb fragment is the vector and the 1011bp and 991bp fragment is the excised cloned inserts of FimC and UreF, respectively. 100bp ladder used in (A) and 1Kb ladder used in (B).
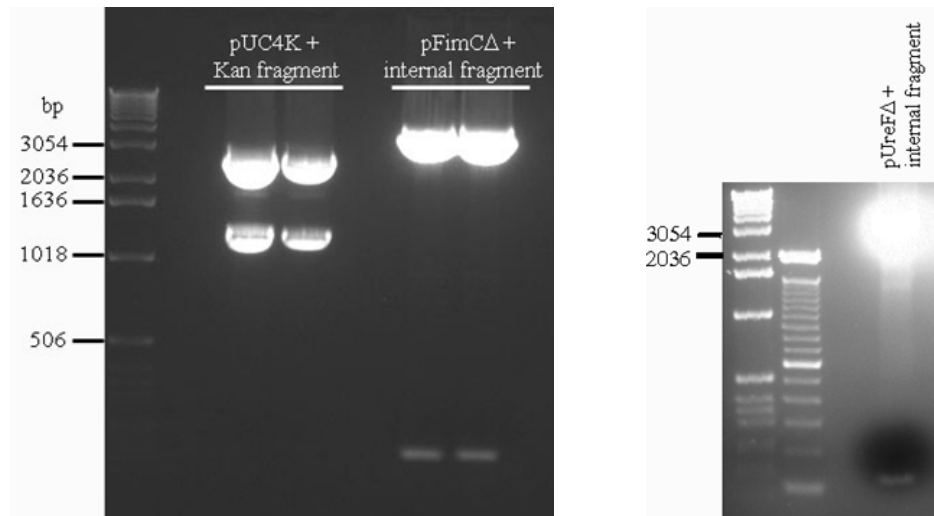
Figure V.6 Generation of pFimCΔ and pUreFΔ
Plasmids were digested to remove fragments of interest. pUC4K was digested with PstI to remove the 1.2Kb Kanamycin resistance gene. pFimC was digested with BlpI and BseRI to remove a 155bp internal fragment. pUreF was digested with Bpu10I and BlpI to remove a 100bp internal fragment. 1Kb ladder and 100bp ladder are shown.

B

Expected:

| UreF 5' | KanR | UreF 3' |

2 Kb

Actual:

| UreF 5' | ~500bp repeat | KanR | UreF 3' |

2.5 Kb

A

Kb
6
3
2

1 2 3

pFimCΔK digest

pUreFΔK digest

Figure V.7 FimCΔK and UreFΔK Fragment Isolation and Analysis

The kanamycin resistance gene flanked by FimC and UreF sequences were obtained by digesting pFimCΔK and pUreFΔK with NotI and Acc65I, unique restriction sites flanking the vector's cloning site (A). The 3Kb band represents the vector and the 2.5Kb band is the FimCΔK and UreFΔK fragment. A schematic diagram of the sequenced UreFΔK fragment is shown (B).

230

FimC and UreF genes. These fragments and the suicide vectors, pWM91 and pKAS32, were digested with NotI (Figure V.8A). FimCΔKan^R and UreFΔKan^R were ligated into pWM91 and pKAS32 forming plasmids 101, UreFΔKan^R in pKAS32; 102, FimCΔKan^R in pKAS32; 103, UreFΔKan^R in pWM91; and 104, FimCΔKan^R in pWM91. These plasmids were then transformed into *E. coli* strain 47084 and plasmid preps from the bacterial transformants were PCR amplified using FimC and UreF specific primers to confirm ligation (Figure V.8B). Strain 47084 containing plasmid 103, strain H103, was mixed with *K. pneumoniae* 43816 and aliquots of the conjugation mixture were plated onto LB-sucrose plates. Strain 47084 containing plasmids 101 and 102, strain H101 and H102, respectively, were mixed with a streptomycin resistant derivative of *K. pneumoniae* 43816, 43816S, and the conjugation mixtures were plated on LB-streptomycin plates.
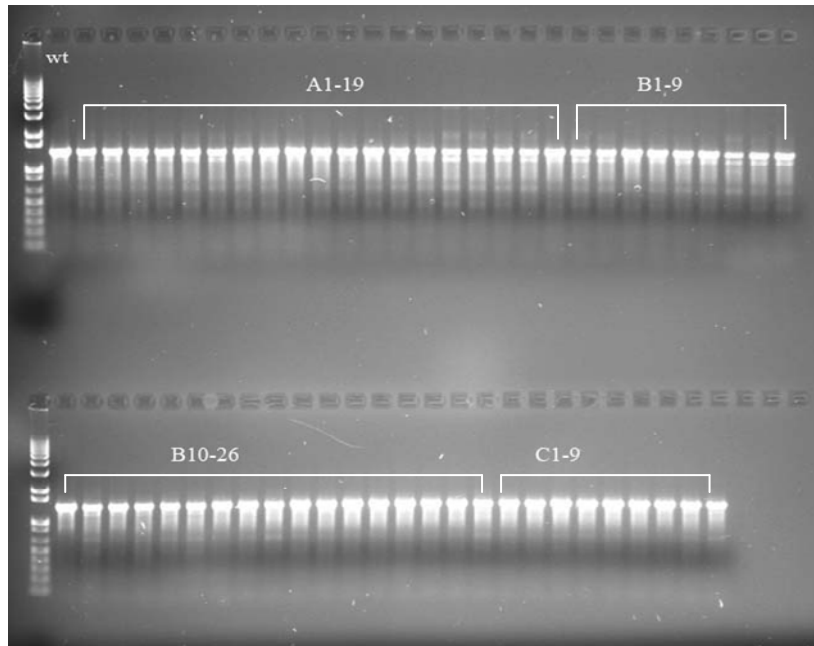
Nineteen transconjugants from mating 43816S and H101, 26 transconjugants from mating 43816S and H102, and 9 transconjugants from mating 43816 and H103 were obtained and analyzed via colony lysate PCR using the respective FimC and UreF primers (Figure V.9). None of the transconjugants harbored the insertionally inactivated genes.

Allelic exchange using temperature sensitive plasmid

Primers were generated containing Acc65I restriction enzyme recognition site, 40 nucleotides homologous to the FimC gene, and P1 or P2 sequences flanking the kanamycin resistance cassette in pKD4 (Table II.4). Using pKD4 as template, the primers were used to construct FimCΔKan^R, an insertionally inactivated FimC sequence.
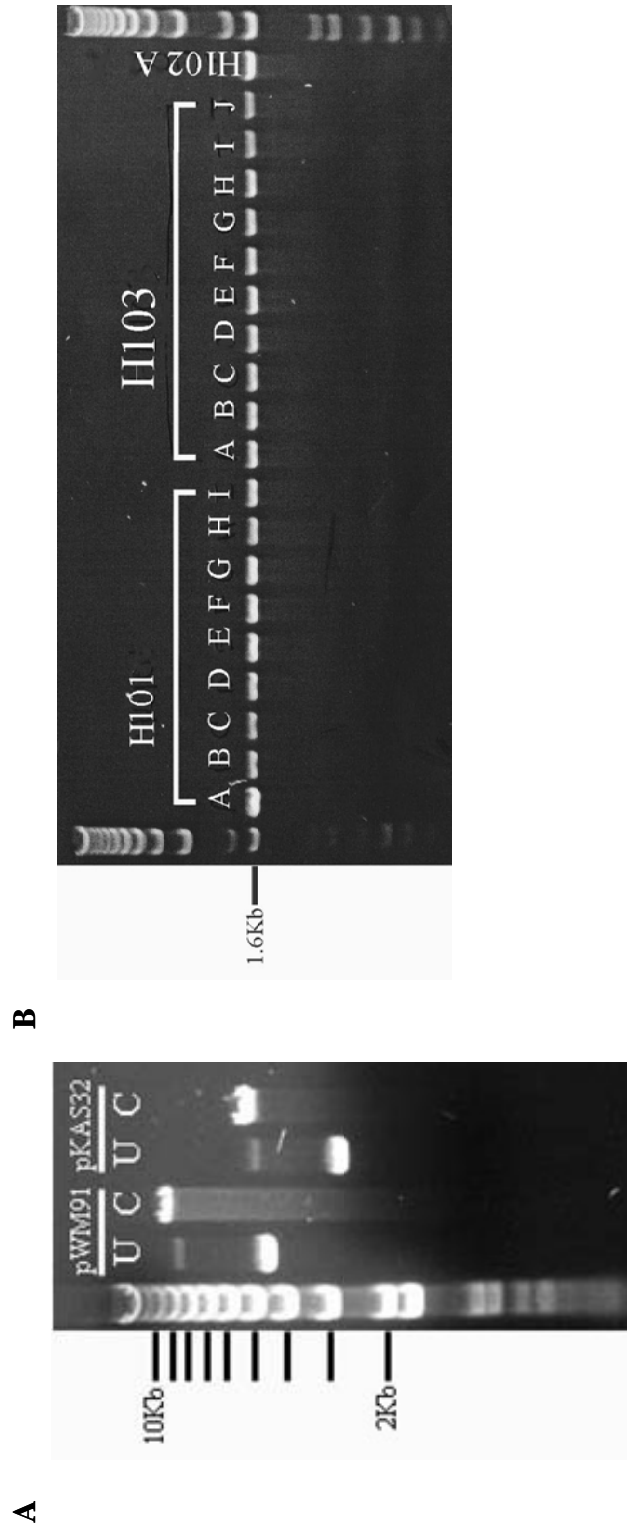
Figure V.8 Generation of Strains H101, H102 and H103

pWM91 and pKAS32 were digested with NotI (A). U, uncut plasmid; C, cut plasmid. NotI digested UreFΔKan^R and FimCΔKan^R fragments were ligated into the digested pWM91 and pKAS32 vectors and cloned into *E. coli* strain 47084. PCR was performed on plasmids isolated from the bacterial transformants using the respective FimC and UreF primers (B). FimC and UreF amplicons were 1592bp.

Figure V.9 Colony Lysate PCR of Transconjugants
Strain 43816S was conjugated to strains H101 and H102. Strain 43816 was conjugated to strain H103. 19 transconjugants from mating 43816S and H101, 26 transconjugants from mating 43816S and H102, and 9 transconjugants from mating 43816 and H103 were obtained and analyzed via colony lysate PCR using the respective FimC and UreF primers. Wild-type amplicon for UreF is 1329bp and for FimC is 1225bp. Mutant amplicon for UreF is 2546bp and 1954bp for FimC. wt denotes FimC amplicon for original 43816 strain.

This was cloned into the Acc65I digested pKD78, a chloramphenicol resistance gene containing vector, whose replication in a bacterial host is temperature dependent. This was then transformed into *K. pneumoniae* strain 43816. Bacterial colony lysate PCR was performed on a bacterial transformant and strain BW26949, a strain harboring pKD78, using 2 set of primers specific for plasmid sequences and the kanamycin resistance gene (Figure V.10). The plasmid specific and kanamycin resistant gene sequences were present in strain 43816 harboring FimCΔKan^R ligated into pKD78. Strain BW26949 only contained the plasmid specific sequences as expected. Strain 43816 harboring FimCΔKan^R ligated into pKD78 was grown overnight at the permissive temperature to select for 43816 bacteria harboring the plasmid and then for 2 days at the non-permissive temperature to induce integration of the plasmid into the chromosome. The cultures were diluted onto LB-chloramphenicol plates and a robust colony was chosen and grown for several days at the permissive temperature to select for bacteria that have excised plasmid sequences. Aliquots of this culture were patched onto LB-chloramphenicol plates and bacteria that were chloramphenicol sensitive and kanamycin resistant were analyzed for FimCΔKan^R chromosomal integration via PCR with FimC and kanamycin resistance cassette specific primers (Figure V.11A and B, respectively). None of the colonies selected contained the disrupted FimC gene.

Allelic recombination using the lambda red recombinase system

The lambda red system was also used in this study to obtain *K. pneumoniae* 43816 mutants. For this method, the FimC gene was targeted for insertional inactivation. Figure V.12 illustrates the wild-type FimC gene and the area targeted for deletion as well
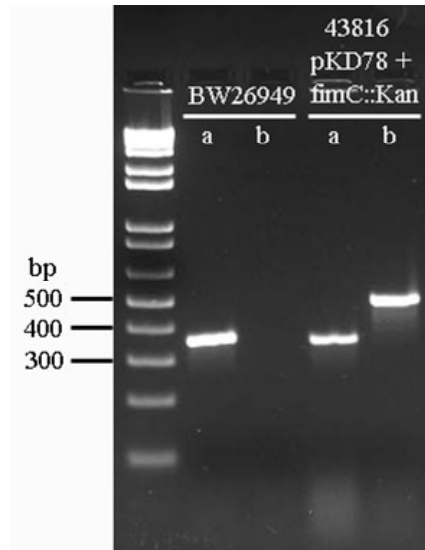
Figure V.10 Generation of a Temperature Sensitive Plasmid Containing FimCΔKan^R
The FimΔKan^R fragment was cloned into pKD78 and then transformed into strain 43816.
Colony lysate PCR was performed on that strain and strain BW26949, which contains pKD78
without the cloned fragment. Gam (a) and kanamycin cassette (b) amplifying primers were
used. Gam primers amplify a 349bp region and the kanamycin primers amplify a 471bp
region. 1Kb ladder is shown.
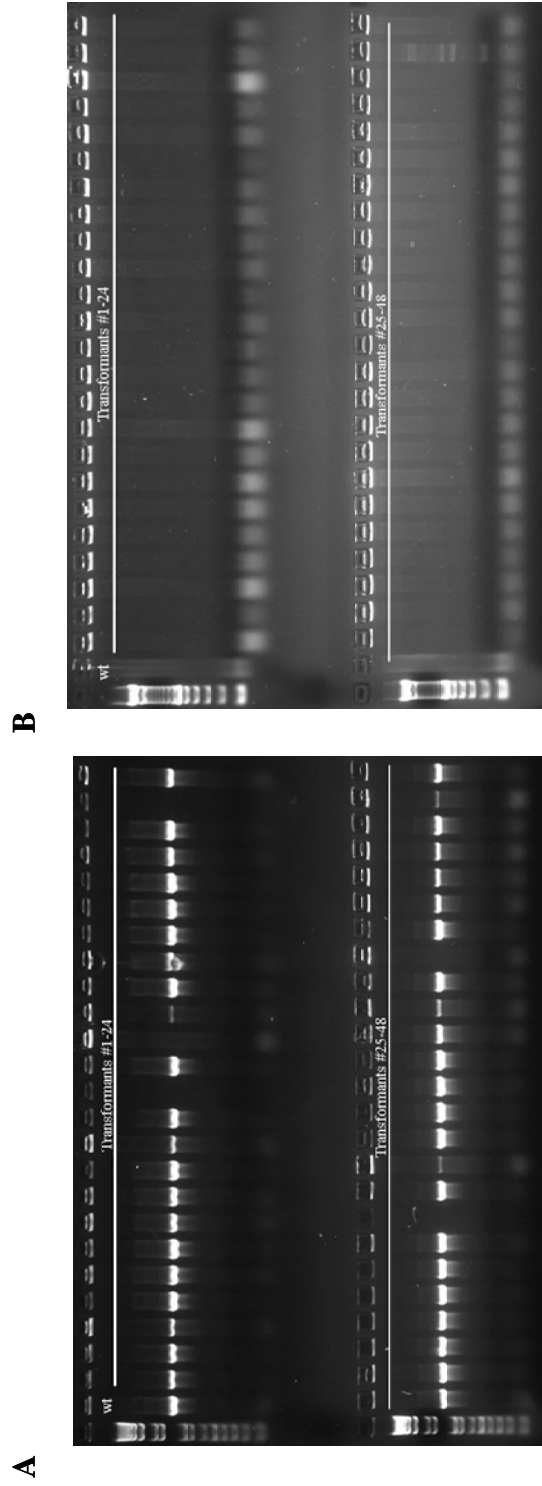
Figure V.11 Growth of 43816 Transformed with pKD78 containing FimCΔKan^R PCR of colonies that grew on LB-Kanamycin plates using PCR Test FimC1 and FimC2 (A) and kanamycin cassette (B) primers was performed. None of the transformants contained the disrupted FimC gene. Wild-type (wt) FimC gene expected size is 1225bp. Mutated FimC gene expected size is 1938bp. Kanamycin cassette amplicon is 471bp. 1Kb ladder is shown for each gel.

236

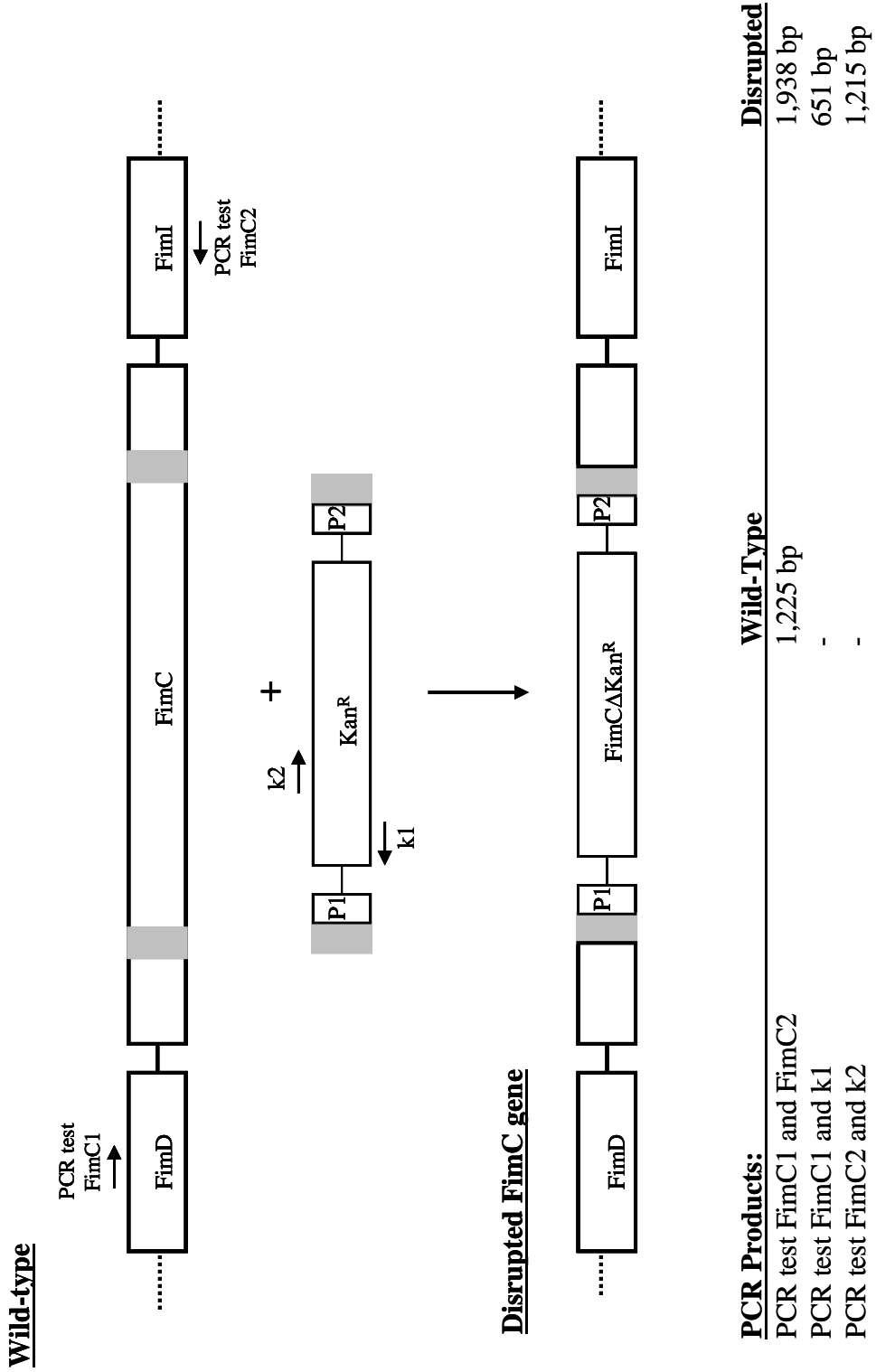**Figure V.12 Lambda Red Recombinase Scheme and Products**

PCR Products:	Wild-Type	Disrupted
PCR test FimC1 and FimC2	1,225 bp	1,938 bp
PCR test FimC1 and k1	-	651 bp
PCR test FimC2 and k2	-	1,215 bp

237

as the expected PCR products from amplification of wild-type and mutant DNA. Primers

were constructed containing 40 nucleotides homologous to the FimC gene, and P1 or P2

sequences flanking the kanamycin resistance cassette in pKD4 (Table II.4). The linear

dsDNA fragment, FimCΔKan^R depicted in Figure V.12 was constructed using those

primers and pKD4 as template (Figure V.13A). pKD78 was transformed into strain

43816, transformants are designated HL078. Bacterial lysate colony PCR was performed

on those transformants using primers generated from plasmid specific sequences (Figure

V.13B). FimCΔKan^R was electroporated into HL078 and the cells were grown on LB-

kanamycin plates. Allelic exchange of the disrupted FimC gene with the wild-type gene

was screened for via PCR using FimC primers flanking the targeted deletion site (Figure

V.13C). None of the bacterial cells contained the mutated FimC gene.

Two modifications to the lambda red system were made to facilitate *K.*

pneumoniae strain 43816 mutagenesis. In the first modification, bacteriophage ϕX174

HaeIII-digested DNA was added to the solution of FimCΔKan^R fragments at a ratio of

100:1 to circumvent the possibility that *K. pneumoniae* exonucleases were digesting the

linear dsDNA fragment preventing FimCΔKan^R from integrating into the chromosome.

This mixture was electroporated into HL078 cells and transformants analyzed by PCR

(Figure V.14). None of the bacterial cells contained the mutated FimC gene.

In the second modification, more gene homology regions flanking the kanamycin

resistance gene was added to increase efficiency of allelic exchange. Construction of a

UreA disrupted gene fragment has been previously described [3] and thus a similar

approach was used in this study. The diagram for the construction of UreAΔKan^R is

shown in Figure V.15. Not to spoil the ending, but this construct proved very difficult to
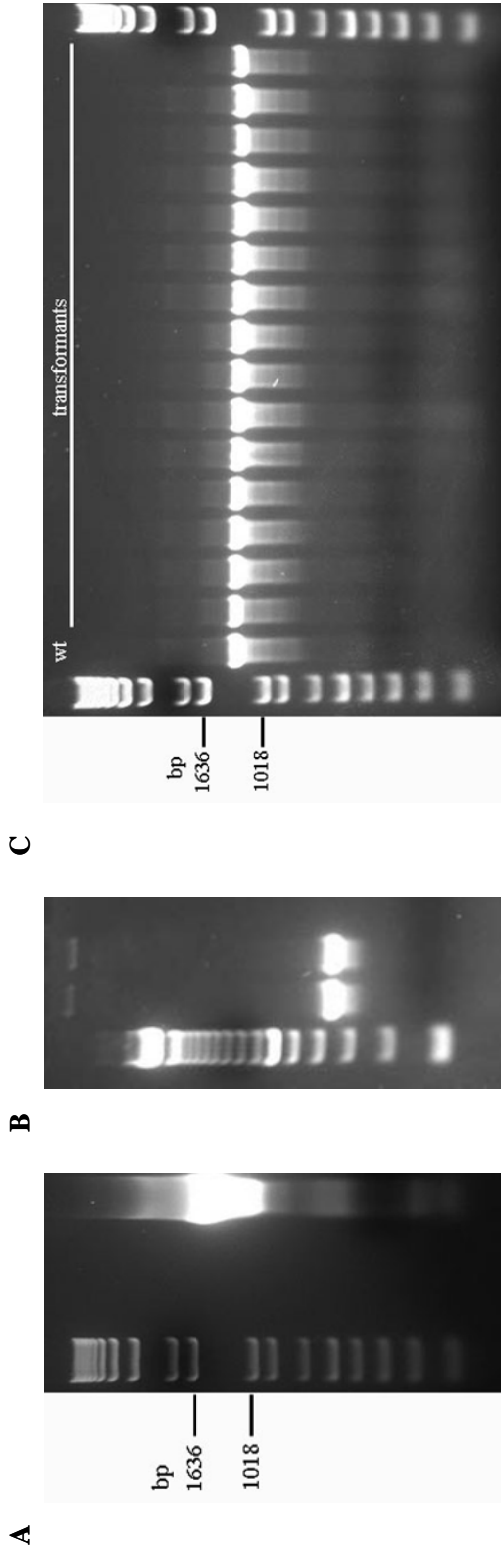
Figure V.13 Mutagenesis of 43816 using the Lambda Red System

(A)Primers P1-H1 FimC and P2-H2 FimC were used to construct the lambda red fragment, FimC∆Kan^R using the plasmid, pKD4 as template DNA. The expected size is 1594bp. 1Kb ladder is shown.

(B) Primers amplifying the gam gene on the pKD78 plasmid were generated. Bacterial colony lysate PCR was performed on BW26949, the strain containing pKD78 (Lane 1) and HL078 (Lane 2). Expected size of PCR product is 349bp. 100bp ladder is shown.

(C) PCR of colonies that grew on LB-Kanamycin plates using PCR Test FimC1 and FimC2 primers was performed. None of the transformants contained the disrupted FimC gene. Wild-type (wt) FimC gene expected size is 1225bp. Mutated FimC gene expected size is 1938bp.

239
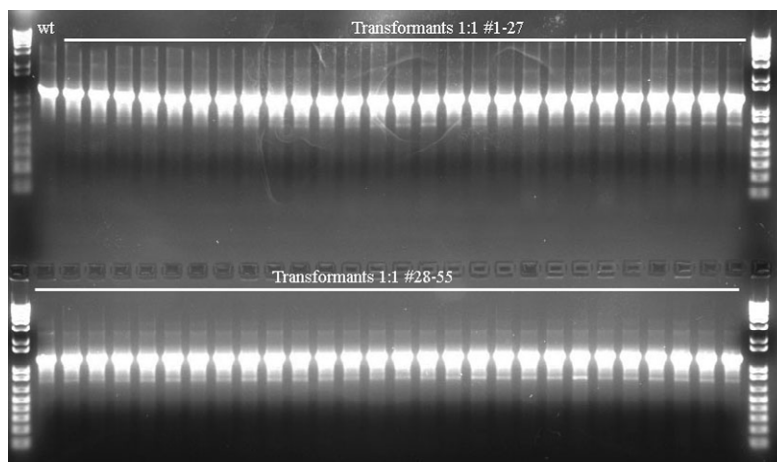
Figure V.14 Mutagenesis of 43816 using the Lambda Red System and Decoy DNA
Bacteriophage φX174 HaeIII-digested DNA was added to the solution of FimCΔKan^R fragments at a ratio of 100:1. This was electroporated into HL078. PCR of colonies that grew on LB-kanamycin plates using PCR Test FimC1 and FimC2 primers was performed. None of the transformants contained the disrupted FimC gene. Wild-type (wt) FimC gene expected size is 1225bp. Mutated FimC gene expected size is 1938bp.

Urease deletion scheme:

ureD   ureA   ureB   ureC

5′ …GCCCGGTGATTGGCGAAACCTTCAGCC…CTGGCTGACTTAAGAGAGAAACGTTATGGAA…CTGAGGTAGCGCCATGATCCCC…CGACATCCAGCCAACGTCACCATCC… 3′

3′ …CGGGCCACTAACCGCTTTGGAAGTCGG…GACCGACTGAATTCTCTTGCAATACCTT…GACTCCATCGCGGTACTAGGGG…GCTGTAGGTCGGGTTGCAGTGGTAGG… 5′

643bp   V   VII   1022bp   1322bp   VIII   VI   1972bp

ureA::Kanᴿ Fragment: (383 + 1,496 + 651 = 2,530bp)

5′ …GCCCGGTGATTGGCGAAACCTTCAGCC…CTGGCTGACTTAAGAGAACGTTATGGTGTAGGCTGGAGCTGCTTCGAA…CGCATGATGATTGAA…TTCTTCTGAGCG…TATGGACCATGGTAATTCCCATAGGTAGCGCCCAACGTCACCATCC… 3′

3′ …CGGGCCACTAACCGCTTTGGAAGTCGG…GACCGACTGAATTCTCTTGCAATAC CACATCCGACCTCG ACGAAGCTT…GGTACTAACTT…AAGAAGACTCGC…ATACCTGGTACCGTTAGGGTA TCCATCGCGGTACCGTTAAGGGTA…GCTGTAGGTCGGGTTGCAGTGGTAGG… 5′

     V   VII – P1   VIII – P2   VI

V - VII-P1 product   VI - VIII-P2 product

403bp   671bp

(383 + 20)   (651 + 20)

P1	GTGTAGGCTGGAGCTGCTTC
P2	ATGGGAATTAGCCATGGTCC
V	CGGTGATTGGCGAAACCTTCA
VI	TGGTGACGTTGGGCTGGATG
VII-P1	GAAGCAGCTCCAGCCTACACCCATAAACGTTCTCTTAAGTCAGC
VIII-P2	GGACCATGGCTAATTCCCATAGGTAGCGCCCATGATC

Figure V.15 Diagram of UreAΔKanᴿ Fragment for use in the Lambda Red Recombinase System

241

generate. The primary author of the paper this protocol was obtained from indicated that making this construct was a little tricky – a huge understatement.

The 403bp (V – VII-P1) 5' and 671bp (VI – VIII-P2) 3' end of the UreAΔKan^R fragment were generated via PCR using 43816 genomic DNA as template (Figure V.16). Those fragments were then combined with the P1 and P2 primer amplified kanamycin resistance cassette from pKD4 and subjected to three various PCR conditions to obtain the 2,530bp UreAΔKan^R fragment (Figure V.17). PCR conditions for Condition #1 were 94ºC for 5 minutes and 35 cycles of 94ºC for 1 minute, 63ºC for 30 seconds, and 68ºC for 2.75 minutes. PCR conditions for Condition #2 were 94ºC for 5 minutes and 35 cycles of 94ºC for 30 seconds, 63ºC for 30 seconds, and 72ºC for 3 minutes. PCR conditions for Condition #3 were 7 cycles of 94ºC for 1 minute and 63ºC for 45 seconds followed by 35 cycles of 94ºC for 1 minute, 63ºC for 30 seconds, and 72ºC for 3 minutes.   These conditions did not yield the desired product.

Using a different approach, fragment A, consisting of the 403bp end and kanamycin cassette, and fragment B, consisting of the kanamycin cassette and the 671 bp end, were generated and those fragments were gel purified (Figure V.18). Those fragments were then incubated with the V and VI primer in various PCR conditions to generate the UreAΔKan^R fragment (Figure V.19). PCR conditions for Condition #1 were 10 cycles of 94ºC for 1 minute and 55ºC for 1 minute followed by 40 cycles of 94ºC for 45 seconds, 55ºC for 45 seconds, and 72ºC for 3 minutes. PCR conditions for Condition #2 were 94ºC for 5 minutes; 10 cycles of 94ºC for 5 minutes and 55ºC for 2 minutes; followed by 40 cycles of 94ºC for 1 minute, 55ºC for 2 minutes and 72ºC for 3 minutes. PCR conditions for Condition #3 were 94ºC for 5 minutes followed by 30
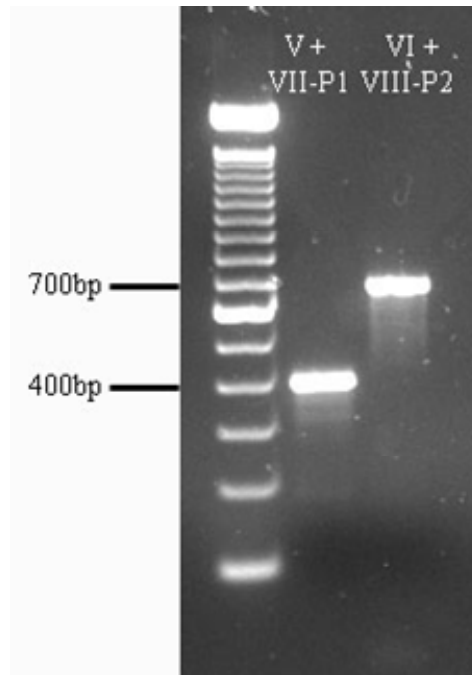
Figure V.16 Left-handed and Right-handed Fragments of UreFΔKan^R
Using 43816 genomic DNA as template, primers V and VII-P1 (Lane 1) and
primers VI and VIII-P2 were used to amplify the left and right hand fragments
of UreFΔKan^R. Expected sizes are 403bp and 671bp. 100bp ladder is shown.
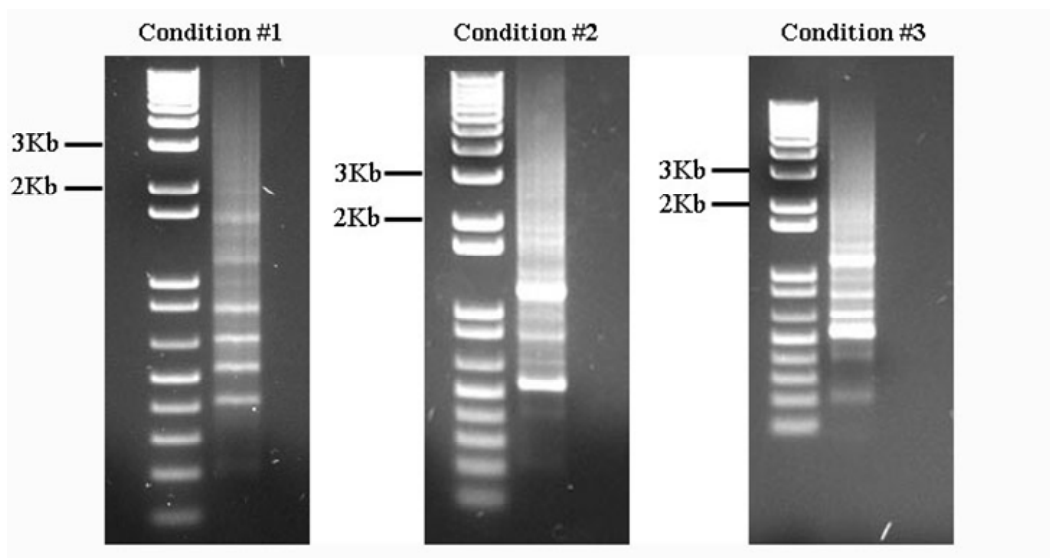
Figure V.17 Results of Various PCR Conditions Used to Generate UreFΔKan^R
Expected product size is 2530bp. None of the PCR conditions used generated the desired product.
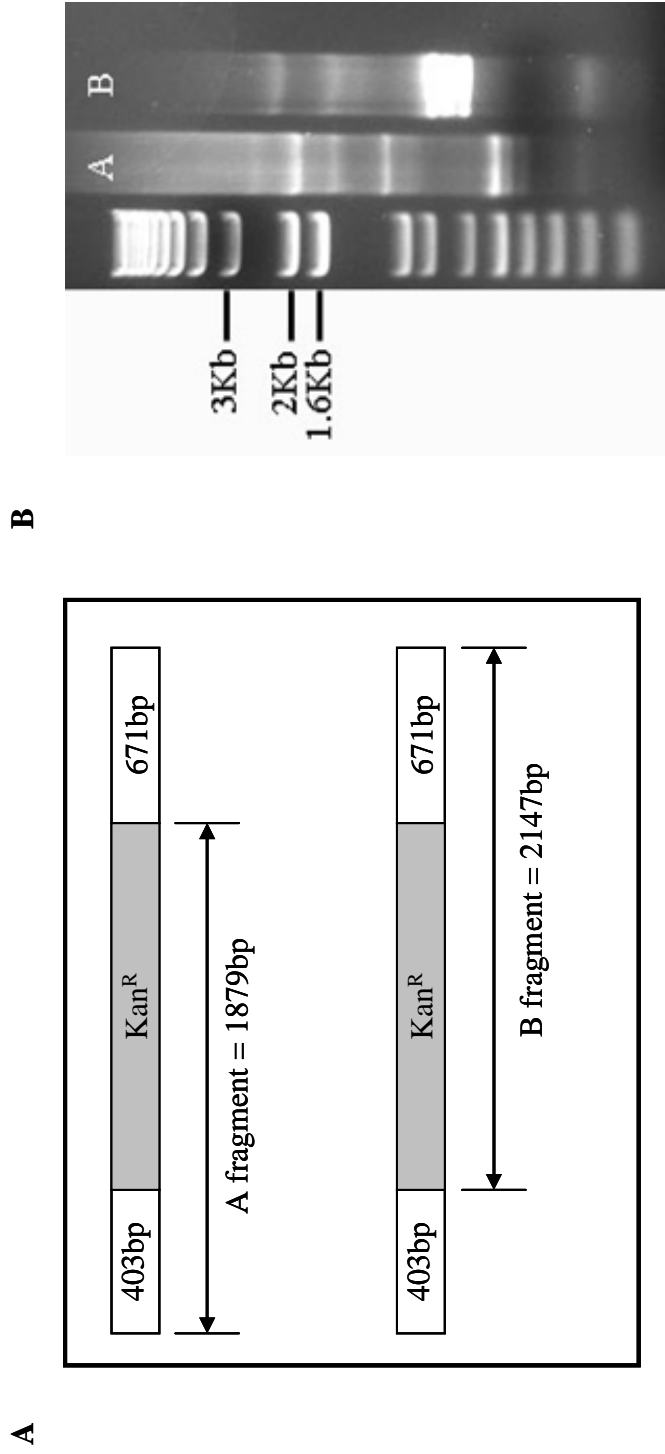
Figure V.18 A and B Fragments of UreFΔKan^R
Diagram of fragments A and B are shown in (A). Fragments corresponding to those sizes were obtained and agarose gel purifed (B).
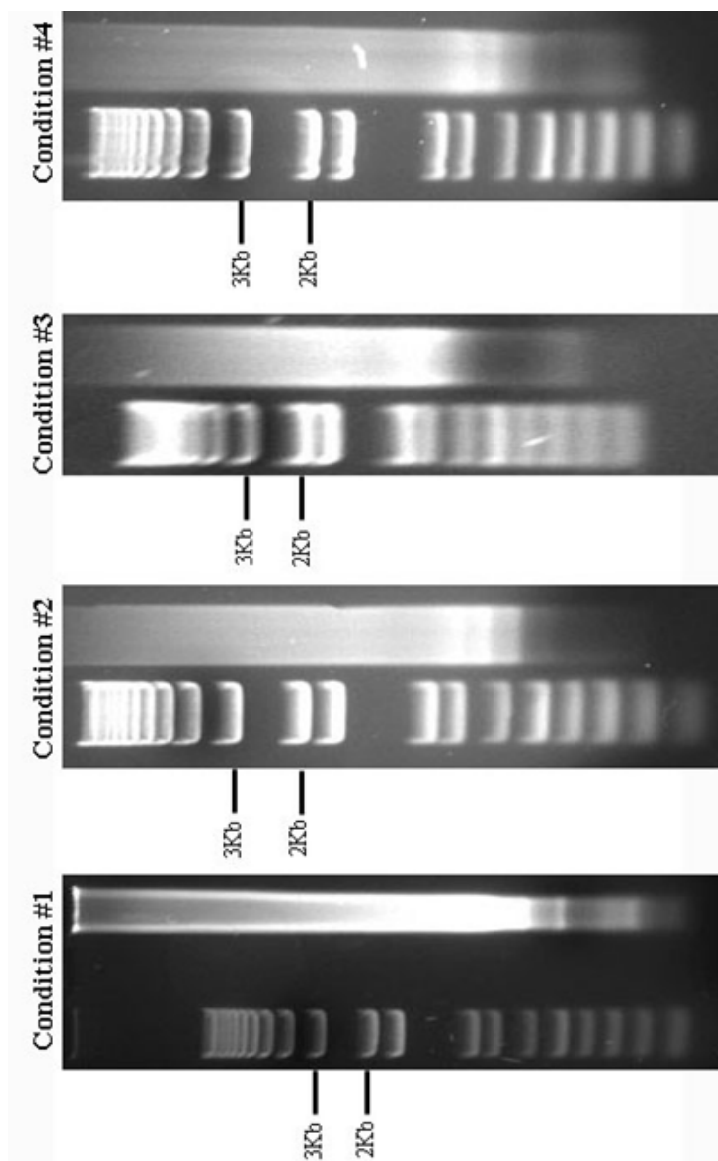
Figure V.19 Results of PCR Conditions Using A and B to Generate UreFΔKan^R Expected product size is 2530bp. None of the PCR conditions used generated the desired product.

cycles of 94ºC for 1 minute, 55ºC for 2 minutes, and 72ºC for 3 minutes. PCR conditions

for Condition #4 were 94ºC for 5 minutes followed by 30 cycles of 94ºC for 2 minutes,

55ºC for 5 minutes, and 72ºC for 3 minutes.   These conditions did not yield the desired

product.

In one final attempt to generate the UreAΔKan^R fragment, varying mixtures of

Taq and Pfu DNA polymerase were in the PCR reaction (Figure V.20). The Taq

polymerase used in these reactions do have 3' to 5' exonuclease proofreading activity due

to an exogenously added enzyme (see Materials and Methods). However, Pfu has natural

3' to 5' exonuclease activity and the half-life is significantly longer than Taq polymerase.

Two reactions were run with the 403bp and 671 bp fragments as primers and the

kanamycin cassette as the template. The PCR products in lane 1 were obtained from

using only Taq polymerase in the reaction mix. The PCR products in lane 2 were

obtained from using Taq and Pfu polymerase at a ratio of 0.75 units to 0.25 or 3:1.

Surprisingly, using the Taq and Pfu polymerase mix did yield a band at 2.5Kb, the

expected size of UreAΔKan^R (Figure V.20, Lane 2, arrow). This band was excised, gel

purified and used as a template in PCR reactions with primers V and VI. However, PCR

products always contained multiple bands when run on a gel with none of them being the

correct size of 2.5Kb.
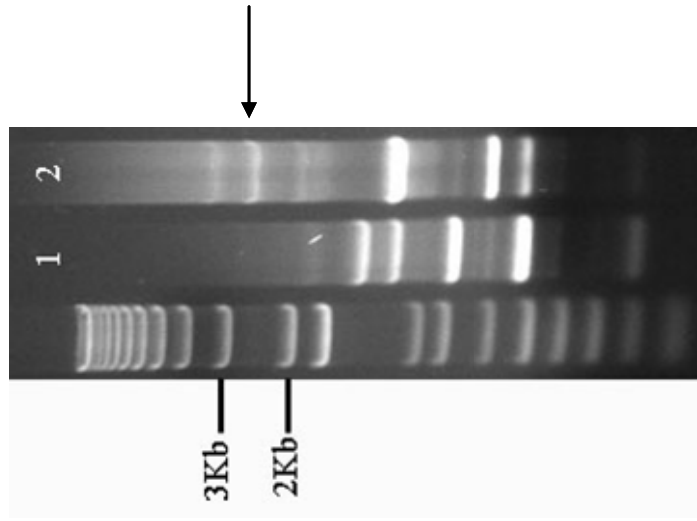
Figure V.20 Use of Various DNA Polymerases to Generate UreFΔKan^R^
DNA Taq polymerase (Lane 1) and a 3:1 mixture of Taq:Pfu DNA polymerase (Lane 2) was used in PCR reactions to obtain the UreFΔKan^R^ fragment. Arrow points to a band of the desired product size, 2530bp.

Discussion of *K. pneumoniae* mutagenesis attempts

As alluded to earlier, genes have been successfully deleted from *K. pneumoniae* strain 43816 in other studies. Specifically, mutants in the siderophore transporter component of the yersiniabactin system (*ybtQ*), the galactosyltransferase necessary for O1 O-antigen synthesis (*wbbO*), and a DNA adenine methylase (*dam*) have been previously described [1, 2, 10]. It is unclear why mutants in the same 43816 strain background could not be constructed in this study. However, it is possible that the technical expertise required to perform the mutagenesis was beyond the scope of this researcher's ability.

Virulence Factors versus Factors associated with Virulence

As discussed in Chapter I, environmental surface water isolates of *K. pneumoniae* were found to be just as capable of expressing virulence factors as clinical isolates. In addition, when evaluated in murine models of UTI and intestinal colonization, these environmental isolates were as virulent as strains of clinical origin. These studies have strong implications for the description and definition of *K. pneumoniae* virulence properties.

"Virulence factors" describe those factors that by themselves enable the organism to cause disease. Examples include the lethal factor and oedema factor enzymes produced by *Bacillus anthracis* [11] and the shiga toxin produced by enterohaemorrhagic *E. coli* [12]. On the other hand, "factors associated with virulence" describe those factors that when given the opportunity to cause infection, aid the microbe in pathogenesis. In other words, commensal and environmental strains may contain these "factors associated

with virulence" but rarely are in the situation where host conditions are right to cause an infection. Yet, when the conditions are right, UTI, pneumonia, septicemia and other *K. pneumoniae* infections ensue. This correlates to the findings which indicate that some pneumonia causing strains of *K. pneumoniae* originate from the flora of hospitalized patients suggesting that those *K. pneumoniae* strains carry "factors associated with virulence".

However, because strain IA565 was unable to cause disease even under extreme immunosuppressive conditions, it is unclear whether or not some *K. pneumoniae* strains even have the aforementioned "factors associated with virulence". It is possible there are *K. pneumoniae* opportunistic pathogens that colonize various mucosal sites waiting to take advantage of the immunocompromised state of the host to flourish. And, as this study suggests, there are *K. pneumoniae* strains that are simply commensal organisms. Should the species designation of strain IA565 be renamed from *K. pneumoniae* to *K. commensiae*? It is very clear that strain 43816 and IA565 significantly differ in their *in vivo* pathogenicity and IA565 is unique in its mucosal tissue colonization patterns.

Summary of IA565 Colonization Data

Table V.1 summarizes the ability of strain IA565 to colonize the lungs, nasal cavity and GI tract of wild-type, immunodeficient and GF mice. Strain IA565 is unable to grow and persist in the lung. However, similar levels of nasal cavity colonization can be achieved in immunocompetent, immunocompromised and germ-free mice. This is in contrast to IA565 GI tract colonization where the absence of the gut microbiota leads to increased IA565 growth.

Table V.1 Summary of IA565 Colonization in the Murine Host[a]

	Various Host Conditions		
Organ	**Wild-Type Animals**	**Absence of Innate Immunity**	**Absence of Microbiota**
Lungs	-	-	-
Nasal cavity	+	+	+
GI Tract	+	n.d.	++

[a]n.d., no data. +, growth and ++, increased growth in that organ

K. pneumoniae Commensalism

The studies carried out in this project identifies strain IA565 as a murine commensal and the endogenous (both host and microbiota) mechanisms controlling commensal growth. Furthermore, during non-specific gut inflammation and not during inflammation specifically directed towards another enteric organism, IA565 intestinal growth significantly increased suggesting host mediated inflammatory conditions effect commensal behavior. Furthermore, the microbiota in certain areas of the host was also found to have an effect on commensal colonization. The absence of the nasal cavity flora versus the absence of the gastrointestinal flora had a differential effect on IA565 colonization in those respective areas with the latter resulting in extremely high titers of IA565 bacteria. This suggests that commensal colonization in two different distal mucosal sites of the host can be modulated by the microbiota.

Normally, potential pathogens and commensals cannot be found in the lung because of effective microbial clearance mechanisms. However, even in the absence of two major lung phagocytes and T and B lymphocytes, strain IA565 was unable to persist in that environment. This suggests that strain IA565 lacks "factors associated with virulence" necessary for pulmonary pathogenesis and thus, is truly a commensal organism.

Strain IA565 is a clinical isolate and was cultured out of the tracheal aspirate of hospitalized patient. The patient's history and reasons for hospitalization is unknown. However, results of this study suggest that strain IA565 was most likely not the causative agent of disease in that patient. It is more likely that the tracheal aspirate sample was

contaminated with this organism and this bystander was mistaken for an opportunistic

pathogen.

Future Directions

It would have been interesting to identify differentially expressed sequences in

IA565 that are absent or less expressed in strain 43816. Unfortunately, at the time the

SSH was done, there was a greater interest in identifying putative *K. pneumoniae*

virulence factors rather than identifying genes not associated with pathogenicity.

Commensals are currently not very well studied. However, with recent studies

implicating the involvement of the gut microbiota in oral and mucosal tolerance, the

study of commensal interactions with the host immune system and the genetic factors

dictating these processes will soon become more conventional. Thus identification of

sequences unique to strain IA565 and not 43816 will provide some insight into the factors

influencing and directing commensalism. Is IA565 commensal behavior an active

process relying on expression of commensal factors? Or is this behavior totally passive

and attributable to the absence of virulence factors and those factors associated with

virulence? In addition, what are the specific interactions of IA565 with the mucosal

immune system? One of the ways to address that question would be to explore whether

or not IA565 bacteria are translocated into the mesenteric lymph nodes (MLN) during GI

colonization and determine cytokine profiles generated at those sites.

The host mucosa is highly adapted to the presence of commensals and their

antigens inducing a state of immunological hyporesponsiveness, known as oral tolerance.

Peyer's patches and MLN are part of the gut associated lymphoid tissues that serve as the

immunologic inductive sites. Effector cells are distributed throughout the mucosa with dendritic cells (DCs) being generally agreed upon as the most important mediator of intestinal immunity [13]. Normally, gut antigens (food proteins or commensal components) are presented in the absence of inflammatory signals by quiescent DCs, resulting in tolerance. Interestingly, Macpherson et. al. demonstrated that intestinal DCs are able to harbor live commensals internally for several days allowing DCs to selectively induce IgA and inhibit commensals from crossing the mucosal barrier [14]. However, studies have shown that non-pathogenic commensal bacteria are able to translocate across intact gut epithelium [15, 16]. Thus, the host's intestinal barrier function, rather than specific virulence properties of enteric microbes, facilitates bacterial translocation.

In vitro cultures of DCs isolated from the MLN when incubated with *Lactobacillus* and *Bifidobacterium* have been shown to secrete the regulatory cytokines, IL-10 and TGF-β. However, DCs isolated from peripheral blood mononuclear cells produced the inflammatory cytokines, TNFα and IL-12 in response to those same commensal organisms [17]. Thus, the induction of immune responses to microbes, especially commensal organism, is highly compartmentalized and tightly regulated.

Future studies that determine the presence of IA565 bacteria in the inductive site of the MLN as well as intestinal DC responses to IA565 will provide insights on how this murine commensal can potentially play a role in mucosal tolerance.

References

1. Mehling, J.S., H. Lavender, and S. Clegg, *A Dam methylation mutant of Klebsiella pneumoniae is partially attenuated.* FEMS Microbiol Lett, 2007. **268**(2): p. 187-93.

2. Shankar-Sinha, S., et al., *The Klebsiella pneumoniae O Antigen Contributes to Bacteremia and Lethality during Murine Pneumonia.* Infect Immun, 2004. **72**(3): p. 1423-1430.

3. Maroncle, N., C. Rich, and C. Forestier, *The role of Klebsiella pneumoniae urease in intestinal colonization and resistance to gastrointestinal stress.* Res Microbiol, 2006. **157**: p. 184-193.

4. Lai, Y.C., et al., *Identification and characterization of KvgAS, a two-component system in Klebsiella pneumoniae CG43.* FEMS Microbiol Lett, 2003. **218**(1): p. 121-6.

5. Koraimann, G., *Bacterial Conjugation: Cell-Cell Contact-Dependent Horizontal Gene Spread.* Microbial Evolution: Gene Establishment, Survival, and Exchange, ed. R.V. Miller and M.J. Day. 2004, Washington, D.C.: ASM Press.

6. Metcalf, W.W., et al., *Conditionally replicative and conjugative plasmids carrying lacZ alpha for cloning, mutagenesis, and allele replacement in bacteria.* Plasmid, 1996. **35**(1): p. 1-13.

7. Skorupski, K. and R.K. Taylor, *Positive selection vectors for allelic exchange.* Gene, 1996. **169**(1): p. 47-52.

8.   Poteete, A.R., *What makes the bacteriophage lambda Red system useful for genetic engineering: molecular mechanism and biological function.* FEMS Microbiol Lett, 2001. **201**(1): p. 9-14.

9.   Murphy, K.C., *Use of bacteriophage lambda recombination functions to promote gene replacement in Escherichia coli.* J Bacteriol, 1998. **180**(8): p. 2063-71.

10.   Lawlor, M.S., C. O'Connor, and V.L. Miller, *Yersiniabactin is a virulence factor for Klebsiella pneumoniae during pulmonary infection.* Infect Immun, 2007. **75**(3): p. 1463-72.

11.   Turk, B.E., *Manipulation of host signalling pathways by anthrax toxins.* Biochem J, 2007. **402**(3): p. 405-17.

12.   Beutin, L., *Emerging enterohaemorrhagic Escherichia coli, causes and effects of the rise of a human pathogen.* J Vet Med B Infect Dis Vet Public Health, 2006. **53**(7): p. 299-305.

13.   Mowat, A.M., *Dendritic cells and immune responses to orally administered antigens.* Vaccine, 2005. **23**(15): p. 1797-9.

14.   Macpherson, A.J., et al., *A primitive T cell-independent mechanism of intestinal mucosal IgA responses to commensal bacteria.* Science, 2000. **288**(5474): p. 2222-6.

15.   Clark, E., et al., *Interferon gamma induces translocation of commensal Escherichia coli across gut epithelial cells via a lipid raft-mediated process.* Gastroenterology, 2005. **128**(5): p. 1258-67.

16.   Reddy, B.S., et al., *Commensal bacteria do translocate across the intestinal barrier in surgical patients.* Clin Nutr, 2007. **26**(2): p. 208-15.

17. O'Mahony, L., et al., *Differential cytokine response from dendritic cells to commensal and pathogenic bacteria in different lymphoid compartments in humans.* Am J Physiol Gastrointest Liver Physiol, 2006. **290**(4): p. G839-45.